Université de Montréal

Bihemispheric reorganization of neuronal activity during hand movements after unilateral inactivation of the primary motor cortex

Ian Moreau-Debord

Département de Neurosciences

Faculté de Médecine

Thèse présentée à la Faculté de Médecine

en vue de l'obtention du grade de Philosophiae Doctor (Ph.D.)

en Neurosciences

3-530-1-1

Mai 2022

Université de Montréal

Unité académique : Département de Neurosciences, Faculté de Médecine

---

This thesis, entitled

Bihemispheric reorganization of neuronal activity during hand movements after unilateral inactivation of the primary motor cortex

Presented by

Ian Moreau-Debord

Was evaluated by a jury of the following individuals

Dr. Arlette Kolta

Chairman of the jury

Dr. Numa Dancause

Research director

Dr. Elvire Vaucher

Member of the jury

Dr. Christopher Pack

External examiner

Abstract

After brain injuries such as stroke, the primary motor cortex (M1) is often damaged leading to motor deficits that include a loss of fine motor skills of the contralateral limbs. Recovery from M1 lesions is accompanied by hemodynamic reorganization in motor areas distal to the site of injury in both hemispheres that are most pronounced early after injury. However, we have limited understanding of the rapid neuronal reorganization that occurs in this complex and distributed cortical motor network. As these neural changes reflect the landscape on which subacute plasticity involved in motor recovery will take place, an exploration of the rapid reorganization in neural activity that occurs in motor regions of both hemispheres is long overdue.

In the current thesis, we set out to explore the impact of a localized, unilateral and reversible cortical injury to the M1 hand area on neuronal activity in motor-related areas of both the ipsi and contralesional hemispheres as non-human primates performed a reach and grasp task. Our inactivation model allowed us to continuously record isolated neurons before and after the onset of motor deficits. In a first study, the rapid reorganization taking place in the ventral premotor cortex (PMv) of both hemispheres was investigated (**Chapter 2**). The PMv is an area well-known to be critically involved in hand motor control and recovery from M1 lesions. In a second study, the rapid reorganization taking place in the contralesional M1 (cM1) was studied and compared to those occurring in bilateral PMv (**Chapter 3**). The cM1 has a complex role in recovery of dexterous hand movements following injury to its homologue.

We reveal extensive, and much more complex than expected, neuronal reorganization in both hemispheres at the very onset of motor impairments. Our data demonstrate that neuronal changes occurring within minutes after brain injury are heterogenous both within and across areas of the cortical motor network. They occur in the two hemispheres during movements of both the paretic and non-paretic arms, and they vary during different phases of movement. These findings constitute a first step in a much needed and timely effort to unravel the complex neuronal correlates of the reorganization that takes place across the distributed motor network after brain injury.

Keywords: premotor cortex, primary motor cortex, neuronal reorganization, non-human primate, hand, grasping, inactivation, plasticity, stroke

Resumé

Le cortex moteur primaire (M1) est souvent endommagé lors des lésions cérébrales telles que les accidents vasculaires cérébraux. Ceci entraîne des déficits moteurs tels qu'une perte de contrôle des membres controlatéraux. La récupération des lésions M1 s'accompagne d'une réorganisation hémodynamique dans les zones motrices intactes des deux hémisphères. Cette réorganisation est plus prononcée dans les premiers jours et semaines qui suivent la lésion. Toutefois, nous avons une compréhension limitée de la réorganisation neuronale rapide qui se produit dans ce réseau moteur cortical complexe. Ces changements neuronaux nous informent sur l'évolution possible de la plasticité subaiguë impliquée dans la récupération motrice. Par conséquent il était grand temps qu'une caractérisation de la réorganisation rapide de l'activité neuronale dans les régions motrices des deux hémisphères soit entreprise.

Dans cette thèse nous avons exploré l'impact d'une lésion corticale localisée, unilatérale et réversible dans M1 sur l'activité neuronale des zones motrices des hémisphères ipsi et contralésionnel lorsque des primates non humains ont effectués des mouvements d'atteinte et de saisie. Notre modèle d'inactivation nous a permis d'enregistrer en continu des neurones isolés avant et après l'apparition des déficits moteurs. Dans une première étude, la réorganisation rapide qui se produit dans le cortex prémoteur ventral (PMv) des deux hémisphères a été étudiée (**Chapitre 2**). Le PMv est une zone connue pour être impliquée dans le contrôle moteur de la main et la récupération des lésions M1. Dans une seconde étude, la réorganisation rapide du M1 contralésionnel (cM1) a été étudiée et comparée à celles se produisant dans les PMv bilatérales (**Chapitre 3**). Le cM1 joue un rôle complexe dans la récupération des mouvements de précision de la main suite à une blessure à son homologue.

Nous révélons une réorganisation neuronale importante et beaucoup plus complexe que prévu dans les deux hémisphères lors de l'apparition initiale des déficiences motrices. Nos données démontrent que les changements neuronaux survenant quelques minutes après une lésion cérébrale sont hétérogènes à la fois dans et entre les zones du réseau moteur cortical. Ils se produisent dans les deux hémisphères lors des mouvements des bras parétiques et non parétiques, et ils varient au cours des différentes phases du mouvement. Ces découvertes constituent une première étape nécessaire pour démêler les corrélats neuronaux complexes de la réorganisation au travers du réseau moteur des deux hémisphères à la suite d'une lésion cérébrale.

Mots-clés: cortex prémoteur, cortex moteur primaire, réorganisation neuronale, primates non-humains, main, préhension, inactivation, plasticité, accidents vasculaires cérébraux

Table of Contents

List of Figures

List of Abbreviations

ACS: alternating current stimulation

AIP: anterior intraparietal area

ANOVA: analysis of variance

BCI: brain computer interface

BOLD: blood oxygen level dependent

CIMT: constraint-induced movement therapy

cM1: contralesional primary motor cortex

CMA: cingulate motor area

CNS: central nervous system

cPMd: contralesional dorsal premotor cortex

cPMv: contralesional ventral premotor cortex

cSMA: contralesional supplementary cortex

CS: corticospinal

D2, D3-5: digit 2, digit 3-5

DCS: direct current stimulation

EMG: electromyographic activity

FMA: floating microprobe array

fMRI: functional magnetic resonance imaging

GABA: γ-aminobutyric acid

ICMS: intracortical microstimulation

iM1: ipsilesional primary motor cortex

iPMd: ipsilesional dorsal premotor cortex

iPMv: ipsilesional ventral premotor cortex

iSMA: ispilesional supplementary motor area

M1: primary motor cortex

MEG: magnetoencephalography

NIBS: non-invasive brain stimulation

PC1-PC2: principal component 1, principal component 2

PLC: perilesional cortex

PMd: dorsal premotor cortex

PMv: ventral premotor cortex

rmANOVA: repeated measures analysis of variance

rTMS: repetitive transcranial magnetic stimulation

S1: primary somatosensory cortex

S2: secondary somatosensory cortex

SD: standard deviation

SDE: spike density estimate

SEM: standard error of the mean

SMA: supplementary motor area

tACS: transcranial alternating current stimulation

TBS: theta burst stimulation

tDCS transcranial direct current stimulation

TMS: transcranial magnetic stimulation

VIP: ventral intraparietal area

χ^2: Chi-square test

Acknowledgements

First of all, I would like to thank my supervisor Dr. Numa Dancause for his guidance, patience and support during my time in his laboratory. Through his supervision I have become a better scientist and a better writer, and I have gained much from his wisdom. Thank you for all the trust you placed in me, for allowing me to work independently, and for tolerating my sometimes chaotic work schedules.

I feel privileged to have gotten the chance to get to know so many wonderful people who shared my passion for neuroscience. I would specifically like to thank Stephan Quessy for all his advice, hard work and feedback that allowed these projects to come to fruition. I would also like to extend a big thanks to Eleonore Serrano, my lab partner on all these projects, we made a good team and had a blast working with the monkeys. Other specific people I would like to thank include Lucie Luneau and Boris Touvykine, for being generally awesome and endlessly supportive during these long years of study.

I would like to thank my family for their unfaltering support and for encouraging me to achieve my dreams throughout the years. Thank you Mom and Dad for always believing in me and thank you Cedric for being the great brother that you are. I would also like to extend a heartfelt thanks to Valeriane Guillaud for her presence, support, patience and understanding as I wrote this thesis. To all these people words cannot describe my gratitude and the extent to which I appreciate their presence in my life.

Finally, I would like to thank the monkeys Sierra and Maika, without whom none of this would have been possible.

Chapter 1- Introduction

1. A cortical control of arm and hand movements

Reaching in the environment to grasp objects is a fundamental and ethologically relevant behavior in humans and other primates (Kaas et al., 2013). The coordination between numerous cortical structures is involved in generating reach to grasp with the upper limb (Kalaska et al., 1997; Shadmehr and Wise, 2005), with each contributing to different extents to various components of the movement. This network includes the primary motor cortex, considered to be the main executor of motor actions, as well as the premotor cortex, which encode higher-order, motor-related processing. Of particular importance to the current thesis, the ventral premotor cortex has mostly been implicated in the control of hand grasping. In this section an overview of the role of these two areas in the control of dexterous movements will be presented, with an emphasis on motor control of the arm and particularly the hand.

1.1 The primary motor cortex

Among the many cortical areas that are decidedly motor-related (Dum and Strick, 1991; Luppino et al., 1991; He et al., 1993; Luppino et al., 1993; He et al., 1995; Dum and Strick, 2002), the primary motor cortex (M1) is considered to be the cortical motor area with the most robust and direct connections with the body's contralateral motor apparatus (Biber et al., 1978; Murray and Coulter, 1981; He et al., 1993, 1995). Indeed, M1 has numerous connections with the spinal cord, a large part of which are projections to spinal interneurons that synapse onto the motoneurons that innervate the musculature (Maier et al., 2002). Of these corticospinal projections, 90% are to the contralateral spinal cord (Dum and Strick, 1996; Brosamle and Schwab, 1997; Lacroix et al., 2004; Rosenzweig et al., 2009; Morecraft et al., 2013). Of those that remain ipsilateral, most bifurcate and synapse bilaterally, such that very few synapse purely with motoneuron pools that control ipsilateral muscles (Rosenzweig et al., 2009). As a consequence, M1 outputs are highly lateralized. In addition, some of M1 neurons with corticospinal projections to the cervical segments of the spinal cord synapse directly onto the

motoneurons that innervate contralateral hand muscles (Bortoff and Strick, 1993; Maier et al., 1993; Bennett and Lemon, 1996; McKiernan et al., 1998; Rathelot and Strick, 2006, 2009; Smith and Fetz, 2009). No such connections have been shown to occur to ipsilateral motoneurons (Soteropoulos et al., 2011). These corticomotoneuronal connections are only present in humans and other primates with a great manual dexterity (Bortoff and Strick, 1993; Maier et al., 2002) and have been suggested to be instrumental in controlling independent movement of the digits of the contralateral hand (Lemon, 1993, 2008).

1.1.1 Movement representation in M1

The origin of our knowledge about the motor cortex stems from classical studies in humans and other animals that demonstrated that an electrical stimulation of the surface of the brain, in a region of the frontal lobe just anterior to the central sulcus, could evoke movements in the side of the body contralateral to the hemisphere stimulated (Ferrier, 1874; Leyton and Sherrington, 1917; Penfield and Boldrey, 1937; Fritsch and Hitzig, 2009). Across this surface, the entire contralateral musculature was found to be represented with major body segments arranged in a medio-lateral fashion, with leg movements evoked at the medial extent of this region and mouth movements at the lateral extent (Penfield and Boldrey, 1937; Woolsey et al., 1952). Thus, these studies demonstrated that there was a somatotopic organization within the motor cortex, the 'homonculus', with different cortical territories dedicated to specific body movements. Notably, these territories were shown to occupy more or less cortical space based on the complexity of possible movements that can be evoked from the territory, rather than on the size of the body parts represented. As a consequence, the representation of the hand is notably large relative to other body parts such as the leg, occupying a large extent of the homunculus consistent with its functional complexity.

While it was the initial view that M1's somatotopic cartography was orderly with different muscle representations occupying discrete locations (Asanuma, 1975), subsequent cortical mapping investigations using electrical stimulation in anesthetized primates revealed that motor cortex is organized as a mosaic, where certain representations of the body, such as the hand and the forearm, overlap partially (Gould et al., 1986; Huntley and Jones, 1991; Donoghue et al., 1992; Park et al., 2001). Indeed, the arm representation area of M1 can be divided into

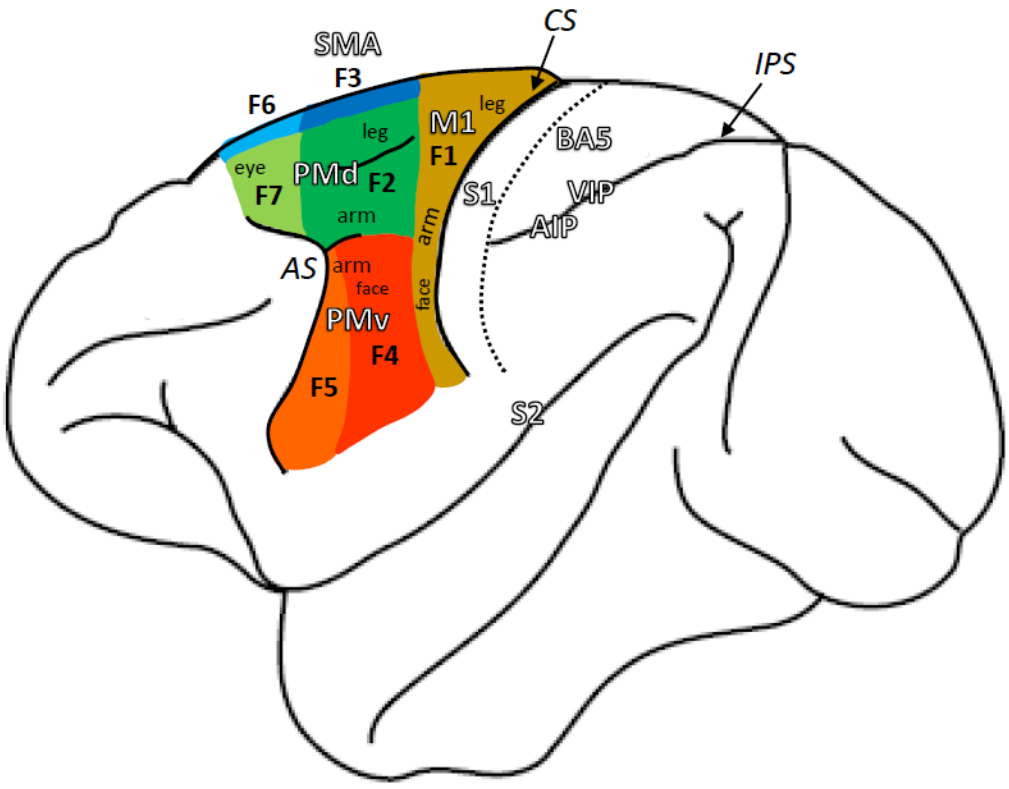

Figure 1.1 *Cortical motor areas.*

Schematic representation of the different cortical motor areas of the macaque monkey discussed in the current thesis. Some of the most commonly used nomenclatures to refer to these areas are shown. The primary motor cortex M1 (also known as F1) is shown in beige. The ventral premotor cortex PMv can be subdivided into two territories, F4 (red) and F5 (orange), as can the dorsal premotor cortex PMd, into the two territories F2 (green) and F7 (light green). The SMA proper (F3, blue) and pre-SMA (F6, light blue) are also shown; these territories wrap around the medial wall of the hemisphere, and thus are only partially visible here. Other areas of interest that are referred to in the thesis are also present. This includes the primary somatosensory cortex S1, the extent of which is shown by the dotted line, as well as secondary somatosensory cortex S2, located mostly in the lunate sulcus. The parietal areas shown include area 5 (BA5) and two areas located in the intraparietal sulcus, the ventral intraparietal area VIP and the anterior intraparietal area AIP. Also shown are approximate locations of some of the arm (includes hand), face, leg and eye representation areas of the motor and premotor cortex. CS: central sulcus; AS: arcuate sulcus; IPS: intraparietal sulcus.

three major sections, with an inner central zone near the anterior wall of the central sulcus that evokes distal movements only (e.g. hand), an outer enveloping zone that evokes proximal movements only (e.g. shoulder), and a transitional zone between them where both distal and proximal movements can be evoked (Park et al., 2001). Furthermore, localized stimulation and even activation of individual corticospinal (CS) neurons can evoke complex patterns of activity across several muscles, for example of the forearm (Cheney and Fetz, 1985) or the hand (Buys et al., 1986). Anatomical studies of M1 provide further support that muscles are represented in a distributed manner. For example, CS neurons can terminate on several motoneurons innervating different hand muscles, and CS neurons that control a specific hand muscle can be found spread out across the territories of several functionally related muscles, such as those of the shoulder or upper arm (Shinoda et al., 1981; Lawrence et al., 1985; Rathelot and Strick, 2006). This general somatotopographic organization complete with functional overlap between muscles would allow M1 to coordinate the activity of numerous muscles during complex multi-joint movements such as reaching towards and grasping objects in the environment (Park et al., 2001). Thus, M1's organization and projections point to this region as being a primary executor of dexterous motor actions.

1.1.2 Functional contributions of M1 to contralateral limb use

The electrophysiological responses of M1 neurons during motor performance also support the preferential role of M1 in purely motor processing. Evarts (Evarts, 1968) was the first to record neural activity in M1 and demonstrated that the greater the neural activity, the more pronounced the evoked contralateral movement. Since then, numerous studies in non-human primates have set out to explore M1 neurons' response properties in greater complexity during voluntary limb movements, particularly reaching movements to spatial targets. To do so, they have performed experiments designed to dissociate different motor-specific variables, such as hand trajectory, force, direction, amplitude, velocity, and joint configuration during reaching (Thach, 1978; Kalaska et al., 1989; Riehle and Requin, 1989; Alexander and Crutcher, 1990a; Crutcher and Alexander, 1990; Bauswein et al., 1991; Werner et al., 1991; Georgopoulos et al., 1992; Fu et al., 1993; Riehle et al., 1994; Riehle and Requin, 1995; Scott and Kalaska, 1995, 1997). These studies have found evidence that M1 is involved in the computation of limb kinematics, such as the position, direction and speed of limb segments and joints in space during reaching

movements (Kalaska and Hyde, 1985; Kalaska et al., 1989; Riehle and Requin, 1989; Alexander and Crutcher, 1990a; Crutcher and Alexander, 1990; Fu et al., 1993; Fu et al., 1995; Riehle and Requin, 1995) as well as the computation of limb dynamics, such as the amount of muscle force and joint torques required to perform a reaching movement (Thach, 1978; Kalaska and Hyde, 1985; Kalaska et al., 1989; Crutcher and Alexander, 1990; Bauswein et al., 1991; Werner et al., 1991; Georgopoulos et al., 1992; Riehle et al., 1994; Riehle and Requin, 1995; Scott and Kalaska, 1995, 1997). Nonetheless, the extent to which M1 encodes purely kinematics versus dynamics of movement is an ongoing debate, and M1 neurons may best be viewed as encoding an amalgamation of different kinematic and dynamic parameters of movement (Kakei et al., 1999).

Studies have also specifically explored M1 neural activity during dexterous use of distal musculature to elucidate its role in voluntary control of the hand and fingers. In humans, functional imaging reveals extensive activation of M1 during hand use (Ehrsson et al., 2000; Takasawa et al., 2003; Kuhtz-Buschbeck et al., 2008) and transcranial magnetic stimulation (TMS) can be used to alter M1 neural excitability and corticospinal motor outputs, altering motor behavior of the hand during voluntary behavior (Lemon et al., 1995; Chouinard et al., 2005; Schabrun et al., 2008). Studies in primates have shown that M1 neural activity is strongly modulated during hand and finger movements, being very active during grasping, including precision or power grasps (Wannier et al., 1991; Maier et al., 1993; Gardner et al., 2007; Umilta et al., 2007; Hendrix et al., 2009), and information related to different grasp configurations can also be found in M1 local field potentials (Spinks et al., 2008). In addition, M1 neurons are sensitive to different properties of the objects to be grasped, for example being modulated by texture or weight (Picard and Smith, 1992) or grasp force required to hold the object (Wannier et al., 1991; Maier et al., 1993; Hepp-Reymond et al., 1999; Hendrix et al., 2009).

Finally, the importance of M1 as a motor controller can be readily seen following lesions to this area, which have profound effects on motor performance (Travis, 1955; Rouiller et al., 1998). Large lesions of the M1 arm area makes movements with the contralateral limb weaker and slower, perturbing movement kinematics and normal patterns of muscle activity (Hoffman and Strick, 1995). Even small lesions of the M1 hand area lead to deficits in fine motor control of the contralateral digits, highlighting the crucial role of this area in the generation of motor

commands for grasping and other hand movements (Friel and Nudo, 1998). Complimentarily, the use of pharmacological agents such as muscimol, a GABA-A receptor agonist, have been used to locally and precisely inactivate cortex to produce reversible 'lesions' (Martin, 1991; Matsumura et al., 1991; Martin and Ghez, 1993; Schieber and Poliakov, 1998; Brochier et al., 1999) (see section 4). Such an approach allows one to explore M1 contributions to motor control without the mechanical damage, tissue inflammation, or hemorrhaging that can accompany actual brain damage. Using a variety of tasks that challenge the dexterity of the hand, studies in primates have demonstrated decreased speed, longer reaction and movement time, weakness of hand muscles and decreased grip force, and loss of independent finger movements following muscimol injection in the M1 hand area (Matsumura et al., 1991; Kubota, 1996; Schieber and Poliakov, 1998; Brochier et al., 1999; Fogassi et al., 2001). Fine motor control, such as precision grip which requires opposition of the index and thumb, can become impossible to execute (Brochier et al., 1999; Fogassi et al., 2001). Thus, these studies solidify the critical role of M1 in voluntarily-generated hand movements such as grasping.

Overall, the studies described above highlight the centrality of this area in direct control of the contralateral musculature. Nonetheless, it has been argued that M1 activity may also have a role in other processes that are not purely motor, such as cognitive processes (Georgopoulos et al., 1989; Georgopoulos et al., 1993; Georgopoulos, 1995), or in the processing of somatosensory information (Mountcastle et al., 1992). For example, as part of its role in motor control M1 responds to proprioceptive feedback about contralateral limb position (Evarts and Tanji, 1976; Wolpaw, 1980; Pruszynski et al., 2011; Takei et al., 2018) and represents loads applied to the contralateral limb (Kalaska et al., 1989; Cabel et al., 2001; Herter et al., 2009; Omrani et al., 2014; Pruszynski et al., 2014). In addition, M1 has been suggested to participate in the sensory or associative processing of visuospatial information for reaching (Georgopoulos et al., 1989; Alexander and Crutcher, 1990b; Hocherman and Wise, 1991; Lurito et al., 1991; Shen and Alexander, 1997a), which is generally considered the purview of premotor cortex (see next section). For example, in a task that dissociated the location of reach targets from the movements required to reach them, some neurons in M1 are target-dependent, representing the location of a reach target irrespective of the type of reach performed (Alexander and Crutcher, 1990b; Shen and Alexander, 1997a). Other neurons show more complex, associative relationships between the position of targets and reach movements, being modulated by both

such that their activity is target- and limb-dependent (Shen and Alexander, 1997a). Of course, many neurons are also present that only care about movement direction, i.e. are purely limb-dependent. Whereas target-dependent neural activity was more pronounced prior to movement during motor planning, limb-dependent activity was dominant during the movement (Shen and Alexander, 1997a). The presence of these different signals, and their progression as motor processes occur, suggests that M1 partakes in a sensorimotor transformation converting information about the visuospatial position of targets into motor commands to reach to the designated spatial location (Shen and Alexander, 1997a).

1.1.3 Cortical inputs to M1

The intrahemispheric connections of M1 support its role in motor control. In particular, M1 is strongly interconnected with several areas related to somatosensory processing. Somatosensory connections with M1 are primarily with areas 3a, 1, 2 (and 3b to a lesser extent) of the primary somatosensory cortex (S1), as well as area S2 in the parietal operculum, and area 5 of the posterior parietal cortex (Stepniewska et al., 1993; Dea et al., 2016; Hamadjida et al., 2016). The S1 is well known to be responsible for the processing of somatic sensations, including touch, proprioception, nociception, and temperature. It plays a critical role in processing afferent somatosensory input and contributes to the integration of sensory and motor signals for skilled movement. The interactions between M1 and S1 are critical for motor control. For example, inactivation of S1 induces errors in finger coordination and the application of grasp and lifting forces when interacting with objects (Brochier et al., 1999). In addition, projections from the sensory to the motor cortex are important for the learning of motor skills in the monkey, such as catching food pellets being dropped (Pavlides et al., 1993). Area S2 is involved in higher-order processing of tactile information, such as object recognition and expected feedback from object interaction (Murray and Mishkin, 1984; Romo et al., 2002; Del Vecchio et al., 2019; Del Vecchio et al., 2020). Area 5 (also referred to as Broadmann Area 5) is involved in somatosensory processing to represent spatial information for limb movement (Kalaska et al., 1983; Lacquaniti et al., 1995). Thus, both these higher-order somatosensory areas provide M1 with important information for limb motor control.

In addition to these somatosensory interactions, M1 is strongly interconnected with the premotor cortex (Stepniewska et al., 1993; Dum and Strick, 2002; Dea et al., 2016; Hamadjida et

al., 2016). The role of the premotor cortex, and its interactions with M1, have important functional implications for motor control, and are the subject of the next sections.

1.2 The premotor cortex

Reaching and grasping an object in the environment, such as a glass of water, requires performing a temporally precise sequence of movements, from reaching out towards the glass, grabbing it, lifting it, and moving it towards the mouth. To perform this movement, the brain must take sensory information about the physical properties of the object and the visuospatial position of the hand and object relative to each other and transform it into a motor plan that can execute the required actions. It must also take into account more abstract, context-dependent task requirements, such as choosing the correct glass among several. The premotor cortex, a frontal region situated just rostrally relative to M1, contributes critically to these sensorimotor transformations. It has classically been considered to perform more complex, or 'higher-order' processing than the computations performed in M1. Premotor areas are defined as regions of the cortex that project directly to M1 as well as the spinal cord (Dum and Strick, 2002). Initial exploration of the premotor cortex began at the start of the 20th century, when a new hypothesis emerged suggesting that the motor cortex was not a singular entity but rather could be subdivided into several cortical regions. In 1905, Campbell performed a cytoarchitectonic analysis that demonstrated that the motor cortex could be separated into a posterior region that contained a dense population of large pyramidal cells, and an anterior region that did not contain such cells (Campbell, 1905). Furthermore, Campbell speculated that there were functional differences between these areas, with the posterior region, the primary motor cortex M1, focused on controlling simple movement parameters, whereas the anterior region controlled more higher-order, complex parameters of movement. Subsequent studies supported this hypothesis of non-uniformity of motor cortex (Broadmann, 1909; Vogt and Vogt, 1919) and the anterior region was given the moniker of "premotor" cortex (Fulton, 1935). While initially it was suggested that only the medial cortex may actually be premotor (Penfield and Welch, 1951; Woolsey et al., 1952), subsequent investigations supported the inclusion of a premotor region located on the lateral surface of the cortex anterior to M1 (Roland et al., 1980; Weinrich and Wise, 1982; Weinrich et al., 1984; Matelli et al., 1985; Gentilucci et al., 1988; Rizzolatti et al., 1988). Since then, it is the

consensus that voluntary motor control does not emerge from one cortical region, but rather from several sub-regions that work together. Of particular importance to the current thesis, on the lateral surface of the cortex is situated the ventral premotor cortex (PMv). This area and its connections with M1 have been implicated in parietofrontal circuits involved in grasping. Other premotor areas include the dorsal premotor cortex (PMd), the supplementary motor area (SMA), and the cingulate motor areas (CMA) located on the median wall of the cortex. In this section, an overview of the organizational and functional properties of the PMv in relation to unimanual motor control of the arm and hand will be presented.

1.2.1 The ventral premotor cortex

The ventral premotor cortex (PMv) is situated on the lateral surface of the cortex, lateral to the genu of the arcuate sulcus. Similar to M1, the PMv contains a somatotopic representation of the contralateral body and contains neurons with corticospinal projections. However, in contrast to M1, the somatotopic representation of PMv is mostly limited to the arm and face (Gentilucci et al., 1988; Rizzolatti et al., 1988; Hepp-Reymond et al., 1994; Preuss et al., 1996). The PMv can be subdivided into two main sections based on anatomical and functional differences, a caudal area F4 and a rostral area F5 (Geyer et al., 2000; Rizzolatti and Luppino, 2015). Stimulation of area F4 using electrodes in the anesthetized monkey can evoke arm, neck, face and mouth movements (Gentilucci et al., 1988). Area F5 is located more rostrally on PMv than area F4 and continues in part into the arcuate sulcus. Area F5 has been shown to contain a motor representation of the hand that is located more dorsally, and a representation of the mouth more ventrally, that overlap considerably (Kurata and Tanji, 1986; Gentilucci et al., 1988; Rizzolatti et al., 1988; Hepp-Reymond et al., 1994; Maranesi et al., 2012).

Both areas are a source of corticospinal outputs and provide input to M1. The corticospinal projections of the F5 hand area are made to the intermediate zone of the cervical spinal cord (Dum and Strick, 1991; He et al., 1993; Borra et al., 2010). While there are some weak projections to the C6-T1 segments where motoneuronal pools of contralateral hand muscles are located, the projections are mainly to the C2-C5 segments, which contains propriospinal neurons that mediate disynaptic pyramidal excitation to contralateral forelimb motoneurons (Isa et al., 2006; Isa et al., 2007). Areas F4 and F5 are also strongly connected with M1 in a somatotopically consistent manner. More specifically, area F4 sends direct projections to

the arm and mouth representation areas of M1 (Matelli et al., 1986). In parallel, area F5 is robustly and extensively connected to the hand field of M1 (Borra et al., 2010; Gerbella et al., 2011). This connection may be critical to PMv's ability to control grasping movements. Indeed, while corticospinal F5 neurons show grasp-related activity (Kraskov et al., 2009; Kraskov et al., 2014), motor actions evoked by microstimulation of the PMv hand area seem to depend in large part on cortico-cortical interactions with M1, modulating its neural activity and corticospinal outputs (Cerri et al., 2003; Shimazu et al., 2004; Umilta et al., 2007; Schmidlin et al., 2008; Prabhu et al., 2009; Kraskov et al., 2011).

The neural activity in PMv is suggested to contribute to the sensorimotor control of arm and hand movements in several important ways. Briefly, area F4 has been implicated in encoding the peripersonal space, which is the space around the body that is within reaching distance (Gentilucci and Rizzolatti, 1990; Graziano et al., 1994; Fogassi et al., 1996; Rizzolatti and Luppino, 2015) In parallel, neural activity in area F5 has been implicated in the visuomotor control of grasping movements. The role of PMv in both of these processes will be discussed in turn, with a strong emphasis on the latter, before concluding with a concise overview of the inputs to PMv associated with these functions.

1.2.1.1 PMv encodes the peripersonal space for reaching

The computation of peripersonal space in PMv comes from observations of neurons with multimodal sensory responses in area F4. A large majority of neurons in this area have sensory responses to tactile and visual stimuli (Rizzolatti et al., 1981a, b; Gentilucci et al., 1983; Gentilucci et al., 1988; Graziano and Gross, 1994). Neurons whose sensory responses are limited to tactile stimuli have been called "unimodal", whereas others that respond to both visual and tactile stimuli have been labelled "bimodal" neurons (Fogassi et al., 1996). Bimodal neurons have also been referred to as simply visuo-tactile (Brozzoli et al., 2012). Both unimodal and bimodal neurons have large tactile receptive fields that are located on the face, arm and upper torso, consistent with its motor somatotopy (Gentilucci et al., 1988). The visual responses of bimodal F4 neurons are characterized by three-dimensional receptive fields that are positioned in conjunction with their tactile receptive fields. These receptive fields are contained within the space around the body that is in reaching distance and are best evoked by moving objects. Thus, their visually evoked responses are modulated based on the distance between the visual object

and the tactile receptive field. In addition, these visual fields are often fixed in place relative to the body, such that changes in gaze direction do not alter the position of the neurons' visual fields (Fogassi et al., 1996; Rizzolatti and Luppino, 2015). As such, sensory information in PMv is mostly encoded relative to the body, such as the arm or face, instead of relative to the eye, as appropriate to be used in motor processes (Gentilucci et al., 1983; Fogassi et al., 1992; Graziano et al., 1994; Fogassi et al., 1996). This suggests that bimodal F4 neurons could be implicated in transforming the position of reach targets located in the peripersonal space, into motor actions that involve those targets.

1.2.1.2 A central role of PMv in visuomotor control of grasp

Neurons in both subdivisions of PMv are active during the preparation and execution of movements that are guided mainly by vision (Kurata and Tanji, 1986; Gentilucci et al., 1988; Rizzolatti et al., 1988). Nonetheless, neural activity in area F5 is much more strongly related to hand motor acts, consistent with its somatotopy (Gentilucci et al., 1988; Fluet et al., 2010; Nelissen and Vanduffel, 2011; Maranesi et al., 2012; Theys et al., 2012, 2013). Neurons in this area have also been shown to encode mouth or combined hand and mouth motor acts (Godschalk et al., 1995; Maranesi et al., 2012), and some neurons located in the convexity of the arcuate sulcus are specifically active during monkey vocalization (Coude et al., 2011).

The PMv has been strongly implicated in the processing of sensorimotor transformations that underlie visuomotor control of the hand (Jeannerod et al., 1995; Borra et al., 2017). In particular, the PMv has been shown to be critically involved in the preshaping of the hand that occurs prior to contact with a target object. When reaching to an object, the hand first progressively opens with the fingers straightening out, before the grip is closed until it matches object size as tactile contact becomes eminent (Jeannerod, 1984; Gentilucci et al., 1991; Jakobson and Goodale, 1991; Paulignan et al., 1991). This process is considered to be the behavioral consequence of a visuomotor transformation that is using visual information about object properties to progressively shape the hand and fingers into an orientation that facilitates object interaction. When experimenters unilaterally inactivated the PMv of monkeys using the GABA-A agonist muscimol, contralateral hand preshaping was severely affected (Fogassi et al., 2001). More specifically, the inactivation induced a mismatch between the hand shape required to grasp the object and the intrinsic properties of the object. As such, the shape of the hand was

inappropriate to properly grasp the object based on its size and form when tactile contact is made (Fogassi et al., 2001).

Neurons in the PMv hand area display motor and sensory responses that strongly implicate it in visuomotor control of the hand. It is well known that different subpopulations of neurons in PMv are tuned to the execution of specific configurations of the grasping hand (Rizzolatti et al., 1988; Spinks et al., 2008; Fluet et al., 2010; Bonini et al., 2012; Schaffelhofer and Scherberger, 2016). In a classic study using macaque primates trained to perform a reach and grasp task towards a variety of objects, Rizzolatti et al. (1988) classified neurons in the PMv hand representation area that were related to distal motor acts into three categories: precision grip neurons, finger prehension neurons, and whole hand prehension neurons. Precision grip neurons were active during the opposition of the thumb and index finger, finger prehension neurons during the opposition of the thumb with the four other digits, and whole hand prehension neurons were selective for flexions that involve closing all the digits around the object (Rizzolatti et al., 1988). Thus, neurons in F5 display activity that is correlated with very specific goal-related hand motor behaviors, such as grasping and manipulating objects, rather than precisely controlling individuated, single digit movements as seen in M1 activity (Rizzolatti, 1987; Rizzolatti et al., 1988; Murata et al., 1997; Umilta et al., 2007). Indeed, they show a much greater affinity for particular objects and the grasp associated with that object than M1 neurons (Umilta et al., 2007). These grasp preferences occur independently of vision, being maintained in the dark (Raos et al., 2006).

Many of these grasp neurons also show sensory responses to visual stimuli. “Canonical” visuomotor neurons are modulated when objects of certain size, shape and orientation become visible, and during subsequent grasping with them (Rizzolatti et al., 1988; Gallese et al., 1996; Murata et al., 1997; Rizzolatti and Fadiga, 1998). The activation of these visuomotor neurons occur even if objects are simply observed, and no hand movement is requested by the task (Murata et al., 1997; Raos et al., 2006; Umilta et al., 2007; Fluet et al., 2010; Vargas-Irwin et al., 2015). Thus, neurons in PMv are conditionally modulated by visual stimuli or ongoing movement depending on the specific type of grasp involved.

Consistent with this role of PMv in encoding more abstract motor representations, area F5 is also home to a significant proportion of visuomotor neurons with particular properties,

named mirror neurons (di Pellegrino et al., 1992; Gallese et al., 1996; Rizzolatti et al., 1996; Rizzolatti and Craighero, 2004; Kraskov et al., 2009; Papadourakis and Raos, 2017). Such neurons discharge not just when a monkey performs a hand or mouth movement, but also when the animal visually observes another human or monkey perform a similar action. Notably, they are not responsive to the visual presentation of a grasp object alone, such that their responses are related to the motor act itself. Thus, PMv neurons can show a specific preference for a grasp type not just during motor preparation and execution, but also during motor observation, with important implications for observational learning (Murata et al., 1997; Raos et al., 2006). Furthermore, by mapping these observed actions onto the corresponding motor representations that are used to produce voluntary motor actions in the brain, these neurons could be used to allow the observer to understand what the agent they are observing is attempting to accomplish (Rizzolatti et al., 2014). Since their initial discovery in PMv, mirror neurons have also been found in other motor areas, including PMd (Papadourakis and Raos, 2019) and M1 (Vigneswaran et al., 2013), highlighting the close computational bond shared between these regions. Thus, PMv neural activity, while motor-related, appears to be involved in more complex, even cognitive processes.

Based on the neural responses described above, it has been strongly implied that PMv may encode the goal of the motor act and not just the motor action itself (Rizzolatti and Luppino, 2015). Following this interpretation, the PMv would contain a motor "vocabulary", or lexicon, of internal representations of goal-directed hand and/or mouth motor acts , where each "word" is represented by populations of F5 neurons encoding these motor actions in more or less abstract terms (Rizzolatti and Luppino, 2001; Rizzolatti et al., 2014). Within this framework, neural responses like those of canonical or mirror visuomotor neurons reflect sensorimotor transformations, where the extraction of object-specific characteristics by sensory means automatically induces the activation of the repertoire, or vocabulary, of potential motor acts that would underly possible hand-object interactions (Rizzolatti and Luppino, 2001; Castiello and Begliomini, 2008; Rizzolatti and Luppino, 2015). Subsequently, the appropriate motor act from this list of potential actions would be selected based on task requirements and behavioral constraints, and executed via PMv's interactions with M1 (Umilta et al., 2007).

Such abstraction could extend to tool use. For example, in one study monkeys were trained to grasp small objects using either "normal pliers", where the object was grasped by the tool via first opening the hand and then closing it, or "reverse pliers", where the object was grasped by using the opposite movement sequence where the hand was first closed and then opened (Umilta et al., 2008). Interestingly, neurons that discharged when the hand was opening with normal pliers also discharged when the hand was closing with reverse pliers, such that the discharge remained linked to the initial phase of the motor act (i.e. closing the tool around the object). Thus, neurons in F5 encoded the temporal organization necessary to reach the goal, and not the hand movement itself (Umilta et al., 2008).

Finally, more recent studies have demonstrated that the complete kinematics of the contralateral arm, hand and finger movements can be decoded from PMv population neural activity (Bansal et al., 2011; Bansal et al., 2012; Kang et al., 2012; Menz et al., 2015; Takahashi et al., 2017). Furthermore, PMv has been shown to encode the kinematics of both reaching and grasping muscle synergies in single neurons (Takahashi et al., 2017). Neurons in PMv have also been shown to encode some dynamic aspects of movement, as they are modulated by the amount of grip force required to hold an object (Hepp-Reymond et al., 1994). As such, in addition to being implicated in abstract representations of motor acts, it has been suggested that PMv may also represent kinematic and dynamic information about hand movements to a similar extent as what is seen in M1 neural activity (Menz et al., 2015). Thus, PMv may encode a full range of movement-related information, from more sensory to purely motor.

1.2.1.3 Cortical inputs to PMv

The PMv receives inputs from parietal and somatosensory areas that support its roles in the computation of peripersonal space and visuomotor control of grasping. Area F4, which encodes peripersonal space, is strongly interconnected with several areas in the inferior parietal lobule related to sensory processing for motor action, such as area PF, which contains somatosensory information related to the face and mouth (Rozzi et al., 2008), and the ventral intraparietal area (VIP), which is involved in the processing of visual targets (Luppino et al., 1999). Area VIP is well known to receive inputs from what is known as the dorsal visual stream, which includes areas such as MT, MST and FST, which are involved in analysis of motion perception for action (Colby, 1998; Rizzolatti et al., 1998). Furthermore, VIP also contains bimodal visual neurons

with similar functional properties as F4 bimodal neurons (Colby, 1998). As such, areas VIP and F4 appear to be involved in the processing of visual information to create peripersonal space representations useful for actions such as reaching (Rizzolatti et al., 1997; Colby, 1998; Rizzolatti et al., 1998). As part of this processing, bimodal neurons in both areas likely play an essential role in the neural circuit that transforms the position of reach targets located in the peripersonal space, into motor actions that involve those targets, such as reaching towards or away from them (Fogassi et al., 1996).

The inputs to area F5 support the role of PMv in the computation of sensorimotor transformations for grasping. Area F5 is well interconnected with several areas of the inferior parietal lobule related to sensory processing for motor action, particularly the anterior intraparietal area (AIP) (Luppino et al., 1999; Tanne-Gariepy et al., 2002; Gregoriou et al., 2006; Gerbella et al., 2011; Gharbawie et al., 2011b). AIP is critically relevant to visuomotor grasp control, being a hand-related field in the rostral part of the lateral bank of the intraparietal sulcus and contains many neurons that discharge during the execution of specific grasping movements (Sakata et al., 1995). Neurons in AIP also discharge passively during object fixation in absence of movement, and appear to reflect the intrinsic properties of the observed object. Other neurons, in addition to discharging during object fixation, also discharge during observation of hand movements and hand/object interactions, and thus can be considered mirror neurons (Sakata et al., 1995). Furthermore, inactivation of AIP leads to grasping deficits that reflect errors in visuomotor transformations, similar to inactivation of F5 (Gallese et al., 1994). Thus, it is clear that AIP and PMv are part of a circuit that play an important role in visuomotor grasping.

In addition to these parietal connections, PMv is strongly interconnected with somatosensory area S2 (Gerbella et al., 2011; Gharbawie et al., 2011b). S2 is a somatosensory area in the parietal operculum, that is in turn also strongly interconnected with AIP (Rozzi et al., 2006; Borra et al., 2008) and M1 (Gharbawie et al., 2011a; Gharbawie et al., 2011b). It is involved in higher-order processing that contributes to the tactile recognition of objects, and in coding the tactile feedback expected from an upcoming interaction with an object. As such, the interaction between S2 and area F5 may be instrumental in providing information about tactile recognition and expected tactile feedback, important for selecting which grasping motor action to be performed, and controlling digit forces to stabilize grasping of an object. Finally, PMv is also

connected with somatosensory areas 3a, 1 and 2 of S1, and can thus receive proprioceptive and tactile inputs from these areas to help in grasp control (Dancause et al., 2006a; Stepniewska et al., 2006).

To resume, PMv is involved in different aspects of reach to grasp behavior, from the encoding of peripersonal space for reaching movements to visuomotor transformations for grasping. Neural activity can reflect various stages of sensorimotor processing, and is involved in more abstract representations of movement when compared to M1. Nonetheless, similar to M1, it also encodes kinematic and dynamic motor parameters of movement.

1.3 Intrahemispheric interactions of premotor and motor cortex

In the sections above, we described the functional properties of the M1 and PMv separately, mostly in relation to contralateral arm and hand use. However, these areas do not work in isolation. Rather, the planning and execution of arm and hand movements involves the coordination of numerous cortical areas (Kalaska et al., 1997; Shadmehr and Wise, 2005), with each contributing to various extents to components of the reaching and grasping movement. This is supported by the anatomical connections that exist between these areas. Intrahemispherically, neuroanatomical tracing in the primate has shown that the hand region of M1 is the site of major inputs from the PMv, as mentioned earlier (Dum and Strick, 2005; Dancause et al., 2006c). Conversely, the hand motor field of PMv receives numerous projections from M1. Together, the PMv and M1 hand areas are considered to be part of the "visuomotor grasping network" (Jeannerod et al., 1995; Borra et al., 2017), utilizing information obtained from sensory modalities to plan and execute grasping movements.

Functionally, premotor areas can modulate M1 activity and outputs in humans (Civardi et al., 2001; Koch et al., 2007; Davare et al., 2008; Davare et al., 2009; Groppa et al., 2012; Vesia et al., 2018) and monkeys (Tokuno and Nambu, 2000; Prabhu et al., 2009; Quessy et al., 2016; Cote et al., 2017; Cote et al., 2020). Studies exploring these interactions used double or paired pulse protocols using electrode or transcranial magnetic stimulations. These experimental protocols involve using a subthreshold stimulation in one area, which does not evoke a motor response, followed by a suprathreshold stimulation in another area, that does evoke a motor

response. Thus, it becomes possible to quantify the modulatory effect of the subthreshold stimulus on the motor response evoked by the suprathreshold stimulus. The modulation of M1 outputs by the premotor cortex can be very diverse, with facilitation or inhibition being observed based on many factors such as the time between stimulations, the intensity of stimulation used, and the state of the system when stimulation occurs.

The effects of PMv on M1 outputs are complex, but often facilitatory. In the anesthetized monkey, PMv exerts much more facilitation than inhibition (Quessy et al., 2016; Cote et al., 2017; Cote et al., 2020). In awake monkeys, the PMv can modulate the activity of neurons in the M1 (Tokuno and Nambu, 2000; Kraskov et al., 2011), and can induce both facilitatory and inhibitory effects on M1 outputs to contralateral hand musculature depending on the type of grasping required to interact with different objects (Prabhu et al., 2009). For example, much more facilitation is observed during precision grip than whole-hand grasp. In humans, PMv has an inhibitory effect on M1 outputs at rest, but facilitates them during precision grip (Davare et al., 2008). In addition, during preparation to grasp, PMv facilitates activity specifically in the contralateral hand muscles that will be used to execute the movements (Davare et al., 2009). As such, PMv plays a clear functional role in modulating M1 outputs to facilitate complex hand movements such as grasping.

2. A bihemispheric control of arm and hand movements

The role of the a given hemisphere is not limited to simply control of the contralateral limb, but is also involved in the control of the ipsilateral limb (Bundy and Leuthardt, 2019). Indeed, many studies have shown robust neural activity during ipsilateral arm and hand movements in M1 (Tanji et al., 1988; Donchin et al., 1998; Kermadi et al., 1998; Cisek et al., 2003; Bundy and Leuthardt, 2019) and PMv (Rizzolatti et al., 1988; Tanji et al., 1988; Kurata, 2007). There is debate as to the function of ipsilateral motor activity and to what extent it contributes to ipsilateral movement. This is particularly relevant considering that motor outputs are highly lateralized, such that the contralateral hemisphere is the dominant contributor to ipsilateral movement control. There is evidence that the ipsilateral hemisphere can drive some movements on its own, but not others. For example, humans are still able to produce voluntary movements with the arm contralesional to large and significant lesions caused by hemispherectomies (Gardner, 1933). In split-brain monkeys where connections between hemispheres have been severed, the ipsilateral hemisphere can initiate proximal movements of the arm on its own (Brinkman and Kuypers, 1973). However, the ipsilateral hemisphere is unable to appropriately control the distal musculature, i.e. the hand and fingers (Brinkman and Kuypers, 1973). Thus, while a given hemisphere clearly encodes a complete motor plan of the movement to be produced with the contralateral hand, it might only contribute to some aspects of the planning and execution of an ipsilateral movement. Below, the extent to which neural activity in M1 and PMv represents movement-related information differently for each limb will be discussed. Subsequently, an overview of how the ipsilateral PMv can modulate the outputs of the contralateral M1 will be presented.

2.1 Bilateral representation of arm and hand movements in motor cortex

In M1, while the majority of neurons are specifically modulated by movements with the contralateral limb, many neurons are also active during ipsilateral movement (Evarts, 1966; Tanji et al., 1987, 1988; Aizawa et al., 1990). Among these neurons, there exists a small subset of them, about 8%, that exclusively respond to ipsilateral movement, without changing their firing patterns during use of the contralateral limb (Tanji et al., 1988). These neurons have been shown

to be specifically tuned to the movement direction of the ipsilateral arm (Cisek et al., 2003). In addition, different parameters such as speed, velocity, joint angles and muscle activations of the ipsilateral arm can be decoded from monkey M1 neural activity (Ganguly et al., 2009; Ames and Churchland, 2019). In humans, non-invasive techniques such as electrocorticography over the ipsilateral motor cortex can also be used to decode kinematics of ipsilateral arm reaching movements (Ganguly et al., 2009; Bundy et al., 2018). Thus, it seems that M1 may compute, or contain a copy, of the motor parameters required to drive ipsilateral arm movements.

Several studies have set out to specifically explore how M1 represents movement of the contralateral limb relative to that of the ipsilateral limb in its neural activity. To do so, they have studied M1 activity through the perspective of dynamical system models (Shenoy et al., 2013; Pandarinath et al., 2018) and have focused on investigating the latent factors that make up the computations occurring in neural populations. These studies have confirmed that there is a notable redundancy of motor information in the M1 of both hemispheres during unimanual movements in monkeys (Michaels and Scherberger, 2018; Ames and Churchland, 2019; Heming et al., 2019) and humans (Downey et al., 2020). They have also shown that the encoding of specific movement parameters is performed differently for each limb.

In monkeys, the M1 of both hemispheres contain similar information in their neural activity during movement of one arm or the other (Ames and Churchland, 2019; Heming et al., 2019). More specifically, during a novel cycling task with the upper limbs, muscle activity of the arm can be decoded from the M1 of either hemisphere with equivalent precision, meaning that motor control signals present in one hemisphere were also present in the other, and with the same signal strength (Ames and Churchland, 2019). Furthermore, the information related to movement of each arm was decorrelated, with neural activity related to each arm occupying orthogonal subspaces. This means that it was possible to separately decode information related to movement of each arm, such that decoded activity from M1 is enough to fully control two separate robotic arms using a brain-machine interface. Similarly, it has been shown that the neural activity that occurs in M1 in response to mechanical perturbation of the ipsilateral or contralateral arm is also separated, occupying orthogonal subspaces (Heming et al., 2019). Thus, M1 appears to contain complete, and distinct, computational representations of each arm.

However, this sort of discrete encoding may not be the case for hand motor control. Recent electrophysiological recordings in the M1 of human tetraplegic and spinal patients show that ipsilateral grasp tuning is strongly correlated to contralateral grasp tuning, unlike for arm movements (Downey et al., 2020). Thus, it may be difficult to extract separate information from M1 concerning each hand if both hands are used simultaneously. This result is consistent with the observation that, during bimanual finger movements in humans, functional magnetic resonance imaging (fMRI) activations in M1 that are related to ipsilateral finger movements disappear, being dominated by activations related to contralateral finger movements (Diedrichsen et al., 2013). Thus, these results suggest that neural representations for ipsilateral and contralateral hand movements may not occupy distinct neural subspaces in M1, and instead are dominated by contralateral hand use.

2.2 Bilateral representation of the limb in the premotor cortex

The premotor cortex is well known to perform more abstract, higher-order processing of sensorimotor information than M1. It is possible that this processing may be strongly lateralized such that it is discretely represented for each limb like in M1. However, a great deal of task-related information encoded by premotor cortex, such as the position of movement targets, the size and orientation of grasping objects, grasp-type, or the associative meaning of sensory cues, does not necessarily need to be encoded in a limb-dependent manner. Initially, it was shown that during tasks where movements are performed with either arm or both together, premotor neurons will show a variety of movement-specific responses, include being active during use of each arm separately, but not during bimanual movements, or being active during use of one limb exclusively, or being active during bimanual movements exclusively (Rizzolatti et al., 1988; Tanji et al., 1988). Thus, they can show substantial context-dependent movement relationships in tasks that involve both arms. Since these initial investigations, several studies have set out to explore the extent to which processing of different task parameters and movements have a bilateral representation in premotor cortex (Hoshi and Tanji, 2002; Cisek et al., 2003; Hoshi and Tanji, 2006; Kurata, 2007, 2010; Michaels and Scherberger, 2018).

2.2.1 Bilateral representation of the arm and hand in PMv

The PMv is particularly well known to be active during the planning and execution of movements with either limb (Rizzolatti et al., 1988; Tanji et al., 1988; Kurata, 2007). During the planning of arm reaches, PMv neurons will respond to visual cues regardless of whether they are presented in the contra or ipsilateral visual hemifield. They also exhibit a tight relation to their spatial locations regardless of which arm will perform the movement (Hoshi and Tanji, 2002, 2006). Indeed, up to 60% of PMv neurons are tuned to target selection, but not arm use, during movement planning (Hoshi and Tanji, 2002). Nonetheless, neurons do show tuning to arm use, particularly as movement execution draws near, with a preference for the contralateral limb. As such, PMv contains bilateral representation of both visuospatial information and arm effector information (Hoshi and Tanji, 2006). A recent study set out to specifically explore the extent to which PMv neural activity during grasping with the ipsilateral or contralateral hand is lateralized (Michaels and Scherberger, 2018). During grasp planning, much of the neural activity represented the grasp invariant of which hand would perform the action. However, as planning gave way to movement execution, PMv neural activity became tuned to hand used, and this hand-dependent signal persisted throughout the movement (Michaels and Scherberger, 2018). Interestingly, information related to the orientation of the grasping hand was strongly hand-dependent, being encoded in neurons with a preference for the contralateral hand. Limb-independent activity may reflect more abstract encoding of the motor act as part of PMv's "vocabulary" of internal representations of goal-directed movements (Rizzolatti and Luppino, 2001; Rizzolatti et al., 2014; Rizzolatti and Luppino, 2015). Limb-independent and limb-dependent activity in PMv may also reflect different stages of a visuomotor transformation. More precisely, limb-independent information may reflect an earlier stage of processing of task-related visual information that does not require limb-specificity, whereas the more lateralized neural activity may reflect later stages of processing into more motor-centric movement information where limb-specificity becomes important (Hoshi and Tanji, 2002, 2006; Kurata, 2007, 2010). Overall, these results suggest that visuomotor grasp with either hand is well-represented in PMv and that a great deal of similar processing occurs in both hemispheres.

2.3 Interhemispheric interactions of premotor and motor cortex

While the control of ipsilateral movements by the ipsilateral cortex could be mediated in part by ipsilateral descending outputs, the dominant source of control of the ipsilateral hand remains the contralateral hemisphere. Indeed, there is a lack of evidence for a direct corticospinal control of the ipsilateral forelimb by M1 in the healthy monkey (Soteropoulos et al., 2011). Thus, it is likely that any contribution of the ipsilateral hemisphere to ipsilateral hand control involves coordination with the contralateral hemisphere and modulation of the outputs of the contralateral M1. This coordination between the premotor and primary motor cortex of each hemisphere is mediated in large part by their interconnections via the corpus callosum (Jones and Wise, 1977; Jenny, 1979; Gould et al., 1986; Kaas, 1995). Such interactions may play a particularly important role in ipsilateral hand motor control. Indeed, as stated earlier, when interhemispheric connections are severed the ipsilateral hemisphere can drive reaching with the ipsilateral arm to some extent but it cannot contribute to appropriate pre-shaping of the ipsilateral hand whatsoever (Brinkman and Kuypers, 1973). Based on neuroanatomical studies, the main interhemispheric connections of M1 and premotor cortex are with their homologues in the contralateral hemisphere (Rouiller et al., 1994; Marconi et al., 2003; Boussaoud et al., 2005; Dancause et al., 2007). For example, 45% of interhemispheric projections from the hand region of PMv are made to the contralateral PMv (Dancause et al., 2007). Interestingly, while the arm area of monkey M1 is callosally interconnected, the hand area of M1 appears to be mostly devoid of callosal terminals (Pandya and Vignolo, 1971; Zant and Strick, 1978; Jones et al., 1979; Gould et al., 1983). In contrast, the premotor cortex of one hemisphere is interconnected with the contralateral M1 hand area, although much less so than with the ipsilateral M1 (Muakkassa and Strick, 1979; Dancause et al., 2007). As such, ipsilateral motor and premotor cortex can influence contralateral M1 both via its direct connections, and indirectly via interactions with contralateral premotor areas that can then influence contralateral M1 activity and outputs. Some of these interhemispheric interactions are described below.

The primary motor cortex of one hemisphere has been shown to have both inhibitory and facilitatory effects on the activity and outputs of its homologue (Ferbert et al., 1992; Meyer et al., 1995; Hanajima et al., 2001). Most studies exploring these interactions have been performed in humans. For example, one study using transcranial magnetic stimulation (TMS) paired pulse

protocols in humans while simultaneously recording descending spinal volleys via an implant demonstrated that conditioning stimulation of M1 can reduce motor potentials produced by a test stimulus applied over the M1 of the other hemisphere (Di Lazzaro et al., 1999). This decreased spinal activity was associated with deceased electromyographic (EMG) activity evoked by the test stimulus. While this suggests that M1 can produce interhemispheric inhibition of its homologue, it has also been suggested that facilitation can occur. For example, the motor potentials evoked in a contralateral limb muscle by M1 TMS stimulation in humans become facilitated when subjects are asked to perform submaximal contractions of the homonymous muscle in the ipsilateral limb (Stedman et al., 1998; Tinazzi and Zanette, 1998; Muellbacher et al., 2000; Stinear et al., 2001). Facilitation versus inhibition of M1 by its homologue may depend on task requirements. For example, increased facilitation occurs as more complex patterns of finger movements are produced (Tinazzi and Zanette, 1998). In addition, whereas phasic, low-force movements are associated with greater inhibition between motor cortexes, tonic, high-force movements are associated with greater interhemispheric facilitation (Liepert et al., 2001). Finally, it has been reported that the extent of transcallosal inhibition depends on phases of movement preparation and execution. Whereas inhibition is reduced during movement preparation of fast movements, it becomes increased during motor execution (Tazoe and Perez, 2013). Taken together, while the modulation of M1 by its homologue can be complex and task dependent, such interactions play functionally relevant roles in motor control of unimanual movements.

The premotor cortex of one hemisphere can have complex modulatory effects on the M1 outputs of the opposite hemisphere. In the anesthetized monkey, modulatory effects of PMv on contralateral M1 outputs to the ipsilateral hand are more inhibitory than facilitatory (Quessy et al., 2016; Cote et al., 2017; Cote et al., 2020). During behavior in humans, PMv has a facilitatory effect on the outputs of the contralateral M1 during preparation and execution of ipsilateral hand movements. However, the PMv has an inhibitory effect on contralateral M1 outputs when the task requires that ipsilateral hand movement be suppressed (Buch et al., 2010). It has been suggested that inhibition of the contralateral M1 could help prevent mirror movements during the planning and execution of a unilateral movement (Mayston et al., 1999; Beaule et al., 2012). Taken together, modulation of contralateral M1 activity and outputs by premotor cortex appear to play important functional roles during unimanual movements.

3. Bihemispheric reorganization in the sensorimotor system following cortical injury

The distributed, bihemispheric nature of sensorimotor control can also be demonstrated by the changes in activity that occur following localized perturbations to this network at short and long timescales. At short timescales after a perturbation (minutes to hours), studies have highlighted that there are important changes in sensory processing that can occur in both hemispheres (Meyer et al., 1985; Sakatani et al., 1990; Clarey et al., 1996; Sigler et al., 2009; Ding et al., 2011; Mohajerani et al., 2011). On longer timescales of weeks to months, it is well-known that cortical damage to motor cortex, such as that often caused by stroke, induces a cortical plasticity that leads to important functional reorganization within the motor network as recovery occurs (Dancause, 2006; Nudo, 2006; Dancause, 2013). Together, these observations promote the concept that recovery requires the understanding of how signals are rerouting within a sensorimotor "connectome" that underlies sensorimotor control (Grefkes and Fink, 2014; Silasi and Murphy, 2014). Below, these different topics will be discussed in turn.

3.1 Rapid changes in information processing following localized perturbations

Studies that have explored the rapid reorganization that can occur following a cortical injury have focused on changes in cortical sensory processing. Hours or even minutes following unilateral inactivation or lesion of sensorimotor cortical areas in rodents, cats or primates, sensory processing becomes altered in both the lesioned and in the "intact" hemisphere (Meyer et al., 1985; Sakatani et al., 1990; Clarey et al., 1996; Mohajerani et al., 2011). In the ipsilesional hemisphere of rodents, as early as 30 min after a lesion, sensory-evoked responses that occur when touching locations on the paretic forelimb normally encoded by the lesioned area become concentrated instead within adjacent cortical areas, particularly the peri-infarct somatosensory and motor cortex (Sigler et al., 2009; Mohajerani et al., 2011). Furthermore, stimulation of the intact forelimb ipsilateral to the lesioned hemisphere produces enhanced sensory responses in peri-infarct somatosensory hindlimb representation, as well as motor and barrel cortex of the lesioned hemisphere (Mohajerani et al., 2011). Changes in sensory processing are also observed in the contralesional, intact hemisphere. For example, 30-50 minutes after acute stroke in the rodent enhanced contralesional sensory responses can be observed when stimulating either the paretic or non-paretic forelimb, in both evoked response amplitude and extent of cortical area

becoming active. These changes observed in the somatosensory system are suggested to reflect wide-scale bihemispheric circuit level rearrangements despite the absence of new structural connectivity, due to the short time frame within which they occur (Mohajerani et al., 2011). Furthermore, no such changes in evoked sensory responses were observed for stimulation of either hindlimb in either hemisphere, showing the changes were functionally dependent in the sense that they were specific to the type of effector targeted by the lesion. Thus, changes occurred specifically within circuits closely related to the lost function.

Similar changes in the processing of sensory responses following cortical injury have been observed in primates. For example, in monkeys the inactivation of primary somatosensory cortex of one hemisphere using cooling will induce the immediate expansion of somatosensory receptive fields in the other hemisphere as well as increases in the response amplitude of neurons to peripheral stimulation (Clarey et al., 1996). These changes may reflect an unmasking of latent functional connections, possibly by disinhibition of the intact hemisphere. Interestingly, after prolonged inactivation (50+ minutes), the receptive fields return to baseline, perhaps reflective of a homeostatic mechanism occurring within the network, as a response to the ongoing, altered pattern of activity (Clarey et al., 1996). Thus, it seems that the somatosensory network attempts to "re-balance" itself following a localized perturbation.

However, it is not known how these rapid changes extend to motor processing specifically. There are some indications that similar changes may occur in motor cortex, at least at a longer timescale of weeks to months after stroke, which is the subject of the next section. For example, it has been shown that the intact hemisphere of stroke patients finds itself with a lower threshold for producing movement when stimulated with TMS (Volz et al., 2015). In parallel, the motor output of the ipsilesional hemisphere is diminished (Escudero et al., 1998). As such, additional studies are required to explore how rapidly such effects take place and progress after cortical injury specifically in the motor network. Notably, an exploration of the neural changes that take place in motor areas of both hemispheres in the immediate aftermath of a cortical injury presents an important gap in the literature.

Nonetheless, there are indications that the motor system can respond very rapidly to perturbations in order to preserve and restore network integrity. In a study performed in the mouse that probed the robustness of neural representations about an upcoming tongue movement

in both hemispheres, preparatory activity in a given hemisphere was extremely robust to large-scale, transient unilateral silencing of that hemisphere using optogenetics (Li et al., 2016). The optogenetic silencing was applied during movement preparation and was used to abolish "ramp-up" neural activity associated with the upcoming movement. However, when the perturbation ended prior to movement onset, the neural dynamics associated with the upcoming movement were quickly and selectively restored in several hundred milliseconds. More precisely, neurons showed accelerated ramping after the end of photoinhibition such that their activity "caught up" to reach the same level of activity as they would have had at that time if they had been left unperturbed. Importantly, severing the corpus callosum prevented this process of recovery from occurring. In addition, no recovery was observed if bilateral silencing was performed. Thus, it appears that a callosal-mediated interhemispheric dialogue between "nodes" in each hemisphere that contain redundant but functionally relevant information about the upcoming movement underlies this process (Li et al., 2016).

3.2 Long-term reorganization of motor cortex following cortical injury

In contrast to the paucity of information available concerning rapid (minutes to hours) reorganization of motor cortex after injury, long-term motor reorganization has been the subject of many studies. Cortical damage to the motor cortex induces a long-term plasticity that leads to important functional reorganization within the motor network (Dancause, 2006; Nudo, 2006; Dancause, 2013). This plasticity can involve reorganization that is localized within the affected region, particularly with smaller lesions (Lashley, 1929, 1930); however, as the extent of damage becomes more widespread, the motor network recruits more and more distal regions that reorganize to support lost function. These regions, while not initially directly performing the function of the damaged region, can demonstrate an adaptive plasticity known as vicariation of function to "take on" the role once performed by the lesioned site (Munk, 1881; Ogden and Franz, 1917; Glees et al., 1950).

The most common source of strokes is middle cerebral artery occlusion, which often cause cortical lesions that include M1, and thus lead to devastating consequences for motor function. Indeed, in human studies, functional outcomes and motor function correlate with the extent to which corticospinal projections are disrupted (Pineiro et al., 2000; Zhu et al., 2010). In

particular, hand function is notoriously difficult to recover, as even patients with good recovery following stroke will often suffer from chronic motor deficits of the hand (Lai et al., 2002). It is therefore critical to understand the mechanisms that allow recovery of hand function following injury and the rules that subserve the plasticity of the motor network that accompanies it.

Importantly, this plasticity can include not just regions located in the affected hemisphere but also in the other, intact hemisphere. Below, the reorganization that can occur in the ipsilesional hemisphere following motor cortex lesions will be presented, followed by an overview of contralesional hemisphere reorganization. In addition, a brief portrayal of how these bihemispheric changes can be seen through the lens of a network "connectome" will be discussed.

3.2.1 Reorganization in the ipsilesional cortex

Ipsilesional motor areas can undergo extensive reorganization following unilateral damage to M1 that bear functional relevance to recovery. In monkeys with a small lesion to the M1 hand area, functional rehabilitation training of the affected limb can induce the cortical representation of the digits to expand into the intact, perilesional cortex initially containing shoulder and elbow representations (Nudo et al., 1996; Friel et al., 2007). Importantly, this plasticity is associated with the recovery of hand motor function, demonstrating that ipsilesional M1 can contribute to recovery (Nudo and Milliken, 1996; Nudo et al., 1996). Thus, with a small infarct, the surviving M1 tissue appears sufficient to support recovery. This mechanism of plasticity requires rehabilitative treatment, since without it, there is instead a reduction of digit representation, with sites evoking digit or wrist instead evoking shoulder or elbow movements (Nudo and Milliken, 1996).

However, with larger lesions of M1, the remaining perilesional M1 tissue is not sufficient to support functional recovery. As a consequence, more distal, but related, regions that were not initially subserving the function of the injured area are recruited to vicariously take over the lost function via adaptive plasticity mechanisms (Dancause, 2013). Importantly, premotor areas are well placed to take over lost M1 function, due to several key factors. In particular, as discussed in earlier sections, they are extensively interconnected with the rest of the motor network, they boast their own corticospinal projections, and they are already involved in motor-related computations. It is not surprising that human studies, while not discussed in detail here, have

reported changes associated with functional recovery occurring in CMA, SMA, PMd, and PMv *e.g.* (Loubinoux et al., 2003; Miyai et al., 2003; Fridman et al., 2004; Carey et al., 2005; Seitz et al., 2005; Carey et al., 2006). Below, several studies performed in monkeys will be presented, that have particularly highlighted the functional reorganization of PMv for recovery of hand motor control.

The ventral premotor cortex has been shown to undergo important functional reorganization following a unilateral lesion to the M1 hand representation area, as long as the lesion was sufficiently large (Frost et al., 2003). In a series of experiments, lesions of different sizes were performed in the region of M1 representing the distal forelimb. Monkeys then underwent three months of functional training using a Kluver board to improve their reach and grasp performance with the paretic hand. Following this recovery, intracortical microstimulation (ICMS) mapping revealed an up to 53.8% increase in the PMv cortical surface dedicated to the paretic hand, as compared to pre-lesion cortical maps. The extent of this increase was dependent on the size of the M1 lesion, such that larger lesions affecting at least 50% of the M1 distal forelimb area led to greater increases of hand cortical representation in PMv, whereas smaller lesions did not (Frost et al., 2003).

These changes in PMv cortical representation are accompanied by anatomical rewiring. Using anatomical tracers injected in PMv, it has been shown that axons that initially projected to M1 show abrupt changes in trajectory at the periphery where the M1 lesion starts, changing paths to now orient towards S1. As such, there is a substantial increase in PMv-S1 connections, particularly with area 1/2 (Dancause et al., 2005). Such an anatomical change could represent a bypassing of the lesion site in M1, possibly to reestablish the sensorimotor loop that normally involves M1 (Asanuma and Pavlides, 1997).

Finally, the role of the premotor cortex in recovery can also be seen in primate studies that inactivated different motor regions following post-lesion reorganization and functional training (Liu and Rouiller, 1999; Murata et al., 2015). For example, Liu and Rouiller (1999) explored the functional role of surviving premotor areas in monkeys trained on a precision-grip task that had undergone a permanent lesion of the hand representations of M1 and part of S1. Following recovery 9 months after the initial lesion, muscimol was injected into different motor areas of the ipsilesional hemisphere. They demonstrated that the combined inactivation of the

ipsilesional PMv and PMd reinstated deficits, whereas inactivation of each area in isolation did not, suggesting that either area by itself can take over part of the lost hand function (Liu and Rouiller, 1999). In another study, a focal lesion of the M1 hand digit area was performed using ibotenic acid in monkeys (Murata et al., 2015). They then performed daily postlesion motor training to induce functional recovery of hand movements including precision grip and used positron emission topography (PET) to image regional cerebral blood flow associated with this recovery. Interestingly, they observed that there was enhanced activity of the ipsilesional PMv during the early post-recovery period (1-2 months following lesion) that persisted during the late post-recovery period (>2months following lesion) and increased functional connectivity within perilesional M1 during the late post-recovery period. The causal roles of these areas in recovery at these different post-recovery periods were confirmed using muscimol. Specifically, inactivation of either ipsilesional M1 or PMv during the early or late post-recovery period led to a reinstatement of deficits. Thus, taken together, both the primary motor and premotor cortex appears to play a role in functional recovery, with PMv suggested to play a particularly important role during the early post-recovery period, and perilesional M1 reorganization contributing to functional recovery more intensely during the late post-recovery period (Murata et al., 2015).

3.2.2 Reorganization in the contralesional cortex

The contralesional hemisphere, while spared from direct damage, can display changes in activity and organization induced by a lesion of the other hemisphere (Buetefisch, 2015). For example, fMRI experiments performed in both rodents and human patients suggest that there is an increase in brain activity in the spared hemisphere as functional recovery occurs (Dijkhuizen et al., 2001; Weber et al., 2008; Rehme et al., 2011a). In monkeys, it has been shown using PET that the contralesional PMv will show increased activity during the early post-recovery period, which corresponded to 1-2 months after a unilateral M1 lesion (Murata et al., 2015).

In rodents, the extent to which the contralesional hemisphere can show changes in activity or reorganization are dependent on the size of the lesion (Kim and Jones, 2010; Touvykine et al., 2016), the severity of motor deficits (Dijkhuizen et al., 2003) and the rehabilitation treatment used (Allred et al., 2010; Jones and Jefferson, 2011). For example, using ICMS mapping in the rat it has been shown that larger unilateral lesions of M1 in one hemisphere can induce a greater expansion of distal limb representations in the contralateral

motor and premotor cortex (Kim and Jones, 2010; Touvykine et al., 2016). Complimentarily, in chronic stroke patients, there is a relationship between abnormally increased activity in contralesional M1 associated to the paretic hand and the extent of CS tract damage (Schaechter and Perdue, 2008).

There is some debate as to the extent to which these changes in activity and reorganization in the contralesional hemisphere may be beneficial or detrimental for the functional recovery of the paretic limb (Buetefisch, 2015). For example, it has been shown that while the contralesional M1 seems to support function in some patients after stroke (Lotze et al., 2006), it may interfere with recovery in others (Mansur et al., 2005; Fregni et al., 2006). Nonetheless, studies that have looked at corticomuscular coherence, which is the synchrony of the neural activity of cortical areas with muscle activity, in human patients with stroke or brain lesions have suggested increased contributions of the contralesional hemisphere to the muscular activity of the paretic hand after injury (Gerloff et al., 2006a; Rossiter et al., 2012). It has also been shown that there is an association between increased excitability of contralesional M1 and good recovery of hand function in patients during the subacute phase of strokes that affected M1 or its CS projections (Butefisch et al., 2003). Furthermore, recovery from motor deficits is associated with increased connectivity between the ipsilesional M1 and contralesional areas, as determined using fMRI in stroke patients (Wang et al., 2010; Eickhoff and Grefkes, 2011). In rodents having recovered from a large ischemic infarct, it has been shown that inhibiting the contralesional hemisphere leads to greater behavioral deficits of the paretic limb relative to what is observed when inhibition is performed in controls (Biernaskie et al., 2005).

Inactivation experiments in non-human primates have also been performed exploring the role of the contralesional hemisphere following recovery from lesions to M1 or the CS tract. However, results have been mixed. On the one hand, in a study where the CS tract from one hemisphere was mostly severed via a spinal lesion, inactivation of the contralesional M1 or PMv during early recovery led to impairments of paretic hand function (Nishimura et al., 2007). On the other hand, muscimol inactivation of contralesional M1 during the early (1-2 month) or late (>2 month) post-recovery period following a unilateral M1 lesion did not induce a change in behavioral performance on a precision grip task (Murata et al., 2015). Furthermore, the same study demonstrated that while there is increased activity in contralesional PMv during the early

post-recovery period following a unilateral M1 lesion, its inactivation with muscimol also did not affect performance on a precision grip task. Interestingly, there were differences between subjects during the late post-recovery period. While inactivation of contralesional PMv at this time point had no effect in one monkey, it did lead to decreased hand motor performance in a second monkey. In contrast to the unaffected primate, this latter monkey showed a continued increased activation of the contralesional PMv during late post-recovery (Murata et al., 2015). Nonetheless, 9 months after a unilateral lesion of M1 and S1 hand representational areas, the inactivation of the contralesional PMv and PMd did not reinstate deficits (Liu and Rouiller, 1999). These different results could be due to variations in lesion sizes or locations, as well as differences in how cortical reorganization occurred between subjects.

In addition, there may be an important temporal relevance to the contributions of the contralesional hemisphere to recovery following stroke. In cross-sectional studies of stroke patients during use of the paretic hand, it has been shown that there is an initial abnormal bilateral activation of motor areas in subacute stroke patients (Chollet et al., 1991; Weiller et al., 1992; Cramer et al., 1997; Cao et al., 1998; Johansen-Berg et al., 2002; Small et al., 2002; Ward et al., 2003b; Butefisch et al., 2005; Nair et al., 2007) that shifts towards a more normal unilateral activation pattern of ipsilesional motor regions in chronic stroke patients (Ward et al., 2003b). This activation shift, based on a longitudinal study of stroke patients, has been associated with good recovery (Ward et al., 2003b). In contrast, persistence of the abnormal bilateral activation pattern is not, instead being associated with poor functional outcome (Ward et al., 2003b). For example, patients with over-activity in the unaffected hemisphere that does not go away 6-12 months after stroke, in the chronic phase, demonstrate poor recovery. These are patients that often have substantial corticospinal damage (Ward, 2007). Overall, in stroke patients with good recovery the contralesional hemisphere appears to contribute to the degree of functional recovery (Gerloff et al., 2006b; Lotze et al., 2006; Braun et al., 2007), whereas in patients with poor functional recovery, the contralesional hemisphere appears to have a more detrimental role, possibly by losing what may be initially supportive effects (Grefkes et al., 2008; Rehme et al., 2011a). Thus, the role of the contralesional hemisphere in recovery is complex and remains to be fully elucidated.

3.2.3 A bihemispheric sensorimotor connectome

As outlined in the above sections, motor control involves a large and distributed network that includes numerous areas from both hemispheres. This bihemispheric network is not just involved in unimanual hand control, but also in functional recovery of dexterous hand movements after cortical damage. The interconnectedness of this network, and of the brain in general, has led several to refer to it as a "connectome".

Currently, there is a push to view recovery from lesions, such as stroke, in the lens of signals rerouting within the bihemispheric connectome (Grefkes and Fink, 2014; Silasi and Murphy, 2014). Within this paradigm, even small and localized perturbations can have widespread consequences over the whole connectome. In a study using connectivity data determined from resting-state fMRI scans in humans, where individuals are at rest ("resting-state") and no motor activity is being performed, the effects of a unilateral small virtual stroke (5% of area) when simulated could lead to network-wide bihemispheric effects (Alstott et al., 2009). Indeed, actual studies using longitudinal imaging techniques in both animals and humans show that the initial impact of brain injury is widespread, inducing profound changes across multiple areas in both hemispheres (Dijkhuizen et al., 2003; Rehme et al., 2012).

Furthermore, these effects tend to be focused specifically on related structures. In resting state fMRI experiments, it was shown that patients with lesions show cortical dysfunction that, while widespread, stays within the limits of existing interconnected networks that are functionally correlated with the lesion sites (Nomura et al., 2010). For example, patients that show motor impairments, but no visuospatial neglect, show abnormal connectivity in the motor system but normal connectivity in attention-related networks (Carter et al., 2010). This is reminiscent of the rapid changes in somatosensory processing discussed earlier that occur following cortical injury to forelimb representations, where alterations in evoked sensory responses were observed during forelimb, but not hindlimb, stimulation (Mohajerani et al., 2011).

Notably, as briefly mentioned earlier, good recovery is associated with a shift towards more normal functional connectivity in the affected network, and particularly with a refocusing of activity in the M1 of the ipsilesional hemisphere (Grefkes and Fink, 2014). For example, in rats or human patients recovering from stroke, resting-state measurements showed that while

initial behavioral deficits were correlated with decreased interhemispheric connectivity between sensory and motor regions of both hemispheres, subsequent functional recovery was associated with a return to normal of interhemispheric connectivity (Carter et al., 2010; van Meer et al., 2010). Indeed, as functional recovery progresses there is a steady increase of resting-state connectivity between contralesional areas and the ipsilesional M1 (Wang et al., 2010; Golestani et al., 2013).

Finally, and importantly, there is a relationship between early changes in activity and the extent of functional recovery. For example, magnetoencephalography (MEG) and fMRI studies in human patients have shown that initially higher connectivity estimates within the motor system in the acute or subacute phases of stroke is correlated with better functional recovery 3-6 months later (Park et al., 2011; Westlake et al., 2012). Furthermore, and importantly, the magnitude of early hemodynamic changes can be used to predict the extent of motor recovery that will occur (Marshall et al., 2009; Rehme et al., 2015; Hannanu et al., 2017). As such, the rapid, early changes observed in the sensorimotor connectome are informative of the direction that the long-term reorganization of the motor system will take and are therefore directly linked to the potential for and extent of recovery. Unfortunately, while a great deal of information about the connectivity of the brain and the roles of these different sensory and motor areas in recovery has been gleaned from the studies presented above, the rapid, early changes occurring in the activity of motor-related neurons of these areas remains unknown.

4. Muscimol as a tool to explore the central control of movement

The use of muscimol injections as a model of acute cortical injury has been well established (for review see Martin and Ghez 1999). As the use of muscimol forms a critical element of the current thesis, a concise overview centered on this topic is warranted. More specifically, we will provide a brief characterization of this drug, its mechanism of action, and how it has been used in the study of motor control.

4.1 Muscimol, a GABA-A receptor agonist

Muscimol, an analog of GABA, is a psychoactive drug obtained from the caps of Amanita muscaria mushrooms, widely used as a selective GABA-A receptor agonist (Michelot and Melendez-Howell, 2003; Johnston, 2014). GABA is the most widely distributed inhibitory neurotransmitter in the mammalian central nervous system (CNS), being released by up to 40% of neurons, and GABA-A receptors are responsible for the fast inhibitory synaptic transmission in the CNS (Seeburg et al., 1990; Bowery and Smart, 2006; Hinton and Johnston, 2018). When GABA released by the presynaptic neuron binds to the receptors at the postsynaptic site, the ion channel opens and chloride diffuses into the cell, thus hyperpolarizing the post-synaptic neuron.

Specifically, muscimol is a 3-hydroxyisoxazole bioisostere of the carboxylate of GABA. Muscimol has comparable potency to GABA, and is orthosteric, binding to the same active site on the GABA-A receptor complex as GABA itself (Johnston, 2014). It is inactive at GABA-B receptors and is a more potent partial agonist at GABA-C receptors. It is a weak inhibitor of GABA uptake and is not a substrate for GABA transaminase, the enzyme that breaks down GABA (Johnston, 2014). Only receptor bound, but not free, muscimol has physiological activity.

Muscimol is commonly injected into the nervous system in order to focally inactivate regions that contain neurons expressing GABA-A receptors, to study the induced behavioral and neuronal consequences of its use and thus infer brain function and neural interactions (Mink and Thach, 1991; Dias et al., 1995; Partsalis et al., 1995; Zhang et al., 1995; Kubota, 1996; Rouiller et al., 1998; Schieber and Poliakov, 1998; Brochier et al., 1999; Martin and Ghez, 1999; Waitzman et al., 2000; Baron et al., 2002; Stepniewska et al., 2014). When muscimol is locally injected in brain tissue, neural activity adjacent to the site of delivery becomes rapidly and totally

suppressed (Arikan et al., 2002; Edeline et al., 2002) with hypometabolism in the affected region (Martin, 1991). For example, following a 0.1 μL muscimol injection into the nucleus basalis magnocellularis of rodents, spontaneous activity of neurons 500 μm from the tip of the cannula used to deliver the drug falls to less than 20% of its initial value 2 min after muscimol injection. From 25 min onwards, and until the final timepoint of the experiment 2 h later, spontaneous activity was completely suppressed (Edeline et al., 2002). When injecting muscimol into rodent cortex or cerebellum, 1 μL causes a spread to a 1.5 to 2 mm radius total (Martin, 1991; Arikan et al., 2002). At .5-1.5 h after injection, neural discharge is completely suppressed in a roughly 2 mm diameter, with cellular activity being attenuated in an area roughly 4 mm in diameter (Arikan et al., 2002). This suppression can last for more than 5 h with graded, partial return of activity over time that progresses from the periphery of the attenuated area inwards. For example, at 4.5-5.5 h after inactivation, the areal extent where cellular activity is still at least weakly inhibited was roughly 1 mm in diameter (Arikan et al., 2002).

4.2 Muscimol as a model of primary motor cortex injury

The motor cortex provides a salient target for the use of muscimol as a model of acute cortical injury and its functional consequences. In M1, GABAergic signaling is ubiquitous, as it contains many neurons that are GABAergic as well as numerous neurons that strongly express GABA-A receptors as shown across a variety of animal models, such as rodents and primates, including humans (Houser et al., 1983; Lidow et al., 1989; Wisden et al., 1992; Petri et al., 2003). For example, in the rhesus macaque, the GABA synthesizing enzyme, glutamic acid decarboxylase (GAD), which can be used as a marker of GABAergic neurons, is markedly present throughout M1 (Houser et al., 1983). All GAD-positive neurons are non-pyramidal cells, and are found in all layers of motor cortex, often serving as inhibitory interneurons. GAD-positive putative axon terminals (puncta) are present throughout motor cortex, and can be found immediately adjacent to the somata, dendrites and initial axon segments of GAD-negative pyramidal cells, which includes corticospinal neurons (Houser et al., 1983). Indeed, M1 pyramidal cells are extremely receptive to GABA. For example, in healthy humans, mRNA histological analyses have shown that most pyramidal neurons in layers III and V (~80%) express mRNA associated with different subunits that make up the GABA-A receptors (Petri et al., 2003). Pyramidal cells are not unique

in their sensitivity to GABA; small and medium sized cells in the same layers also express such mRNA, albeit more moderately (~60%) (Petri et al., 2003). As such, the motor cortex is highly sensitive to muscimol-induced inactivation of its neural activity, with important consequences to motor function.

The behavioral consequences of M1 muscimol inactivation are comparable to those observed acutely after M1 permanent injury in monkeys. For example, during reach and grasp tasks, both inactivation and lesions to the M1 hand/arm area induce decreased movement speed and trajectory errors during reaches, and impaired dexterous hand control such as digit muscle weakness and a loss of independent finger movement during grasp (Matsumura et al., 1991; Hoffman and Strick, 1995; Kubota, 1996; Schieber and Poliakov, 1998; Brochier et al., 1999; Fogassi et al., 2001; Nudo et al., 2003; Hoogewoud et al., 2013). The behavioral effects of muscimol inactivation can last as long as 24 h, peaking at roughly 1 h post injection and then regressing with time (Martin and Ghez, 1993; Collins et al., 2005). Overall, there is a consensus that muscimol is an effective tool to study the acute effects of brain injury.

Finally, there are several advantages to using muscimol relative to other approaches in the study of motor control and the functional consequences of acute focal M1 injury. For example, an important advantage of muscimol is its specificity, as it only inactivates local neurons, unlike blockers of sodium channels (e.g. tetrodoxin) or local anesthetics (e.g. lidocaine) which additionally prevent the occurrence of action potentials from fibers of passage (Hilles, 1966, 1977; Ritchie, 1979). There are important differences between using a reversible drug like muscimol versus actual brain injury. Normally, brain injury is accompanied by a host of consequences that extend beyond a mere perturbation of healthy neuronal network dynamics. For example, stroke doesn't just disrupt descending motor commands due to a loss of cortical/subcortical inputs to muscles, but also leads to other processes such as inflammation, which has its own cascade of consequences (Block et al., 2005; Muir et al., 2007). Furthermore, it can also induce damage to other brain regions that have synaptic connections with the primary lesion location but were not directly affected by the injury. For example, following a medial cerebral artery occlusion, there is secondary neural death, gliosis, and axonal degeneration in spared regions that are not normally irrigated by the medial cerebral artery, such as the thalamus, substantia nigra, and distal pyramidal tract (Forno, 1983; Ogawa et al., 1997; Schmitt et al.,

1998; Schmitt et al., 2000; Buss et al., 2004; Buss et al., 2005). As such, muscimol is a powerful tool to study motor control as it allows elucidating the precise role of the inactivated tissue and the neuronal dynamics of the circuitry that it is part of while limiting confounds that can arise.

5. Thesis research question and objectives

Previously, direct in-vivo recordings that have explored the rapid neuronal reorganization that occurs after brain lesions have been limited to somatosensory cortex. As presented above, these studies were conducted in sedated animals and using externally applied passive stimulation. In parallel, much work has been done using non-invasive imaging methods to probe bihemispheric sensorimotor reorganization following brain injury. These studies relied on indirect measures such as changes in hemodynamic activity, and therefore are unable to apprise of the actual neural changes that are taking place. Thus, while informative, these direct and indirect studies have left us with a very limited understanding of how brain injury specifically affects neural activity related to the generation of impaired hand movements, particularly at very short time scales. Notably, such early changes in neuronal activity can affect reorganization during the subacute phase of a cortical injury such as stroke, with important consequences for recovery.

The work in this thesis addresses the general question of how neural activity in the distributed motor network of both hemispheres rapidly reorganizes following a localized, unilateral and reversible cortical injury in the non-human primate. To do so, we take the approach of quantifying the short-term, rapid changes which occur in neurons of motor-related areas of both hemispheres in the immediate aftermath of the suppression of one area, namely the M1 hand representation area, during performance on a functional reach and grasp task. We focused in particular on neural changes taking place during grasping, as the most pronounced deficits are expected to occur during use of the hand. The results of these experiments are divided into two chapters.

In **chapter 2**, we set out to quantify the rapid reorganization of neural activity in the ipsilesional and contralesional PMv, two areas that have been shown to be heavily implicated in the control of grasping and in recovery of dexterous hand movements following M1 lesions.

In **chapter 3**, we quantified the rapid reorganization of the contralesional M1, which has a complex role in recovery of dexterous hand movements following injury to its homologue. In addition, comparisons of the extent of reorganization taking place in M1 and the premotor areas studied in chapter 2 were performed.

Chapter 2 - Rapid and Bihemispheric Reorganization of Neuronal Activity in Premotor Cortex after Brain Injury

Ian Moreau-Debord[1], Eléonore Serrano[1], Stephan Quessy[1], and Numa Dancause[1,2]

[1]Département de Neurosciences, Faculté de Médecine, Université de Montréal, Montréal, Canada

[2]Centre interdisciplinaire de recherche sur le cerveau et l'apprentissage (CIRCA), Université de Montréal, Montréal, Canada

Published in *Journal of Neuroscience*, 41(44):9112-9128, Nov 3, 2021.
DOI: 10.1523/JNEUROSCI.0196-21.2021

Abstract

Brain injuries cause hemodynamic changes in several distant, spared areas from the lesion. Our objective was to better understand the neuronal correlates of this reorganization in awake, behaving female monkeys. We used reversible inactivation techniques to “injure” the primary motor cortex, while continuously recording neuronal activity of the ventral premotor cortex in the two hemispheres, before and after the onset of behavioral impairments. Inactivation rapidly induced profound alterations of neuronal discharges that were heterogeneous within each and across the two hemispheres, occurred during movements of either the affected or nonaffected arm, and varied during different phases of grasping. Our results support that extensive, and much more complex than expected, neuronal reorganization takes place in spared areas of the bihemispheric cortical network involved in the control of hand movements. This broad pattern of reorganization offers potential targets that should be considered for the development of neuromodulation protocols applied early after brain injury.

Introduction

Moving the hand to grasp an object is associated with modulation of neuronal activity in several cortical areas, including the primary motor cortex (M1) (Schieber and Hibbard, 1993; Kakei et al., 1999) and premotor areas (Tanji et al., 1987, 1988; Cisek et al., 2003; Nakayama et al., 2015). Interestingly, the cortical network supporting unimanual movements extends to both hemispheres, also involving premotor areas and even M1 ipsilateral to the hand (Donchin et al., 1998; Ames and Churchland, 2019; Heming et al., 2019). In the ventral premotor cortex (PMv), for example, many neurons show little selectivity to the hand used, but are rather coding for the location of the target, its shape, or the configuration of the hand to grasp that target (Tanji et al., 1988; Rizzolatti and Luppino, 2001; Michaels and Scherberger, 2018). Although the ipsilateral hemisphere is not specifically driving the production of corticospinal outputs (Soteropoulos et al., 2011; Li et al., 2015), at least some components of the control of unimanual hand movements involve widespread coordination of neural activity across several cortical areas, in the two hemispheres. In this distributed framework, dysfunction or injury in one region is expected to have far-reaching impacts across multiple areas of the ipsilesional and contralesional hemispheres (Grefkes and Fink, 2014; Silasi and Murphy, 2014).

Not surprisingly, there is extensive support that lesions in the brain cause bihemispheric reorganization. However, most studies have used noninvasive imaging methods based on indirect metabolic measures (Ward, 2015; Crofts et al., 2020). To date, direct *in vivo* recording of the impact of brain injury on neuronal activity has revealed that cortical inactivation or lesion profoundly alters processing of sensory information in the two hemispheres (Meyer et al., 1985; Takatsuru et al., 2009; Sweetnam and Brown, 2013; Kokinovic and Medini, 2018), even within minutes after injury (Sakatani et al., 1990; Ding et al., 2011; Mohajerani et al., 2011). Such rapid neuronal changes can be viewed as consequences of the lesion on the network's homeostasis (von Monakow, 1914; Carrera and Tononi, 2014), with a questionable active involvement in motor function at this stage. They are, however, precursors that form the landscape on which subacute plasticity later takes place and, as such, are likely to have profound effects on recovery after brain injury.

Previous studies on rapid neuronal reorganization after brain lesions have been essentially limited to the sensory cortex, conducted in sedated animal preparations, and using

passive stimulation. They have left us with a limited understanding of the early consequences of brain injury on neuronal activity associated with the generation of impaired hand movements. This knowledge is particularly timely and could have a far reaching impact, now that noninvasive neuromodulatory approaches, such as transcranial magnetic stimulation (TMS), are being used to favor motor recovery after brain damage (Grefkes and Fink, 2014). Current stimulation strategies are largely based on concepts of network connectivity and interactions. Stimulations are often used to alter the excitability of areas spared by the injury to remotely help reestablish the functional state across the network involved in the generation of movements. The refinement of the hypotheses underlying the development of these treatments would thus greatly gain from a better understanding of the impact of brain injury on neuronal activity across the motor network.

To address some of these issues, we investigated neuronal reorganization associated with the loss of fine control of hand movements in adult macaque monkeys. Motor deficits were induced using reversible inactivation techniques in the hand representation of M1 while continuously recording before and after cortical injury. This allowed us to identify changes in individual neurons in a highly sensitive and powerful way. In the present report, we focused on recordings in PMv, an area known to undergo physiological and anatomic reorganization after brain lesions that cause impairments of hand movements (Dancause et al., 2005; Dancause et al., 2006b; Murata et al., 2015; Yamamoto et al., 2019).

Materials and Methods

Experimental model and subject details

Two adult female rhesus macaques (*Macaca mulatta*), Monkey M (5.5 kg) and Monkey S (5.7 kg), were used in the present study. All surgical and experimental procedures were performed in accordance with the guidelines set forth by the Canadian Council on Animal Care and were approved by Comité de Déontologie de l'Expérimentation sur les Animaux of the Université de Montréal.

Surgical procedures

Surgical procedures were conducted under sterile conditions. Anesthesia was induced with ketamine hydrochloride (15 mg/kg; Ketaset; Pfizer) and maintained with ~2%-3% isoflurane (Furane; Baxter) in 100% oxygen. Monkeys were given atropine (atropine sulfide; 0.04 mg/kg; Rafter 8 Products) and dexamethasone 2 (Dexacort 2, 0.5 mg/kg; Rafter 8 Products) as well as an intravenous injection of mannitol 20% (1500 mg/kg; Fresenius Kabi Canada) to prevent inflammation and swelling of the brain. Lactated Ringer's solution was injected continuously to maintain hydration (10 ml/kg/h, i.v.). Body temperature was kept near 36.5°C with a self-regulating heating blanket (Harvard Apparatus), and blood oxygen saturation and heart rate were monitored throughout the procedures.

Muscles were intramuscularly implanted with insulated, multistranded microwires (Cooner Wire) for recording of EMG signals. Each microwire was tunneled subcutaneously from the target muscle to a connector embedded in bone cement on the top of the head. Accurate placement of the EMG wires was tested by electrical stimulation of the muscles with the implanted wires and observation of the evoked movements, both during the surgery and in later sessions in the awake state, while the monkey was sitting quietly. We implanted the deltoideus, biceps brachii, brachioradialis, palmaris longus, flexor carpi ulnaris, flexor carpi radialis, flexor digit communis, extensor carpi ulnaris, extensor carpi radialis, extensor digit communis, first dorsal interosseus, adductor of the thumb, and abductor of the thumb. Only channels with clear EMG signals for all selected recording sessions were kept for analysis (see Figure 2.3). In the

present set of analyses, the EMG signals were used primarily to control for the appearance of covert movements after inactivation.

Craniotomies and durectomies were performed to expose M1 and the lateral premotor cortex in both hemispheres. Multielectrode arrays were implanted in the left PMv and dorsal premotor cortex (PMd) and the right PMv, PMd, the M1, and primary somatosensory cortex (S1) (see Figure 2.1 B). In the left hemisphere, the dura was left intact over the central sulcus and a chronic chamber (2 × 2 cm opening; Plexiglas) was positioned to provide access to the dura over the M1 hand representation. The chamber was used to perform muscimol inactivation (see next section) in the left hemisphere, which we refer to as the "ipsilesional" hemisphere. Consequently, the right hemisphere was opposite to the lesion, and referred to as the "contralesional" hemisphere in both monkeys. With this configuration, the right hand was the affected or "paretic" hand.

The placement of the arrays was guided by anatomic landmarks, including the arcuate and central sulcus. In Monkey M, 370 electrodes were implanted. In the ipsilesional hemisphere, one 96-electrodes Utah array (Blackrock Microsystems) was placed in PMd (ipsilesional PMd [iPMd]), and one 32-electrodes and one 16-electrodes floating microprobe array (FMA; Microprobes for Life Science) were placed in PMv (ipsilesional PMv [iPMv]). In the contralesional hemisphere, one 96-electrodes Utah array was placed in M1 (contralesional M1 [cM1]), as well as four 32-electrodes FMAs, two each in PMv and PMd (contralesional PMv and PMd; cPMv and cPMd, respectively). In Monkey S, a total of 448 electrodes were implanted. In the ipsilesional hemisphere, one 96-electrodes Utah array was placed in iPMv, and two 32-electrodes FMAs were placed in iPMd. In the contralesional hemisphere, two 96-electrodes Utah arrays were placed, one in cM1 and one in cPMv, and two 32-electrodes FMAs were placed in cPMd and one in S1. Signals from arrays implanted in iPMv and cPMv were used for the present set of analyses.

At the end of each surgery, monkeys were given Baytril (5 mg/kg; enrofloxacin, Bayer) to protect against infection, another injection of dexamethasone 2 (0.5 mg/kg; Dexacort 2, Rafter 8 Products) to prevent brain swelling, as well as carprofen (4 mg/kg; Rimadyl, Zoetis Canada) and buprenorphine (5 µg/kg; Temgesic, Schering-Plough) to prevent inflammation and pain,

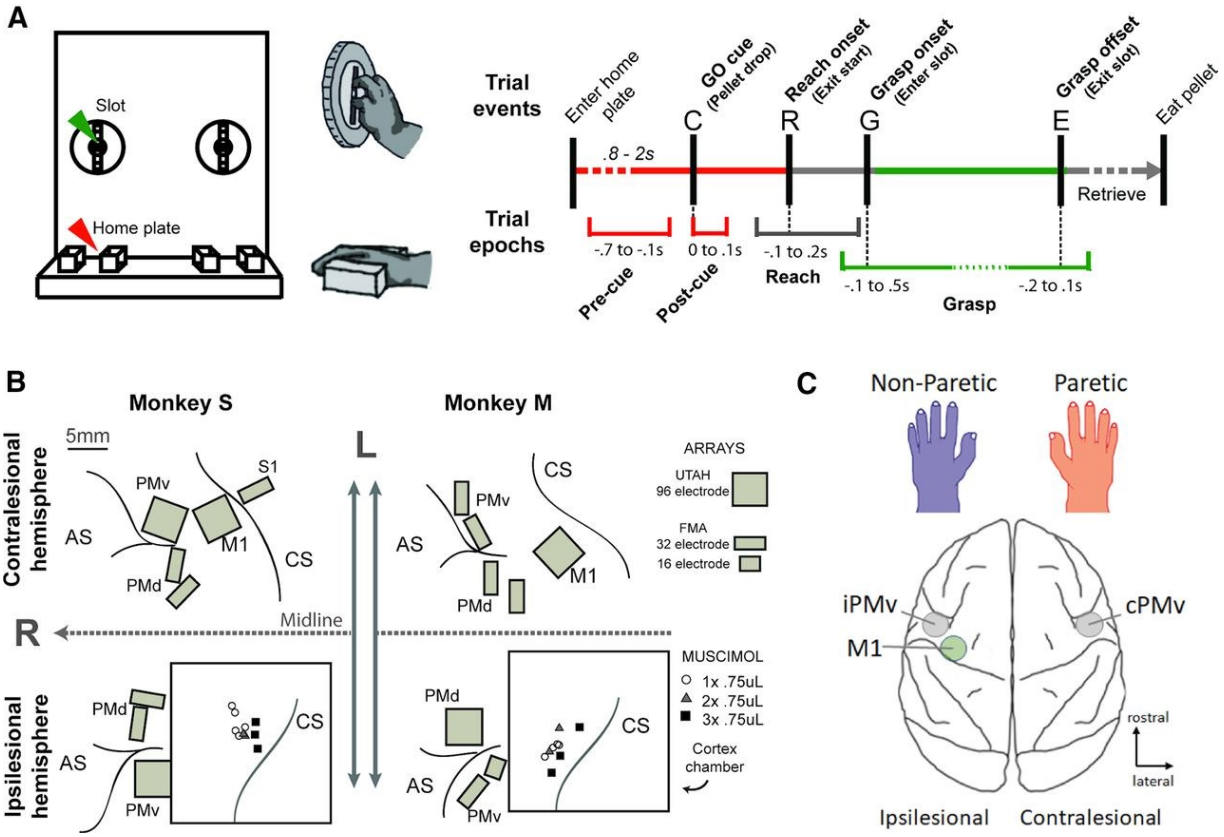

Figure 2.1. *Experimental design*

A, Illustration of the task (left). To initiate trials, the monkey placed the hand in the home plate (red arrowhead; bottom right inset). After a variable delay, a pellet was delivered in a distribution slot (green arrowhead) containing a food well (top right inset). Trial events and epochs (right). The home plates and slots were equipped with infrared LED sensors that reported trial events used to define trial epochs for neuronal analyses (see Materials and Methods). ***B***, Reconstruction of the location of the electrode arrays in the 2 monkeys relative to the sulci and the location of the chamber (black square). The muscimol injection sites for the different experiments are shown in the chamber. AS, Arcuate sulcus; CS, central sulcus; L, lateral; R, rostral. ***C***, Schematic representation of iPMv and cPMv, and the paretic and non-paretic hands in relation to the location of the inactivation, which was always in the left M1.

respectively. Additional doses of Baytril and Carprofen were given for 2 d after the surgery or longer, following the recommendations of the veterinarian.

Behavioral task

The monkeys were brought to the laboratory to conduct the neuronal recording sessions. They sat in a custom-made primate chair placed in front of a pellet retrieval task (see Figure 2.1 A, top). The chair had an opening in front of the mouth and removable panels on both sides to allow the use of one hand or the other in different blocks of trials. The pellet rewards (190 mg Dustless Precision Pellets; BioServ) were delivered in a target consisting of a well behind a vertical slot (1.3 cm × 5.5 cm) that was positioned ~10 cm below the shoulder height and 20 cm from the monkeys. To get the rewards, the animals had to reach with either the left or the right hand and use a precision grip (opposition of the thumb and index) with the forearm pronated. Video recordings of the behavioral task were collected using two computer webcams placed above and on the left side of the animal. The task was controlled by a Tucker-Davis Technologies acquisition system using two RZ2 BioAmp processors and custom software designed for this experiment.

The hand used was determined by which side panel on the chair was removed. Each trial began when the animal placed the hand on the home plate located in front of them, 15 cm below the target. The home plate contained an infrared laser sensor, which detected the presence of the hand. Trial progression is shown in Figure 2.1 A (right). After a variable delay period (0.8-2 s), a pellet was delivered into the well by a pellet distributor (80209 Pellet Dispenser, Campden Instrument). The clicking sound associated with the pellet delivery served as GO cue. The animal then had 2 s to perform a self-paced reach toward the target. The movement of the hand out of the home plate was signaled by the sensor and marked the onset of reach. The animal entered the target to grasp the pellet. A second infrared laser placed in the slot containing the food well signaled the hand entering and leaving the target, which were used to mark the onset and offset of grasp. After grasp, the monkey brought the pellet to its mouth, before placing its hand back in the start position to initiate the next trial. The intertrial interval was 3 s.

In each recording session, the monkeys performed 25 trials with the left hand and then 25 trials with the right hand. In inactivation experiments (see below), additional recording sessions were conducted to collect blocks of trials at different time points after the inactivation, always in the same order. Each recording session took ∼10 min to perform.

EMG recording and analysis

The EMG signals were recorded using a Tucker-Davis Technologies acquisition system. The continuously recorded raw EMG signals were sampled at 4.069 kHz, and separated into individual trials using a custom-built software, before being further analyzed using custom code written in MATLAB (The MathWorks). For each recording session, we took a rectified mean of the activity across a block of trials during use of a given hand, aligned on different task epochs (see below for epoch descriptions). The mean EMG signals were then low-pass filtered at 50 Hz using a second-order Butterworth filter.

To quantify potential changes of EMG after inactivation, we normalized the mean rectified and filtered activity for each muscle using the 500 ms period before the onset of movements for a given block of trials (from −0.6 to −0.1 s from reach onset). The area under the curve of the mean and rectified EMG trace was extracted with data aligned on grasp onset (−0.1 to 0.5 s from event), and on grasp offset (−0.2 to 0.1 s from event). Values of all muscles in one arm for a given block of trials were averaged (e.g., with non-paretic arm, Pre-inactivation). Two paired *t* tests were used to compare the Pre-inactivation to the Post-inactivation blocks of trials: one test with data aligned to grasp onset and the other with data aligned to grasp offset. This was done for EMG data in both the moving and the resting arm. Recordings from all inactivation experiments were included in these analyses (see below).

Muscimol inactivation experimental procedures

In the first two recording sessions after the implantation of cortical arrays and chamber, we confirmed the location of the hand representation in left M1 with intracortical microstimulation trains. A custom-made borosilicate glass-coated tungsten electrode was lowered within the

chamber, perpendicular to the dura, while the animal was sitting quietly. Trains were delivered at 1 Hz, and each train consisted of 13 monophasic cathodal pulses of 0.2 ms at 350 Hz (Dancause et al., 2008). We included in the hand representation all cortical sites from which digit, wrist, or forelimb (i.e., pronation/supination) movements were evoked and located its borders. At the rostral and medial borders, proximal movements were evoked (i.e., elbow or shoulder). At the lateral border, movements of the face were evoked (e.g., lip, tongue, or pinna). The caudal border was located deep in the central sulcus, at cortical sites that did not evoke movement with low stimulation intensity (i.e., ≤ 30 µA). For cortical sites within the hand area, we identified the depth at which the lowest stimulus intensity was required to evoke a movement. These sites and depths were used to guide the muscimol injections.

A total of 13 inactivation experiments were included in the present analyses. Six of these experiments were conducted in Monkey M, and 7 in Monkey S. For most experiments ($n = 9$, 4 from Monkey M, 5 from Monkey S), we did one injection of 0.75 µl of the GABA-A receptor agonist muscimol (5 mg/ml) in the hand area of the left hemisphere. In each monkey, we also included one additional experiment in which we injected muscimol at two sites (2 × 0.75 µl) and one other experiment in which we injected muscimol at three sites (3 × 0.75 µl) in the hand area (see Figure 2.1 B).

For each inactivation experiment, we first recorded baseline behavioral performance and neural data in a "Pre-inactivation" data collection session. Animals performed a block of trials ($n = 25$) with the left hand followed by a block with the right hand. Then, the M1 hand representation was reversibly inactivated with muscimol, delivered with a 5 µl Hamilton syringe with a beveled 26-gauge needle (Hamilton). The syringe was positioned in the brain using a micromanipulator (David Kopf Instruments) with stereotaxic frame mounted to the primate chair. At each targeted cortical site, 0.75 µl of muscimol was injected at a rate of 4 nl/s with a microinjector (Harvard Apparatus) at different depths adjusted based on intracortical microstimulation data (range ~4.5-7 mm from top of the dura). Thirty minutes after the injection of muscimol, the animal was required to perform two more blocks of trials ($n = 25$ trials), first with the left hand and then with the right hand, in a second recording session (Post 0.5 h). The animals showed some clear deficits (see Results) while still being able to perform some trials successfully. Notably, neural activity was recorded continuously throughout the Pre-inactivation

session, the injection of the muscimol, and the Post 0.5 h session. After the Post 0.5 h recording session, the monkeys were returned to the home cage, where they could move freely and have unlimited access to water.

To follow the progression and extent of motor deficits, monkeys were brought back to the laboratory to record additional sessions 3 h (Post 3 h) and 10 h (Post 10 h) after the inactivation. At Post 3 h after inactivation, the impairments had progressed to the point that monkeys were not able to perform the task with the paretic hand (see Results). To evaluate behavior, the experimenter presented food morsels in front of the monkey with large forceps held vertically, which led the monkeys to attempt reaches and grasping with the forearm in pronation. Deficits were milder at Post 10 h and no longer visible on the following day, confirming the transitory effect of the pharmacological manipulation. We always had a minimum of 72 h between subsequent inactivation experiments.

Neural recordings and identification of neurons

We focused the present neuronal analyses on Pre-inactivation and Post 0.5 h recording sessions for two main reasons. First, at this time point, the monkeys were still able to successfully perform the task, at least in some trials. This allowed us to compare the neuronal activity in a similar behavioral context, before and after the inactivation. Second, since neuronal activity was recorded continuously from Pre-inactivation to Post 0.5 h, this allowed us to unequivocally follow individual neurons throughout these sessions and to perform "within-neuron" analyses (see below), in which we quantified the changes of activity caused by the inactivation in the discharge pattern of clearly isolated and continuously recorded neurons. To increase the number of neurons in the control condition, we included sessions in which the monkey performed the task, but no inactivation was induced (i.e., Unmanipulated sessions).

We simultaneously recorded neural activity from 256 channels, the maximum possible count with our equipment. In different experiments, we alternated the areas/arrays we focused on. Recordings included in the present analyses are from sessions that prioritized recordings from the arrays implanted in PMv. Neuronal data were sampled at 24,414.1 Hz, bandpass filtered between 100 and 5000 Hz, and recorded digitally using a Tucker-Davis Technologies acquisition

system. An automatic threshold (×4 SDs above the baseline noise) was used on all channels that was locked in place for the duration of the recording. When this threshold was crossed, a 1228 μs sample was recorded. These suprathreshold waveforms were sorted offline using principal component analyses in Plexon Offline Sorter (Plexon). Waveforms from a given unit were categorized as "well-isolated" when the waveform cluster was clearly separated from other recorded signals using the first three principal components. Only well-isolated units were included in the current analyses. Then, we verified the stability and isolation of the principal components of each unit for the entire time of recording by plotting the first 2 principal components over time. For the within-neuron analyses (see below), we discarded any unit that completely disappeared or appeared after inactivation or for which the PC1-PC2 cluster isolation in relation to other signals was lost at any point during recording. Thus, although some neurons in these analyses had very few spikes during reaching and grasping in post-inactivation trials (e.g., see Figure 2.5 F), they were sufficiently active during intertrial intervals or between blocks of trials to follow their isolation from the beginning to the end of recording. It should be noted that this approach could have resulted in the removal of neurons that truly shut off or started discharging after inactivation and consequently to an underestimation of the number of neurons with lower or higher firing rate after the inactivation. However, we preferred this potential underestimation to an overestimation of the impact of inactivation. Initial sorting was done by one experimenter (I.M.-D.) and the quality of the isolation of sorted waveforms confirmed by a second (S.Q.). After sorting, we confirmed that units had no refractory period violation (0%) using an interspike interval of ≤1 ms, before and after inactivation.

We ensured that most neurons included in the study were sampled only once in iPMv (66 of 94; 70.2%) and in cPMv (103 of 138; 74.6%) for within-neuron analyses. For this subpopulation, only signals from a single inactivation experiment were selected for any given electrode (i.e., 0% chance of double sampling). We verified that all analyses using "within-neuron" data gave similar results with this subpopulation of neurons. However, because muscimol could potentially affect the activity of a given neuron differently (e.g., depending on the specific location of the injection in relation to the hand representation or the level and nature of impairment it caused), we considered each inactivation experiment as an independent sampling. We thus included signals from more than a single recording session for some of the electrodes in iPMv and cPMv in the total population of neurons (see Results).

Task epoch modulation of individual neurons

To give an appreciation of the discharge pattern of the total population of neurons, we produced heat plots of discharge rates in relation to the onset of grasp (see Figure 2.4 A,B). In these plots, for each neuron the spike density estimate (SDE) of spike discharge at each moment in time was divided by the average SDE across the time window of interest (−1 to 1 s around Grasp Onset) to highlight when neurons had their peak discharge. To characterize if neurons were modulated during one or several epochs of the task, we compared the average firing during the pre-cue epoch (0.7 to −0.1 s before the Go cue), which served as a baseline of neural activity, to the firing rate during other epochs of the task using two-tailed *t* tests. The different epochs of interest, in chronological order, were pre-cue, post-cue, reach, and grasp. The post-cue epoch was the first 0.1 s following the GO cue, and the reach epoch ranged from −0.1 to 0.2 s from Reach Onset, when the monkey's hand left the home plate. The current set of analyses mostly focused on the grasp epoch, which ranged from −0.1 s before the fingers entered the slot (Grasp Onset) to 0.1 s after the fingers had left the slot with the pellet (Grasp Offset). Since the grasp epoch encompasses both the Grasp Onset and Grasp Offset events, the *t* test was performed on spike times aligned on each event separately for some analyses. The two windows of time used were −0.1 to 0.5 s from Grasp Onset and −0.2 to 0.1 s from Grasp Offset. A neuron whose firing rate was modulated according to the *t* test ($p < 0.05$) within either of these windows was considered tuned to grasp during that block of trials. To visualize the modulation of individual neurons during the task, in addition to raster plots, we calculated SDEs of the firing rate across trials for each neuron (Nawrot et al., 1999), with spike times aligned at Grasp Onset (see Figure 2.5). The SDEs were performed using a Gaussian kernel function with a kernel of 50 ms.

Effect of inactivation on the total population of recorded neurons

To explore changes in the general discharge of neurons when the animals were at rest, we looked at the firing rate of control and Post 0.5 h PMv neurons during the pre-cue epoch (−0.7 to −0.1 s from cue) when the animal waited with either hand in the start position. For each neuron, we determined the mean firing rate during the pre-cue epoch for each block of trials (right or left

arm, pre or post 0.5 h inactivation). We compared the proportion of neurons modulated during grasp (i.e., identified with the two-tailed *t* test; see above) before and after inactivation (see Figure 2.6 A,B) and the proportion of neurons modulated in function of the hand used (see Figure 2.6 C,D). All available control and Post 0.5 h neurons were used for these comparisons. When performing these analyses, "control" always included PMv neurons from both hemispheres pooled together, using their activity during ipsilateral or contralateral hand movements, as appropriate. For other analyses, we only used neurons that remained clearly isolated throughout the inactivation experiments, both before (Pre) and Post 0.5 h after inactivation ("within-neuron"; see below).

Quantification of changes within continuously recorded neurons before and after inactivation ("within-neuron" analyses)

To take into account differences in grasp duration within a given trial block, but also following inactivation, we normalized the duration of grasp for our "within-neuron" analyses (see Figures 2.7–2.11). The SDE of each trial was resampled, attributing a value of "0" at the time of Grasp Onset and "100" at the time of Grasp Offset, such that time is visually represented as percentage (%) of grasp completed. In this normalized time, each time bin represents 1/1000th (0.1%) of grasp duration. The mean trial SDE during the pre-cue epoch for a block of trials served as a baseline, which was then subtracted from the resampled SDE curves.

Incidence of neurons with increases and decreases of discharge rate during grasp

We were first interested in determining how many neurons increased or decreased activity during grasp following inactivation (see Figure 2.7). For each neuron, and at each moment in normalized time, we determined whether there was an increase or decrease of neural discharge following the inactivation by subtracting the Post-inactivation SDE values from the Pre-inactivation SDE values at that moment in time. We also performed unpaired *t* tests on the SDE values obtained in trials performed before and after inactivation. This provided counts of neurons whose discharge increased or decreased at each moment during grasp and for how many neurons these changes were substantial (i.e., "significant" change reported by the *t* test). Furthermore, to provide an alternative quantification of increases or decreases of neural activity throughout

grasp, we calculated cumulative sums of neurons with higher and lower firing rates after inactivation at each moment in time according to the following formula:

$$Cumulative\ sum = \sum_{i=1}^{n} \frac{Neurons\ higher(i) - Neurons\ lower(i)}{Total\ neurons\ x\ 1200} x\ 100$$

Where *i* is the time bin ranging from 1 to the total number of time bins per trial considered for this analysis, *n* = 1200 (1000 bins for grasp duration, plus the last 100 bins before grasp onset, and the first 100 bins after grasp offset). *Total neurons* represent the number of neurons included in the population, which could either have higher (*Neurons higher*) or lower (*Neurons lower*) firing rates after inactivation compared with Pre-inactivation values, at time *i*, regardless of whether changes were significant or not. Accordingly, values are expressed as a percentage of the maximum sum of neurons with increase possible (i.e., if only increases would occur across the population throughout grasp). Positive values report that the proportion of neurons with higher activity surpassed the proportion of neurons with lower activity as grasping progressed. This reflects an increase of activity in the neuronal population after inactivation. Negative values report that a greater proportion of neurons with lower activity cumulated along grasp and reflects that the neural population became less active after inactivation. To better visualize the effect of the inactivation on the cumulative traces compared with chance, we used Monte Carlo methods. For each neuron, the firing rate at each time bin in the Pre- and Post-inactivation blocks of trials was pooled. Two new artificial SDE traces were generated by randomly selecting data points from this pool of bin values, with replacement. Then, we subtracted the two artificial SDE traces to calculate the increase or decrease of firing rate at each time bin. The same procedure was done for all neurons in a hemisphere and for a block of trials (e.g., iPMv, nonparetic hand trials) and the cumulative sum of this population was calculated. This process was repeated 1000 times. The mean and 95th percentile from all these artificial traces are shown in relation to real values in Figure 2.7.

Changes of peak discharge time and burst rate

For both the peak discharge time (see Figures 2.8 and 2.9) and rate (see Figures 2.10 and 2.11), we wanted to investigate further the changes of activity in neurons that specifically had a burst of activity during grasp (in contrast to neurons modulated according to the *t* test). Because of the

time devoted to each epoch, the *t* test is insensitive to neurons with either low spiking rate or with discharge burst of short duration. Therefore, for these analyses, we opted to include neurons that had a maximal discharge value >1 SD from baseline (i.e., pre-cue epoch) in the grasp epoch of the normalized SDE curves, either before or after inactivation. For each neuron with such a burst during grasp, we identified the time of maximal discharge rate during grasp before and after inactivation (see Figure 2.8 C,D) and quantified the change by subtracting the two values (see Figure 2.9 B).

For the analyses of burst rate, since neurons could have peaks at different moments during the grasp epoch before and after inactivation, we characterized the amplitude and time of the peak in both recording sessions, when present. For each neuron, we compared the firing rate at the time of the peak for pre-inactivation (i.e., Pre Peak; see, e.g., Figure 2.10 A) to the firing rate at the same moment in normalized time in Post 0.5 h and averaged the changes across the population of neurons. This approach highlights the change of activity at the time when the neuron was most active before the inactivation and emphasizes decreases of neural activity. Similarly, we took the time of peak discharge in Post 0.5 h (i.e., Post 0.5 h Peak; see, e.g., Figure 2.10 C) and compared the firing rate of each neuron in the pre-inactivation to the Post 0.5 h at this time and averaged changes across the population. This highlights the change of activity at the time when the neuron was most active after the inactivation and emphasizes increases of neural activity.

Finally, we verified that neural changes followed the time course of behavioral impairments induced by the inactivation (see Figure 2.11). We selected well-isolated neurons with a significant burst during grasp with the non-paretic hand and with consistent waveform characteristics across recording sessions for a given inactivation experiment (i.e., Post 0.5 h; Post 3 h and Post 10 h). These analyses were exclusively conducted with trials of the non-paretic hand because monkeys were not able to complete trials with the paretic hand in at least one of the recording sessions. We compared the peak amplitude of neurons in the different sessions after inactivation to the pre-inactivation values, similarly to what was described above. For each neuron, we calculated the mean of the SDE values of trials of a given session in a 1200 bin window that spanned across grasp duration (1000 bins for grasp duration, plus the last 100 bins before grasp onset, and the first 100 bins after grasp offset). Complimentarily, we also performed

the same analysis using the discharge amplitude of the population at the time of maximal discharge before inactivation (see Figure 2.11 D).

Statistical analysis

Quantification of muscimol effects on movement duration and EMG

The effects of muscimol on movement duration were evaluated using unpaired *t* tests (see Figures 2.2 and 2.3). For each arm, one test compared the duration of the reach period and one test compared the duration of grasp ($p < 0.05$). To compare the area under the curve of average EMG signals before and after muscimol injections, we used paired *t* tests ($p < 0.05$). Cohen's *d* was used to measure effect sizes when appropriate. In some cases when the sample was too small (i.e., $n < 20$), we used Hedges' *g* to measure the effect size.

Quantification of muscimol effects on the total population of recorded neurons

To identify neurons significantly modulated during one or several epochs of the task, we used paired *t* tests (*t* test $p < 0.05$). The discharge of neurons at rest, when the animal waited with the hand in the start position using a 600 ms window before Cue onset (−0.7 to −0.1 s), were compared using a three-way ANOVA ($p < 0.05$), using area (iPMv, cPMv), arm (non-paretic, paretic), and session (control, Post 0.5 h) as factors. The effect size for ANOVAs was estimated using the partial η squared (η_p^2). Finally, the proportion of neurons modulated during grasp or in function of the hand used was compared using χ^2 tests ($p < 0.05$) followed by *post hoc* two-proportion *Z* tests with Bonferroni correction (see Figure 2.6). The effect size for the χ^2 tests and *Z* tests was calculated using Cramer's *V* and the correlation coefficient *r* ($r = z/\text{sqrt}(n1 + n2)$), respectively.

Quantification of changes within continuously recorded neurons

We compared the variance of peak discharge time after inactivation to control neurons recorded for ∼1 h using Bartlett's test, followed by *post hoc* two-sample *F* tests with Bonferroni correction (see Figure 2.9). Comparison of spike discharge rate before and after inactivation was done using paired *t* tests (see Figure 2.10).

For the progression of changes with time after muscimol injection (see Figure 2.11), we evaluated the effect of time and cortical area (iPMv and cPMv) with two-way repeated-measures ANOVAs, one for mean spike firing rate during grasp (see Figure 2.11 B) and one for discharge amplitude of neurons at the time of their maximal discharge (see Figure 2.11 C,D). Since in both cases, there was no effect of area nor interaction between area and session, we merged data from the two hemispheres. Values from each post-inactivation session (i.e., Post 0.5 h; Post 3 h and Post 10 h) were then compared with pre-inactivation using a *t* test, and the *p* value adjusted using a Bonferroni correction ($p < 0.017$).

Results

We trained 2 adult female rhesus macaques on a reach-to-grasp task (Figure 2.1 A), in which monkeys retrieved food pellets using precision grip with the right or the left hand. Both animals were implanted with chronic electrode arrays in PMv of the two hemispheres (Figure 2.1 B). In addition, a chamber was placed over the left M1, giving access to the dura. After implantation, we located the hand representation in the chamber using intracortical microstimulation trains before initiating inactivation experiments. In each inactivation experiment, we first recorded the neuronal activity during grasping before inactivation (i.e., recording session Pre). Then, the GABA-A receptor agonist muscimol was injected in the hand area of the left M1 through the chamber to induce a reversible inactivation (see Materials and Methods). With this design, the left PMv was always in the same hemisphere as the "lesion" (i.e., "ipsilesional" PMv or iPMv) and the right PMv was in the opposite hemisphere (i.e., "contralesional" PMv or cPMv) (Figure 2.1 C). The monkey resumed performing trials ∼30 min after the injection of muscimol (i.e., session Post 0.5 h). Recordings were uninterrupted throughout these different steps, allowing us to quantify the effect of inactivation on individual neurons.

As previously reported when using comparable inactivation techniques (Matsumura et al., 1991; Schieber and Poliakov, 1998; Brochier et al., 1999), both monkeys showed clear impairments with the contralateral, right hand, which we refer to as the "paretic hand." In session Post 0.5 h, animals were still able to perform some trials on the task with the paretic hand (minimum = 5, maximum = 25; average ± SD =21.4 ± 5.5), albeit with clear impairments. Examples of deficits included difficulty to oppose the thumb to the index and a reduction of individuated movements of the index (e.g., D2 and D3-5 being moved together), increased number of digit flexions to grasp the pellet, and abnormal coordination between the hand and forearm. Reaching and grasping movements with the paretic hand became slower at Post 0.5 h (*t* test: reach $T_{(586)} = 5.15$, $p = 3.57 \times 10^{-7}$, $d = 0.43$; grasp $T_{(586)} = 7.49$, $p = 2.41 \times 10^{-13}$, $d = 0.62$) (Figure 2.2). In contrast, we found no change in reach ($T_{(642)} = 1.26$, $p = 0.21$, $d = 0.099$) or grasp duration ($T_{(642)} = -1.36$, $p = 0.17$, $d = -0.11$) with the left, "non-paretic hand." For EMG signals, the pattern of activation was generally well-preserved during movements of the non-paretic arm (Figure 2.3). However, changes were apparent in some muscles of the paretic arm during reach

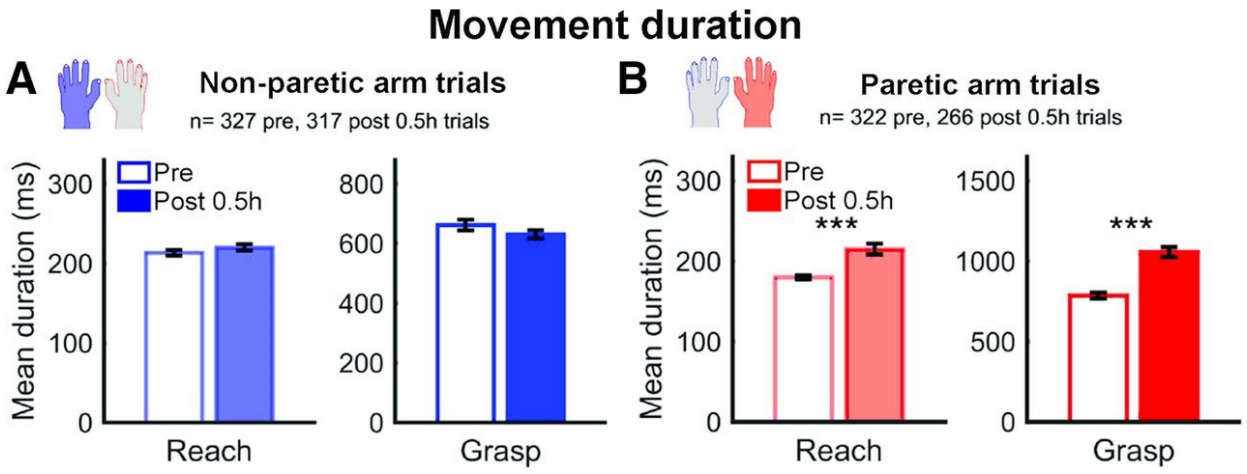

Figure 2.2. *Impact of the inactivation on movement duration 0.5 h after injection of muscimol*

A, ***B***, Average reach and grasp duration (±SEM) before (Pre) and 0.5 h after injections of muscimol (Post 0.5 h) during movement of the non-paretic (***A***) and paretic arm (***B***). Data from all sessions for both monkeys are combined. While no changes were observed with the left, "non-paretic hand" (blue bars), both reach and grasp duration were increased with the right, "paretic hand" (red bars). ***$p < 0.001$ (unpaired *t* tests).

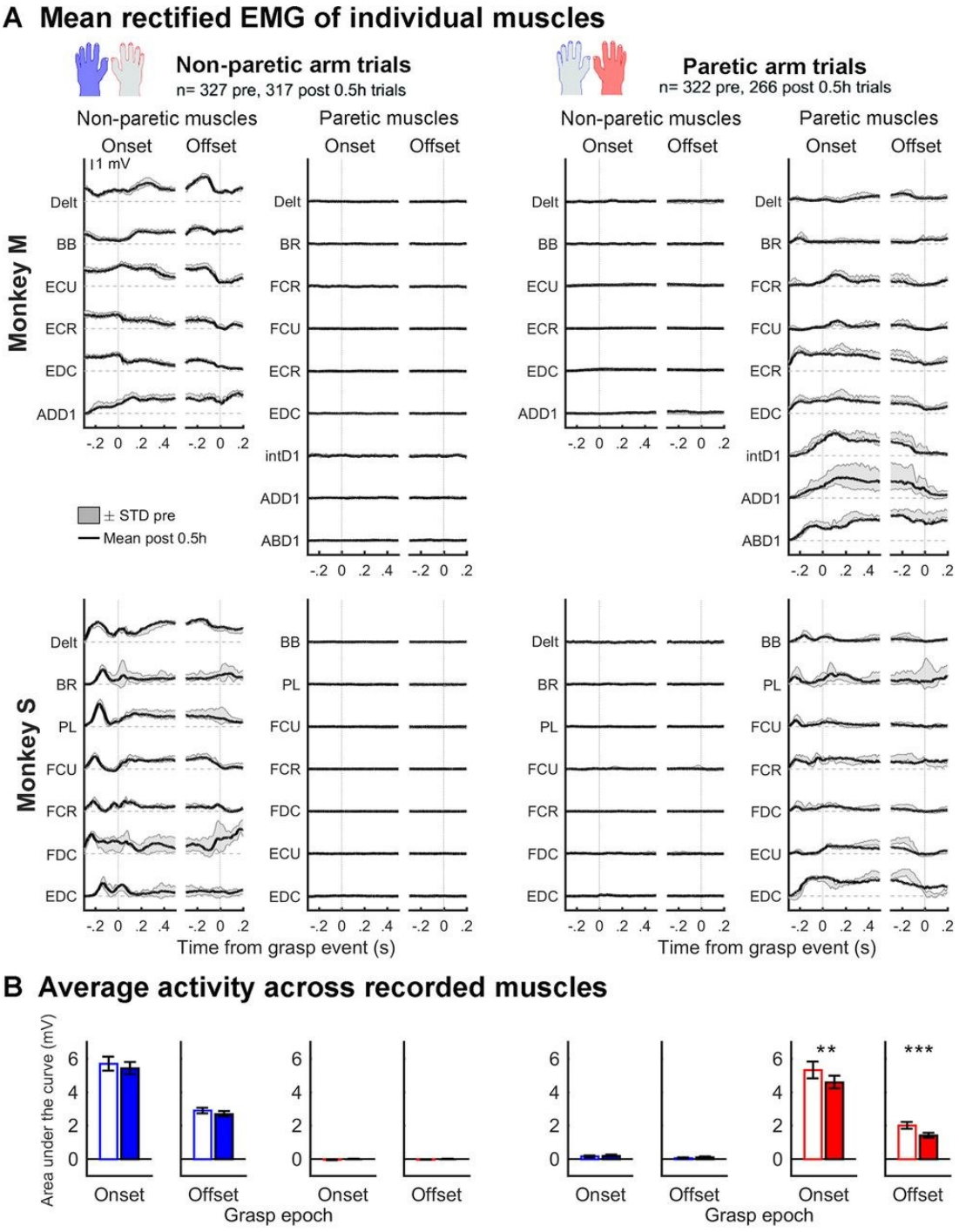

Figure 2.3. *Impact of the inactivation on EMG activity 0.5 h after injection of muscimol*

A, Mean rectified and filtered EMG traces in the various muscles recorded during grasp with the non-paretic arm (left) and the paretic arm (right) in Monkey M (top) and Monkey S (bottom). In each plot, EMG traces are shown aligned on Grasp Onset and Grasp Offset using the same time widows used for the neuronal analyses. For each monkey, data from successful trials across

inactivation experiments are combined. For each muscle, the average EMG trace of trials collected after inactivation (Post 0.5 h; black line) is overlapping the SDs from the mean of trials collected before inactivation (shaded gray). ***B***, Quantification of EMG changes after inactivation using the area under the curve of the average EMG trace (± SEM) across recorded muscles. During trials with the non-paretic arm (left plots), there were no significant changes of EMG activity in the moving arm (i.e., non-paretic arm, blue bars) after inactivation. The error bars show standard errors. This was true both at the onset and the offset of grasp. Little EMG activity was present in the resting arm (i.e., paretic arm), and the inactivation did not cause any changes. During trials with the paretic arm (right plots), there was little activity in the non-paretic arm (i.e., resting arm), both before and after the inactivation. However, there was a significant decrease of EMG activity in the paretic arm (i.e., moving arm; red bars), both at the onset and the offset of grasp. $^{**}p < 0.01$. $^{***}p < 0.001$.

and grasp after inactivation (Figure 2.3 A), and there was a significant decrease of EMG amplitude in this arm (Figure 2.3 B; paired *t* test: aligned on Grasp Onset, $T_{(12)} = -4.129$, $p = 0.0014$, $g = -0.44$; aligned on Grasp Offset, $T_{(12)} = -5.985$, $p = 6.36 \times 10^{-5}$, $g = -0.85$). In addition, no activity was observed in the "resting" arm (i.e., opposite to the one performing trials) before or after inactivation. Thus, changes of neuronal activity after inactivation cannot be explained by the appearance or disappearance of covert, "mirror like" EMG activity in the resting arm. After the Post 0.5 h recording session, the monkeys were brought back to the home cage, where they could move freely, with unlimited access to water.

We monitored the progression and extent of deficits caused by inactivation in additional recording sessions, 3 h and 10 h after the injection of muscimol. After 3 h (Post 3 h), impairments with the right hand were so profound that the monkeys could no longer perform the task. However, they still attempted grasping when presented fruits. In some cases, this revealed a limited ability to move digits and an incapacity to produce a precision grip. In other cases, the paretic hand was completely flaccid. Importantly, in all cases, the monkeys attempted to reach to the fruit and eat it with no obvious proximal arm or orofacial movement deficits. This confirmed that the inactivation accurately targeted the M1 hand representation and was seemingly limited to this part of the brain in all inactivation experiments selected in the present study. At 10 h post-inactivation (Post 10 h), the deficits were generally much milder, and they were completely resorbed on the next day.

The population of neurons recorded in PMv in the control condition

Neuronal data from both monkeys were obtained during 21 recording sessions. For 8 of these sessions, there was no inactivation (Unmanipulated sessions). The 13 others were inactivation experiments. Combining data from the Unmanipulated sessions with data recorded before the injection of muscimol in the inactivation experiments (i.e., session Pre), we identified 520 well-isolated "control" PMv neurons across both hemispheres.

We characterized the population of neurons recorded by our arrays by determining their preferred epoch and hand (maximal discharge rate), as well as quantifying modulation patterns across epochs (*t* test $p<0.05$; see Materials and Methods). The population comprised neurons active throughout the various epochs of the task (Figure 2.4). However, we found that there was a greater proportion of neurons with a maximal discharge rate (36.9% across both hands; Figure

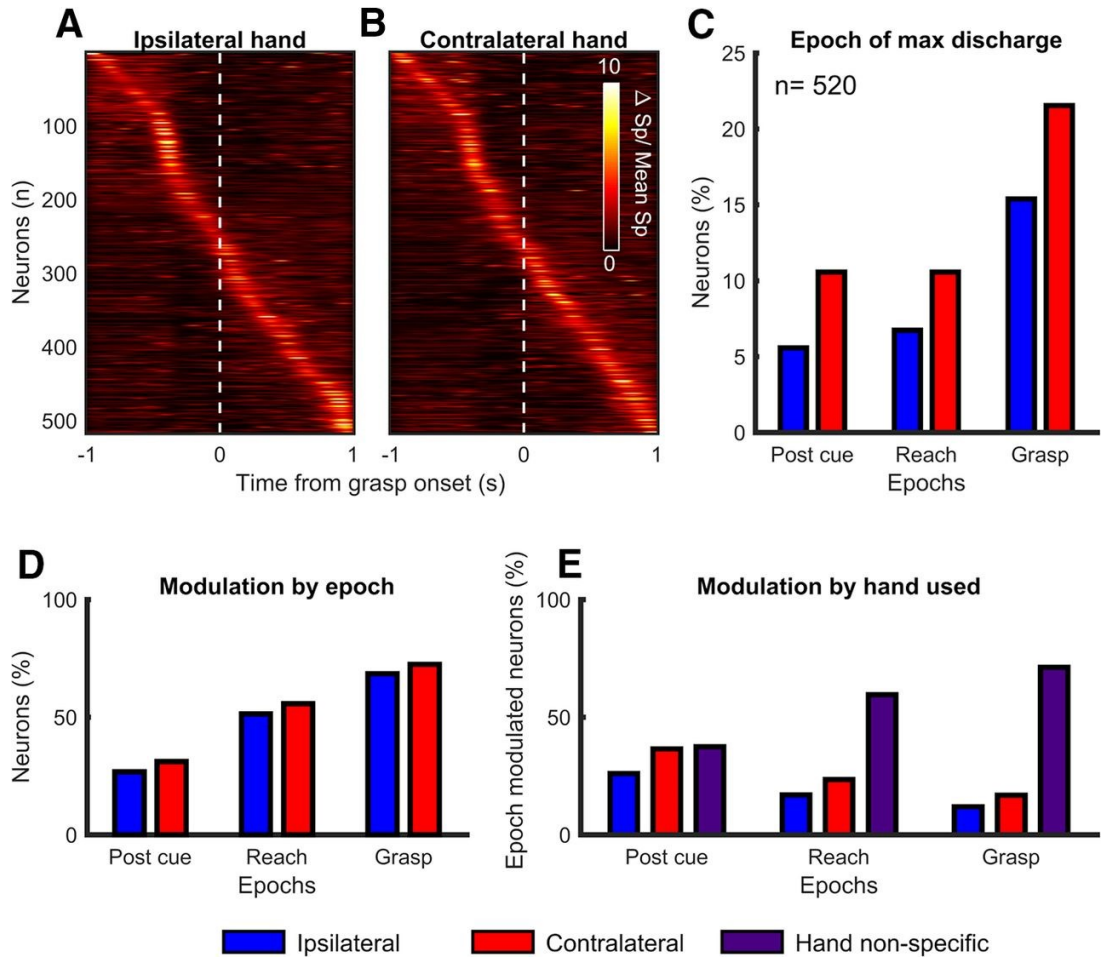

Figure 2.4. *Population of control neurons recorded in PMv*

Data from the two hemispheres in both monkeys were pooled for analyses of control neurons. Heat plots of the SDE normalized to the average value in a 2 seconds window around Grasp Onset for all PMv neurons during movements of the ipsilateral (***A***) and contralateral (***B***) hand. Neurons are ordered separately for each hand based on the time of maximal discharge relative to Grasp Onset. Time is in seconds. ***C***, Proportion of neurons with their maximal discharge rate in the various task epochs, during movement of either the ipsilateral or contralateral hand. There is only one count per neuron, across both the task epochs and hand used. There was a greater proportion of neurons with a maximal discharge rate during the grasp epoch and with the contralateral hand. ***D***, Proportion of neurons with significant modulation of discharge rate during the various task epochs (*t* test; $p<0.05$). Categories are not mutually exclusive. There was a greater proportion of neurons being significantly modulated during the grasp epoch. ***E***, Modulation of neurons during the various task epochs in function of the hand used. For each epoch, only neurons modulated during the use of either hand in that specific epoch are included (sum = 100% per epoch.) Most grasp-related neurons were significantly modulated during movements of both hands.

2.4 C) or being significantly modulated (82.3% across both hands; Figure 2.4 D) during the grasp epoch. This was expected since the arrays were implanted in the region of PMv where the hand representation and neurons contributing to grasp are typically found (Tanji et al., 1988; Schmidlin et al., 2008). Neurons that were not modulated during any of these epochs of interest (9.4% across both hands) often showed modulation after the end of grasp or between trials, several seemingly related to orofacial movements, such as chewing the reward.

Most grasp-related neurons were significantly modulated during movements of both hands (i.e., hand non-specific; 71.3%; Figure 2.4 E). Fewer neurons were modulated during movements of the contralateral hand only (16.8%) and fewer still during movements of the ipsilateral hand only (11.9%). Together, these results demonstrate that a large proportion of PMv neurons recorded from our arrays were involved in grasping, and were active during movements of both hands, albeit with a slight predominance of modulation with movements of the contralateral hand. These findings are very much in line with previous reports of neuronal activity in PMv during hand movements while performing comparable tasks (Rizzolatti et al., 1988; Tanji et al., 1988; Umilta et al., 2007; Michaels and Scherberger, 2018).

The impact of inactivation on the pattern of modulation of all recorded neurons

After muscimol injection, we identified 293 well-isolated post-inactivation neurons, 138 in iPMv and 155 in cPMv. The inactivation of M1 in the left hemisphere induced changes of neural activity in both hemispheres that were readily observed in individual neurons (Figure 2.5). After inactivation, both decreases and increases of neural discharge rates were observed. In extreme cases, neurons completely stopped discharging during movements (e.g., Figure 2.5 F), or neurons with little activity started to discharge large bursts (e.g., Figure 2.5 L). The most pronounced changes were often observed in the grasp epoch, suggesting that neuronal activity was particularly affected during movements of the digits.

We compared the entire population of control neurons to the population of post-inactivation neurons (i.e., not limited to within-neuron analyses). To verify if the inactivation had an effect on PMv neurons when the animals were at rest, we looked at the firing rate during the

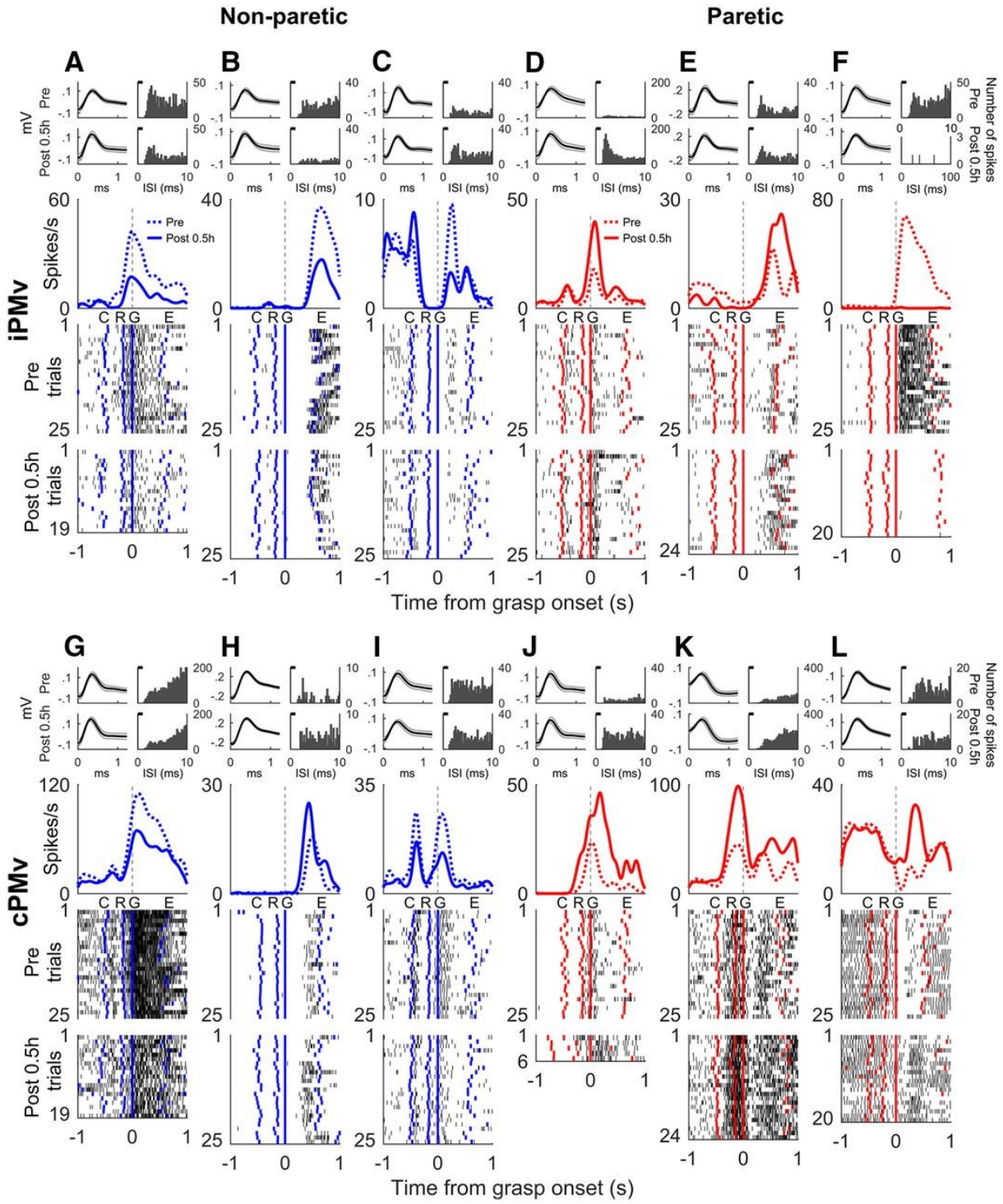

Figure 2.5. *Example neurons with altered pattern of discharge after inactivation*

Neurons recorded in iPMv (***A–F***) and cPMv (***G–L***) during movements of the non-paretic (left, blue) and paretic hand (right, red). For each neuron, the top panel shows the average spike shape (±SD with gray shading; left) and the interspike interval count histogram (right), before (top) and after inactivation (bottom). Below are the SDE curves and finally the raster plot of individual

trials before (Pre) and 0.5 h after inactivation (Post 0.5 h). Data are aligned on Grasp Onset (time = 0), and time is in seconds. Colored markers in the raster plots represent the timing of other events in each trial (C, GO cue; R, Reach Onset; G, Grasp Onset; E, Grasp Offset). While many neurons were affected in both hemispheres, there was a great variability in the nature of the changes observed in each area.

pre-cue epoch when the hand was at the home plate. We found that the discharge rate during the pre-cue epoch was similar in both hemispheres and regardless of which hand would be used, and that there were no interaction effects between these factors (three-way ANOVA $p < 0.05$; see Materials and Methods). However, the firing rate of PMv neurons was significantly lower after inactivation ($F_{(1,1618)} = 14.4$, $p = 0.0002$, $\eta_p^2 = 0.0088$). These results support that the inactivation resulted in a general decrease of neuronal activity in both hemispheres when the monkeys were not actively involved in the task.

The M1 inactivation also affected the proportion of neurons modulated during grasp with the paretic hand in both iPMv ($\chi^2_{(2,\ N = 658)} = 9.36$, $p = 0.0093$, $V = 0.084$) and cPMv ($\chi^2_{(2,\ N = 675)} = 19.76$, $p = 5.11 \times 10^{-5}$, $V = 0.12$) (Figure 2.6 A,B). When looking at the type of neurons affected, we found little difference in the proportion of neurons with a significant burst during grasp. Instead, neurons with a decrease of firing rate, or trough, during grasp were primarily affected (iPMv −12.4%, Bonferroni-corrected z test, $z = -2.91$, $p = 0.0071$, $r = -0.22$; cPMv −12.2%, $z = -3.01$, $p = 0.0053$, $r = -0.22$). Finally, the inactivation affected the selectivity of neurons to the hand moved in both the iPMv ($\chi^2_{(2,\ N = 543)} = 9.85$, $p = 0.0073$, $V = 0.095$) and cPMv ($\chi^2_{(2,\ N = 543)} = 15.05$, $p = 5.39 \times 10^{-4}$, $V = 0.12$) (Figure 2.6 C,D). Compared with controls, the post-inactivation population had a greater proportion of neurons only modulated during use of the non-paretic hand in both iPMv (11.6%; $z = 3.14$, $p = 0.0051$, $r = 0.36$) and cPMv (16.2%; $z = 3.84$, $p = 3.65 \times 10^{-4}$, $r = 0.37$). It also had a lower proportion of hand non-specific neurons that was significant in cPMv (−15.6%; $z = -3.18$, $p = 0.0043$, $r = -0.17$). A similar trend was observed in the iPMv, although it did not reach significance (−9.5%; $z = -1.96$, $p = 0.15$, $r = -0.1$). This suggests that the lower proportion of neurons with trough during grasp with the paretic hand may be largely due a loss of neurons broadly tuned to movements of either hand (i.e., hand non-specific) that became only active during grasp with the non-paretic hand.

Increases and decreases of firing rate in individual neurons during grasp

The greatest strength of our data is that the continuous recording before and after inactivation allowed us to quantify changes within individual neurons that remained well-isolated throughout any given inactivation experiment (within-neurons analyses; 94 in iPMv and 138 in cPMv). The rest of our analyses were focused on this subpopulation of neurons.

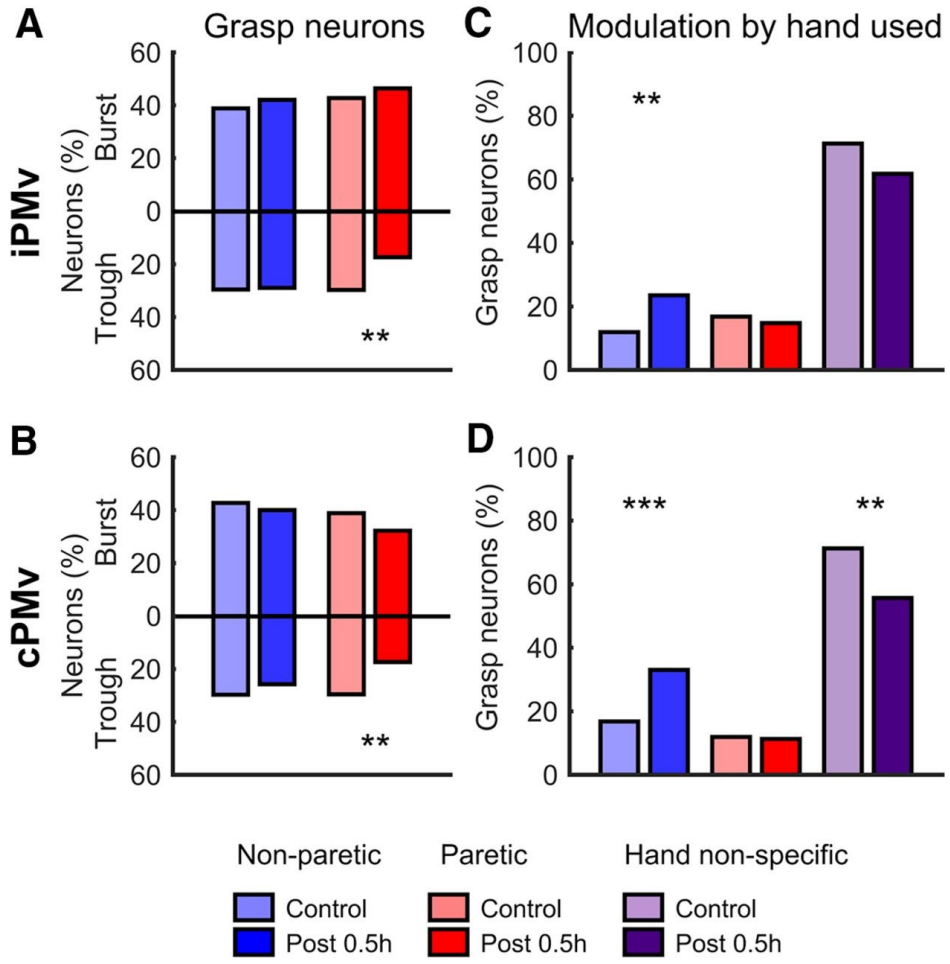

Figure 2.6. *Changes across the PMv neuronal population after inactivation*

A, ***B***, Proportion of neurons modulated during grasp (*t* test, $p < 0.05$) in iPMv (***A***) and cPMv (***B***) during movement of the non-paretic (blue bars) and paretic hand (red bars). The proportion of neurons with increased discharge rates during grasp, or bursts, is shown above the *x* axis, and the proportion of neurons with decreased discharge rate, or trough, is below. After inactivation, there was a lower proportion of neurons with trough during grasping with the paretic hand in both hemispheres. ***C***, ***D***, Proportion of neurons modulated in function of the hand used in iPMv (***C***) and cPMv (***D***). After inactivation, there was a higher proportion of neurons modulated only during movements of non-paretic hand (blue bar) in both hemispheres and a decrease of neurons modulated during grasp with either hand (i.e., "hand non-specific"; purple bar) in cPMv. $^{**}p < 0.01$. $^{***}p < 0.001$.

We quantified the incidence of neurons with increases or decreases of neural discharge rate at each moment in time throughout the grasp epoch (Figure 2.7). Changes in both iPMv and cPMv, with movements of either hand, were highly heterogeneous. While many neurons had increased firing rates, many others decreased their activity, perhaps to counterbalance each other. Nevertheless, specific and different general trends were present in the two hemispheres. In iPMv, a greater proportion of neurons decreased firing rate after inactivation, in particular when monkeys used the non-paretic hand. In contrast, a greater proportion of neurons increased discharge rate in cPMv, and the largest changes occurred at the end of grasp with the paretic hand. These effects were clearly outside the realm of what could be expected by chance, when compared with Monte Carlo simulated population changes (see Materials and Methods). We confirmed that this increased neuronal activity during movement of the paretic arm was not associated with the appearance of covert EMG activity in the non-paretic arm (see Figure 2.3).

Changes of peak timing in individual neurons following inactivation

We investigated the effects of M1 inactivation on the timing of peak discharge of iPMv and cPMv neurons during grasp. When looking at all clearly isolated neurons before and after inactivation (Figure 2.8 A,B), we found that timing was perturbed for many neurons in both hemispheres, and these changes were greater during paretic hand movements. We quantified the changes of peak discharge timing for neurons with a clear burst during grasp (>1 SD increase from pre-cue epoch) and found a similar pattern of reorganization with this subpopulation (Figure 2.8 C,D). In both iPMv and cPMv, several neurons showed altered peak discharge time, and more so during movements of the paretic hand. We interpret this as a desynchronization of PMv neurons' activity in relation to the various components of grasping movements after inactivation, that simultaneously occurs in both hemispheres. Interestingly, many well-isolated neurons in iPMv with a burst during grasp lost this burst after inactivation (n = 18, 18.9%; Figure 2.8 C), and more so during movements of the non-paretic hand (n = 11, 25.0%; left). In contrast, many neurons in cPMv that did not have peaks during grasp before inactivation had one after inactivation (n = 27, 20.6%; Figure 2.8 D), and more so during movements with the paretic hand (n = 22, 30.1%; right).

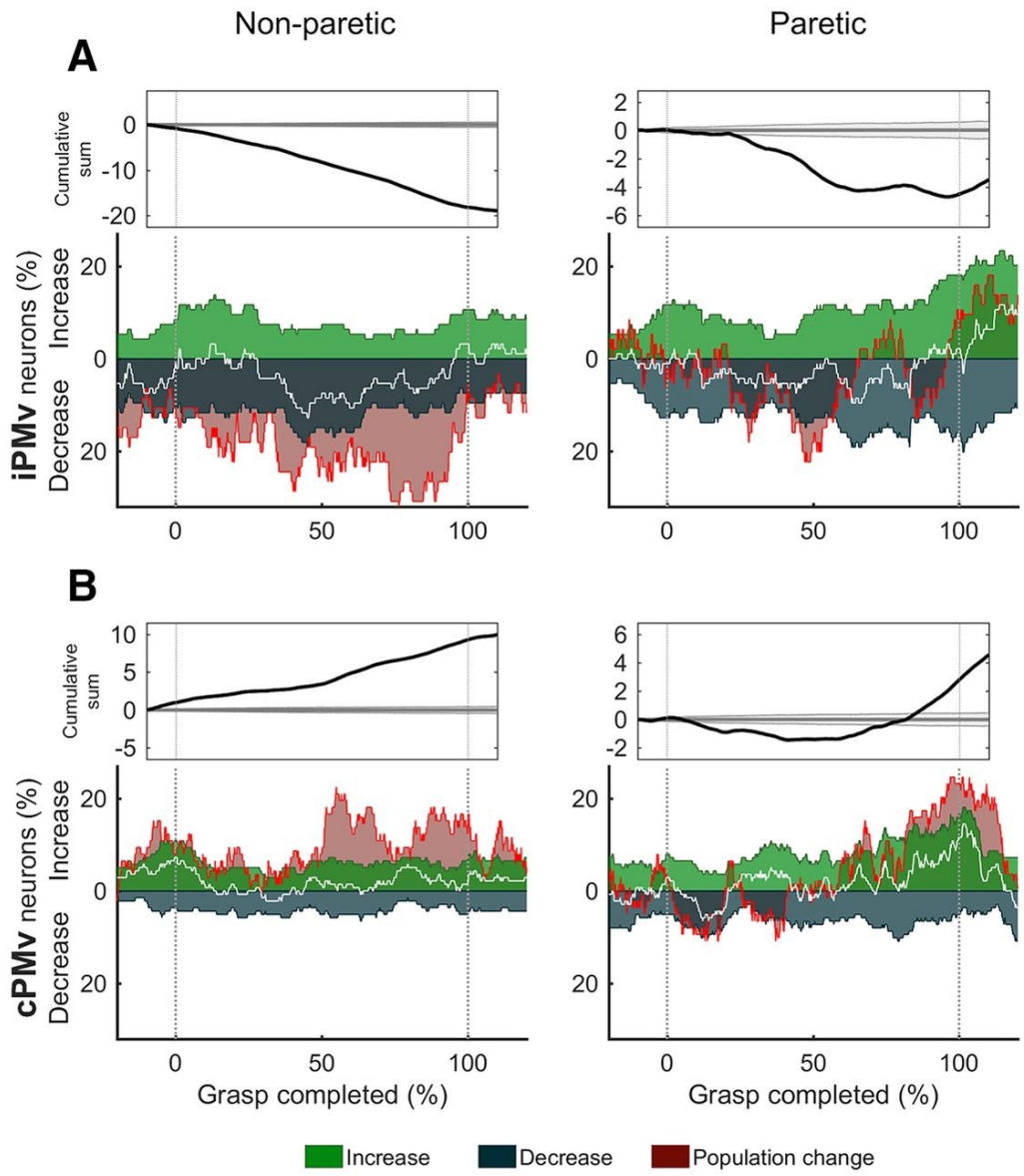

Figure 2.7. *Incidence of neurons with increases and decreases of discharge rate during grasp*

Changes of firing rate in iPMv (***A***) and cPMv (***B***) across normalized time during grasp with the non-paretic hand (left column) and the paretic hand (right column). All clearly isolated neurons before and after inactivation are included in this analysis, independently of their tuning to the task epochs (n = 94 in iPMv; n = 138 in cPMv). In each panel, top plots represent the cumulative sum of the difference between the total population of neurons with increases and decreases of firing rate across time bins (black trace) with the mean and 95% quantile of randomly simulated values (gray line and shadow). Bottom color plots represent the percentage of neurons with "significant" (unpaired t tests with $p < 0.05$; see Materials and Methods) increases (green) or decreases (gray-blue) in discharge rate at each moment during grasp. White trace represents the difference in the proportion of all clearly isolated neurons with "significant" increases and

decreases of activity. Red shaded area and line represent the same difference but using all neurons, including those with “nonsignificant” changes. In iPMv, more neurons showed decreased discharge rate after inactivation. This population accumulated with time during grasp, in particular with the non-paretic hand. In cPMv, more neurons showed decreased discharge rate after inactivation. This population accumulated with time during grasp, in particular with the paretic hand. 0 = Grasp Onset; 100 = Grasp Offset.

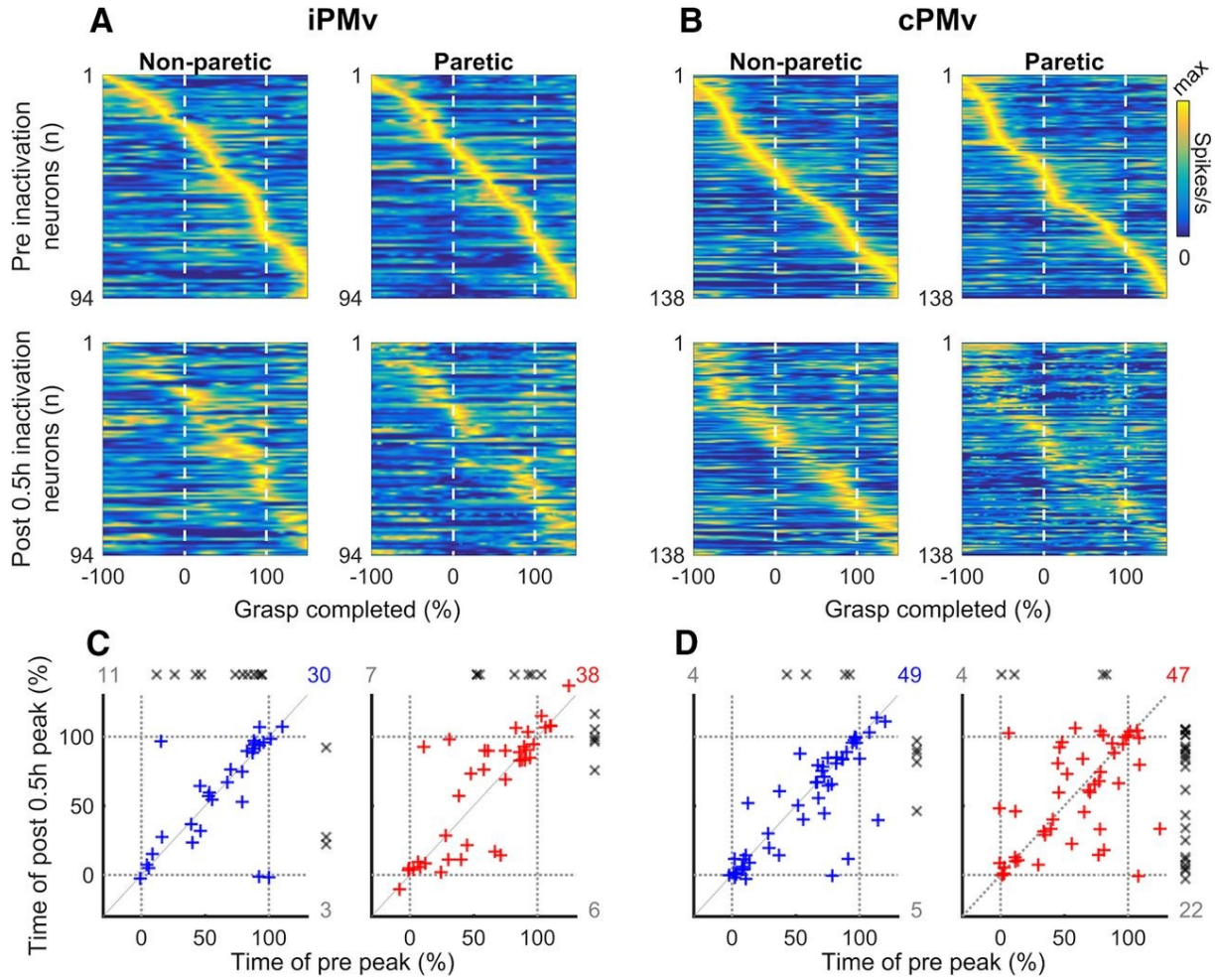

Figure 2.8. *Changes in the timing of peak discharge during grasp after inactivation*

A, ***B***, Heat plots of the SDE during grasp for all iPMv (***A***) and cPMv (***B***) neurons well isolated both before and after inactivation (within-neuron analysis) in normalized time. Left and right panels represent activity during movements with the non-paretic and paretic hand, respectively. To emphasize timing shifts over changes in firing rate, the discharge rate of each neuron across time is normalized to its peak value. Neurons are ordered based on the time of their peak discharge relative to Grasp Onset before inactivation (Pre; top row), and the order is kept constant 0.5 h after the inactivation (Post 0.5 h; bottom row). 0 = Grasp Onset; 100 = Grasp Offset. ***C***, ***D***, Peak discharge time of iPMv and cPMv neurons with clear discharge burst during grasp before inactivation ("Pre-Peak," *x* axis) and/or after inactivation ("Post-Peak," *y* axis) in normalized time. Colored symbols (+; blue = non-paretic hand; red = paretic hand) and numbers are for neurons with detectable bursts (>1 SD increase from pre-cue epoch) before and after the inactivation. Additional well-isolated neurons that either stopped or started having a detectable burst during grasp after inactivation are plotted along the axes (gray x symbols and numbers). The inactivation affected the temporal pattern of neuronal discharge in both iPMv and cPMv, more so during use of the paretic hand. In iPMv (***C***), many well-isolated neurons with a burst

during grasp lost this burst after inactivation. When considering the entire population of neurons that had detectable burst during grasp, either before and/or after inactivation (n = 44 for the non-paretic arm and n = 51 for the paretic arm), a total of 18 neurons (18.9%) lost this burst after inactivation (n = 11 for the non-paretic arm and n = 7 for the paretic arm; gray x symbols and count on top of plots). Thus, the loss of modulated neurons was greater during movements of the non-paretic arm (11 of 44; 25.0%). ***D***, In cPMv, many neurons that did not have peaks during grasp before inactivation had one after inactivation. Out of the entire population (n = 58 for the non-paretic arm and n = 73 for the paretic arm), 27 neurons (20.6%) showed a new burst of activity after inactivation and many more during movements of the paretic arm (22 of 73; 30.1%).

To give a better appreciation of the effect of the inactivation on the timing of peak discharge, we compared the effect of the inactivation with the impact of time during a control session that lasted ~1 h. When comparing the peak discharge time of all the well-isolated neurons at the beginning and the end of that recording session (Figure 2.9 A), the timing of discharges appeared much more stable than what we found after inactivation. Using neurons with a clear burst during grasp, we compared the changes of peak discharge time for these control neurons to the ones caused by inactivation (i.e., neurons from Figure 2.8 C,D). The variance of peak discharge time was significantly lower in the control session (Bartlett's statistic $\chi^2_{(4,\ N\ =\ 199)} = 70.53$, $p = 1.76 \times 10^{-14}$). This was true for iPMv neurons during movements of the non-paretic and paretic arm (*post hoc* two-sample *F* tests $F_{(34,29)} = 0.053$, $p = 4.16 \times 10^{-13}$ and $F_{(34,37)} = 0.081$, $p = 7.29 \times 10^{-11}$, respectively), and for cPMv also during movements of the non-paretic and paretic arm (*F* tests $F_{(34,48)} = 0.11$, $p = 1.53 \times 10^{-9}$ and $F_{(34,46)} = 0.041$, $p = 1.08 \times 10^{-15}$, respectively).

Overall, it seems that M1 inactivation led to a profound alteration of peak discharge timing in PMv that was generalized to both hemispheres, and during grasping with the non-paretic and the paretic arm. These circuit-wide changes also involved the disappearance of discharge bursts for many neurons in iPMv and the emergence of novel discharge bursts for many neurons in cPMv.

Changes of peak amplitude at the time of peak discharge of individual neurons

To consider both firing rate and peak timing, we looked at firing frequency at the time of peak discharge of individual neurons (Figure 2.10). For iPMv, given the large count drop of neurons with a detectable peak after inactivation, we identified peak discharge time during grasp before inactivation for each neuron and compared the discharge rate at this time before and after inactivation. This time alignment highlights that iPMv neurons had a large decrease of activity at the time during grasp when they were most active before inactivation. These changes were greater during movements with the non-paretic hand (Figure 2.10 A). When comparing the firing rate at the time of peak discharge (Figure 2.10 B), there was a significant decrease during

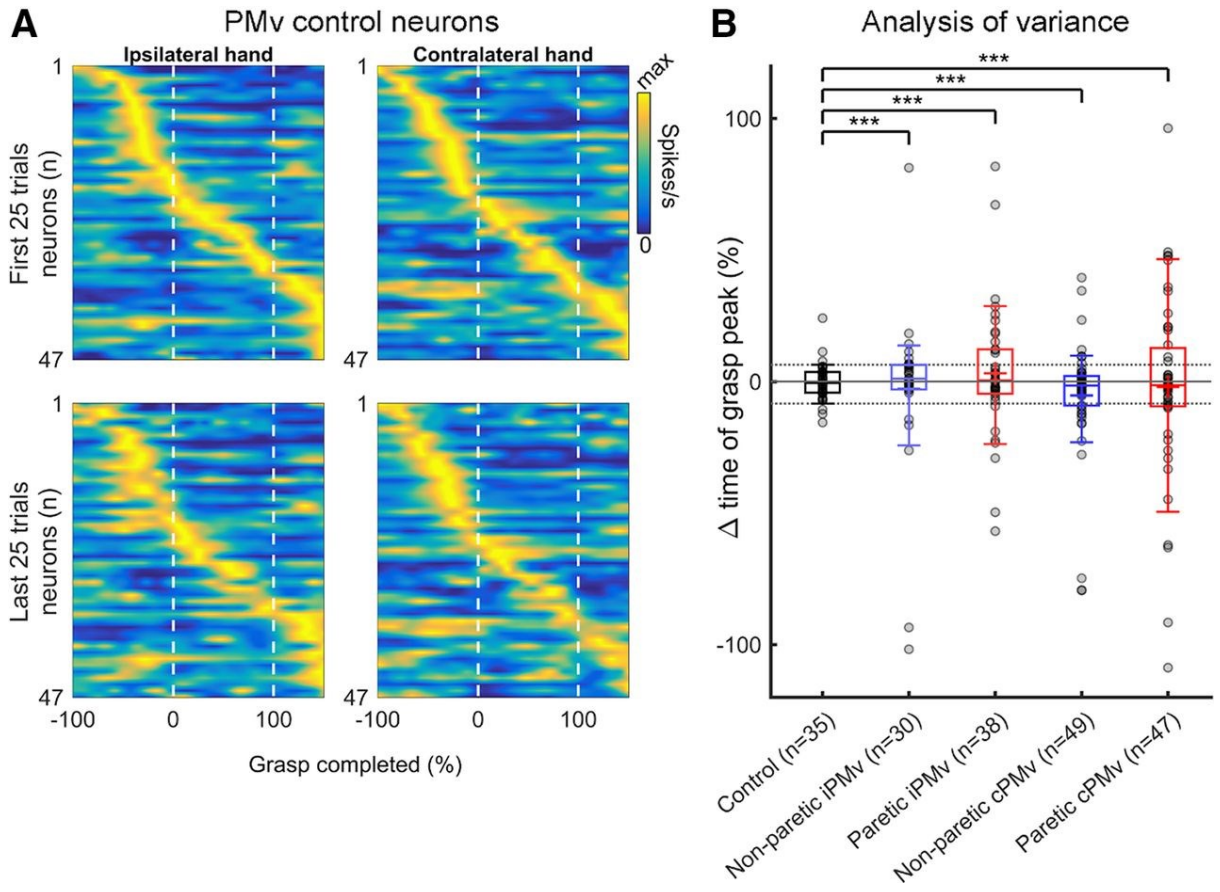

Figure 2.9. *Comparison of variability for the timing of peak discharge in an unmanipulated session*

A, We selected the longest unmanipulated session during which we recorded continuously (duration ~1 h) and identified all well-isolated units in PMv of both hemispheres. As in Figure 2.8 A, B, the heat plots represent the SDE of these control neurons during the first 25 trials (top) and last 25 trials (bottom). Left and right plots represent data during trials with the ipsilateral and contralateral hand, respectively. Peak discharge timing was largely preserved across control neurons. 0 = Grasp Onset; 100 = Grasp Offset. ***B***, Box-and-whisker plot of the change of peak discharge time of PMv neurons with clear discharge burst during grasp. The plot compares PMv neurons from the same unmanipulated recording session (black) to neurons recorded in iPMv and cPMv in inactivation experiments (i.e., from Figure 2.8 C,D). The variance of peak discharge time was significantly greater after inactivation, for both iPMv and cPMv neurons, and this was true during movements of the non-paretic (blue) and paretic arm (red). ***$p < 0.001$.

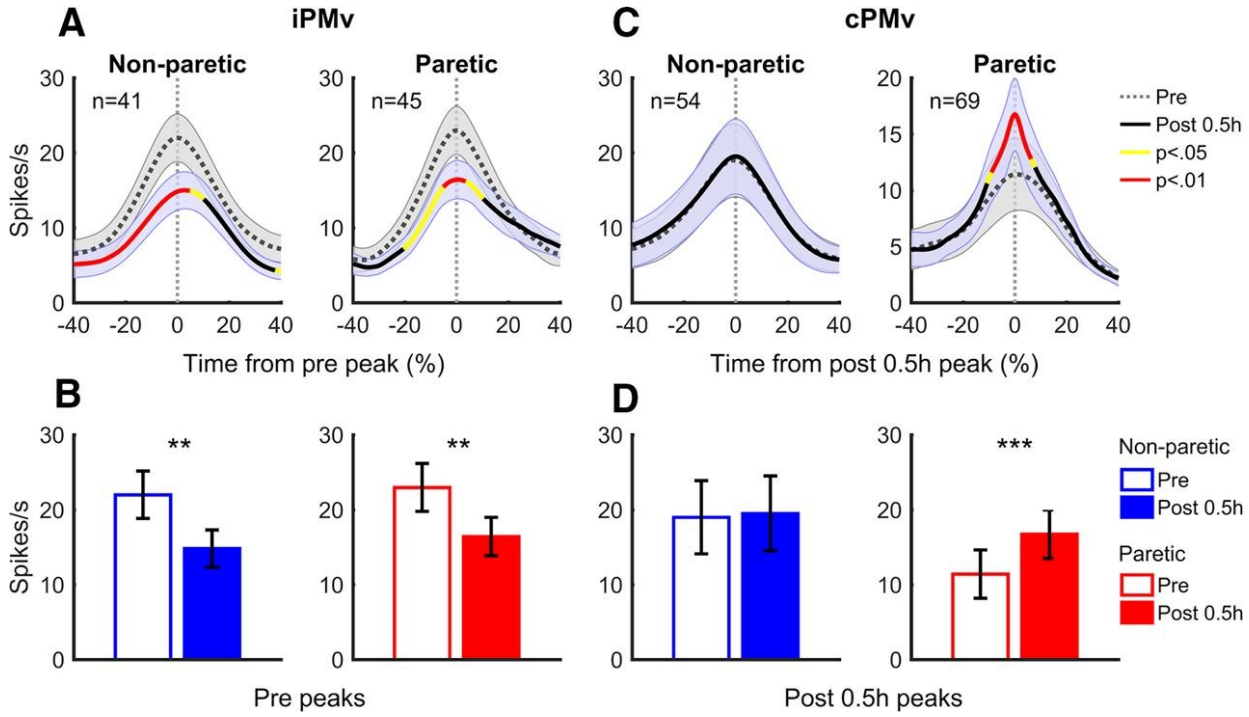

Figure 2.10. *Changes induced by inactivation at the time of peak discharge*

A, Average spike density of iPMv neurons during grasp before (dotted line; gray shade represents SEM) and after inactivation (solid line; blue shade represents SEM), when the activity is aligned to the time of peak discharge before inactivation, in normalized time. Colors on the solid line report time bins for which the average firing rate of the population was "significantly" different after inactivation (yellow represents paired *t* test $p < 0.05$; red represents paired *t* test $p < 0.01$). There was a decrease of activity during grasp that was more pronounced during movements of the non-paretic hand (left). ***B***, Comparison of average spike discharge rate of iPMv neurons (± SEM) before and after inactivation (paired *t* test at time 0). There was a significant decrease of peak firing rate with movements of both the non-paretic (left; blue) and paretic hand (right; red). ***C***, Average discharge rate of cPMv neurons, when the activity is aligned to the time of peak discharge after inactivation. There was a sharp increase of activity during movements of the paretic hand (right). ***D***, There was a significant increase of peak firing rate with movements of the paretic hand at the time of maximal discharge during grasp (right; red). $^{**}p < 0.01$. $^{***}p < 0.001$.

movements of the non-paretic ($T_{(40)} = -3.25$, $p = 0.0023$, $d = -0.51$) and the paretic hand ($T_{(44)} = -2.94$, $p = 0.0052$, $d = -0.44$). No such decrease was observed in cPMv using this time alignment ($p > 0.05$).

In cPMv, because many neurons started to have significant bursts only after inactivation, we identified the peak discharge time of each neuron after inactivation and compared the discharge rate at this time before and after inactivation. While there was no change when monkeys moved the non-paretic hand, there was a sharp increase of maximal discharge rate during grasp with the paretic hand (Figure 2.10 C). This time alignment highlights that, during movements with the paretic hand, cPMv neurons had increased discharge or new bursts at a time during grasp when they were much less active before inactivation. Peak firing frequency of cPMv neurons was unaffected during movement with the non-paretic hand (Figure 2.10 D; $T_{(53)} = 0.55$, $p > 0.05$, $d = 0.074$) and was significantly increased during grasp with the paretic hand ($T_{(68)} = 6.37$, $p = 1.90 \times 10^{-8}$, $d = 0.77$). Using this timing alignment, no such increase was observed in iPMv ($p > 0.05$).

Although these population changes were supported by neurons that either lost their discharge peaks (i.e., in iPMv) or had new ones (i.e., in cPMv), the same trends were observed when only looking at neurons that had detectable peaks before and after inactivation. Within this subpopulation of neurons, there was also a decrease of activity in iPMv during grasp with the paretic (−6.15 spikes/s; $T_{(37)} = -2.37$, $p = 0.023$, $d = -0.32$) and the non-paretic hand (−5.69 spikes/s; $T_{(29)} = -3.1$, $p = 0.0043$, $d = -0.38$). In cPMv, there were no changes during movements of the non-paretic hand ($p > 0.05$), but a sharp increase of activity during movements of the paretic hand (4.06 spikes/s; $T_{(46)} = 3.97$, $p = 2.49 \times 10^{-4}$, $d = 0.58$).

Together, these findings confirm that two very different phenomena occurred simultaneously in iPMv and cPMv after inactivation. Neurons in iPMv decreased firing at the time when they were most active and neurons in cPMv started bursting at a time when they were less active before inactivation.

Progression of altered neuronal discharge pattern with time after muscimol injection

Finally, we wondered whether the changes in neural activity observed at the onset of impairments would increase along with time and the progression of motor deficits after the muscimol injection. We tracked a subset of electrodes with stable recordings across Post 0.5 h, 3 h, and 10 h sessions (i.e., consistently well-isolated and similar spike shape), and thus that we could reasonably assume to come from the same neurons. In addition, these neurons all had their maximal peak discharge during grasp with the non-paretic hand before inactivation (n = 11 iPMv, 34 cPMv neurons). We focused on the non-paretic hand since the monkeys were unable to perform the task with the paretic hand at Post 3 h (see above).

Looking at individual neurons, we found examples with increases and with decreases of activity following inactivation (Figure 2.11 A). We quantified the mean spike firing rate during grasp of the neuronal population and compared the different data collection sessions. Since we did not observe a main effect of area (iPMv, cPMv) nor interaction between area and session (Pre, Post 0.5 h, 3 h, 10 h) (repeated-measures two-way ANOVA; $F_{(3,129)} = 0.67$, $p = 0.57$, $\eta_p^2 = 0.013$), we merged the neuronal populations from the two hemispheres. With this analysis, there was a trend of a progressive decrease of firing rate for Post 0.5 h and Post 3 h sessions and a return toward baseline for Post 10 h (Figure 2.11 B). However, the main effect of session was not significant ($F_{(3,132)} = 1.84$, $p = 0.14$, $\eta_p^2 = 0.04$). We then compared the discharge amplitude of the population at the time of their maximal discharge before inactivation (Figure 2.11 C,D). Again, since we did not observe any significant interaction between area and session ($F_{(3,129)} = 0.52$, $p = 0.66$, $\eta_p^2 = 0.012$), we merged the two populations. With this analysis, there was a significant effect of session ($F_{(3,132)} = 4.21$, $p = 0.007$, $\eta_p^2 = 0.087$). While there was no difference between Pre and Post 0.5 h (Bonferroni-corrected paired t test; $T_{(44)} = -1.72$, $p = 0.08$, $d = -0.26$), there was a significant decrease in peak neural activity at Post 3 h ($T_{(44)} = -3.49$, $p = 6.67 \times 10^{-4}$, $d = -0.52$), when behavioral deficits were most pronounced. At Post 10 h, neural activity seemed to have recovered, returning to Pre-inactivation levels ($T_{(44)} = -1.17$, $p = 0.24$, $d = -0.17$). These analyses support that the changes of neuronal activity at Post 0.5 h reflect the level impairments and that they likely progressed in a similar manner, becoming more pronounced as behavioral deficits worsened.

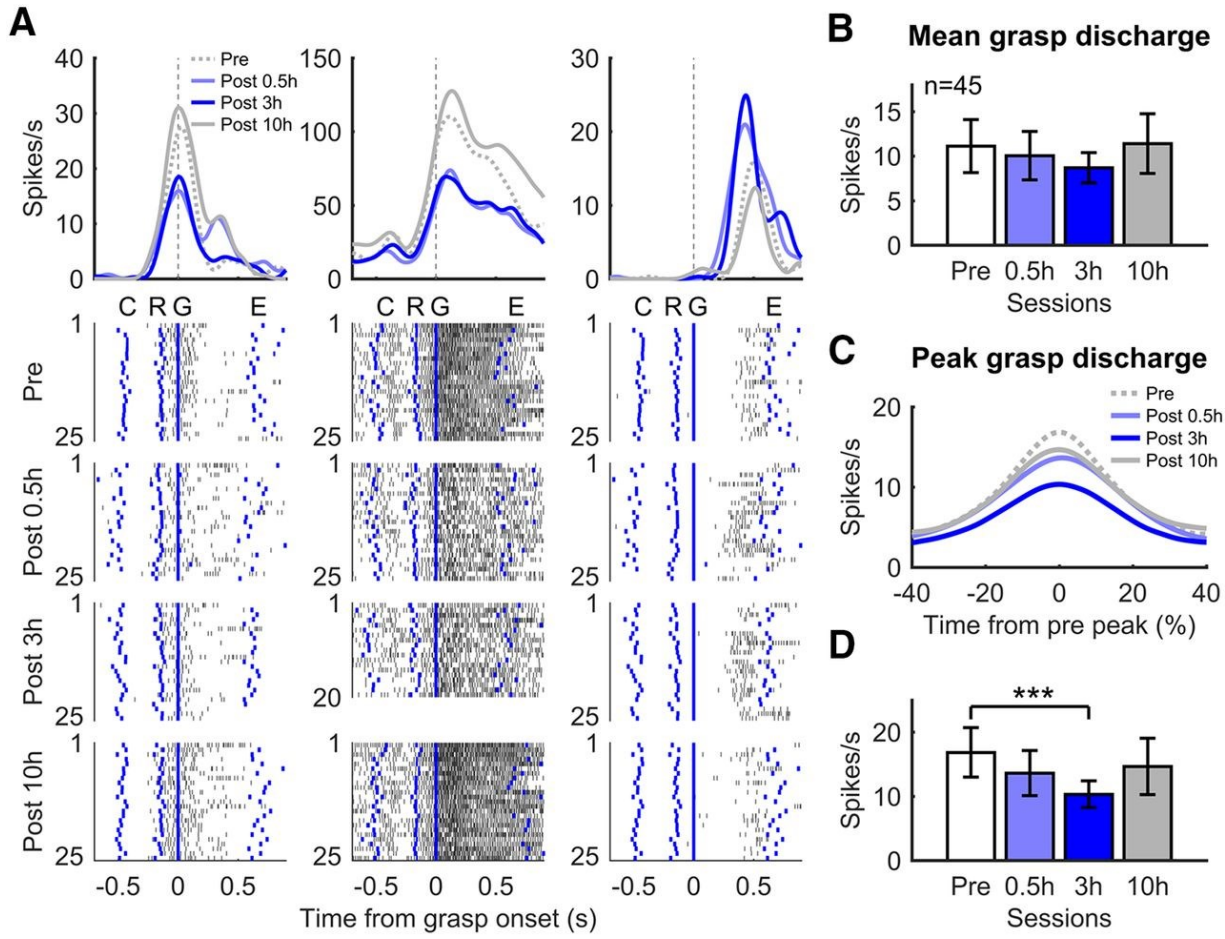

Figure 2.11. *Progression of neuronal changes in PMv with time after muscimol injection*

A, Examples of well-isolated neurons, showing decreases (left and middle column) and increases (right column) of activity during use of the non-paretic hand in real time (seconds). There is a clear impact of the inactivation on neural activity at time Post 0.5 h and Post 3 h. At time Post 10 h, the firing rate tended to return toward pre-inactivation values. ***B***, Average firing rate (±SEM) during grasp. The neuronal population showed a similar trend across different data collection time points. The largest change from baseline was observed at Post 3 h, with a return toward baseline at Post 10 h. ***C***, Profile of peak discharge of PMv neurons at Post 0.5 h, Post 3 h, and Post 10 h, when aligning data using the time of peak maximal discharge of each neuron before inactivation in normalized time (Pre-Peak). The average firing rate progressively decreased at Post 0.5 h and Post 3 h and then came back toward pre-inactivation values at Post 10 h. ***D***, Maximal peak discharge rate (±SEM) using Pre-Peak time alignment. There was a significant decrease at Post 3 h. At Post 10 h, neural activity seemed to have recovered, returning to Pre-inactivation levels. ***$p < 0.001$.

Discussion

We investigated the impact of a cortical lesion in M1 on neuronal activity of PMv in the ipsilesional and contralesional hemispheres while monkeys produced grasping movements. To do so, we used reversible inactivation of M1 with a receptor agonist of the neurotransmitter GABA, muscimol. GABA is ubiquitously present in the neocortex, and cortical injections of muscimol lead to hyperpolarization of all neuron types (Matsumoto, 1989; Martin and Ghez, 1999). The discharge rate of these neurons is profoundly reduced or completely abolished (Hess and Murata, 1974), causing hypometabolism in the affected region (Martin, 1991). Several experiments support that the behavioral effects of muscimol inactivation are comparable to the ones observed acutely after permanent brain lesions. For example, muscimol inactivation or permanent lesion in the motor cortex can both cause movement trajectory errors, impaired dexterous hand control, and loss of independent finger movements (Martin and Ghez, 1993; Hoffman and Strick, 1995; Schieber and Poliakov, 1998; Brochier et al., 1999; Nudo et al., 2003; Hoogewoud et al., 2013). Muscimol is thus considered an acceptable tool to study the acute effects of injuries in the brain.

In the present study, we favored reversible inactivation techniques over more clinically relevant brain injury models to continuously record isolated neurons before and after the onset of motor deficits. This powerful approach helped us reveal that extensive and complex neuronal reorganization takes place in both hemispheres, at the very onset of behavioral impairments. We view this rapid reorganization as a consequence of the disruption of the motor network's homeostasis (von Monakow, 1914; Carrera and Tononi, 2014). We thus expect that changes of comparable magnitude simultaneously take place in other brain regions interconnected with the site of injury. Because of the very short delay after injury, molecular and cellular processes specific to the type of injury (e.g., traumatic or ischemic, etc.) probably have little impact on neuronal reorganization at this point but instead become involved later during recovery. Accordingly, the changes we describe should have many common features with the ones evoked acutely after any type of lesion in the brain.

Bihemispheric detuning of neuronal activity in PMv during grasp with the paretic hand

It is well known that some PMv neurons pause during movements of the hand (Tanji et al., 1988). After inactivation of M1, we found that trough neurons in both hemispheres were more likely to lose their tuning to grasp with the paretic hand. In the oculomotor system, inhibitory interneurons are tonically active to prevent unwanted movements. When they pause, the release of inhibition favors the firing of excitatory neurons driving motor outputs (Evinger et al., 1982; Pare and Guitton, 1998). One possibility is that trough neurons in PMv serve a comparable purpose. If so, their loss in iPMv after brain injury could favor the generation of undesirable co-contractions and impair individuated finger movements (Lang and Schieber, 2004). The presence of such a gating mechanism in the premotor cortex is, however, uncertain (Kaufman et al., 2010). In cPMv, the decrease of hand nonspecific neurons and the increase of neurons modulated with movement of only the non-paretic hand could support compensatory behavior with the non-paretic hand (Jones, 2017).

A conspicuous impact of inactivation was the alteration of discharge burst timing during grasp. These changes were also observed in iPMv and cPMv, and more pronounced with movements of the paretic hand. Similarly, stroke in the somatosensory cortex induces chronic impairments in the temporal fidelity of responses to peripheral stimulation (Sweetnam and Brown, 2013), which could be because of a dysfunction of the corticothalamic feedback circuit involved in the inhibition of thalamocortical neurons (Paz et al., 2010). In the visual system, corticothalamic feedback from the visual cortex to the lateral geniculate nucleus is involved in spike-timing precision of thalamic neurons' responses to incoming visual signals (Hasse and Briggs, 2017). It is thus possible that changes in the timing of neuronal activity in PMv during grasp are because of the loss of corticothalamic signals from M1 that indirectly affect inputs to PMv. Alternatively, timing abnormality could be caused by the loss of feedback of cortical projections from M1 to iPMv and cPMv (Dancause et al., 2007; Hamadjida et al., 2016). In any case, our results suggest that brain injuries immediately have a major impact on the timing of neuronal activity in spared cortical areas, across the bihemispheric network. The restoration of proper timing or retuning of the neuronal discharges in these areas may thus be an important contributor to recovery. Along these lines, activity-dependent stimulation was used to resynchronize the neuronal activity of spared motor and somatosensory cortex after brain injury

in rats (Guggenmos et al., 2013). Remarkably, this precisely timed, closed-loop approach contributed more effectively to recovery than stimulation delivered using arbitrary timing, in an open-loop design.

Hemisphere-specific alteration of neuronal activity in PMv

The reorganization of iPMv and/or cPMv activity during movement of the paretic hand is one of the most consistent findings across human imaging studies after stroke (Rehme et al., 2012). The neuronal correlate to this metabolic reorganization is, however, largely unknown. Previous invasive studies have shown that cortical injury can induce bihemispheric neuronal reorganization, with a decrease of responses in the ipsilesional and an increase in the contralesional hemisphere (Sigler et al., 2009; Mohajerani et al., 2011). However, these studies have provided little insight into changes that occur in the motor network during active generation of movements and have been essentially limited to rodents. This is further complicated by the equivocal homology between the rostral motor area in rodents and premotor cortex of primates (Rouiller et al., 1993; Touvykine et al., 2020). Our findings clarify these issues by showing rapid and heterogeneous effects of brain injury on neuronal activity in the premotor cortex of nonhuman primates during the generation of hand movements.

Several of our analyses indicate a decrease of activity in iPMv. This decrease might in part explain the reduction of EMG activity observed during the movement of the paretic hand. However, it is worth nothing that iPMv activity was more affected during movements with the non-paretic arm, for which we found no changes of EMG. This suggests that at least some reorganization in iPMv was because of other factors, such as, for example, a disruption of interactions between neurons within iPMv or with cPMv across the hemispheres. In addition, the decreased firing rate of some iPMv neurons could be caused by changes of interactions with other neurons in distant cortical areas of the grasping network (Davare et al., 2011), also likely affected by the injury.

Among ipsilateral premotor areas, PMv has the most numerous projections to M1 (Dum and Strick, 2005) and bears powerful facilitatory effects on M1 outputs (Cerri et al., 2003; Quessy et al., 2016). Interestingly, several studies in monkeys looking at iPMv in the chronic

phase of recovery after brain injury have reported profound physiological and anatomic reorganization (Dancause et al., 2005; Dancause et al., 2006b; Yamamoto et al., 2019). The contribution of iPMv to recovery has also been supported in pharmacological inactivation studies (Murata et al., 2015). If the decrease of neuronal activity in iPMv persists during recovery, it could thus contribute to impairments of movements with the paretic hand. To counter the acute decrease of activity in iPMv, it may be interesting to deliver excitatory neuromodulatory protocols to this area early after stroke, for example using high-frequency repetitive TMS (Pascual-Leone et al., 1994).

Our data also highlight that, in awake monkeys, the increased neuronal activity in the contralesional hemisphere is movement- and effector-specific. After injury, the firing rate in PMv of both hemispheres was actually lower at rest. The neuronal activity in cPMv was only increased with movements of the paretic hand, at the end of grasp. This timing suggests that it occurred while the monkeys attempted to hold the reward and initiate the movement back to the mouth. The novel activity may thus be caused by a mismatch between the predicted and effective movement (Wolpert and Miall, 1996) or the visual detection of end-point errors (Inoue et al., 2016). If this is the case, it is intriguing that such an error signal would be present in cPMv, but not detectable in iPMv. Regardless of its cause, increased neuronal discharges in cPMv could potentially have negative effects on the generation of paretic hand movements. Inversely to iPMv, cPMv exerts strong inhibition on the production of M1 outputs (Quessy et al., 2016; Cote et al., 2020). The application of inhibitory stimulation protocols over cPMv early after brain injury, for example using low-frequency repetitive TMS (Chen et al., 1997), could thus be a valid strategy to help recovery of hand movements. However, given the specificity of neuronal changes in cPMv, perhaps activity-dependent, closed-loop modulation would be more effective. This could be achieved, for example, using disruptive single TMS pulse to this area (Day et al., 1989) at the end of grasp with the paretic hand.

The impact of rapid neuronal reorganization after brain injury on recovery

Longitudinal imaging studies in both animals and humans tend to support that the initial impact of brain injury is profound, inducing changes across multiple areas in both hemispheres (Dijkhuizen et al., 2003; Rehme et al., 2012). Behavioral recovery is accompanied by a return

toward normal functional connectivity in the network and refocusing of activity in the ipsilesional hemisphere, in particular in M1 (Grefkes and Fink, 2014). It should be kept in mind that these correlational studies provide limited information about the functional role of the changes that take place in the brain. Early changes could reflect negative processes that contributed to impairments. Alternatively, they may reflect rapid adjustments in the circuit to compensate for the neuronal loss caused by the lesion and preserve some residual function. Either way and importantly, the magnitude of early hemodynamic changes correlates with impairments (Weber et al., 2008; Rehme et al., 2011a; van Meer et al., 2012) and has a predictive value for motor recovery (Marshall et al., 2009; Rehme et al., 2015; Hannanu et al., 2017). Early shifts of neuronal activity can thus affect subacute reorganization and, consequently, recovery.

Despite the general trends in the two hemispheres, one striking feature in our data was the heterogeneity of effects across neurons. This diversity likely reflects the complexity of neuronal processing that takes place in PMv (Rizzolatti and Luppino, 2001). The initial impact of the lesion on a PMv neuron may vary with its function before the lesion and the specific interactions it entertained with the site of injury. This heterogeneity may create an unstable state that is particularly malleable, and that offers a window of opportunity for external manipulation. Supporting this view, inactivation of the contralesional hemisphere in rats increased recovery when initiated rapidly after stroke, but failed to do so when longer delays were used (Mansoori et al., 2014; Dancause et al., 2015). Similarly, in humans after stroke, repetitive TMS seems to be more beneficial when started early after the lesion (van Lieshout et al., 2019). With time after injury, shifts in the neuronal population may become more uniform across the area and stabilize, decreasing the potential impact of treatments. Obviously, the progression of neuronal reorganization after brain injury will have to be investigated to verify these hypotheses. However, our data clearly highlight the complexity of the reorganization triggered by acute brain injuries, at the very onset of motor impairments. A better knowledge of these changes will lead to the elaboration of new hypotheses for the design of neuromodulatory strategies that target specific neuronal mechanisms, in different components of the network, to favor recovery.

Chapter 3 – Rapid Reorganization of Neuronal Activity in Contralesional Motor Cortex after Brain Injury

Abstract

After traumatic brain injuries such as the ones caused by stroke, the primary motor cortex (M1) is often damaged leading to motor deficits such as a loss of fine motor skills of the contralateral limbs. Imaging studies have shown that there is atypical hemodynamic activity in spared regions, including the contralesional cortex. However, we have limited understanding of the neuronal reorganization that occurs in this complex and distributed cortical network. We used reversible inactivation techniques in non-human primates to "injure" the M1 hand representation area of one hemisphere while continuously recording neural signals of the intact M1 before and after the onset of behavioral impairments. We also compared the extent of rapid reorganization occurring in M1 with that of the ventral premotor cortex (PMv) of both hemispheres collected in the same series of experiments. The inactivation induced changes in M1 that were heterogenous across neurons and could be observed during reach and grasp movements performed with either the affected or nonaffected arm. However, contralesional M1 neural activity appeared to be particularly resilient to inactivation of its homologue as it was less perturbed, and showed less changes, than the PMv of both hemispheres. Our results provide important insights into the changes that take place within neurons of these different motor areas and suggest that premotor cortex, more so than intact M1, may provide salient targets for the development of neuromodulation protocols applied early after brain injury.

Introduction

The planning and execution of upper limb movements is an extremely complex behavior that involves several motor-related cortical areas (Kalaska et al., 1997; Shadmehr and Wise, 2005) that together form a network, with each area contributing to various extents to different aspects of the movement. Among these areas, M1 is considered to be the main executor of motor actions, boasting the most robust and direct connections with the body's contralateral musculature (Biber et al., 1978; Murray and Coulter, 1981; He et al., 1993, 1995). However, the role of the a given hemisphere is not limited to simply control of the contralateral limb, with many studies showing robust neural activity during ipsilateral arm and hand movements in M1 (Tanji et al., 1988; Donchin et al., 1998; Kermadi et al., 1998; Cisek et al., 2003; Bundy and Leuthardt, 2019). One manner in which this activity could arise is through bihemispheric cooperation with the M1 and premotor cortex in the other hemisphere, connected via the corpus callosum (Jones and Wise, 1977; Jenny, 1979; Gould et al., 1986).

Interestingly, analysis of the ipsilateral and contralateral activity has revealed that there is a notable redundancy of information in the motor cortex of both hemispheres during unimanual arm movements (Ames and Churchland, 2019; Heming et al., 2019). Indeed, the M1 of each hemisphere contain similar information in their neural activity during movement of one arm or the other (Ames and Churchland, 2019; Heming et al., 2019). As such, a given hemisphere contains the necessary motor information to drive movement with either arm. Thus, the neural processes underlying unimanual arm movements appear to involve a great deal of bihemispheric communication and coordination taking place across a large and distributed sensorimotor network.

The perturbation of this network can lead to rapid and widespread changes in activity patterns that extend across both hemispheres. Recently, we demonstrated that unilateral inactivation of the M1 hand area in primates leads to extensive, and much more complex than expected, neural reorganization in the PMv of both hemispheres at the very onset of behavioral impairments (Moreau-Debord et al., 2021). The profound alterations of neuronal discharges were heterogeneous within each and across the two hemispheres and were present during use of both the paretic and non-paretic hand. As this rapid reorganization is likely a consequence of the disruption of the motor network's homeostasis (von Monakow, 1914; Carrera and Tononi, 2014),

we expect that changes of comparable magnitude simultaneously take place in other brain regions interconnected with the site of injury. More specifically, the rapid changes occurring in neurons of the contralesional M1 (cM1) following cortical injury remain to be quantified and are the focus of the experiments reported here.

The reorganization that takes place in the cM1 is likely to be different to what we previously observed in the PMv, as these areas play different roles in hand motor control, and their neural populations encode motor information in different ways. In the PMv, many of the task and motor parameters are encoded bilaterally in a non-effector specific manner (Rizzolatti et al., 1988; Tanji et al., 1988; Hoshi and Tanji, 2002, 2006; Kurata, 2007; Michaels and Scherberger, 2018), such that, for example, grasp type can be encoded the same regardless of which hand will be used to execute the movement. In contrast, M1 neural activity is highly lateralized with effector specific activity, and a dominant preference for the contralateral musculature (Tanji et al., 1988; Donchin et al., 1998; Cisek et al., 2003). As such, while we found substantial reorganization of PMv neural activity in both hemispheres after unilateral M1 inactivation, it is not clear if or what kind of changes will occur in cM1 neural activity. However, we do expect neural reorganization to occur, as numerous fMRI studies have shown that there are important changes in cM1 blood flow taking place following injury to its homologue (Butefisch et al., 2005; Rehme et al., 2011a; Rehme et al., 2012; Buetefisch, 2015).

Characterizing this reorganization is important, as the contralesional M1 has been implicated in recovery processes following unilateral cortical lesions, and many exploratory therapeutic protocols have focused on this area as a main neuromodulatory target (Buetefisch, 2015; Wessel et al., 2015). These interventions seek to modulate cM1 excitability, for example using non-invasive transcranial magnetic stimulation (TMS), with the goal of re-balancing the network's homeostasis and promoting network plasticity towards a functional state capable of appropriately controlling movement. However, little is known about how neural activity in the cM1 changes following unilateral damage to its homologue. As these neural changes reflect the landscape on which subacute plasticity involved in motor recovery will take place, an exploration of the rapid reorganization in neural activity that occurs in cM1 is long overdue.

In the current experiments, we explored the neuronal reorganization that accompanies the loss of fine motor control of the hand in two adult macaque monkeys. We used reversible

inactivation techniques to target the M1 hand representation area unilaterally and induce motor deficits while simultaneously recording neural signals before and after the cortical injury (Wilke et al., 2012)**.** A particular strength of this approach is that it allows the characterization of changes induced by the inactivation in individual neurons in a very powerful and sensitive way (Restani et al., 2009). Whereas previously we reported changes occurring in the PMv of both hemispheres (Moreau-Debord et al., 2021), here we extend these investigations to the cM1. Finally, we compared changes occurring in cM1 and the PMv of both hemispheres to provide a better overall understanding of the neural changes occurring in this distributed, bihemispheric motor network.

Methods

Experimental model and subject details

The present study was performed using two adult female rhesus macaques (*Macaca mulatta*), Monkey M (5.5 kg) and Monkey S (5.7 kg). The surgical and experimental procedures used in the study were done in accordance with the Canadian Council on Animal Care guidelines and approved by the Comité de Déontologie de l'Expérimentation sur les Animaux of the Université de Montréal.

Surgical procedures

Surgical procedures were described previously (Moreau-Debord et al., 2021). We used ketamine hydrochloride (15 mg/kg; Ketaset; Pfizer Inc, New York, NY, USA) to induce anesthesia, which was then maintained using ~2-3% isoflurane (Furane; Baxter, Deerfield, IL, USA) in 100% oxygen. To maintain hydration a solution of lactated Ringer was continuously injected intravenously (10 ml/kg/h). In order to prevent inflammation and swelling of the brain, Atropine (Atropine Sulfide; 0.04mg/kg; Rafter 8 Products, Calgary, AB, Canada) and Dexamethasone 2 (Dexacort 2, 0.5 mg/kg; Rafter 8 Products, Calgary, AB, Canada) were given intramuscularly, and Mannitol 20% (1500 mg/kg; Fresenius Kabi Canada Ltd., Richmond Hill, ON, Canada) was injected intravenously. A self-regulating heating blanket (Harvard Apparatus, Holliston, MA, USA) was used to keep monkey's body temperature near 36.5°C. Furthermore, we monitored heart rate and blood oxygen saturation during the procedures.

Craniotomies and durectomies were performed in both hemispheres over the primary motor cortex (M1) and the ventral and dorsal premotor cortex (PMv, PMd). We implanted multi-electrode arrays in the PMv and PMd of both hemispheres. In addition, in the right hemisphere we also placed electrodes in the M1 and primary somatosensory cortex (S1). In the left hemisphere, in order to provide later access to the M1 hand representation, a chronic chamber made of plexiglass (2x2 cm opening) was placed over the central sulcus and the dura left intact. This chamber allowed us to directly inactivate the left M1 using muscimol injections (see next section). Therefore, the left hemisphere is referred to as the 'ipsilesional' hemisphere, whereas the right hemisphere opposite to the lesion is referred to as the 'contralesional' hemisphere.

Thus, the right hand contralateral to the lesion site was the 'paretic' hand, whereas the left hand was the 'non-paretic' hand. This was the same in both monkeys.

To guide the placements of the arrays we used anatomical landmarks, notably the arcuate and central sulcus. We implanted 370 electrodes in Monkey M and 448 electrodes in Monkey S. For Monkey M, in the ipsilesional hemisphere, we placed one 96-electrode Utah array (Blackrock Microsystems, Salt Lake City, Utah, USA) in the PMd (ipsilesional PMd; iPMd), and one 32-electrode and one 16-electrode Floating Microprobe Arrays (FMA; Microprobes for Life Science, Gaithersburg, MD, USA) in the PMv (ipsilesional PMv; iPMv). In the contralesional hemisphere, we placed one 96-electrode Utah array in M1 (contralesional M1; cM1), two 32-electrode FMAs in PMv (contralesional PMv; cPMv), and two 32-electrode FMAs in PMd (contralesional PMd; cPMd). For Monkey S, in the ipsilesional hemisphere we placed one 96-electrode Utah array as well as two 32-electrode FMAs in the iPMd. For the contralesional hemisphere, in each of the cM1 and cPMv we placed one 96-electrode Utah array. We placed two 32-electrode FMAs in cPMd. Finally, we also placed one 32-electrode FMA in S1. The present analyses concern signals obtained from arrays implanted in the cM1.

At the end of each surgery, to prevent infection and brain swelling monkeys were given Baytril (5 mg/kg; Enrofloxacin, Bayer Inc., Mississauga, ON, Canada) and injected with Dexamethasone 2 (0.5 mg/kg; Dexacort 2, Rafter 8 Products, Calgary, AB, Canada), respectively. To prevent inflammation and pain, they were also given Carprofen (4 mg/kg; Rimadyl, Zoetis Canada Inc., Kirkland, QC, Canada) and Buprenorphine (5 µg/kg; Temgesic, Schering-Plough, Kenilworth, NJ, USA), respectively. Based on the recommendations of the veterinarian, additional doses of both Baytril and Carprofen were given for a minimum of two days or more after the surgery.

Behavioral task

The neural recording sessions were performed in the laboratory. Monkeys sat in a custom-made primate chair that was brought to the laboratory and placed in front of a pellet retrieval task. To allow the monkeys to use one hand or the other during the task, the chair had removable panels on both sides. In addition, there was an opening in front of the mouth in order for the animals to

consume food rewards. With regards to the pellet retrieval task, the pellet rewards (190 mg Dustless Precision Pellets; BioServ, Flemington, NJ, USA) were placed in a small well located behind a vertical slot (1.3 cm x 5.5 cm) that was 20cm away from the monkeys and ~10 cm below the shoulder height. In order to obtain the rewards, the animals had to perform a reaching movement with the left or right hand in different blocks of trials that cumulated in a precision grip (opposition of the thumb and index) with the forearm pronated. To collect video recordings of the behavioral task, a computer webcam was placed above the animal and another on their left side. We used a TDT acquisition system with two RZ2 BioAmp processors and custom software to control the task (Tucker-Davis Technologies (TDT), Alachua, FL, USA).

In order to perform the task one or the other side panel on the chair was removed, which determined which hand would be used. To start each trial, monkeys were instructed to place their hand on the home plate in front of them, 15 cm below the vertical slot, which served as the target of the reach and grasp movement. An infrared laser sensor contained within the home plate detected the presence of the hand. The progression of a given trial is shown in Figure 2.1. Following a variable delay period of 0.8-2 s, a pellet distributor (80209 Pellet Dispenser, Campden Instrument Ltd.) dropped a pellet into the well located behind the vertical slot. The sound made by the pellet distributor as it released the pellet served as a GO cue for the animal to initiate a self-paced reach towards the target. The animal had two seconds to initiate the reach, and the onset of the reach was signaled by the hand moving out of the home plate by the infrared sensor. The slot contained a second infrared laser sensor, which signaled when the hand entered the target to grasp the pellet (grasp onset) and left the target with the pellet (grasp offset). Having exited the target, the monkey then brought the pellet to its mouth to consume the reward before re-placing its hand in the home plate to start the next trial. There was an interval of 3 seconds between trials.

For a given recording session the animals performed a block of 25 trials first with the left hand and then another block of 25 trials with the right hand, for a total of 50 trials. Subsequently, following inactivation with muscimol (see below), an additional recording session was conducted where animals performed two more blocks of trials in the same order, i.e. first one with the left and then with the right hand. Each recording session took about 10 minutes to complete.

Muscimol inactivation experimental procedures

After the animals recovered from the implantation of the cortical arrays and the plexiglass chamber, we confirmed the location of the left M1 hand representation area using intracortical microstimulation (ICMS) trains during the first two recording sessions. To do so we used a custom-made borosilicate glass coated tungsten electrode. The electrode was lowered into the chamber while the animal waited calmly in the primate chair. ICMS trains consisted of 13 monophasic cathodal pulses of 0.2 ms at 350 Hz, delivered at 1 Hz (Dancause et al., 2008). We used ICMS to determine the borders of the M1 hand representation area, which included sites that evoked forelimb movements including those of the wrist and digits. We determined the depth at which the lowest stimulus intensity was required to evoke a movement in the hand area, and these sites and depths were used to guide the muscimol injections.

The present analyses include data obtained from a total of 13 inactivation experiments (N = 6 from Monkey M, N = 7 from Monkey S). Of these experiments, most involved one injection of 0.75 µL of muscimol, a GABA-A receptor agonist (5 mg/ml) in the hand area of the left hemisphere (n = 9, 4 from Monkey M, 5 from Monkey S). In addition, for each monkey we also included an addition experiment where muscimol was injected at two sites (2 × 0.75 µL) and another experiment where muscimol was injected at three sites (3 × 0.75 µL), always in the hand area (Figure 2.1).

Each inactivation experiment contained a “Pre-inactivation” and “Post 0.5 h inactivation” data collection session. In the Pre-inactivation session we recorded baseline behavioral performance and neural data, where animals were required to perform a block of 25 trials with the left hand and then another block of 25 trials with the right hand. Once these two blocks were completed, muscimol was used to reversibly inactivate the M1 hand representation area via a 5 µL Hamilton syringe with a beveled 26 gauge needle (Hamilton Company, Reno, NV, USA) held in place by a micromanipulator (David Kopf Instruments, Tujunga, CA, USA) with stereotaxic frame that was affixed to the primate chair. Once properly positioned, 0.75 µL of muscimol was injected at a rate of 4 nL/s with a microinjector (Harvard Apparatus, Holliston, MA, USA) at each cortical site and at different depths as informed by the previously-collected ICMS data (range ~4.5-7 mm from top of the dura). Once the injection of muscimol complete

(roughly thirty minutes after the start of the injection), as part of the Post 0.5h inactivation data collection session monkeys performed two additional blocks of 25 trials, first with the left and the right hand. As the animals showed some clear deficits with the right hand, they were still able to perform at least some trials successfully with that hand. Importantly, the neural activity was recorded continuously throughout the inactivation experiments, i.e. during the Pre-inactivation session, the injection of muscimol, and the Post 0.5 h session. Following this last session the animals were returned to their home cage and provided with water ad libitum. There was always a minimum of 72 hrs between subsequent inactivation experiments, and all deficits were resorbed by the following day after an inactivation.

Neural recordings and identification of neurons

We recorded neural activity from 256 channels simultaneously during a given experiment, which was the maximum possible with our equipment. Thus, in different experiments we focused on different areas and arrays to sample all implanted electrodes. In the current analyses we focus on recordings that involved the arrays implanted in cM1. The neuronal data was sampled at 24,414.1 Hz, band-pass filtered between 100 and 5000 Hz, and recorded digitally using a Tucker-Davis Technologies acquisition system (Tucker-Davis Technologies Inc, Alachua, Florida, USA). As part of the acquisition process during the recording session, on all channels an automatic threshold (x4 SDs above the baseline noise) was set and locked in place that when crossed led to a 1228μs suprathreshold waveform sample being saved. These waveforms were then sorted offline using Plexon Offline Sorter (Plexon Inc, Dallas, Texas, USA) using principal component analyses. Using the first 3 principal components, we determined whether the waveform cluster of each unit could be categorized as “well-isolated”, i.e. whether it was clearly separate from the other recorded signals. The well-isolated status of each cluster was verified by confirming that its stability and isolation was maintained throughout the recording by plotting the first 2 principal components over time. Only well-isolated and verified M1 units are included in the analyses presented here, and none of them had a refractory period violation (0%) based on an inter-spike interval of $\leq$1ms either before or after inactivation.

Task epoch modulation of individual neurons

We produced heat plots of the discharge rates of neurons aligned on the onset of grasp in order to provide an overview of the discharge pattern of the total population of neurons (Figure 3.2). As part of these plots, to highlight when neurons had their peak discharge, for each neuron the spike density estimate (SDE) of spike discharge at each moment in time was divided by the average SDE across the time window of interest (-1 to 1 s around Grasp Onset). The different epochs of the task were the pre-cue, post-cue, reach and grasp epochs. The pre-cue epoch ranged from -0.7 to -0.1 s before the Go cue. The post-cue epoch was the first 0.1 s following the GO cue. The reach epoch ranged from -0.1 to 0.2 s from Reach Onset, when the monkey's hand left the home plate. Finally and most importantly, the grasp epoch ranged from -0.1s before the fingers entered the slot (Grasp Onset) to 0.1 s after the fingers had left the slot with the pellet (Grasp Offset). To determine whether neurons were modulated by one or more epochs of interest, we compared the firing rate during the post-cue, reach, grasp to the average firing rate during the pre-cue epoch using two-tailed *t* tests. Because the grasp epoch encompasses both the Grasp Onset and Grasp Offset events, to determine whether neurons were modulated the *t* test was performed on spike times aligned on each event separately for some analyses. The two windows of time used were -0.1 to 0.5 s from Grasp Onset, and -0.2 to 0.1 s from Grasp Offset. A neuron whose firing rate was modulated according to the *t* test ($p < 0.05$) within either of these windows was considered tuned to grasp during that block of trials. Finally, we calculated SDEs of the firing rate across trials using a Gaussian kernel function of 50 ms for each neuron (Nawrot et al., 1999), with spike times aligned at Grasp Onset to visualize task modulation.

Effect of inactivation on the total population of recorded neurons

We explored the changes in the general discharge rate of neurons when the animals were at rest (Figure 3.4 A). To do so we looked at the firing rate of M1 neurons before (Pre) and after (Post 0.5 h) inactivation during the pre-cue epoch where the animal was at rest with either hand placed in the start position. This was done for each neuron by determining the mean firing rate during the pre-cue epoch that took place during the block of trials with the right or left arm, during the pre or post 0.5 h inactivation session. Furthermore, we explored the changes that occurred in the proportion of neurons identified as being modulated during grasp (see above) before and after

inactivation as well as the proportion of grasp neurons that were modulated for both hands or only the left or right hand specifically (Figure 3.4 B,C). For these analyses we used all neurons, without taking into consideration whether neurons were the same well-isolated units in both the pre and post 0.5 h sessions.

Quantification of changes within continuously recorded neurons before and after inactivation ('within-neuron' analyses)

From this point on, all the analyses were performed using neurons that were clearly isolated both before and after the inactivation, which we refer to as 'within-neuron' analyses. Since there were differences in grasp duration before and after inactivation as well as within a given trial block, the duration of grasp was normalized for all of our 'within-neuron' analyses (Figures 3.5-3.10). To do so, we resampled the SDE of each trial such that time became visually represented as a percentage (%) of grasp completed, using a value of "0" for the time of Grasp Onset and "100" for the time of Grasp Offset. In normalized time each time bin represented $1/1000^{th}$ (0.1%) of total grasp duration. Finally, for each neuron we subtracted baseline activity from the resampled SDE curves. Baseline activity was calculated using the mean trial SDE during the pre-cue epoch for a block of trials.

Incidence of neurons with increases and decreases of discharge rate during grasp

We determined the proportion of neurons with increases and decreases of activity during grasp following inactivation (see Figure 3.5). For each neuron and at each moment in normalized time we subtracted the Post-inactivation SDE values from the Pre-inactivation SDE values to determine whether neural discharge had increased or decreased following the inactivation. Furthermore, we determined the proportions of neurons that showed substantial, i.e. 'significant', increases or decreases of discharge at each moment during grasp using unpaired *t* tests on the SDE values of trials performed before and after inactivation. To provide an additional, complimentary quantification of increases or decreases of neural activity throughout grasp, we also calculated the cumulative sums of neurons that had higher and lower firing rates after inactivation at each moment in time using the formula:

$$Cumulative\ sum = \sum_{i=1}^{n} \frac{Neurons\ higher(i) - Neurons\ lower(i)}{Total\ neurons\ x\ 1200}\ x\ 100$$

Where *i* is the time bin, which ranges from 1 to the total number of time bins per trial considered for this analysis, n = 1200 (1000 bins for grasp duration, plus the last 100 bins before grasp onset, and the first 100 bins after grasp offset). *Total neurons* represent the total number of neurons in the population studied. *Neurons higher* and *Neurons lower* were the number of neurons with higher or lower firing rates after inactivation relative to Pre-inactivation values, respectively, at time *i*, and regardless of whether neuron changes were significant or not. The cumulative sum is expressed as a percentage of the maximum sum of neurons if they had all shown increases, i.e. it represents the total number of neurons if only increases of discharge had occurred in all neurons of the population throughout grasp. A positive value of the cumulative sum means that there was a greater proportion of neurons with increased activity than neurons with decreased activity as grasp progressed, meaning that there was an overall increase of activity after inactivation in the population of neurons studied. In contrast, negative values indicate that there was a greater proportion of neurons with lower activity than higher activity after the inactivation as grasp progressed, meaning that there was an overall decrease of activity in the neural population after inactivation.

We used Monte Carlo methods in order to provide a better visualization of the effect of the inactivation on the cumulative sum traces by comparing them to what would be expected to be observed by chance. To do so, for each neuron, first the firing rate at each time bin in both the Pre-and Post-inactivation blocks of trials were pooled together. Then we randomly sampled data points with replacement from these pooled values to generate two new but artificial SDE traces. These two SDE traces were subtracted from each other to calculate the increase or decrease of firing rate at each time bin. This process was done for all neurons and for a given block of trials (non-paretic, paretic hand). At this point the cumulative sum of this simulated population was calculated. This provided one artificial cumulative sum trace for the neural population studied during use of a given hand. We repeated this process to generate 1000 cumulative sum traces, and determined the mean and 95th percentile from these 1000 traces to compare them to the real values shown in Figures 3.5 and 3.8.

We compared the incidence of 'significant' neurons showing increases or decreases of activity during grasp between the area studied here (cM1) and those studied previously (iPMv,

cPMv; Moreau-Debord et al., 2021), shown in Figure 3.8. We chose to perform this analysis using three windows of interest: the start of grasp (the last 100 bins before grasp onset and the first 100 bins after grasp onset), the end of grasp (the last 100 bins before grasp offset and the first 100 bins after grasp offset), and the total grasp duration (1000 bins for grasp duration, plus the last 100 bins before grasp onset, and the first 100 bins after grasp offset). For each neuron and at each trial, we took a mean of their activity before and after inactivation across the time bins of interest and used unpaired *t* tests ($p < 0.05$) on the mean trial values to determine if the neuron showed a 'significant' increase or decrease of discharge rate during the window of interest. We then summed the numbers of neurons showing 'significant' increases of decreases of discharge rate.

Changes of maximal discharge time

We determined the time of maximal discharge rate during the task before and after inactivation in a window centered around grasp duration (-100% to 150% of grasp duration; the window of time used for Figure 3.6 A). For each within-neuron and during use of a given hand we subtracted the time of maximal discharge before and after inactivation to quantify the change in maximal discharge timing, to provide a measure of the stability of neural discharge timing during the task (Figure 3.9).

Changes of peak discharge burst rate

We were interested in further exploring changes in peak discharge rate of neurons that specifically had a burst of activity during the grasp epoch of the normalized SDE curves (Figures 3.6, 3.10). For a neuron to be considered to have a peak of discharge rate during grasp, it had to have a maximal discharge value during the grasp epoch >1 standard deviation (SD) from baseline (i.e. pre-cue epoch) either before or after inactivation.

Neurons could have peaks of discharge rate at different movements during the grasp epoch before inactivation compared to after inactivation. As such, for analyses of burst rate (Figures 3.7, 3.10), we characterized the time and the amplitude of peak discharge in both the pre and post 0.5 h recording sessions when present. For neurons with grasp peaks during the pre-inactivation session, we took the firing rate at the time of the Pre-inactivation peak (Pre Peak) and compared it to the firing rate that took place at the same moment in normalized time in the

Post 0.5 h inactivation session. We then averaged these changes across the population of neurons. This analysis focuses on the change of activity that took place where the neuron had been most active prior to inactivation, and thus emphasizes decreases of neural activity. We performed a similar analysis for neurons with grasp peaks during the post 0.5 h inactivation session. For those neurons we compared the firing rate at the time of peak discharge in Post 0.5 h (Post 0.5 h Peak) to the firing rate that occurred at that moment in normalized time during the pre-inactivation session. We then averaged those changes across the population of neurons. This analysis focuses on the change of activity that took place where neurons became most active following the inactivation, and thus emphasizes increases of neural activity.

Statistical Analysis

Quantification of muscimol effects on the total population of recorded neurons

To determine which neurons were significantly modulated during which task epochs, we used paired *t* tests ($p < 0.05$). To explore changes in the discharge of neurons at rest, we compared the mean activity that occurred during the pre-cue epoch (-0.7 to -0.1 s from Cue) using a two-way ANOVA for the cM1 with the arm and session as factors. To compare the proportion of neurons modulated during grasp, or in function of the hand used, we used χ^2 tests ($p < 0.05$) and performed post-hoc tests using two-proportion *Z* tests with Bonferroni correction (Figure 3.4).

Quantification of changes within continuously recorded neurons

To compare differences between populations (iPMv, cPMv, cM1) in the incidence of neurons showing increases or decreases of neural activity during grasp, we used χ^2 tests ($p < 0.05$) and performed post-hoc tests using two-proportion *Z* tests with Bonferroni correction (Figure 3.8). To compare the variance of maximal discharge time that occurred after inactivation between the different populations of neurons, we used Bartlett's test for equal variances and performed post-hoc tests using two-sample *F* tests with Bonferroni correction (Figure 3.9). We used paired *t* tests to compare the peak discharge rate of neurons before and after inactivation (Figures 3.7, 3.10). To compare the changes in discharge rate that occurred during the time of peak discharge between the different populations of neurons, we performed two-way repeated measures ANOVAs, one for 'Pre peaks' (discharge rate at the time where neurons were most active prior

to inactivation) and one for ‘Post peaks’ (discharge rate at the time where neurons became most active after the inactivation) where the independent factors were area (iPMv, cPMv, cM1) and arm (non-paretic, paretic) and the dependent factor session (pre-inactivation, post 0.5 h inactivation). We also performed a one-way repeated measures ANOVA specifically on Post peaks during use of the paretic hand, using area and session as factors.

Results

For these series of experiments, two adult female rhesus macaques were trained on a reach-to-grasp task that cumulated in a precision grip with the right or left hand in order to retrieve food pellets from a well. For the purposes of neural recordings, both monkeys were implanted in the right, contralesional M1, using chronic electrode arrays. Furthermore, a plexiglass chamber was placed over the left M1 to provide access to the dura in order to directly inject muscimol via syringe into the M1 hand representation area in awake behaving animals. Following implantation, we used intracortical microstimulation (ICMS) to locate the hand representation in the chamber before performing inactivation experiments. Each inactivation experiment proceeded thustly. First, we recorded the neuronal activity prior to inactivation as animals *p*erformed the task (i.e., recording session Pre). We then induced a reversible inactivation by injecting muscimol, a GABA-A receptor agonist, into the hand area of the left M1. Here, the right M1 was contralesional ('cM1') in the opposite hemisphere (Figure 3.1). Following approximately 30 minutes after the injection of muscimol, the monkey resumed performing trials as deficits appeared (i.e. recording session Post 0.5 h). Because recording was performed continuously throughout this process, we were able to quantify the effect on the inactivation on individual neurons (i.e. 'within-neurons').

As previously discussed (Moreau-Debord et al. 2021), both monkeys displayed clear deficits with the right, 'paretic' hand contralateral to the inactivated M1 during the Post 0.5 h session, consistent with previous reports that used similar inactivation techniques (Matsumura et al., 1991; Schieber and Poliakov, 1998; Brochier et al., 1999). As these results were presented earlier in chapter 2, they will not be discussed in detail here. Briefly, both reaching and grasping movements became slower with the paretic hand (Figure 2.2), and this was accompanied by decreased EMG in muscles of the paretic arm (Figure 2.3). Notably, no changes in EMG or movement duration occurred in the left, non-paretic arm, and no activity was observed in the arm at rest when the other arm was performing trials. Deficits were completely resorbed by the next day.

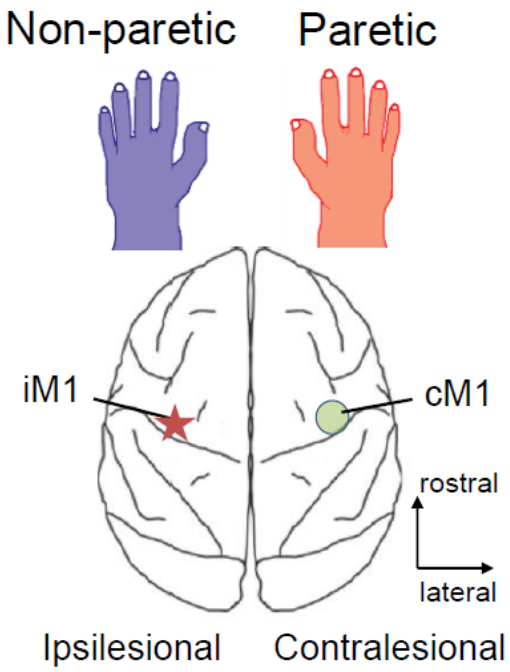

Figure 3.1. *Experimental overview*

Schematic representation of the location of the cM1 recorded area as well as the paretic and non-paretic hand relative to the location of the left M1 inactivation (iM1).

The population of neurons recorded in M1 in the control condition

The neural data discussed here comes from 13 inactivation experiments. Altogether, from the data obtained prior to the inactivation of M1 during the experiments (i.e. session Pre) we identified a total of 164 'control' M1 neurons in the right hemisphere.

We characterized the population of M1 neurons recorded by our arrays in an identical fashion as what was done for PMv previously (Figure 3.2). Specifically, we determined the preferred epoch and hand of each neuron as well as determining their modulation patterns across epochs using maximal discharge rate and *t* tests ($p < 0.05$), respectively. While neurons were active throughout the task, they showed a greater preference for grasp in maximal discharge rate (53.7% across both hands; Figure 3.2 C) and significant modulation (82.3% across both hands; Figure 3.2 D). In addition, there was a greater preference in neural activity for the contralateral limb. Notably, almost half of all M1 neurons maximally discharged during grasp with the contralateral hand (49.4% of neurons; Figure 3.2 C). This result is not surprising, as M1 is known for showing a much greater lateralization of function for the contralateral musculature. Nonetheless, when looking at modulation patterns, we see that the ipsilateral limb is still well represented in the M1 population (51.8% of neurons during grasp with ipsilateral hand; Figure 3.2 D), consistent with the fact that M1 has robust ipsilateral activity (Tanji et al., 1988; Donchin et al., 1998; Kermadi et al., 1998; Cisek et al., 2003; Bundy and Leuthardt, 2019).

Most grasp-related neurons were significantly modulated during movements of either hand, such that they were 'hand non-specific' (55.6% of M1 grasp neurons; Figure 3.2 E). Among grasp-neurons that were only modulated during use of one hand, there was a clear preference for the contralateral hand (37% contralateral vs 7.4% ipsilateral), consistent with the high lateralization of hand function of this area.

Modulation patterns of all recorded neurons are remarkably preserved after inactivation

Following the injection of muscimol into the left M1 hand representation area, we identified a total of 163 well-isolated post-inactivation neurons in cM1. We observed changes of neural activity in individual neurons due to the unilateral M1 inactivation (Figure 3.3). Notably, changes in neural activity were heterogeneous, with both increases and decreases of neural

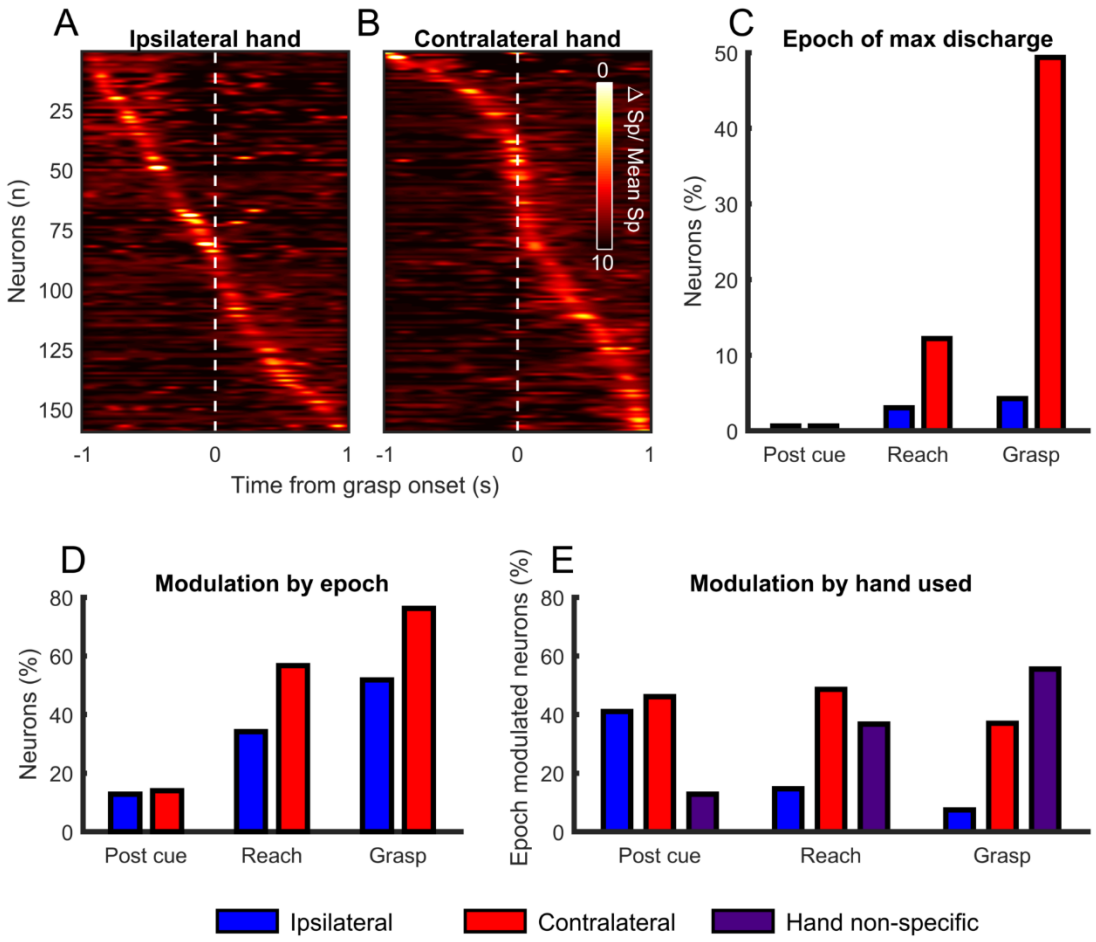

Figure 3.2. *Population of control neurons recorded in the cM1*

Data is pooled from both monkeys. ***A,B,*** Shown are heat plots of the spike density estimates for all M1 neurons during task performance with the ipsilateral (***A***) and contralateral hand (***B***). For each hand, neurons are ordered according to the time of maximal discharge relative to Grasp Onset. Time is in seconds (s). ***C,*** The proportion of neurons that had their maximal discharge occur in the different epochs of the task during use of the ipsilateral or contralateral hand are shown. Note that categories are mutually exclusive, such that each neuron is only counted once. ***D,*** Shown are the proportion of neurons with a significant modulation of their discharge rate during the different task epochs (*t* test; $p < 0.05$). Here, categories are not mutually exclusive such that a given neuron could be counted in several epochs and for both arms. ***E,*** For each epoch are shown the proportions of neurons that were significantly modulated during use of the ipsilateral or contralateral hand only, or for both hands (i.e. hand non-specific) during that epoch. Overall, these plots demonstrate that while different proportions of neurons in the M1 were active for the different epochs of the task and for both arms, there was a greater proportion of neurons modulated during grasp and for the contralateral arm.

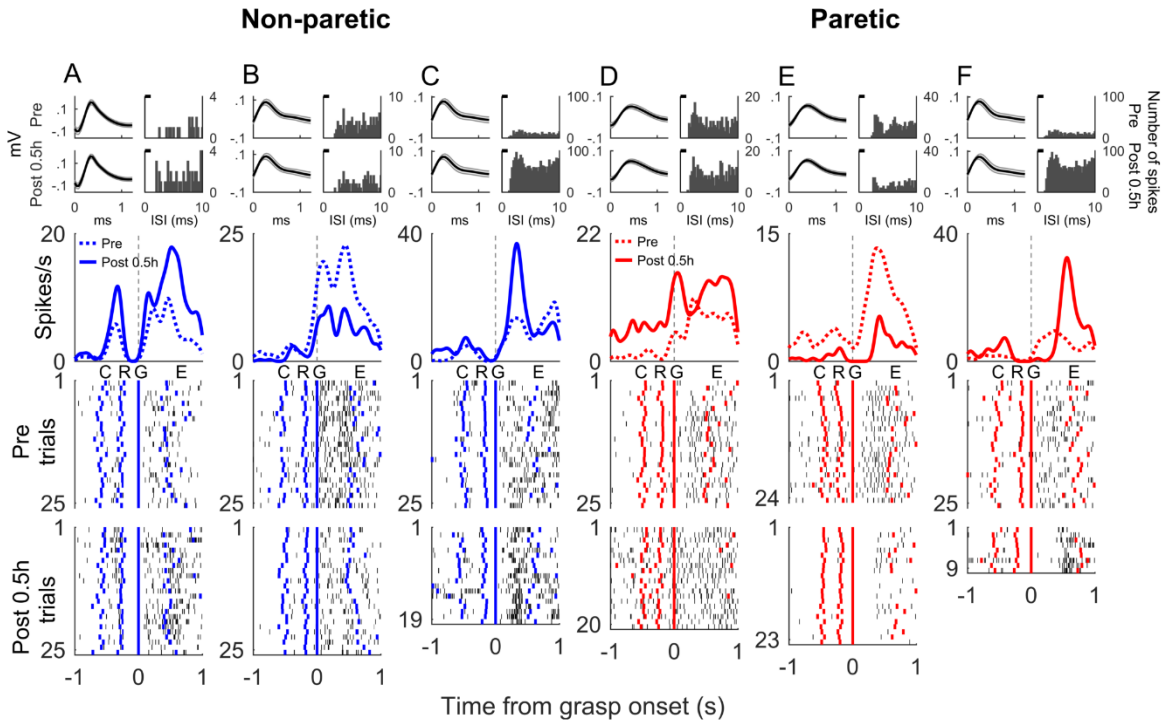

Figure 3.3. *Examples of cM1 neurons that showed altered patterns of discharge after inactivation*

Shown are neurons recorded during use of the non-paretic (***A-C***, blue) and paretic (***D-F***, red) hand. For each neuron the top panel shows the average spike shape on the left (±SD, grey shading) and the interspike interval count histogram on the left, both before (top) and after inactivation (bottom). The middle panel shows the spike density estimate (SDE) curves of discharge rate before and after inactivation. Below that (bottom two plots), the raster plots of individual trials before (Pre) and after inactivation (Post 0.5 h) are shown. All data is aligned on the time of Grasp Onset, and the time is in seconds (s). In the raster plots, the colored markers show the timing of the events in each trial (C=GO cue; R= Reach Onset; G= Grasp Onset; E= Grasp Offset). There was a great variability in the nature of the changes observed that took place during use of either hand.

discharge rates observed in cM1 neurons during use of either hand. These changes could occur throughout the different epochs of the task, but were often observed during grasp, suggesting that neural activity was particularly disturbed during hand use.

To determine how the overall neural cM1 population was affected by the inactivation, we compared the population of 'control' neurons (i.e., pre-inactivation) with the population of post-inactivation neurons (Figure 3.4). Here, no consideration was made as to whether these populations contained neurons present in both pre- and post-inactivation sessions (i.e. not limited to within-neuron analyses). We first determined whether the inactivation had an effect on M1 neurons when the animals were at rest (Figure 3.4 A). To do so, we looked at the firing rate of neurons during the pre-cue epoch, where the animal was not moving with its hand placed on the home plate. There was no difference in discharge rate regardless of which hand was placed in the start position and when comparing activity before and after inactivation (two-way ANOVA, $p > 0.05$). Thus, in contrast to what we previously reported for PMv, where we found that firing rate during the pre-cue period was significantly lower after inactivation ($p < 0.001$; see Chapter 2), the inactivation did not produce any alterations in the cM1 at rest.

Similarly, during movement, the proportions of cM1 neurons modulated during grasp appeared particularly stable despite inactivation of its homologue ($p<0.05$) (Figure 3.4 B). Furthermore, there were no significant changes in the proportions of grasp neurons modulated during use of either or both hands ($p < 0.05$) (Figure 3.4 C). This is again in contrast to what was previously reported for PMv, where important changes at the population level were reported, notably with regards to through neurons. Thus, at the population level, cM1 appears to be particularly stable and relatively unperturbed by the inactivation.

Increases and decreases of firing rate in individual neurons during grasp

We chose to perform continuous recording before and after the inactivation in order to quantify the changes occurring within individual, well-isolated neurons throughout each inactivation experiment. This allowed us to perform 'within-neuron' analyses, which form the greatest strength of our data. In total, 154 cM1 neurons were considered to be within-neurons. From this point on, all analyses will focus on this subpopulation of neurons.

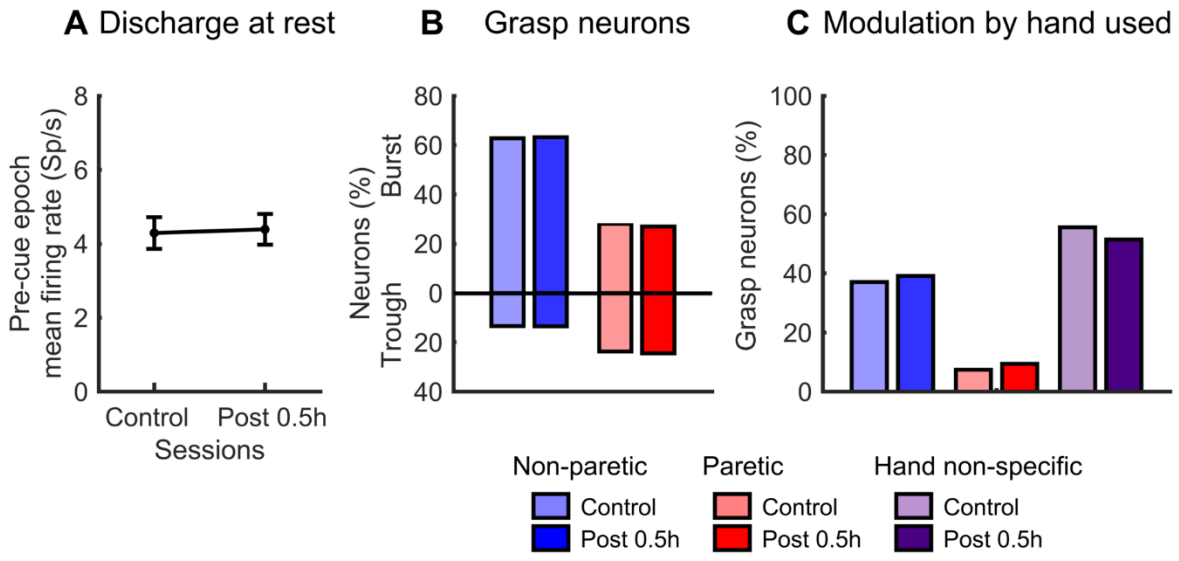

Figure 3.4. *Neuronal cM1 population is stable after inactivation*

A, Shown is the average discharge rate (±SEM) of all cM1 neurons at rest during the pre-cue epoch where monkeys waited with either hand in the start position for the cue to initiate the movement. There was no change in the discharge rate at rest (Sp/s: spikes per second). ***B,*** Shown are the proportion of grasp modulated neurons (*t* test $p < 0.05$) in the cM1 during use of the non-paretic (blue bars) and paretic hand (red bars). Above the x-axis are shown the proportion of neurons with bursts (i.e. increased discharge rates during grasp) and below the x-axis are shown the proportion of neurons with troughs (i.e. decreased discharge rates during grasp). There were practically no changes in the proportion of cM1 burst or trough neurons after inactivation. ***C,*** The proportion of grasp neurons modulated only during use of the non-paretic or paretic hand or modulated during use of either hand (hand non-specific) are shown. We did not observe any significant changes in these proportions after inactivation. Overall, the cM1 was resilient to the inactivation at the population level, such that it appeared unperturbed.

We first quantified the incidence of neurons that showed increases or decreases of neural discharge rate at each moment in normalized time of the grasp epoch (Figure 3.5). We used all within-neurons regardless of whether they were significantly modulated during grasp or not. There was a greater proportion of neurons with decreased discharge rate that accumulated with time in the cM1 during use of the paretic hand (Figure 3.5 B). Changes were less conclusive during use of the non-paretic hand, with cumulative changes alternating directions during grasp such that by the end of grasp the proportion of neurons showing increases or decreases of discharge completely balanced each other out.

Changes of peak timing in individual neurons following inactivation

We quantified the extent to which the timing of peak discharge during grasp of cM1 within-neurons were affected by the M1 inactivation (Figure 3.6). We used all within-neurons regardless of modulation. We found that the timing of peak discharge was perturbed for many neurons, and these changes were more pronounced during movements with the paretic hand (Figure 3.6 A). We then specifically quantified the changes of peak discharge timing of neurons that had a clear burst of discharge rate during grasp (>1 SD increase relative to pre-cue epoch activity). The M1 inactivation induced an important de-synchronization of neural activity related to the various aspects of grasp movements, particularly during use of the paretic hand (Figure 3.6 B).

Furthermore, we observed that there were many neurons that displayed a significant peak grasp discharge in either the pre or post 0.5 h inactivation session, but not in both sessions (grey crosses in Figure 3.6 D-F). This was particularly so during grasp with the hand *ipsilateral* to cM1, i.e. the paretic hand for the cM1 (n = 28, 45.9%). There was not a substantial difference in the proportion of neurons 'losing' their pre-inactivation peaks or 'gaining' a peak after inactivation. It is interesting to note that the cM1 showed a relatively preserved pattern of peak discharge during use of the non-paretic hand. Indeed, among neurons with significant bursts during grasp with the non-paretic hand, most cM1 neurons showed stable timing of peak discharge in both sessions (Figure 3.6 B). Furthermore, there were few neurons that 'lost' or 'gained' peaks of discharge during grasp with the non-paretic hand (n = 20, 17.7%).

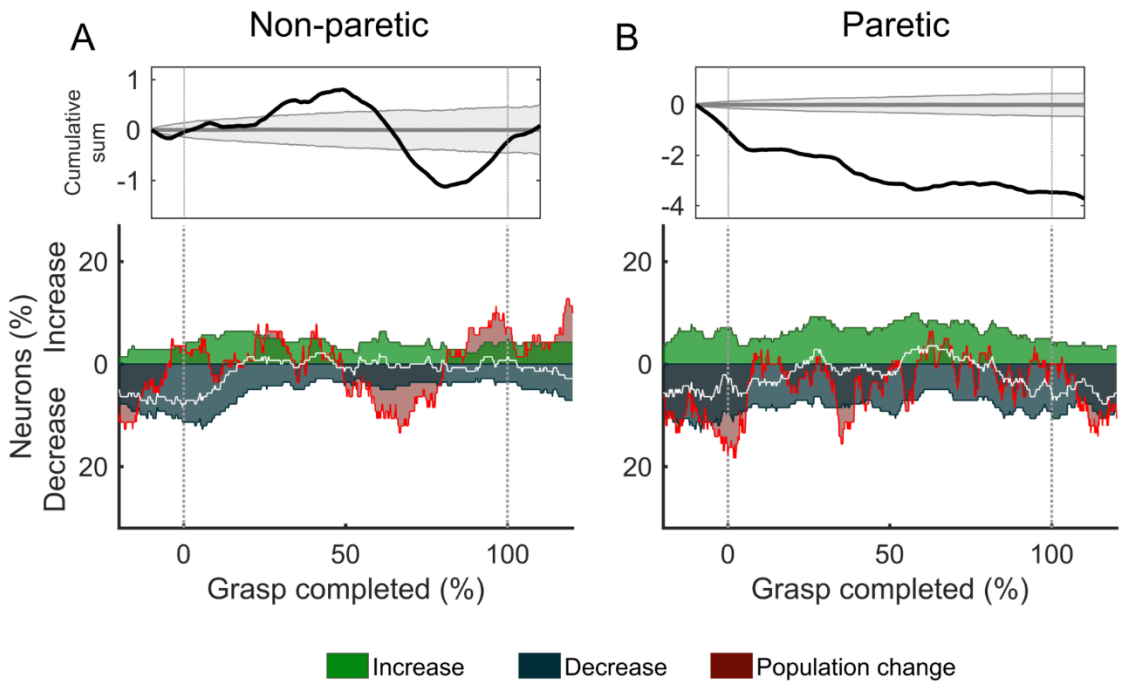

Figure 3.5. *Incidence of neurons showing increases or decreases of discharge rate during grasp*

A,B, Shown are the changes of firing rate of cM1 neurons during grasp with the non-paretic (***A***) and paretic hand (***B***). Time is represented in normalized grasp time (Grasp Onset = 0%, Grasp Offset = 100%). In this analysis, all neurons that were well-isolated both before and after inactivation were included, regardless of whether they were modulated during grasp or not (n = 154). In the top plots of each panel, shown is the cumulative sum of the difference between the total population of neurons with increases versus decreases of firing rate across the time bins (black trace). These traces are compared to the mean and 95% quantiles of randomly simulated values using Monte Carlo methods (grey line and shadow). In the bottom plots of each panel, the percentage of neurons with 'significant' increases (green) or decreases (grey-blue) of discharge rate at each time bin during grasp are shown (unpaired *t* tests with $p < 0.05$; see Methods). Also shown is the difference in the proportion of the neurons with 'significant' increases versus decreases of activity (white trace). Finally, the red line and shaded area show the same difference as the white trace but instead using all well-isolated neurons regardless of whether their changes were 'significant' or not. During use of the non-paretic hand, the accumulation of neurons with increased discharge rate were counterbalanced by the accumulation of neurons with decreased discharge rate, such that by the end of grasp there was no bias in the overall cM1 population. In contrast, we observed an accumulation of neurons with decreased discharge rate during grasp with the paretic hand.

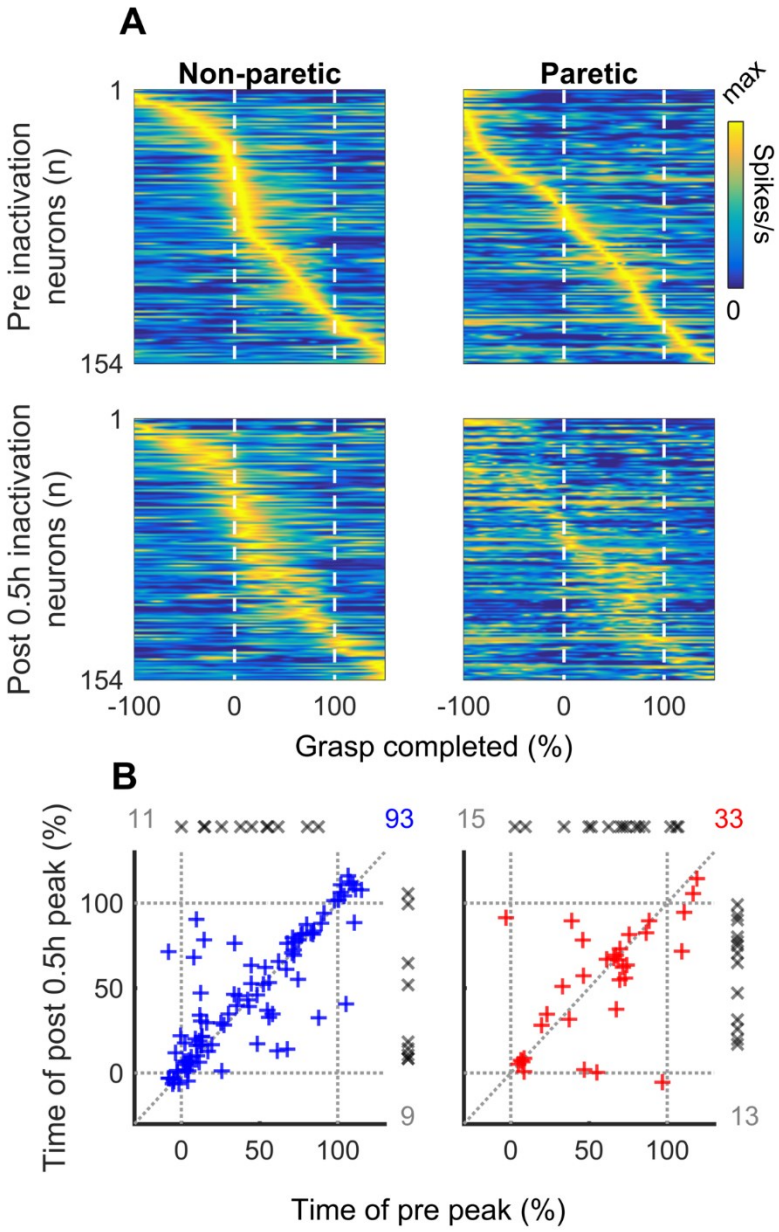

Figure 3.6. *Changes in the timing of peak discharge rate after inactivation*

A, Shown are heat plots of the spike density estimates of all the neurons that were well-isolated both before and after inactivation (i.e. 'within-neurons') in the cM1. The x-axis represents normalized grasp time (Grasp Onset = 0%, Grasp Offset = 100%). The left panels show neural activity during movements with the non-paretic hand, and the right panels show neural activity during use of the paretic hand. In the top row, neurons are ordered based on the time of their maximal discharge before inactivation. This same order is kept in the bottom row, which represents their activity after inactivation during the Post 0.5 h session. The discharge rate of

each neuron is normalized to its maximal value. ***B,*** Shown are the peak discharge times of cM1 neurons that had a clear discharge burst during grasp, before inactivation ('Pre peak', x-axis) and/or after inactivation ('Post 0.5 h peak', y-axis). The colored symbols (+) show the neurons that had 'significant' bursts during grasp both before and after the inactivation (>1 SD increase from pre-cue epoch) during use of the non-paretic (blue) or paretic hand (red). In addition, the blue and red colored numbers show the counts of these neurons. Finally, we also had neurons that only had a 'significant' burst during grasp either before or after inactivation, but not for both sessions. These neurons are shown with grey x symbols and numbers, and plotted along the axes. Overall, we observed that the inactivation affected the temporal pattern of neurons' timing of peak discharge. However, maximal discharge timing (***A***) and peak timing (***B***) appeared to be more perturbed during use of the paretic than non-paretic hand.

Changes of peak amplitude at the time of peak discharge of individual neurons

We explored the changes in the amplitudes of neural discharge that occurred at the time of peak discharge rate during grasp of individual neurons. Since we observed important drops as well as additions in the count of neurons with a significant peak after inactivation, we quantified the changes in discharge rate that occurred before and after inactivation at both the peak discharge time during grasp prior to inactivation ('pre peaks') as well as the peak discharge time during grasp after inactivation ('post 0.5 h peaks').

In the cM1 (Figure 3.7), there were important decreases in discharge rates at the time where neurons had been most active prior to inactivation, during grasp with the non-paretic (-1.78 spikes/sec; $T_{(103)} = -3.43$, $p = 8.75 \times 10^{-4}$, $d = -0.34$) and paretic hand (-2.82 spikes/sec; $T_{(47)} = -3.57$, $p = 8.34 \times 10^{-4}$, $d = -0.52$; Figure 3.7 A,C). In contrast, we observed a significant increase in discharge rate at the time where neurons became most active after the inactivation during use of the paretic hand (2.27 spikes/sec; $T_{(45)} = 2.53$, $p = 0.015$, $d = 0.37$; Figure 3.7 B,D). There was no significant change in discharge rate during use of the non-paretic hand ($p > 0.05$). Thus, overall, we observed decreases in neurons' firing frequency at the time of pre peak discharge, which were accompanied by increases in firing frequency at the time of post 0.5 h peak discharge during use of the paretic hand.

Comparisons of cM1 and PMv changes induced by inactivation

Previously, we characterized the changes in neural activity that occurred in the PMv of both hemispheres after unilateral M1 inactivation (Moreau-Debord et al. 2021). In the subsequent sections, we compare the changes observed in the PMv with those that have been just described for cM1, focusing in particular on three analyses: changes in incidence of neurons with increases and decreases of firing rate during grasp (Figure 3.8), changes of maximal discharge timing during the task (Figure 3.9), and changes of peak amplitude at the time of peak discharge during grasp following inactivation (Figure 3.10).

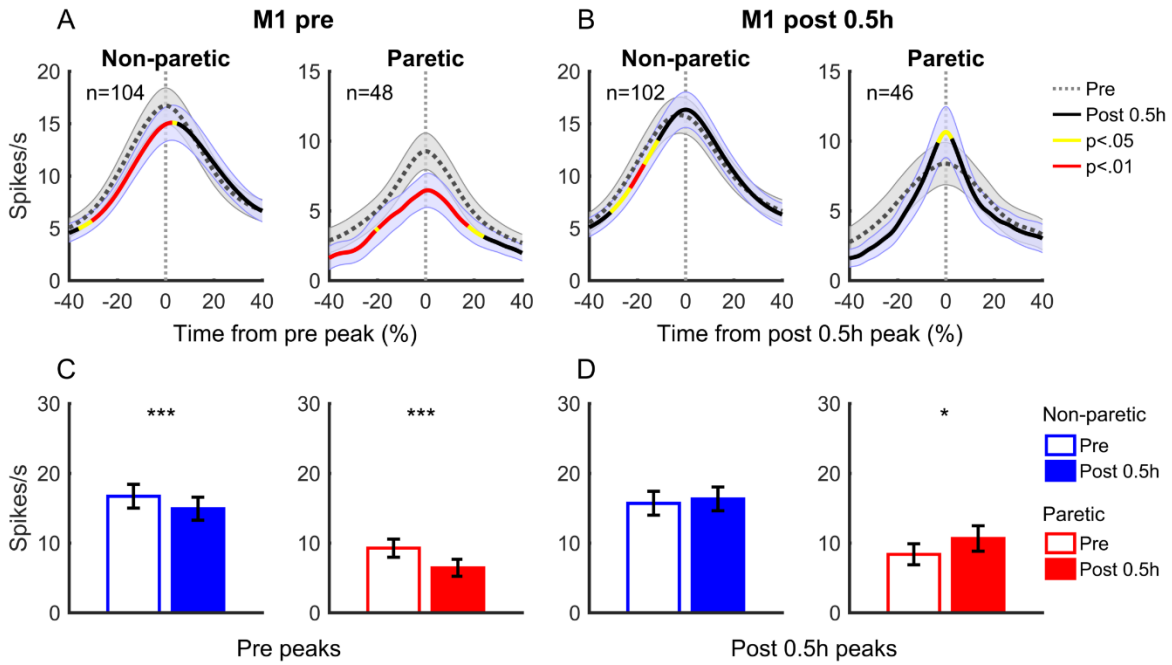

Figure 3.7. *Changes at the time of peak discharge for cM1 neurons induced by the inactivation*

A, The average spike density of cM1 neurons during grasp before (dotted line; gray shade = ±SEM) and after inactivation (solid line; blue shade = ±SEM) are plotted with their activity aligned to the time of peak discharge prior to the inactivation ('Pre peaks'). The colors on the solid 'Post 0.5 h' line represent time bins where the average firing rate of the population was shown to be 'significantly' different after inactivation (yellow: $p < 0.05$; red: $p < 0.01$; paired t tests). ***B,*** Plots are similar to those in A) except the activity is instead aligned to the time of peak discharge after the inactivation ('Post 0.5 h peaks'). ***C,D,*** Comparison of the spike discharge rate of neurons before and after inactivation at the time of Pre peaks (***C***) or the time of Post 0.5 h peaks (***D***), i.e. at the time "0" in the *A,B,* plots, respectively (paired t tests; $*p < 0.05$, $***p < 0.001$). Overall, in the cM1 we noticed a notably significant decrease of discharge rate at the time of Pre peaks during use of the non-paretic and paretic hand. At the time of Post 0.5 h peaks, we observed a sharp increase of discharge rate at the time of Post 0.5 h peaks during use of the paretic hand. There was no change in activity at the time of Post 0.5 h peaks during use of the non-paretic hand.

Incidences of neurons showing increases and decreases of firing rate during grasp in different motor areas

We compared the differences in the incidence of neurons with significant increases or decreases of neural discharge rate during grasp for the area studied here (cM1) and the PMv studied previously (Figure 3.8). A summary of the accumulated difference in the proportion of neurons showing increases versus decreases of discharge rate throughout grasp is shown in figure 3.8 A,B. All neurons regardless of whether they were modulated during grasp were included in this analysis, and the sum of these differences for each area are compared to what would have been predicted to occur by chance as determined by Monte Carlo methods (see Methods). Essentially, the values shown correspond to the last values of the cumulative sum traces of Figure 3.5. During use of the non-paretic hand, each area showed a different result (Figure 3.8 A). The iPMv had a bias of decreased activity of -18.9% and the cPMv a bias of increased activity of 9.95% relative to what would be expected if all neurons showed only increases of activity for all time bins during grasp. In the cM1, there was no significant bias, with results falling within what could be expected by chance, suggesting that cM1 was minimally perturbed during grasp with the non-paretic hand. During use of the paretic hand (Figure 3.8 B), the cPMv showed a greater incidence of neurons with increased discharge during grasp (4.6%). In contrast, both the iPMv (-3.5%) and the cM1 (-3.7%) had more neurons with decreased discharge rate during grasp.

We were also interested in comparing the incidences of neurons with 'significant' increases and decreases in discharge rate (Figure 3.8 C,D). In particular, we previously reported that there were notable changes occurring at the end of grasp in the PMv (Moreau-Debord et al., 2021). Thus, we were interested in comparing the incidence of neurons from the different areas with 'significant' changes that took place at the end of grasp with one hand or the other, but also at the start of grasp, as well as across the entire grasp epoch. For the window of time centered around the start of grasp (mean of 200 bins centered on grasp onset), we did not observe any difference between cM1, iPMv and cPMv in the proportion of neurons with increases, decreases or no change of discharge rate during use of either the non-paretic or paretic hand (χ^2 tests; $p > 0.05$; not shown). Similarly, there was no overall difference between these areas when considering the entire grasp epoch during use of either hand ($p > 0.05$; not shown).

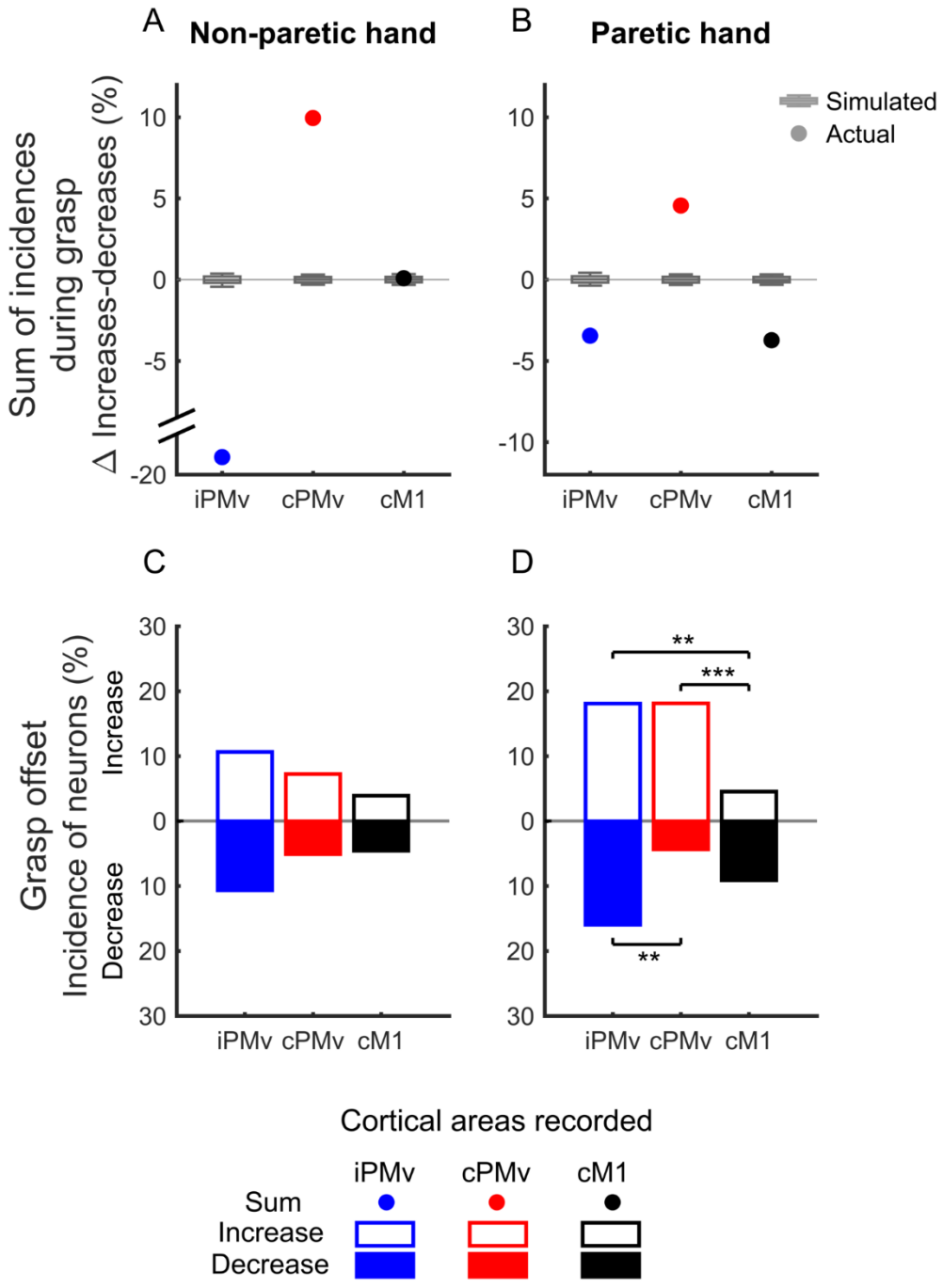

Figure 3.8. *Differences between areas in the incidence of neurons showing increases or decreases of discharge rate during grasp*

A,B, The sum of the difference between the total population of neurons of each area with increases versus decreases of firing rate across all normalized time bins during grasp with the non-paretic (***A***) and paretic hand (***B***). In this analysis, all neurons that were well-isolated both

before and after inactivation were included, regardless of whether they were modulated during grasp or not. These values are compared to distribution of randomly simulated values using Monte Carlo methods (grey whisker plots). The values shown here are equivalent to the last values of the cumulative sum traces of Figure 3.5. During use of the non-paretic hand, the greatest changes clearly took place in the PMv, with a substantial proportion of neurons showing decreases in the iPMv and increases in the cPMv. In contrast, cM1 activity appears to be particularly stable. During use of the paretic hand, there were greater incidences of neurons with increases in the cPMv, whereas both the iPMv and cM1 showed more neurons with decreases of discharge rate throughout grasp. ***C,D,*** Shown are the changes in the firing rate of all cortical areas during a window of time centered at the end of grasp in normalized time (±100 bins from Grasp Offset) during use of the non-paretic hand (***C***) and the paretic hand (***D***). In this analysis, only neurons that showed 'significant' mean increases (clear bars; above the x-axis) or decreases (filled bars; below the x-axis) of discharge rate during the 200 bin window of time were included (unpaired *t* tests with $p < 0.05$; see Methods). Whereas there were no differences between areas in neuron incidences during use of the non-paretic hand, there were significant differences at the end of grasp with the paretic hand. Notably, both PMv had significantly more neurons with increases at the end of grasp than what was observed for the cM1 (*Z* tests; $p < 0.05$). However, the cPMv had significantly less neurons with decreases at the end of grasp than the iPMv ($p < 0.05$). Thus, whereas both PMv had the same proportion of neurons with increased activity at the end of grasp, this was not counterbalanced by neurons with decreased activity in the cPMv, such that this area ended up being much more excitatory at the end of grasp than the other areas studied. Two-sample *Z* tests; $^{**}p < 0.01$, $^{***}p < 0.001$.

However, when looking specifically at the end of grasp (mean of 200 bins centered on grasp offset), while no difference was observed during use of the non-paretic hand ($p > 0.05$; Figure 3.8 C), there was a significant difference in the proportion of neurons showing significant increases, decreases, or no change of neural discharge rate across cortical areas during use of the paretic hand ($\chi^2_{(4,N=386)} = 24.83$, $p = 5.43 \times 10^{-5}$, $V = 0.13$; Figure 3.8 D). With regards to the incidence of increases of discharge rate, we observed that there were significantly more of such neurons in the iPMv compared to the cM1 (18.1% iPMv vs 4.5% cM1; Bonferroni corrected post-hoc two-sample z test for proportions $z = -3.5$, $p = 0.0014$, $r = -0.71$). Similarly, the incidence of neurons with increases of discharge rate in the cPMv was significantly greater than those observed in the cM1 (18.1% cPMv vs 4.5% cM1; $z = -3.71$, $p = 6.31 \times 10^{-4}$, $r = -0.66$). With regards to the incidence of significant decreases of discharge rate, we observed that there was a significant difference between the iPMv and cPMv (16% iPMv vs 4.4% cPMv; $z = -3.03$, $p = 0.0074$, $r = -0.66$). Thus, during use of the paretic hand, it appears that in both PMv a substantial proportion of neurons showed significant increases of their firing rate at the end of grasp, and to a similar extent (iPMv: 18.1%; cPMv: 18.1%). However, whereas in the iPMv these increases were counterbalanced by an almost identical proportion of neurons that significantly decreased their discharge rate at the end of grasp (16%), there were very few of such neurons in the cPMv (4.4%). As such, the cPMv found itself in an overall much more excitatory state at the end of grasp with the paretic hand than did iPMv, or cM1.

Changes of maximal discharge timing in different motor areas following inactivation

We compared the changes of neuron's maximal discharge time (see Figure 3.6 A) induced by the inactivation for the iPMv, cPMv, and CM1, shown in Figure 3.9. All within-neurons were included in the maximal discharge time analysis, regardless of modulation. The change in the timing of maximal discharges after inactivation of the different populations of neurons (cM1, iPMv, cPMv) during task performance with the paretic or non-paretic hand were significantly different (Bartlett's statistic $\chi^2_{(5,N=772)} = 29.13$, $p = 2.19 \times 10^{-5}$). These populations are shown in Figure 3.9. Furthermore, we had noticed that the inactivation appeared to lead to a greater de-synchronization of maximal discharge timing during use of the paretic hand than the non-paretic hand across areas; indeed, when pooling neurons from all areas together, we observed that the variance of maximal discharge time during task performance was significantly greater with the

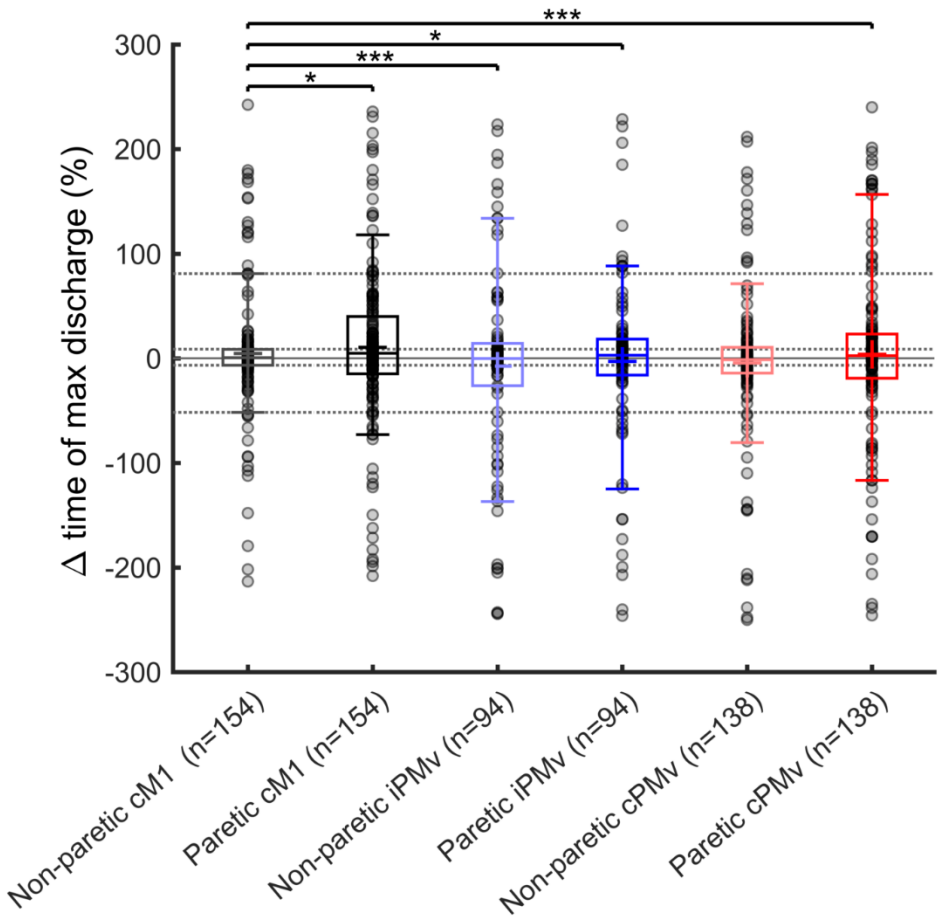

Figure 3.9. *Comparison of the variability of the timing of maximal discharge between cortical areas*

Box and whisker plot of the change of maximal discharge time of the different populations of neurons during use of the non-paretic or paretic hand. All within-neurons are included in this analysis regardless of modulatory profile. The dotted lines (bottom to top) show the 10th, 25th, 50th, and 90th percentiles of the distribution of the cM1 non-paretic population for ease of comparison. While the inactivation perturbed neural timing in all areas and during use of either hand, the smallest variance was observed in the cM1 during use of the non-paretic hand, whereas the greatest variance was observed in the cPMv during use of the paretic hand. The variance of the cM1 population during use of the non-paretic hand was significantly smaller than what was observed for most of the other populations (F test, $p < 0.05$). *$p < 0.05$, **$p < 0.01$, ***$p < 0.001$.

paretic hand relative to the non-paretic hand (two-sample F test for equal variances $F_{(385, 385)} = 0.82$, $p = 0.0477$). The smallest variance was observed in the cM1 during use of the non-paretic hand, that was significantly different than what was observed in the cM1 during paretic hand use (two-sample F test with Bonferroni correction; $F_{(153, 153)} = 0.603$, $p = 0.028$), the iPMv during paretic ($F_{(153, 93)} = 0.54$, $p = 0.011$) and non-paretic hand use ($F_{(153, 93)} = 0.41$, $p = 1.86 \times 10^{-5}$), and the cPMv during paretic hand use, which had the largest variance ($F_{(153, 137)} = 0.48$, $p = 2.14 \times 10^{-4}$). Thus, overall, while neuron's discharge timing was perturbed in all areas and during use of either hand, it was least perturbed during use of the non-paretic hand in cM1, and most perturbed during use of the paretic hand in the cPMv.

Changes of peak amplitude at the time of peak discharge in different motor areas following inactivation

As shown in Figure 3.7, we observed changes in the amplitude of neuron's firing frequency at their time of peak discharge during grasp prior to inactivation ('Pre peaks') and at their time of peak discharge during grasp after inactivation ('Post 0.5 h peaks'). A summary of these changes for the area studied here (cM1) and studied previously (iPMv, cPMv) are shown in Figure 3.10. Notably, during use of either hand, we observed decreases following the inactivation in the amplitude of neuron's firing frequency at their time of peak discharge prior to inactivation (Pre peaks) across all cortical areas (Figure 3.10 A,B). However, we did not observe a main effect of area (iPMv, cPMv, cM1) or hand used (non-paretic, paretic) on these results (repeated measures three-way ANOVA; $F_{(1,339)} = 0.001$, $p = 0.97$, $\eta_p^2 = 2.96 \times 10^{-6}$ for area; $F_{(1,339)} = 0.47$, $p = 0.47$, $\eta_p^2 = 0.0014$ for hand). Therefore, we merged these populations together. With this analysis there was a significant effect of session (repeated measures one-way ANOVA; $F_{(1,341)} = 41.3$, $p = 4.42 \times 10^{-10}$, $\eta_p^2 = 0.11$). Thus, there was a general decrease in pre peak discharge across the motor network regardless of area and during use of either hand.

In contrast, we observed increases in the amplitude of neuron's firing frequency at their time of peak discharge after inactivation (Post 0.5 h peaks) in most areas studied (Figure 3.10 C,D), particularly during use of the paretic hand (D). Indeed, while we did not observe a main effect of area on these changes ($F_{(1,345)} = 0.95$, $p = 0.33$, $\eta_p^2 = 0.0027$), unsurprisingly the main effect of hand used was significant ($F_{(1,345)} = 11.51$, $p = 7.73 \times 10^{-4}$, $\eta_p^2 = 0.032$). Furthermore,

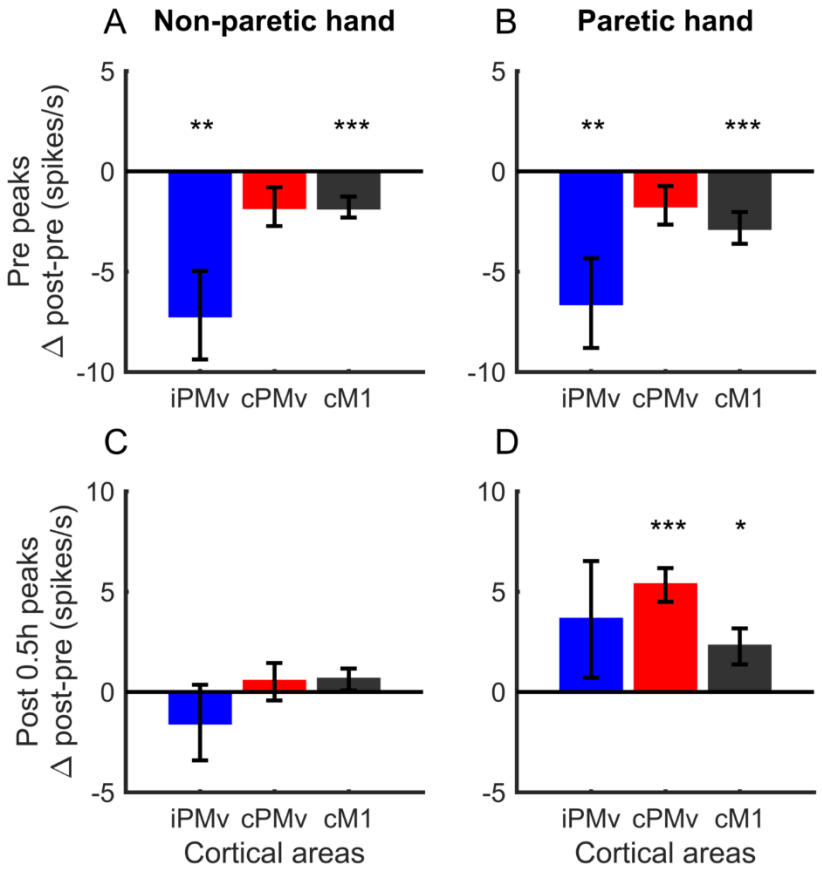

Figure 3.10. *Summary of the inactivation-induced changes at the time of peak discharge for the different cortical areas studied*

A,B, Shown are the changes in discharge rate at the time of Pre peaks, where neurons were maximally active prior to inactivation during grasp with the non-paretic hand (***A***) or paretic hand (***B***). For each area, asterisks denote that the population of 'within-neuron' changes in discharge rate at the time of peak discharge was significantly different after inactivation (paired *t* test, $p < 0.05$). Whereas the iPMv and cM1 showed significantly decreased activity during use of either hand at the time of Pre peaks, there was no significant effect of the factors 'hand' or 'area' on the results (two-way rmANOVA, $p > 0.05$). ***C,D,*** Shown are the changes in discharge rate at the time of Post 0.5 h peaks, where neurons became maximally active after the inactivation during grasp with the non-paretic hand (***C***) or paretic hand (***D***). There was a significant effect of hand used on the changes of discharge rate that occurred at the time of Post 0.5 h peaks (two-way rmANOVA, $p < 0.05$). Thus, overall, increases in discharge rate at the time of Post 0.5 h peaks occurred preferentially during use of the paretic hand. However, there was no effect of area, when either including the data from both hands (two-way rmANOVA, $p > 0.05$) or only data obtained during use of the paretic hand (one-way rmANOVA, $p > 0.05$). Nonetheless, the greatest increase in

discharge rate clearly occurred in the cPMv. rmANOVA= repeated measures ANOVA. *$p <$ 0.05, **$p < 0.01$, *** $p < 0.001$, paired t tests.

when we performed an additional test that only considered the changes occurring at the time of post 0.5 h peaks for the paretic hand specifically, we also did not observe an effect of area (repeated measures two-way ANOVA; $F_{(1,157)} = 1.99$, $p = 0.16$, $\eta_p^2 = 0.013$). Therefore, we merged the paretic hand data from the different areas together. With this analysis there was a significant effect of session (repeated measures one-way ANOVA; $F_{(1,347)} = 14.12$, $p = 2.01 \times 10^{-4}$, $\eta_p^2 = 0.039$). Thus, there was a general increase in post 0.5 h peak discharge across the motor network during grasp with the paretic hand.

In summary, these results demonstrate that during the use of the non-paretic hand, there was no generalized compensation across the motor network for the decreased activity that occurred where neurons were most active prior to the inactivation during grasp. In contrast, during use of the paretic hand the decreased activity that occurred at the time of pre peak discharge became compensated for by the emergence of novel activity at other moments in time during grasp across the motor network.

Discussion

We set out to investigate how neural activity in the contralesional M1 is impacted by a unilateral lesion of the M1 hand area in the other hemisphere as monkeys performed reach and grasp movements with either hand. These results were compared to our previous exploration of changes in PMv neural activity obtained from the same animals (Moreau-Debord et al., 2021). For these experiments we chose to use muscimol, a GABA-A receptor agonist, in order to reversibly inactivate M1. This is a frequently used and accepted technique to study changes after cortical injury as it induces similar deficits to those observed after permanent lesions (Martin and Ghez, 1993; Schieber and Poliakov, 1998; Brochier et al., 1999; Martin and Ghez, 1999). An important advantage of using muscimol concurrently with neural recordings in awake behaving primates is that it allowed us to characterize changes in individual neurons that were well-isolated both before and after the inactivation, such that we were able to perform within-neuron analyses. Overall, our experimental approach demonstrated that a localized perturbation of M1 rapidly induces an extensive and complex reorganization of neural activity across the motor network. This reorganization can be seen immediately as deficits appear and is observable in neurons of the premotor cortices of both hemispheres and the contralesional M1. Nonetheless, the changes observed in the cM1 were quite different from those reported previously for the PMv. Because of the short time scale within which this reorganization takes place, they represent the result of the immediate effect of circuit loss rather than any rewiring or experience-induced plasticity that accompanies long-term reorganization.

Resilience of cM1 neural population activity to inactivation of its homologue

Neural activity appeared to be particularly resilient in the cM1 when compared to the PMv. Previously, we reported that the PMv of both hemispheres were substantially perturbed by the unilateral M1 inactivation, at both the population level and within individual neurons. For the PMv, at the population level we had observed important decreases in both hemispheres in neural discharge rates when animals were at rest with no movement taking place. Furthermore, there were less PMv neurons being modulated during grasp with the paretic hand, as many neurons that were modulated for the non-paretic hand instead became hand non-specific, modulated

during use of either hand. As such, many PMv neurons lost their modulatory specificity. In contrast, the cM1 neural population appeared to be particularly resilient in the face of the inactivation of its homologue (Figure 3.4). At the population level, there was no change in the proportion of neurons modulated during grasp with either hand following the inactivation. This neural stability was also obvious at rest, as there was no change in baseline levels of cM1 neural discharge rates. This is perhaps surprising, since many studies report important changes at the population level in excitability of cM1 after injury to its homologue (Shimizu et al., 2002; Murase et al., 2004; Butefisch et al., 2008; Buetefisch, 2015), such that cM1 might be expected to show greater changes in neural activity than premotor cortex. As discussed below, this resilience was also observed in our within-neuron analyses of cM1 neural activity, most notably during use of the non-paretic hand, but also during grasp with the paretic hand.

Robust tuning of cM1 for contralateral, non-paretic hand movement

While there were important changes in discharge rates that took place in individual cM1 neurons following inactivation, our within-neuron analyses revealed that there was a notable stability of cM1 neural activity during use of the non-paretic hand. This conclusion is driven by several observations. During grasp, the proportion of neurons showing increases or decreases of discharge rate balanced each other out, such that no overall bias emerged, and the area remained stable (Figure 3.5 A and 3.8 A). In addition, relative to the iPMv and cPMv, the cM1 had the least neurons with significant changes in discharge rate at the end of grasp (Figure 3.5 C). At the time of peak discharge where neurons had been most active prior to inactivation, while there was a significant decrease in amplitude due to the inactivation, the extent of this change was quite small, much less than what was observed in the iPMv (Figure 3.10). Finally and most importantly, this stability was most obvious in the neural timing of maximal discharge rates during task performance, as can be seen visually in the heat plots of Figure 3.6 A and confirmed with further analysis in Figure 3.9. Indeed, while the cM1 population showed shifts in neural timing during use of the non-paretic hand following inactivation, these timing shifts were significantly smaller than those observed during use of the paretic hand. They were also much smaller than the timing shifts observed in the PMv of both hemispheres (Figure 3.9). Thus, the neural timing of the cM1 during use of the non-paretic hand was the most stable among all areas

studied, highlighting that the changes taking place in the cM1 following inactivation are quite different from those that occurred in the PMv.

To explain the stability of cM1 neural activity during use of the non-paretic hand, one must consider this area's important lateralization of function in limb motor control. Indeed, among the cortical motor areas (Luppino et al., 1991; Matsuzaka et al., 1992; He et al., 1993; Luppino et al., 1993; He et al., 1995; Dum and Strick, 2002), M1 has the most robust and direct connections with the body's contralateral motor apparatus (Biber et al., 1978; Murray and Coulter, 1981; He et al., 1993, 1995) with up to 90% of its corticospinal projections being made to the contralateral spinal cord (Dum and Strick, 1996; Brosamle and Schwab, 1997; Lacroix et al., 2004; Rosenzweig et al., 2009; Morecraft et al., 2013). In addition, M1 neurons are much more modulated during use of the contralateral than the ipsilateral hand (Tanji et al., 1988; Donchin et al., 1998; Cisek et al., 2003). As such, M1 outputs are highly lateralized, and play a preferential role in purely motor processing of the contralateral musculature. Thus, while the inactivation did perturb processing across the motor network, its specific effect on cM1 motor control of the contralateral, non-paretic hand were minimal, which is reflected in the stability of the neural activity of the cM1.

Specific detuning of cM1 neural activity during use of the paretic hand

Neural activity in the cM1 was more perturbed during use of the paretic hand than with the non-paretic hand. However, once again, these paretic hand changes also reflect a certain resilience of cM1 neural activity. During use of the paretic hand, our within-neuron analyses revealed that cM1 neural activity was principally negatively affected by the inactivation. Many of these changes were noticeably similar to what was observed in the PMv. For example, cM1 neural activity was much more detuned during use of the paretic hand than the non-paretic hand (Figures 3.6 and 3.9), an observation common to all areas studied. Among the changes observed in cM1 some were specifically similar to those observed in the iPMv. In particular, there was an overall greater proportion of cM1 neurons showing decreases of discharge rate during grasp, to the same extent as iPMv, as seen in Figure 3.8 B. In addition, peak neural activity during grasp at the time when neurons were most active prior to inactivation was significantly attenuated (Figure 3.10 B), albeit to a smaller extent than what was seen in iPMv. Other changes were similar to

those observed in the cPMv. Specifically, we observed an emergence of new neural activity in cM1 during grasp with the paretic hand where neurons were not initially maximally active (Figure 3.10 D). However, this novel increase in cM1 peak discharge rate was nonetheless much less pronounced than the increased discharge rate that was observed in the cPMv.

Two common themes appear to emerge from these results. First, they demonstrate that the reorganization observed in the cM1 following inactivation are to some extent a combination of the changes that took place in the iPMv and cPMv. Second, and importantly, they demonstrate that the cM1 changes were for the most part much less pronounced than those that took place in the PMv. As such, these results further highlight the resilience of the cM1 neural population to perturbation of its homologue. A notable demonstration of this stability can be seen at the end of grasp (Figure 3.8 D). While important proportions of PMv neurons in both hemispheres showed increased (or decreased) activity at the end of grasp with the paretic hand when animals had successfully performed the motor task and grasped their food reward, much fewer neurons showed significant changes in cM1.

As stated earlier, it is perhaps unexpected that the cM1 would show such resilience in its neural activity during use of the paretic hand. However, it is important to note that the hand representation area of M1 is not generally considered to have robust cortico-cortical projections to its homotopic analogue in the other hemisphere, the target of our inactivation protocols (Pandya and Vignolo, 1971; Zant and Strick, 1978; Jenny, 1979; Jones et al., 1979; Gould et al., 1983; Rouiller et al., 1994). It is possible that suppressed perilesional M1 activity may indirectly influence cM1 hand area excitability via neighboring homotopic (or heterotopic) cortico-cortical connections. Furthermore, the iPMv exerts a principally facilitatory interhemispheric influence on cM1 (Quessy et al., 2016; Cote et al., 2017; Cote et al., 2020), such that the decreased iPMv activity may contribute to the reduced activity in cM1 that was observed during paretic hand grasping. Overall, the cM1 changes are likely due to widespread diaschisis (von Monakow, 1914; Carrera and Tononi, 2014), albeit extending to the cM1 less directly than say for iPMv, which is much more strongly interconnected with the site of injury (Dum and Strick, 2005).

Patients with stroke often demonstrate increased hemodynamic activity and excitability of contralesional M1 during movements of the paretic limb (Chollet et al., 1991; Weiller et al., 1992; Shimizu et al., 2002; Butefisch et al., 2003; Murase et al., 2004; Tang et al., 2015). Our

results suggest that the abolishment of neural responses in the M1 hand area do not induce increased contralesional M1 neural activity, at least not at the rapid timescale studied. It is possible that such increased cM1 excitability occurs later in time following injury or requires a greater extent of M1 damage. However, meta-analyses of stroke patients have shown that the probability of finding contralesional M1 activity is dependent on multiple, interacting factors, and not related singularly to motor impairment or time post-stroke (Rehme et al., 2012). As such, ischemia itself or inflammation may play a more important role in producing increases in contralesional M1 activity than a mere reduction in ipsilesional M1 activity. In the somatosensory system, it has been shown in rodents that while ischemia in one hemisphere increases evoked somatosensory responses in the unaffected hemisphere produced by stimulation of the paretic limb, pharmacological inactivation of forelimb somatosensory cortex with tetrodoxin does not lead to the development of such responses in the uninjected hemisphere (Mohajerani et al., 2011). A similar mechanism may possibly be at play in the motor system.

Extent of neural changes in each area reflects their functional contributions to unimanual grasping

The manner and extent to which M1 and PMv were affected by the inactivation is likely reflective of their different functional contributions to the motor control of unimanual grasping in the healthy brain. The PMv is well known to play a critical role in in the visuomotor control of grasping (Jeannerod et al., 1995; Fagg and Arbib, 1998; Castiello, 2005; Umilta et al., 2007; Davare et al., 2011; Borra et al., 2017) and in the recovery of hand dexterity after M1 injury (Frost et al., 2003; Dancause et al., 2005; Dancause, 2013; Murata et al., 2015). In the PMv neural code, many task and grasp motor parameters have a bilateral representation (Rizzolatti et al., 1988; Tanji et al., 1988; Hoshi and Tanji, 2002, 2006; Kurata, 2007; Michaels and Scherberger, 2018). This is less true in M1. Whereas the M1 of both hemispheres appears to contain complete, and distinct, computational representations of each arm during bimanual or unimanual movements (Ames and Churchland, 2019; Heming et al., 2019), this sort of discrete encoding may not be the case for hand motor control. Rather, M1 ipsilateral grasp tuning is strongly correlated to contralateral grasp tuning, such that ipsilateral hand signals during bimanual movements are difficult to isolate (Downey et al., 2020). Similarly, fMRI activations in

M1 that are related to ipsilateral finger movements disappear during bimanual movements, being dominated by activations related to contralateral finger movements (Diedrichsen et al., 2013). As such, the cM1, while having a significant involvement in compensatory mechanisms for recovery of the paretic hand (Jones et al., 1989; Cuadrado et al., 1999; Caramia et al., 2000; Butefisch et al., 2005; Ward, 2005; Buetefisch, 2015) may be less computationally flexible, and functionally relevant, in its ability to rapidly contribute to paretic hand grasping than PMv without slower, longer-term rewiring or experience-induced plasticity.

Thus, the motor system may be particularly inclined to enlist the PMv, more so than cM1, to rapidly compensate for unimanual grasping deficits. Indications of such a potential recruitment can be seen in the substantial proportion of iPMv and cPMv neurons showing increased activity at the end of grasp when the monkeys have successfully performed their grasping movements, which was not mirrored in cM1 (Figure 3.8 D). However, as the iPMv was to a great extent negatively affected by the M1 inactivation (Moreau-Debord et al., 2021), it is possible that the motor system had no choice but to become more dependent on the contralesional hemisphere for hand motor processing. This could explain the pronounced and robust emergence of new neural activity in the cPMv, and to a much lesser extent the cM1, during grasp with the paretic hand when neurons were not initially maximally active (Figure 3.10 D). This new activity could reflect adaptation and compensation by the motor network as it attempts to preserve dexterous hand motor function in the face of increasing behavioral deficits induced by the M1 inactivation.

Conclusions

Unilateral M1 inactivation induces rapid reorganization of neural activity across motor areas of both hemispheres. However, the extent of this reorganization was different across the areas studied. Most notably, cM1 neural activity appeared to be particularly resilient to inactivation of its homologue as it was less perturbed, and showed less changes, than the PMv of both hemispheres. Our results provide important insights into the changes that take place within neurons of these different motor areas and highlight that there is a great complexity in the reorganization induced by acute brain injuries when behavioral deficits first appear.

Chapter 4 -General Discussion

1. General summary and discussion chapter overview

Reaching to grasp objects in the environment requires the coordination of numerous cortical structures that together form a network (Kalaska et al., 1997; Shadmehr and Wise, 2005). This cortical network extends to both hemispheres, such that unimanual movements will involve both ipsilateral and contralateral motor-related areas (Donchin et al., 1998; Ames and Churchland, 2019; Heming et al., 2019). In the current thesis we focused in particular on two motor-related cortical regions, the PMv and M1, whose interconnected hand representation areas are considered to be part of the "visuomotor grasping network" (Jeannerod et al., 1995), utilizing information obtained from sensory modalities to plan and execute grasping movements.

Following brain injuries, neural reorganization can occur in distant, spared motor areas from the lesion in both hemispheres. These changes are most pronounced early after the injury, and this rapid reorganization ultimately reflects the landscape on which subacute plasticity involved in motor recovery will take place. However, most explorations of these changes in motor-related areas have been done using indirect measures of neural activity, for example by quantifying hemodynamic changes obtained from noninvasive brain imaging. As such, it has not been clear how brain injuries specifically affect the discharge rates of neurons during ongoing reach and grasp behavior. In the current thesis, we set out to quantify the rapid changes occurring in neuronal activity of bilateral PMv and contralesional M1 after a unilateral inactivation of the M1 hand area. Our results demonstrated that overall, there was widespread detuning in the timing of discharge rates across the motor network, but also the appearance of novel neural activity, notably in the contralesional hemisphere and particularly in cPMv. The specific effects of the inactivation were different for each area, with notable decreases of activity in the iPMv, and increases of activity in the cPMv. In contrast, the cM1 appeared to be more stable. Our results suggest the PMv may be a salient neuromodulatory target for stroke rehabilitation, possibly more so than cM1. Nonetheless, numerous questions remain to be explored in future work.

In this chapter, we will first discuss several general topics that relate to our experiments and results. To start, we will focus on the widespread detuning that we observed and how it may relate to changes in connectivity between motor areas. This will then be followed by an overview of neuromodulatory interventions, both non-invasive and invasive, that have targeted motor cortex for stroke rehabilitation, as well as recent therapeutic interventions that have specifically focused on premotor cortex. Finally, within the context of future research directions that are of interest to pursue following our experiments, we first highlight the value in performing additional analyses specifically exploring changes in neuron preferences for use of one hand relative to the other. We then ask the question of what rapid neural reorganization may take place in other premotor areas, notably the dorsal premotor cortex and the supplementary motor area. Additionally, a quantification of how this rapid reorganization is dependent on lesion size and location will be proposed. Finally, we suggest exploring how single-neuron activity across the bihemispheric motor network evolves during recovery from an actual M1 lesion.

2. Widespread detuning of neural activity in both hemispheres

In the current experiments, we demonstrated that there was a widespread detuning of neuronal activity across the bihemispheric motor network following a localized, unilateral perturbation of the M1 hand area. The most notable evidence of this detuning could be seen in the changes in the timing of maximal and peak discharges during grasp of bilateral PMv and cM1 neurons following the inactivation, as well as in the general suppression of peak discharge rates in iPMv and cM1, at the time where neurons were most active prior to inactivation. As such, the local perturbation of the M1 hand area led to a generalized loss of coordination in neural activity across the bihemispheric motor network, albeit to different extents depending on the cortical area studied and the hand used.

The distributed nature of the perturbation to neural discharge timing across the bihemispheric motor network during ongoing grasp is consistent with observations obtained from human connectivity studies using resting-state fMRI (Grefkes and Fink, 2014; Silasi and Murphy, 2014). Stroke preferentially affects homotopic connections, such that the cortical dysfunction produced by lesions stay within the limits of existing interconnected networks that are functionally correlated with the lesion sites (Carter et al., 2010; Nomura et al., 2010; Siegel et al., 2016). For example, patients that show motor impairments, but no visuospatial neglect, show abnormal connectivity in the motor system but normal connectivity in attention-related networks (Carter et al., 2010). Similarly, interhemispheric connectivity between motor cortices is not affected when patients only display non-motor stroke deficits (Golestani et al., 2013). Widespread, but functionally specific, abnormal changes in somatosensory processing have also been reported following unilateral cortical injury to motor and sensory forelimb representations in rodents (Mohajerani et al., 2011; Sweetnam and Brown, 2013). Indeed, minutes after cortical injury rapid changes in somatosensory evoked responses during stimulation of either forelimb can be observed in both hemispheres, whereas stimulation of either hindlimb maintained normal responses (Mohajerani et al., 2011). In our experiments, while the observed neural detuning was more pronounced during use of the paretic hand, it was still present during use of the non-paretic hand, reinforcing the notion that the unimanual control of hand grasping is driven by a distributed but interconnected network of motor regions in both hemispheres.

There are several additional interesting parallels between connectivity changes following stroke and the neural changes described in our experiments. Furthermore, the way in which these changes in connectivity progress as recovery takes place provide some suggestions as to how the neural reorganization that we observed might be inclined to evolve following an actual cortical lesion. In the ipsilesional hemisphere, influences on motor performance of premotor cortex connectivity are reduced early after stroke in patients with more severe impairments (Grefkes et al., 2008; Rehme et al., 2012). This is consistent with our experiments, where we observed that iPMv neural activity was for the most part negatively affected by the inactivation. However, the influence of premotor cortex increases as motor recovery progresses (Wang et al., 2010; Rehme et al., 2011b). As such, it is likely that the attenuated neural activity that we observed in the iPMv disappears and may even be replaced with increased neural activity as motor recovery progresses, although this hypothesis will have to be tested experimentally.

With regards to the influence of the contralesional hemisphere, within 24 hours after stroke the connectivity between the ipsilesional sensorimotor cortex and contralesional motor areas are reduced (Golestani et al., 2013). In terms of changes in neural activity, this may have been reflected in our experiments by the substantial detuning observed in the contralesional areas due to the M1 injury, as well as the decreased cM1 activity that we reported. As time progresses, increased connectivity between ipsilesional M1 and contralesional motor areas including cM1 and cPMv is associated with recovery (Wang et al., 2010; Golestani et al., 2013; Grefkes and Fink, 2014). Although it remains to be seen, it is likely that such changes are accompanied by a retuning of activity in these areas. In support of this possibility, the re-emergence of coordinated firing of neuron ensembles in the perilesional cortex after a focal M1 stroke in rodents and primates is associated with improved post-stroke performance (Ramanathan et al., 2018; Latifi et al., 2020; Abasi et al., 2021; Khanna et al., 2021; Kim et al., 2021). One interesting question is whether retuning in premotor cortex or M1 occurs first. Initial retuning in premotor cortex could help retune M1 activity (see section 6.3.3 of future directions).

Overall, the cM1 and bilateral PMv are quite regularly observed to display more hemodynamic activity in patients with stroke than in healthy controls and are particularly implicated in the reorganization of the bihemispheric cortical motor network in patients that display motor impairments (Rehme et al., 2012). However, hemodynamic changes occur on a

much slower timescale than changes in neuron discharge rates, and cannot distinguish the direction of neural change (e.g. an upregulation of GABA interneurons would inhibit neural outputs of an area, but still lead to an increase in hemodynamic signals). In our results, we demonstrate very time specific neural changes in relation to ongoing movement that were very different in the two hemispheres, being sustained in the iPMv, and precise at the end of grasp in cPMv. Our experiments thus provide a first glimpse into what this reorganization looks like at the level of individual neurons during ongoing behavior and highlight the importance of exploring how these changes will progress during recovery from an actual lesion of the M1 hand area (see section 6.3.3).

3. Non-invasive neuromodulatory approaches for stroke recovery targeting M1

Recent therapeutic interventions have set out to modulate neural excitability of specific brain regions in order to drive neuroplasticity towards a desired endpoint. In particular, there has been a great deal of interest in non-invasive brain stimulation (NIBS) techniques (Liew et al., 2014), such as TMS (Smith and Stinear, 2016), transcranial direct current stimulation (tDCS) (Orru et al., 2020; Sawan et al., 2020), or transcranial alternating current stimulation (tACS) (Solomons and Shanmugasundaram, 2019) as they are preferable to be used in human patients than more invasive methods. The use of these techniques for stroke recovery has been strongly influenced by the interhemispheric competition model. While these techniques have shown great promise for therapeutic interventions, they have fallen short of being approved for widespread clinical use due to several issues. Following a brief presentation of NIBS techniques, the interhemispheric competition model and its consequences for stroke will be discussed, as well as how it has driven therapeutic NIBS neuromodulatory approaches. The limitations and obstacles faced by NIBS treatments will also be presented, followed by attempts in the field to address some of these issues via the development of theta burst stimulation.

3.1 NIBS techniques: transcranial magnetic and electrical stimulation

Briefly, TMS uses a magnetic field to induce electric fields in cortical tissue. This is done by having an electric current flow through a coil, which generates a magnetic field. This magnetic field then flows to the neural tissue, which generates an electric field in the cortical tissue (Chail et al., 2018). Of notable importance for therapeutic interventions, repetitive TMS (rTMS) involves long periods of stimulation that are made up of short bursts of pulses. Low frequency rTMS (<5 Hz) causes inhibition, whereas high frequency rTMS (>5 Hz) causes excitation (Valero-Cabre et al., 2017). An important advantage of rTMS is that all the equipment used is completely external to the patient, such that it is easy and safe to use up to certain frequencies (~25 Hz; but see subsequent paragraphs). Transcranial electric stimulation techniques, which have been explored less than rTMS for stroke recovery, involve the placement of electrodes on the scalp to electrically stimulate brain areas. In tDCS, low-intensity electrical current flows unidirectionally from one electrode to the other, placed distally from each other such that the current will traverse a large area of cortex (Sawan et al., 2020). The flow of electrons creates a

region under the anode where neuronal activity is facilitated and a region under the cathode where activity is inhibited through modifications of transmembrane neuronal potentials and cortical excitability (Tortella et al., 2015). In tACS, oscillatory electrical stimulation is applied by alternating the current flow between the electrodes, which overrides the endogenous rhythmic activity of the cortical areas through which the current traverses (Antal and Paulus, 2013; Herrmann et al., 2013; Song et al., 2014; Solomons and Shanmugasundaram, 2019). In healthy subjects, these techniques can be used to improve motor performance or motor learning, for example by using high-frequency rTMS or anodal tDCS to increase M1 excitability (Nitsche et al., 2003; Kim et al., 2004; Reis et al., 2008; Reis et al., 2009).

3.2 The interhemispheric competition model and its implications for stroke

In stroke recovery, the application of these NIBS techniques is heavily influenced by the interhemispheric competition model (Buetefisch, 2015; Alia et al., 2017; Boddington and Reynolds, 2017). The model is based on the idea that the neural activity in the motor areas of the brain is functionally coupled between the two hemispheres (Kinsbourne, 1977, 1980; Vallone et al., 2016), such that each cerebral hemisphere inhibits the other in a process called interhemispheric inhibition, exerted via transcallosal connections (Ferbert et al., 1992; Butefisch et al., 2008). Such interhemispheric inhibition is suggested to play an important role in the process of initiating and executing a unilateral movement, and play a part in the lateralization of motor neural activity during movements (Meyer et al., 1995; Di Lazzaro et al., 1999). Experimentally, it has been shown that down-regulation of excitability in one motor cortex will affect the corticomotor excitability of the motor cortex in the opposite hemisphere. For example, inhibitory 1 Hz rTMS applied to the M1 of one hemisphere causes increased corticomotoneuronal excitability in its homologue (Plewnia et al., 2003; Kobayashi et al., 2004) and therefore improved performance in the hand ipsilateral to the site of stimulation (Kobayashi et al., 2004; Buetefisch et al., 2011).

Importantly, following stroke, the interhemispheric competition model posits that the normal inhibitory balance between hemispheres becomes altered, such that the ipsilesional hemisphere cannot effectively inhibit the contralesional hemisphere. In turn, the contralesional hemisphere exerts excessive inhibition onto the ipsilesional hemisphere (Murase et al., 2004;

Duque et al., 2005). Thus, motor deficits in stroke patients are due to not just a reduced output from the lesioned hemisphere, but also from excessive inhibition originating from the unaffected hemisphere due to the interhemispheric imbalance (Kinsbourne, 1977, 1980; Murase et al., 2004; Takeuchi et al., 2005; Nowak et al., 2009; Di Pino et al., 2014). As such, to improve motor deficits, it would follow that one should aim to increase the excitability of the lesioned hemisphere or decrease the excitability of the unaffected hemisphere (Ward and Cohen, 2004; Nowak et al., 2008).

3.3 NIBS approaches towards enhancing stroke recovery

In accordance with the interhemispheric competition model, NIBS studies often set out to upregulate the over-inhibited ipsilesional cortex or downregulate the excessively disinhibited contralesional cortex in order to rebalance the inhibitory dialogue between the hemispheres and enhance functional return (Au-Yeung et al., 2014; Lefebvre et al., 2014; Rocha et al., 2016; Boddington and Reynolds, 2017). Both approaches have shown promise. For the former approach, studies have shown that upregulating ipsilesional M1 excitability of chronic stroke patients can produce modest, but variable, improvements in motor function (Hummel and Cohen, 2005; Khedr et al., 2005; Hummel and Cohen, 2006; Kim et al., 2006; Pomeroy et al., 2007; Ameli et al., 2009; Sandrini and Cohen, 2013) and some of these changes may transiently persist beyond the period of stimulation for several minutes (Khedr et al., 2010). Like in healthy subjects, the effect of ipsilesional stimulation may also extend to the other hemisphere. For example, excitatory rTMS over the affected hemisphere of stroke patients not only facilitates the ipsilesional motor cortex but also appears to reduce neural activity in the contralesional motor cortex (Ameli et al., 2009). Many studies have also focused on stimulation of the contralesional M1 to inhibit its hyperactivity (Hummel and Cohen, 2005; Takeuchi et al., 2005; Fregni et al., 2006; Dafotakis et al., 2008; Hummel et al., 2008; Nowak et al., 2008). For example, downregulating contralesional M1 using low-frequency rTMS or cathodal tDCS in chronic stroke patients can improve movement kinematics (Mansur et al., 2005; Takeuchi et al., 2005; Boggio et al., 2006; Liepert et al., 2007; Dafotakis et al., 2008; Nowak et al., 2008), as well as lead to increased grip strength and better arm motor function on the paretic side when applied over several days (Kirton et al., 2008; Kakuda et al., 2011). This approach appears to not just

cause decreased M1 excitability in the contralesional hemisphere, but also induce increased M1 excitability in the ipsilesional hemisphere (Takeuchi et al., 2005; Takeuchi et al., 2008). In addition, inhibitory rTMS over the unaffected hemisphere has been suggested to reduce interhemispheric connectivity and enhance connectivity in the affected hemisphere between the primary and non-primary motor cortices, which is considered beneficial for recovery (Grefkes et al., 2010; Takeuchi et al., 2010).

However, the extent to which these neuromodulatory approaches produce motor gains appears to be quite variable. Overall, the reported therapeutic benefits gained from "rebalancing" the hemispheres are inconsistent (Ackerley et al., 2010; Seniow et al., 2012; Talelli et al., 2012; Stinear et al., 2015; McDonnell and Stinear, 2017; Xu et al., 2019). Indeed, reviews and meta-analyses looking at the effectiveness of using rTMS or tDCS to rebalance interhemispheric inhibition and produce lasting improvements of motor function in stroke rehabilitation therapy are inconclusive, unable to completely support or reject this approach based on the available evidence (Adeyemo et al., 2012; Hsu et al., 2012; Elsner et al., 2013; Hao et al., 2013). As such, these interventions remain exploratory, and have not been approved for widespread therapeutic use. One reason for these failures may be that the vast majority of these studies have been performed using patients at the chronic stage of stroke (Bates and Rodger, 2015), where limited cortical reorganization is possible. Indeed, there is a brief, time-sensitive window when the post-stroke circuitry is particularly responsive to training and therapeutic interventions that is present early after stroke and becomes less effective, or no-longer effective at all, if initiated later in time (Biernaskie and Corbett, 2001; Biernaskie et al., 2004; Mansoori et al., 2014; Dancause et al., 2015; Dromerick et al., 2015; Zeiler et al., 2016; Boddington et al., 2020; Dromerick et al., 2021; Hordacre et al., 2021).

Another possible contributing factor to the variability observed in NIBS results is that interhemispheric inhibition may not be a static, consistent state of the brain following stroke, but is instead dynamic, being more or less present depending on the phase of a movement being executed (Boddington and Reynolds, 2017). Indeed, interhemispheric inhibition may disproportionately impair motor initiation, being dynamically increased onto perilesional areas during early movement. As such, depending on the movement phase and technique studied, and the timing at which changes in interhemispheric inhibition are measured, the effect of this

increased inhibition on the ipsilesional hemisphere and the efficacy of the chosen intervention may differ from one study to the next (Boddington and Reynolds, 2017).

3.4 Theta burst stimulation as a refinement of rTMS

The paucity of consistent therapeutic gains in NIBS studies may also be explained in part by the fact that these studies often used repetitive TMS of 25 Hz or less due to safety concerns, which may not be the most effective at promoting cortical excitability and synaptic plasticity when that is the objective. Research suggests that the transient cortical excitability induced by rTMS remains enhanced for longer periods of time the higher the frequency and longer the trains of stimulation used (Maeda et al., 2000b, a; Gangitano et al., 2002; Peinemann et al., 2004). To produce powerful effects on synaptic plasticity, animal studies have suggested using repeated, but short bursts (3-5 pulses) of high-frequency stimulation (50-200 Hz) 3-5 times per second, known as theta burst stimulation (TBS) (Hess et al., 1996; Otani et al., 1998; Urban et al., 2002). Fortunately, safe application of low-intensity TBS in humans has been developed as an alternative to traditional low-frequency rTMS, and is suggested to provide much more effective and consistent after-stimulation potentiation of neural circuits (Huang and Rothwell, 2004; Huang et al., 2005). The effects of TBS are dependent on the duration of the stimulation trains. Intermittent TBS, which involves pulse trains up to 2 s, produce purely facilitatory effects. Longer duration trains, for example of 5 s, produce a mixture of facilitatory and inhibitory effects that are ultimately dominated by the latter. Finally, continuous TBS, which involves trains of 20 s or more, are purely inhibitory. Ultimately, very short periods of low-intensity TBS over motor cortex can have powerful effects on physiology and behavior that outlast the conditioning by up to 1 hr (Huang et al., 2005).

TBS applied using rTMS has shown promise as a therapeutic tool. For example, when excitatory, intermittent TBS was applied over ipsilesional M1 of patients within the first two weeks after stroke prior to physiotherapy, they showed better motor recovery than controls 3 months later (Volz et al., 2016). Furthermore, these patients showed higher levels of motor network recovery, such that the intervention appeared to be effective at shaping early reorganization of neural networks. Studies in stroke patients have also shown that inhibitory, continuous TBS applied to the contralesional M1 might enhance rehabilitation, presumably via a

mechanism that attenuates the interhemispheric inhibitory drive to perilesional cortex (Talelli et al., 2007; Ackerley et al., 2010; Meehan et al., 2011) (but see next section). Unfortunately, validating rTMS-TBS as approved clinical intervention has not been successful, as its clinical implementation failed to confirm its efficacy (Talelli et al., 2012). It has been suggested that a main reason for this failure is due to the limited spatial specificity of the rTMS technique, as the stimulation induces widespread activity changes that extend beyond the targeted site (Bestmann et al., 2004). Furthermore, the intensities of rTMS used in clinical settings tend to be very high, which is suboptimal. Animal work has shown that high-intensity TBS is much less effective than low-intensity TBS (Barry et al., 2014; Boddington et al., 2020).

Finally, it is worth noting that some TBS results seem to challenge the underlying assumptions of the interhemispheric competition model. For example, one study applied continuous TBS, which is inhibitory, onto the ipsilesional hemisphere of chronic stroke patients (Di Lazzaro et al., 2013). Interestingly, this approach produced clinical improvements for up to 3 months posttreatment, demonstrating that at least for some patients, inhibition of the ipsilesional hemisphere could be beneficial. As such, a better understanding of how the hemispheres interact at the neural level after injury is needed, and the interhemispheric inhibition model may need to be refined.

Taken together, much of the work done using NIBS techniques within the framework of rebalancing a post-stroke asymmetric interhemispheric inhibition has been promising and informative, but inconclusive. Ultimately, to overcome the limitations of these approaches, it is likely that more specific targeting of the neural elements underlying interhemispheric inhibition and cortical excitability are required, by exploring different stimulation types, locations, and intensities. More invasive methods may provide some solutions to these issues.

4. Invasive neuromodulatory approaches for stroke recovery targeting M1

While much research has been done using NIBS for stroke recovery, more invasive methods have also shown promise. Invasive methods, such as those that involve intracortical or epidural/subdural surface electrodes, have several advantages, such as the ability to use higher frequencies, lower intensities, and deliver stimulation much more focally than NIBS techniques to better target specific populations of neurons. Several approaches will be discussed here. These include using focal subthreshold stimulation to drive cortical reorganization of perilesional motor cortex, applying TBS with electrical stimulation, and targeting underlying neural dynamics to induce a "retuning" of neural activity to drive functional recovery.

4.1 Focal subthreshold stimulation to drive perilesional reorganization

One invasive approach that involved applying high-frequency, subthreshold stimulation to promote functional perilesional reorganization got very close to being approved for widespread therapeutic use in stroke rehabilitation (Levy et al., 2016). To start, in rodent and monkeys with a lesion to the M1 hand area, continuous subthreshold (50-70% of motor threshold) cortical stimulation at 50 Hz or 100 Hz with epidural or subdural surface electrodes placed over perilesional motor cortex improved functional recovery of the forelimb when it was delivered concurrently with motor rehabilitation (Adkins-Muir and Jones, 2003; Kleim et al., 2003; Plautz et al., 2003; Teskey et al., 2003). Importantly, this approach led to improved long-term posttreatment motor outcomes. This stimulation paradigm also led to increased dendritic density in layer V (Adkins-Muir and Jones, 2003), larger polysynaptic evoked potentials (Teskey et al., 2003), and increased forelimb representation in perilesional cortex (Kleim et al., 2003; Plautz et al., 2003).

This invasive, high-frequency subthreshold stimulation approach also showed promise in early-phase clinical trials with small numbers of human stroke patients, with improved motor outcomes after several weeks of stimulation-enhanced rehabilitation training relative to controls (Brown et al., 2003; Brown et al., 2006; Huang et al., 2008; Levy et al., 2008). Unfortunately, when the subsequent large scale phase III trial was performed, there was no overall benefit of the stimulation for functional recovery at 4 weeks posttreatment, and thus this approach did not end

up being approved for widespread clinical use (Plow et al., 2009; Levy et al., 2016). However, post-hoc analyses later revealed that, while the intervention group did not reach their efficacy endpoint at 4 weeks, they did show significantly greater motor ability than controls at 24 weeks posttreatment, demonstrating that the intervention did lead to overall long-term motor improvements. Furthermore, the failure at 4 weeks appeared to be explained by poor patient selection. Indeed, for many patients no motor threshold could be found with the implanted electrodes, and thus an arbitrary level of stimulation intensity was used for therapy in those patients. However, when looking only at patients that had detectable motor thresholds at the start of therapy, and thus whose stimulation parameters could be personalized, this subgroup did show significant improved motor outcome at 4 weeks posttreatment relative to controls (Levy et al., 2016). As such, these studies provide a cautionary tale of the importance of appropriately selecting patients that can benefit from a specific therapeutic intervention strategy- a given approach will not be appropriate for all patients.

4.2 Electrical TBS to target abnormal interhemispheric circuitry

Invasive animal models have also been used to explore how TBS applied using electrical stimulation could be used to enhance stroke recovery. Indeed, intracortical stimulation is much more focal and allows the use of lower intensities, such that it can address the main issues that have plagued clinical application of TBS applied via rTMS (see previous section). Interestingly, it has been shown that low-intensity, intermittent TBS appears to "shut down" interhemispheric inhibition in healthy rodents when delivered intracortically in layer V (Barry et al., 2014). As such, electrical TBS may allow a more selective targeting of the abnormally functioning interhemispheric circuitry. Using this approach, it has been shown that low-intensity intermittent TBS applied onto the contralesional M1 down-regulates interhemispheric inhibition and led to improved recovery in animal models of cortical injury and stroke in the acute phase (Barry et al. 2014) as well as in the sub-acute/ early chronic phase (Boddington et al., 2020). Interestingly, continuous TBS, which is inhibitory, did not improve recovery outcomes when applied onto the contralesional cortex, and even decreased ipsilesional excitability (Boddington et al., 2020). Thus, these results demonstrate that electrical TBS can be used to target very specific neural dynamics, and interventions that aim to simply decrease contralesional excitability with the goal

of promoting ipsilesional reorganization, as has often been been the case with rTMS approaches, may be suboptimal.

4.3 Retuning neural activity to improve post-stroke motor function

Interventions that target the loss of coordinated timing of neural discharge rates after cortical lesions have shown a great deal of promise (Ramanathan et al., 2018; Abasi et al., 2021; Khanna et al., 2021). Notably, stimulation that promotes widespread co-firing of neurons in perilesional cortex during reach and grasp have led to immediate improvements in movement accuracy and trial success (Ramanathan et al., 2018; Khanna et al., 2021). In rodents, when a long, 1-5 min single pulse of anodal DCS was applied via small cranial screws in contact with the dura in awake behaving rodents with persistent sensorimotor stroke deficits (20-150 days post-stroke), the stimulation immediately increased movement accuracy by 73% on a reach and grasp task (Ramanathan et al., 2018). The screws were placed in the ipsilesional hemisphere, rostrally and caudally from the site of injury such the current passed through the lesioned and perilesional cortex. Interestingly, this stimulation was shown to induce a "retuning" of neural timing in perilesional cortex; when turned on, the DCS immediately caused coherent, phasic spiking of neurons whose firing patterns had become chaotic following the stroke. Similar results were observed in monkeys recovering from experimental sensorimotor stroke (Khanna et al., 2021). Low-frequency (3 Hz) epidural ACS applied for 10-15 min during therapy lead to substantial improvements in motor performance on several reach and grasp tasks. Similar to the rodent study, the stimulation was applied using skull screws in contact with the dura and placed away from the site of injury but oriented such that the current passed through the lesioned and perilesional cortex. However, while the caudal electrode was placed in the ipsilesional hemisphere, the rostral electrode was placed in the contralesional hemisphere. As such, the current also passed through premotor cortex bilaterally to some degree. The stimulation tests occurred when monkeys were in an "intermediate" stage of recovery, where their reach movements had recovered, but not grasp. When the tasks were performed during ACS, there was a significant and immediate improvement in hand dexterity, similarly to what had been observed in the rodent study. Interestingly, the more impaired the monkey, the more effective the ACS stimulation on task performance. This improvement was associated to the effects of the ACS on

underlying neural dynamics. In particular, it was shown that ACS increased the co-firing of task-related perilesional cortex neuron ensembles during dexterous behavior, and these changes resembled the natural increases in neural co-firing that normally occurs during recovery. As such, these studies demonstrate that electrical stimulation via epidural electrodes can produce "on demand" improvements in motor function following stroke, and do so by entraining neurons to induce a functionally-relevant retuning of neural activity (Ramanathan et al., 2018; Khanna et al., 2021).

Interestingly, due to the distal placement of the stimulating electrodes from the site of injury, the current passed through large amounts of ipsilesional and even contralesional cortical areas during paretic hand use in these studies. In addition, re-instatement of neural discharge timing in perilesional cortex likely influenced neural synchrony in other, connected areas, even if those areas were not directly affected by the stimulation. In support of this, it has been shown that epidural cerebellar stimulation in rodents with stroke will drive widespread neural synchrony across both the ipsilesional and contralesional M1 (Abasi et al., 2021). As such, these paradigms likely induced a retuning of neural discharge timing not just in perilesional cortex but also across a large swath of the motor network, including premotor cortex. Such widespread retuning may have contributed to the functional motor gains induced by the stimulation, although this remains to be verified.

Taken together, more invasive stimulation strategies targeting primary motor cortex for stroke rehabilitation have shown a great deal of promise. Relative to NIBS, they can allow more specific targeting of neural populations and neural dynamics. However, they rely much more heavily on experimentation in animal models, and for the most part, they are still in the early stages of development. Like NIBS approaches, they will require additional refinement before they can be used habitually in patient populations.

5. Premotor cortex as a target for stroke recovery

While M1 has been extensively explored as a neuromodulatory target for stroke recovery, the premotor cortex has been largely ignored (Plow et al., 2015). This is despite the fact that premotor cortex is known to be fundamentally important for functional recovery after cortical injury in both animal models and human patients (see general introduction). Furthermore, in patients with greater lesions and impairments, premotor areas and their descending projections have a higher probability of survival after stroke than M1 and its corticospinal outputs, such that ipsilesional premotor areas emerge as potentially useful alternatives for brain stimulation approaches (Plow et al., 2015).

In the current thesis, our results strongly pointed towards the PMv as a possible therapeutic target after cortical injury, with the PMv of both hemispheres showing dramatic changes in activity patterns and to a much greater extent than cM1. In human patients after stroke, there is a displacement of motor maps towards the PMv (Alagona et al., 2001) and increased cerebral blood flow in this area (Seitz et al., 1998). In addition, patients with intact PMv show better recovery than patients with damage to that area after a medial cerebral artery occlusion (Miyai et al., 1999), and connectivity between ipsilesional M1 and PMv is important for stroke recovery (Grefkes et al., 2008; Rehme et al., 2011b; Inman et al., 2012; Bajaj et al., 2015).

While a few studies have begun to explore modulation of premotor cortex activity for stroke recovery, they have not generally focused specifically on PMv. Some of the therapeutic intervention studies that involve premotor cortex activity more generally will be described below. While some of these studies have involved directly modulating the excitability of premotor cortex, there has also been other interesting approaches, such as using closed-loop systems to promote communication between somatosensory cortex and premotor cortex, and the use of neurofeedback training to volitionally upregulate bilateral PMv activity in stroke patients.

5.1 Modulating premotor cortex during stroke rehabilitation

There has been interest in using tDCS to potentiate ipsilesional premotor areas of stroke patients concurrently with constraint-induced movement therapy (CIMT) (Taub et al., 2003), which

involves restricting the intact limb for most waking hours such that patients are massively forced to use the paretic limb (Plow et al., 2013; Cunningham et al., 2015). In a proof-of-concept pilot clinical study, chronic stroke patients received anodal tDCS over premotor cortex during 5 weeks of therapy concurrently with CIMT (Cunningham et al., 2015). The location of the anode was such that it likely mostly affected the PMd and SMA, rather than the PMv. Nonetheless, they found that patients with tDCS+CIMT showed better gains in motor function of the affected limb relative to patients that received the CIMT alone. Interestingly, these motor improvements were accompanied by increased excitability of the contralesional hemisphere, rather than the ipsilesional hemisphere, demonstrating once again that interhemispheric interactions are much more complex than initially formulated.

Conversely, some studies explored neuromodulation of the contralesional premotor cortex for stroke rehabilitation (Wang et al., 2014; Ludemann-Podubecka et al., 2016). These studies have shown that inhibition of contralesional PMd can improve motor function of the paretic hand. For example, one study set out to compare the effects of 10 sessions of inhibitory (1 Hz) rTMS applied over the contralesional PMd versus the contralesional M1 in stroke patients during recovery (Wang et al., 2014). Both the PMd and M1 stimulation yielded significant improvements relative to controls on a variety of motor improvement scales and led to similar improvements in the excitability of the ipsilesional motor cortex. However, the effect of the PMd modulation on motor improvement was nonetheless inferior to the M1 modulation. Thus, stimulation of contralesional premotor cortex can also be used to ameliorate interhemispheric imbalance, but does not appear to be overall “better” than cM1 stimulation for motor recovery (For more discussion on PMd, see section 6.2.1 below).

Taken together, these results validate that targeting premotor cortex could be a potentially beneficial approach for stroke therapy, and an alternative to M1. However, these two studies did not target PMv specifically. As such, it remains to be seen whether similar (or better) results could be obtained by shifting the locus of premotor cortex stimulation more ventrally, either ipsilesionally or contralesionally.

5.2 Strengthening communication between premotor cortex and S1

Injury to M1 results in impaired motor performance that is due in part to a disruption of the communication between the somatosensory and motor cortex (Friel et al., 2005), as S1 provides M1 with critical information about the position of the limb in space. Premotor cortex also has long-range corticocortical connections with somatosensory areas, but they are relatively weak compared to those of M1 with somatosensory cortex (Rouiller et al., 1993; Dancause et al., 2005; Fang et al., 2005). Interestingly, after injury to the M1 hand area in monkeys, projections from PMv to M1 will "re-route" towards S1, such that there is a substantial increase in PMv-S1 connections, particularly area 1/2 (Dancause et al., 2005), possibly to reestablish the sensorimotor loop that normally involves M1 (Asanuma and Pavlides, 1997). As such, one possible approach for stroke recovery would involve promoting the communication between premotor cortex and S1. One such proof-of-concept study sought to do exactly that using a closed-loop neural interface in rodents with lesions to the primary motor area (Guggenmos et al., 2013). Their approach involved using an implanted neural prosthesis that consisted of electrodes placed in both the premotor cortex and somatosensory cortex. The device was designed to discriminate neural discharges in premotor cortex, and whenever an individual action potential was detected, the prosthesis would trigger electrical stimulation of the somatosensory cortex. This closed-loop system provided continuous stimulation over several weeks during recovery. This protocol substantially improved motor function and performance on reach and grasp tasks, such that by week 2 of therapy motor function returned to prelesion performance levels. The behavioral improvements of this closed loop approach were much greater than what was observed for animals with no stimulation, as well as animals with open-loop stimulation where S1 stimulation was not correlated with premotor neural discharge. Finally, the closed-loop stimulation enhanced the functional connectivity between premotor cortex and S1. As such, therapeutic intervention strategies that focus on promoting and reinforcing the functional and anatomical reorganization that is known to take place in premotor cortex following motor cortex injury may be an effective alternative approach to neuromodulatory strategies that focus exclusively on M1.

5.3 Neurofeedback training to upregulate PMv activity

Another approach, this time in human patients, explored whether volitional upregulation of PMv activity can be beneficial to recovery (Sitaram et al., 2012). It has been suggested that bihemispheric activation of the PMv can play an important functional role following cortical injury (Rehme et al., 2012; Sitaram et al., 2012; Horn et al., 2016). For example, after three weeks of comprehensive hand motor training, subacute stroke patients showed higher PMv activation in both hemispheres relative to controls during an active motor task that involved fist clenching of a rubber ball with the paretic hand, but not the non-paretic hand, and this was associated with improved motor performance (Horn et al., 2016). One study explored the feasibility of using a real-time fMRI brain-computer interface (BCI) to teach chronic stroke patients to self-upregulate ipsilesional PMv activity (Sitaram et al., 2012). This involved doing neurofeedback training where patients learned to self-regulate the BOLD (blood oxygenation level dependent) signal provided by the real-time fMRI-BCI setup. The neurofeedback training involved several tasks, such as observing a video of a hand grasping a coffee cup, whose frames would be advanced proportionally to the amount of BOLD signal change in the PMv. Patients were then able to "transfer" this learned self-upregulation to situations where they did not have any feedback, such that they were ultimately able to do so during performance on visuomotor grasp tasks outside of the scanner. This neurofeedback training with fMRI-BCI produced bilateral PMv activation and improved task performance in stroke patients. It also improved cortical excitability of M1 outputs to the paretic, contralateral hand as assessed by paired-pulse TMS over ipsilesional PMv and M1. They also tried this approach in healthy subjects, which similarly led to improved task performance. Interestingly, in both healthy subjects and stroke patients, self-upregulation of PMv activation was always bilateral, such that it was never restricted to the hemisphere whose BOLD response was being used for the neurofeedback signal. In addition, some healthy controls and stroke patients actually showed stronger activation of the PMv in the other hemisphere than the one providing the feedback signal during training, i.e. the ipsilateral PMv or contralesional PMv, respectively (Sitaram et al., 2012). Thus, these results provide further support that PMv's contributions to motor planning and execution are strongly bihemispheric. However, this approach also has some controversial elements. Generally speaking, stroke recovery approaches are viewed within the framework that recovery patterns towards normal representation maps are best (Ward et al., 2003a). For example, in humans, it has

been shown that irrespective of the method of modulation, good functional outcomes rely on the return of pre-stroke ipsilesional excitability (Rehme et al., 2012). Here, experimenters instead favored an approach that went in the opposite direction, by favoring much greater activation of PMv than normal (Sitaram et al., 2012). As such, the opinion that "near to normal patterns of activity is good recovery" may not be an absolute.

In conclusion, while studies have largely ignored premotor cortex as a neuromodulatory target for stroke recovery, the results of the experiments presented in this thesis and those of some exploratory studies suggest that intervention strategies should perhaps shift from exclusively targeting M1 to instead including premotor cortex. In particular, the PMv of both hemispheres is emerging as a promising and salient target for neuromodulatory approaches. Based on the plethora of neuromodulatory strategies targeting M1, one might be inclined to suggest that neuromodulation of PMv should follow a similar approach, by down-regulating an "excitable" cPMv, and/or up-regulating an "inhibited" iPMv. However, as discussed in the above sections, such approaches have shown inconsistent results, and the framework that guides them, the interhemispheric competition model, may need to be revisited. Perhaps alternative approaches, such as upregulating bilateral PMv, or focusing on retuning neural activity across the motor and premotor cortex, may be more consistent with the bihemispheric nature of PMv's contributions to motor control, and therefore lead to better functional recovery.

6. Future directions

6.1 Exploring changes in the relative encoding of the non-paretic versus paretic hand in single neurons

In this thesis, we performed numerous different analyses to quantify the changes occurring within neurons during use of the paretic or non-paretic hand separately. An additional analytical direction of interest could more specifically compare the relative preference, or sensitivity, of individual neurons for use of one hand relative to the other during grasp, and how this measure is affected by the unilateral M1 inactivation for the different areas studied. One way to perform this comparison is by calculating hand preference indexes, which can be used to compare the mean activity of a neuron during a given epoch, notably grasp, during use of the non-paretic hand relative to the paretic hand (Donchin et al., 1998; Donchin et al., 2002). Such an index can be calculated as:

$$\text{Hand preference index} = \frac{|Mean_{non-paretic}| - |Mean_{paretic}|}{|Mean_{non-paretic}| + |Mean_{paretic}|}$$

Where "Mean" is the mean discharge rate of the neuron during the grasp epoch. Absolute values are used, because mean baseline activity is removed from the mean discharge rates. As such, both mean increases and decreases of discharge rate relative to baseline activity reflect modulation during use of a given hand. As written, a value of "1" indicates a modulatory preference for the non-paretic hand and a value of "-1" indicates a modulatory preference for the paretic hand, whereas a value of "0" indicates that the neuron was equally modulated during use of either hand (hand non-specific).

The hand preference index of each neuron can be compared before and after inactivation, to quantify how the experimental manipulation affected the extent to which different cortical areas encode one hand relative to the other. Indeed, as discussed previously, unilateral perturbations to the motor system can induce imbalances in neural activity related to use of each limb, and as such shifts in hand preference indexes can help quantify such imbalances.

We performed some initial quantifications of changes in hand preference indexes for the PMv in both hemispheres and cM1 (Figure 4.1). In the figure, the indexes are calculated using mean activity during grasp. Unsurprisingly, we can see that activity in cM1 is much more

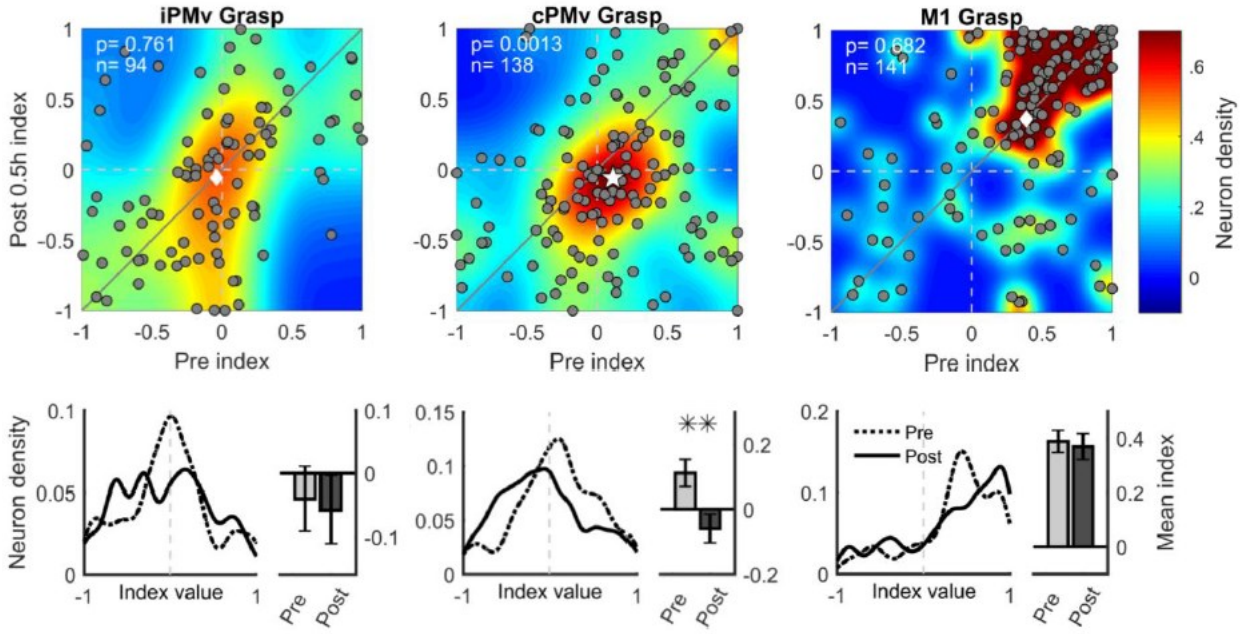

Figure 4.1. *Changes in mean hand preference indexes during grasp induced by the inactivation*

Shown are data for iPMv (left column), cPMv (middle column) and cM1 (right column). All neurons well-isolated both before and after inactivation were used in this analysis (within-neurons). The hand preference index for each neuron was calculated using the mean discharge rate across the grasp epoch in normalized time. Across all graphs, a value of "-1" denotes a preference for the paretic hand, and a value of "1" a preference for the non-paretic hand. *Top row*, heat plots show the mean hand preference index during grasp of each neuron (grey circles) before (x-axis) and after (y-axis) inactivation. The diagonal line represents no change in index. The mean population index across all neurons before vs after inactivation is shown with a white diamond (no significant change) or white star (significant change; paired *t* test, $p < 0.05$). *Bottom row*, the left plots show the density profile of the population of neuron indexes before (dotted line) and after inactivation (solid line). The right plots show the mean population index across all neurons before (light shade) and after inactivation (darker shade). Error bars represent ±SEM. $^{**}p < 0.01$, paired *t* tests.

lateralized towards the contralateral (non-paretic) hand, whereas activity in PMv is much more hand non-specific. After the inactivation, the most pronounced change is seen in cPMv, which shows a significant "shift" in the mean population index towards the paretic hand. In the iPMv, while the mean index stays relatively the same, we can see that the distribution of individual neuron indexes changed, such that there are much less hand non-specific neurons after inactivation (i.e. less neurons with an index value close to "0"). In contrast, the cM1 appeared once again to be minimally perturbed at the population level.

A quantification of shifts in hand preference indexes can also be performed at each point in time as grasp progresses, instead of using mean activity during grasp. This sort of approach allows for the quantification of dynamic changes in hand preference indexes during grasp (Figure 4.2). However, when doing this sort of quantification, for a given neuron the hand preference index should be scaled according to its maximal discharge, to avoid large fluctuations in indexes that can occur when the neuron is minimally active (Figure 4.2 A, center). When scaled, the hand preference index more accurately reflects the dynamic discharge pattern of the neuron (Figure 4.2 A, right). The tentative equation being used is shown below:

$$\text{Scaled hand preference index}_{\,t} = \frac{|NonParetic_t| - |Paretic_t|}{max_i(|NonParetic - Paretic|)_i}$$

Where t is a given bin in normalized grasp time (there are 1000 bins from grasp onset to grasp offset). "NonParetic" and "Paretic" represent the discharge rate of the neuron at time t during use of that hand. The denominator is the absolute maximal difference in firing rate that occurred across all time bins during grasp. With the scaled index, a value of "0" is typical when a neuron was not active (see Figure 4.2 A).

We first explored whether shifts in hand preference indexes occur naturally in the healthy brain as animals perform several hundred trials (Figure 4.2 B). We performed this analysis using the population of PMv neurons recorded during a session where no inactivation occurred, which previously served as a 'control' population for several analyses (see chapter 2). For each moment in time during grasp, we determined the index value of each neuron during the first 25 trials performed with each hand ('early trials'; Figure 4.2 B, left plot) and the last 25 trials performed with each hand ~1hr later ('late' trials; Figure 4.2 B, center). There was little change in the indexes of these neurons, showing that they are normally stable with time (Figure 4.2 B, right).

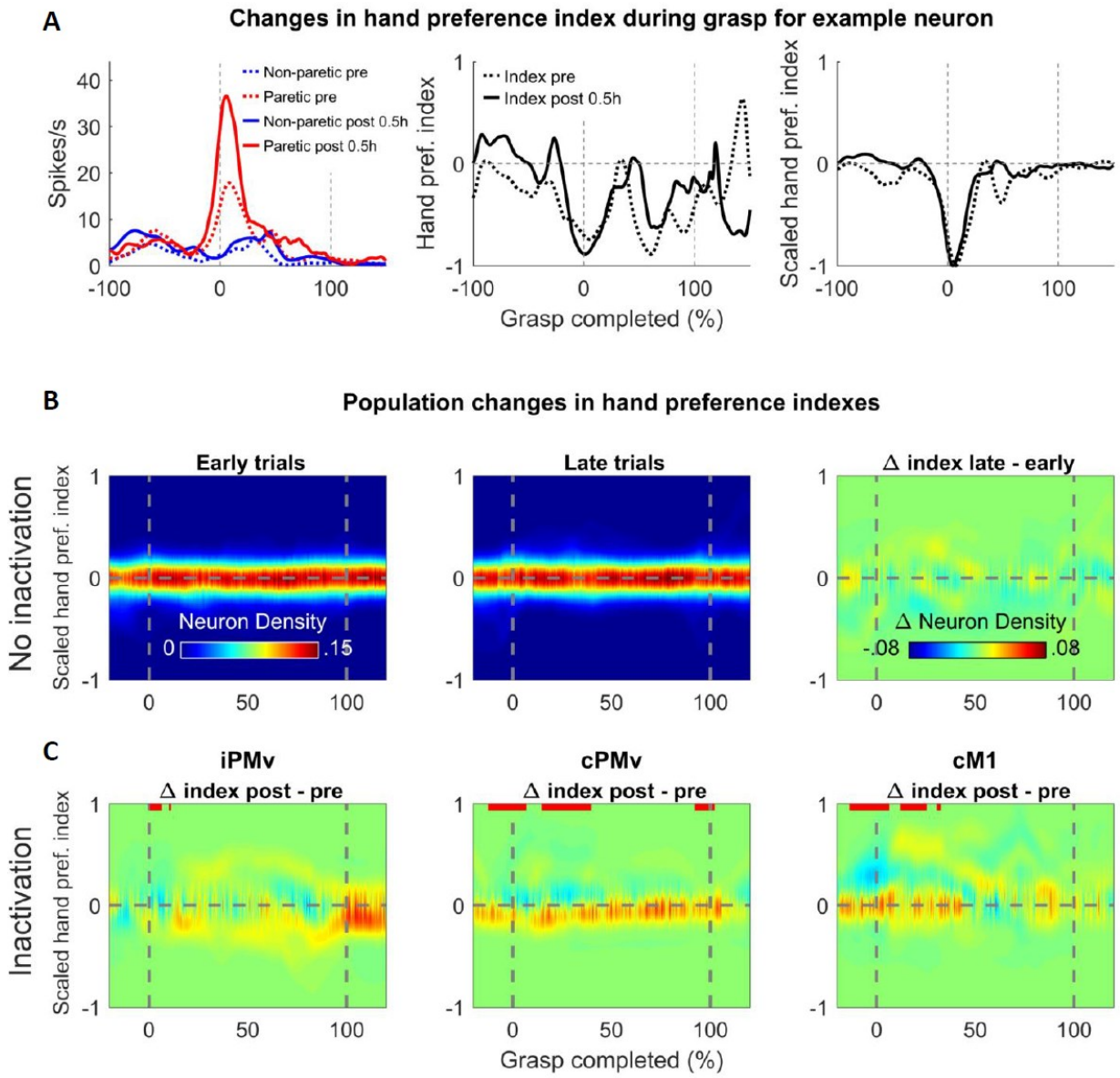

Figure 4.2. *Changes in hand preference indexes during ongoing grasp induced by the inactivation*

A, An example neuron with a clear preference for the paretic hand is shown to illustrate the importance of scaling the hand preference index for this sort of analysis. The index is calculated at each moment in time during grasp. Time is represented in normalized grasp time (Grasp Onset= 0%, Grasp Offset= 100%). ***B,*** Shown is the distribution of indexes during grasp for a population of PMv neurons (n = 49) during a recording session where no inactivation occurred (Moreau-Debord et al., 2021). 'Early trials' include the first 25 trials performed for each hand, and 'late trials' are the last 25 trials performed with each hand. Several hundred trials separate them, such that ~1 hr has passed between the early and late trial blocks. The left and center plot show the density of neuron indexes as grasp progressed during early trials and late trials,

respectively. Here, “-1” represents a preference for the contralateral hand, and “1” represents a preference for the ipsilateral hand. As different neurons show peaks of activity at different moments during grasp, it is normal that throughout grasp the greatest density of neuron indexes is found near “0” (see text). However, slight shifts from this center have meaningful implications. The right plot shows the different in density of neuron indexes during early and late trials. In this plot, the color green represents no change in the density of neurons at a given time and index value. Shifts towards blue and red reflect that less neurons or more neurons displayed that index value, respectively. Note that most of the plot is green, as there was little variation in index values across the population of neurons in the absence of inactivation. ***C,*** Shown in the change in index values of the population of iPMv (left), cPMv (center) and cM1 (right) neurons after unilateral M1 inactivation. The heat scales used are the same as for the ‘control’ PMv neurons (middle row, right). The red traces represent moments in time during grasp where the mean population indexes were significantly different after inactivation (paired *t* tests). In all three areas, noticeable changes in hand preference indexes can be observed.

However, after inactivation, neuron indexes were dynamically perturbed during grasp in both PMv and cM1 (Figure 4.2 C). For all three populations of neurons, significant shifts in population hand preference indexes occurred around grasp onset (red traces; $p < 0.05$, paired t tests). There were other noticeable changes in the distribution of neuron indexes during different windows of time during grasp. In particular, in the cPMv many neurons showed a greater preference for the paretic hand throughout grasp after inactivation, visible by the red hotspots below the origin line. In the iPMv, a noticeable shift in hand preference for the paretic limb appears to develop specifically after the end of grasp. Finally, in the cM1, prior to and during early grasp there seems to be an increase in the number of neurons showing no preference for either hand. This shift seems to be due in part to some neurons "losing" their bias for the non-paretic hand, visible by the blue hotspot at grasp onset. Thus, there appears to be important shifts in hand preferences that occur across the motor network that appear to be mostly directed towards the paretic hand. These initial results validate that a more thorough exploration of the biases in hand preferences that rapidly emerge in different neural populations after cortical injury are warranted.

Future refinement of this approach will seek to better emphasize changes in hand preference indexes occurring when neurons are actually modulated by the task, such that neurons that are not being responsive at a given timepoint during grasp can be distinguished from neurons that were active but truly hand non-specific, as both have a value of "0" in the current formulation of the scaled index. In addition, an exploration of the changes in hand preference indexes occurring specifically at the time where neurons were most active before (Pre peaks) and after inactivation (Post 0.5 h peaks) is warranted.

6.2 Exploring rapid reorganization in other premotor areas

In the current thesis, we focused on quantifying the neural reorganization that takes place on a very short time scale after a unilateral M1 inactivation, in bilateral PMv and cM1. One question that arises is how these rapid changes would look like in other premotor areas that have been implicated in recovery from focal M1 lesions. In particular, both the dorsal premotor cortex and the supplementary motor area have been shown to undergo reorganization that plays a role in recovery.

6.2.1 The dorsal premotor cortex

With regards to the premotor cortex, in this thesis we focused our attention on the PMv specifically, due to its particular role in visuomotor grasping. However, other premotor areas, including notably the dorsal premotor cortex (PMd), are critically involved in the planning and execution of unilateral arm and hand movements. In the monkeys used for the experiments presented in this thesis, we also placed arrays in the PMd of both hemispheres and recorded neural activity from those areas. Unfortunately, the quality of the recordings was lower than for the PMv and M1, and the arrays may not have been optimally placed in the hand representation of PMd. These factors guided our decision not to emphasize their analysis in this thesis. Nonetheless, while not the focus of the current thesis, an overview of the role of the PMd in motor control, and some of the neural changes that the ipsilesional PMd (iPMd) and contralesional PMd (cPMd) undergo following unilateral M1 inactivation with muscimol will be presented here. Finally, the potential implications of PMd reorganization for stroke recovery will be briefly discussed.

6.2.1.1 The PMd in motor control

The PMd is situated on the lateral surface of the cortex, medial to the genu of the arcuate sulcus. Like the other motor regions that have been the focus of this thesis, microstimulation studies have shown that PMd contains a somatotopic representation of certain areas of the contralateral body, which includes distal movements (He et al., 1993, 1995; Preuss et al., 1996; Dum and Strick, 2002; Raos et al., 2003; Raos et al., 2004; Stark et al., 2007). PMd can be subdivided into two subregions based on functional and anatomical differences, a caudal and rostral region, named F2 and F7 respectively (Geyer et al., 2000). F2 has a somatotopic organization that contains an arm and leg representation, that is ventral and dorsal to the superior precentral dimple respectively, whereas the rostral part of PMd, F7, contains neck, trunk, face and eye representations (Preuss et al., 1996; Rizzolatti and Luppino, 2001, 2015). PMd, like all premotor areas, contains corticospinal projections. Those of the hand area of PMd in area F2 project to the inferior cervical segments that contain motoneuron pools innervating the distal musculature of the arm and hand, and thus are able to influence hand movements (He et al., 1993). In addition, PMd also has cortico-cortical connections to the M1 hand area (Marconi et al., 2003; Hamadjida

et al., 2016), and it has been suggested that PMd could influence hand movements like grasping through these direct M1 connections (Raos et al., 2004; Castiello and Begliomini, 2008).

Neurons in the PMd, particularly area F2, have been shown to encode different aspects of reach-to-grasp movements (Raos et al., 2004; Stark et al., 2007; Hendrix et al., 2009; Takahashi et al., 2017; Papadourakis and Raos, 2019). Classically, PMd neural activity has mostly been studied in the context of arm movements. PMd neurons are particularly active during arm movement preparation, while also being active during the execution of planned arm movements (Weinrich and Wise, 1982; Kurata and Wise, 1988; Kurata and Hoffman, 1994; Cisek et al., 2003). Neurons in PMd encode many movement-related parameters similarly to M1. For example, during motor execution, PMd neural activity covaries with kinematic parameters such as the direction and extent of arm movement (Caminiti et al., 1991; Fu et al., 1993; Crammond and Kalaska, 1996, 2000; Messier and Kalaska, 2000; Cisek et al., 2003). However, it is less sensitive to parameters considered to be closer to the motor output of the cortex than M1, such as the posture of the joints and force exerted (Riehle et al., 1994; Crammond and Kalaska, 1996; Scott and Kalaska, 1997; Kakei et al., 1999). Rather, the PMd more preferentially encodes more abstract task-related information (Caminiti et al., 1991; Mitz et al., 1991; Johnson et al., 1996; Wise et al., 1996; Shen and Alexander, 1997b; Wise et al., 1997; Wise et al., 1998; Crammond and Kalaska, 2000; Wise and Murray, 2000).

In contrast to reaching movements, the PMd has been less studied for grasp motor control. One reason for this is that the PMd has a much smaller hand representation area than PMv and even SMA (see next section 6.2.2 for discussion on SMA). Nonetheless, some studies have shown that PMd is involved in encoding grasping to some degree. For example, using tasks that require performing movements to grasp objects, some neurons in PMd have been shown to be selective for the type of grasp required to interact with the different objects, both during movement preparation and execution (Raos et al., 2003; Raos et al., 2004; Stark et al., 2007; Hendrix et al., 2009). Thus, PMd neurons are tuned to grasping similar to PMv. In addition, PMd neurons may maintain in memory, during reach to grasp, a motor representation of the grasp used as well as their encoding of object-related parameters regardless of whether visual feedback is available (Raos et al., 2004; Raos et al., 2006).

The PMd may also encode kinematic and dynamic information about hand movements. For example, it has been demonstrated that whole-arm kinematic parameters, which include the hand, can be decoded from ensembles of PMd neurons or combined ensembles of PMd and PMv neurons (Hatsopoulos et al., 2004; Kang et al., 2012; Aggarwal et al., 2013). In addition, it has been demonstrated that single neurons in PMd can encode the kinematics of both reach and grasp synergies (Takahashi et al., 2017). While there was a preference for the former (reaching) in single neuron activity, the representation of grasp kinematics was nonetheless robust. Finally, it has been suggested that PMd may also encode dynamic aspects of hand movements. PMd neurons appear to be modulated by the application of grasp force similar to M1 during reach-to-grasps such as those that require whole-hand grasping (Hepp-Reymond et al., 1999; Raos et al., 2004; Gardner et al., 2007; Stark et al., 2007; Umilta et al., 2007; Hendrix et al., 2009), although this has been disputed (Boudreau et al., 2001).

The PMd can induce complex modulatory effects on M1 outputs. Like PMv, in the awake monkey ipsilateral PMd can modulate ipsilateral M1 neuron activity (Tokuno and Nambu, 2000), and shows more facilitation than inhibition on M1 outputs to contralateral hand muscles in the anesthetized monkey (Cote et al., 2017; Cote et al., 2020). However, it has less facilitation and more inhibition compared to PMv (Cote et al., 2017; Cote et al., 2020). In humans at rest, PMd has inhibitory effects than become facilitatory as stimulus intensity increases (Civardi et al., 2001; Koch et al., 2007). During movement preparation in humans, PMd facilitates M1 outputs to the contralateral hand muscles used to perform the task (Groppa et al., 2012; Vesia et al., 2018). However, if the task requires use of the ipsilateral hand only and not the contralateral hand, then ipsilateral PMd modulation on ipsilateral M1 becomes inhibitory (Groppa et al., 2012). Complex modulatory effects of the ipsilateral PMd on contralateral M1 have also been reported during unimanual movements. For example, during movement selection in human subjects, the PMd will inhibit the outputs of the contralateral M1 to the ipsilateral hand if this hand has not been selected based on task requirements (Koch et al., 2006; O'Shea et al., 2007). During complex bimanual movements, PMd can show important facilitatory effects on the contralateral M1, and the extent of this facilitation predicts performance on the task (Liuzzi et al., 2011). As such, the modulatory effects of PMd on M1 outputs of both hemispheres are consistent with its complex role in movement selection, and its mixed effects may contribute to fine adjustments of the hand for grasping based on task requirements.

Finally, it is worth noting that the PMv and PMd can also exchange information during arm and hand movements. Anatomically, area F5 from the PMv and the lateral part of F2 from the PMd are interconnected (Marconi et al., 2001; Dancause et al., 2006a; Bruni et al., 2018). Based on the functional roles of these two areas, it has been suggested that PMv may provide PMd with a motor representation of the object that is to be grasped, that in turn combines this representation with visuo-spatial information about the environmental context of the task in order to update the appropriate configuration and orientation of the hand as it closes in on the object (Raos et al., 2004).

Overall, it is clear that PMd, PMv and M1 form a richly interconnected cortical network that works together towards the production of hand motor acts such as reaching and grasping, with complex functional interactions that depend on many factors such as task demands and phases of movement (Dum and Strick, 2005).

6.2.1.2 Changes in bihemispheric PMd neural activity after M1 inactivation

We performed identical analyses on PMd neural activity as those performed on PMv and M1 data. Similarly to the other areas studied, changes in neural activity were heterogeneous, with both increases and decreases of neural discharge rates observed in PMd neurons of both hemispheres during use of either hand. When comparing the population of 'control' PMd neurons (i.e. pre-inactivation; n = 252) to the population of post-inactivation PMd neurons (n = 150 iPMd, 101 cPMd), we found that there was no alterations is discharge rate in either PMd at rest (three-way ANOVA $p > 0.05$; not shown). Furthermore, during movement, there were minimal changes in the proportions of neurons modulated during grasp with either hand, with the notable exception that there were significantly less cPMd neurons modulated during grasp with the paretic hand ($\chi^2_{(2, N = 353)} = 9.19$, $p = 0.01$, $V = 0.11$; not shown). More specifically, there were less cPMd burst neurons during grasp with the paretic hand (-14.3%, Bonferroni corrected z test, $z = -3.03$, $p = 0.0049$, $r = 0.36$). In the healthy brain, during ipsilateral hand movement, the ipsilateral PMd exerts an inhibitory influence on ipsilateral M1, possibly to prevent unwanted movements in the unused hand (Groppa et al., 2012). Such a loss of grasp-modulated cPMd burst neurons during paretic hand movements may play a role in the generation of undesirable movements in the non-paretic hand such as mirror movements, that is sometimes seen after M1 lesions, if such bursting activity has an inhibitory function on M1 outputs. Overall, the iPMd and

cPMd was less perturbed at the population level than PMv, but not quite as unperturbed as cM1. Thus, it appears that the inactivation affected the PMv, PMd, and M1 populations differently.

For our within-neuron analyses, we focused on 113 iPMd, and 75 cPMd neurons that were well-isolated both before and after the unilateral M1 inactivation. When quantifying the incidence of neurons showing increases or decreases of neural discharge rate at each moment in normalized tine of the grasp epoch, changes were quite heterogenous, but general trends emerged (Figure 4.3 A). Notably, in both the iPMd and cPMd during grasp with the non-paretic hand, there were somewhat more neurons with decreases than increases of activity that accumulated with time, whereas with the paretic hand, there was a greater proportion of neurons with increased discharge rate that accumulated with time, as shown with the cumulative sums. These results are different from what was observed in the other areas studied. For example, for both PMv we had observed cumulative decreases in the iPMv and increases in the cPMv during use of either hand. Furthermore, there was a much greater proportion of neurons showing significant changes at each moment during grasp in either PMv compared to the iPMd or cPMd. Thus, once again, the inactivation affected PMd neurons differently than the other areas studied.

When looking at the timing of neuron's maximal discharge, we found that it was perturbed in both the iPMd and cPMd after inactivation (Figure 4.3 B, heat plots). This detuning was most pronounced in the cPMd during use of the paretic hand, similarly to what had been observed for the PMv and cM1. Unfortunately, it was more difficult to find neurons with significant peaks of activity during grasp (>1 SD from baseline), particularly for cPMd (Figure 4.3 B, bottom row). Many neurons "gained" or "lost" significant grasp peaks after the inactivation (grey "x" in figures), further demonstrating how PMd neural activity in both hemispheres was destabilized by the "loss" of the M1 hand area. Furthermore we observed significant decreases in discharge rate that occurred at the time where neurons had been most active prior to inactivation during grasp (Pre peaks; Figure 4.3 C, left) in the iPMd (non-paretic: -1.92 spikes/sec, $T_{(38)} = -4.63$, $p = 4.24 \times 10^{-5}$, $d = -0.74$; paretic: -1.64 spikes/sec, $T_{(46)} = -3.00$, $p = 0.0043$, $d = -0.44$; paired t tests) and the cPMd (non-paretic: -3.24 spikes/sec, $T_{(19)} = -2.66$, $p = 0.015$, $g = -0.29$; paretic: -4.68 spikes/sec, $T_{(15)} = -2.98$, $p = 0.0094$, $g = -0.8$), similar to what was observed in iPMv and cM1. In contrast, we observed increases in discharge rate at the time

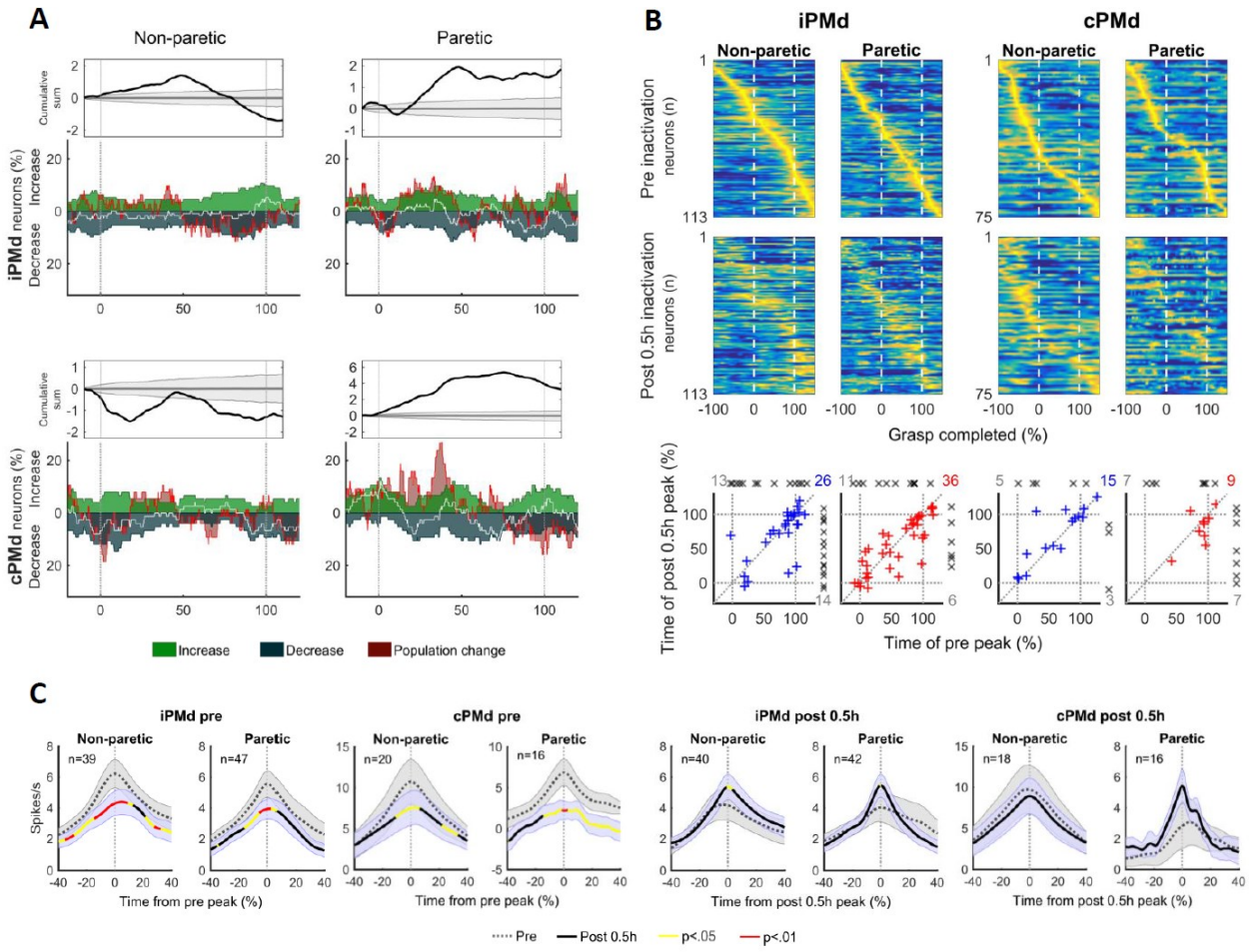

Figure 4.3. *An exploration of neural changes taking place in the PMd of both hemispheres*

A, The incidence of neurons with increases and decreases of discharge rate during grasp. See Figures 2.7 and 3.5 for legend details. During use of the paretic hand, there were more neurons that showed increases of neuronal discharge rates that cumulated with time in both PMd. In contrast, during use of the non-paretic hand there were overall more neurons with decreases that cumulated with time, although this pattern is less consistent. ***B,*** Changes in the timing of peak discharge rate after inactivation. See Figures 2.8 and 3.6 for legend details. Overall, the inactivation affected the temporal pattern of neurons' timing in both PMd and during use of the non-paretic and paretic hand. However, few neurons with significant peaks of discharge rates during grasp were found particularly in the cPMd, limiting our ability to perform peak analyses. ***C,*** Changes at the time of peak discharge of iPMd and cPMd neurons induced by the inactivation. See Figures 2.10 and 3.7 for legend details. In both the iPMd and cPMd we noticed significant decreases of discharge rate at the time of Pre peaks (left plots). At the time of Post 0.5 h peaks, in the cPMv we observed barely significant increases during use of either hand, that are less much convincing than what was observed particularly in cPMv but also cM1.

where neurons became most active after the inactivation (Figure 4.3 C, right) during use of either hand in the iPMd (non-paretic: 1.2 spikes/sec, $T_{(39)} = 2.1$, $p = 0.043$, $d = 0.33$; paretic: 1.43 spikes/sec, $T_{(41)} = 2.02$, $p = 0.049$, $d = 0.31$) and a similar trend during use of the paretic hand in the cPMd (2.6 spikes/sec, $T_{(15)} = 1.61$, $p = 0.13$, $g = 0.48$). However, these post 0.5 h peak increases were much more attenuated and less convincing than what was reported for the cPMv especially, but also for the cM1.

Overall, when comparing these results with those obtained from PMv and M1, the widespread detuning of neural discharges was a consistent observation across all areas studied, further highlighting that the local perturbation of the M1 hand area led to a generalized loss of coordination in neural activity across the bihemispheric motor network. However, aside from the widespread detuning, the results are strongly heterogenous between areas, demonstrating that the inactivation affected the PMd, PMv, and M1 very differently. The M1 inactivation perturbed iPMd and cPMd neural discharge rates and modulatory patterns in both hemispheres to a greater extent than cM1, but the most perturbed areas were by far the iPMv and cPMv, which showed the most pronounced changes in neural activity. These differences may be due in part to the different roles that these areas play in unimanual control of grasping, that seems to involve bilateral PMv more so than bilateral PMd or cM1 in the monkey.

6.2.1.3 A more limited role of PMd reorganization in recovery from focal M1 hand area lesions

There are several possible explanations as to why PMd may have shown less pronounced changes than PMv. Relative to the PMv, functionally the PMd has been more implicated in the control of arm movements than grasping (Jeannerod, 1981; Filimon, 2010; Karl and Whishaw, 2013; Whishaw and Karl, 2014) and is less interconnected with the M1 hand area that was the target of our inactivation paradigm (Dum and Strick, 2005). Furthermore, it is well known that precision grip tasks in particular evoke bilateral PMv activity (Binkofski et al., 1999a; Binkofski et al., 1999b; Ehrsson et al., 2000; Ehrsson et al., 2001). As such, perhaps it is not surprising that PMd activity would be less affected than PMv during grasping specifically. In parallel, some of our PMd arrays may not have been ideally placed in the hand representation area. This could explain the low count of neurons with significant grasp peaks that we observed notably in the

cPMd and contribute to the less pronounced neural changes observed in this area relative to the PMv.

However, the PMd may simply not be the main site of reorganization in this model of focal M1 hand area injury. One piece of evidence for this interpretation is derived from a therapeutic intervention study that looked at the use of cell therapy in monkeys to promote cortical reorganization after a lesion to the M1 hand area (Moore et al., 2013; Orczykowski et al., 2018). Monkeys that received an intravenous injection of human stem cells (umbilical tissue-derived cells, hUTC) 24 hours after cortical injury showed significantly improved paretic hand function relative to controls as early as just 2 weeks into recovery, and improved precision pinch grasping over 12 weeks of behavioral testing (Moore et al., 2013). After the final postoperative assessment testing with the paretic hand at 12 weeks, the monkeys were rapidly perfused and early gene c-Fos expression in cells of the PMv and PMd were quantified (Orczykowski et al., 2018). The expression of c-Fos often occurs when neurons fire action potentials, and thus serves as an indirect marker of recent neuronal activity. Interestingly, they found that there were significantly more c-Fos activated cells in both the iPMv and cPMv of hUTC treated animals compared to controls. Furthermore, increased c-Fos activated cells in bilateral PMv was correlated with decreased recovery time and better grasp performance. In contrast, there was no change in the proportion of these cells in either the iPMd or cPMd of treated animals relative to controls. Thus, they concluded that the cell therapy enhanced cortical reorganization and recovery, and that this recovery of function critically involved bilateral plasticity of the PMv but not of the PMd (Orczykowski et al., 2018).

Additional evidence that reorganization of PMd may not be default path to recovery from focal M1 hand area injury comes from an invasive brain stimulation study that specifically targeted PMd (Plautz et al., 2016). In this proof of principle study, they favored an invasive neuromodulatory approach using monopolar subthreshold stimulation applied via subdural cortical electrodes placed over iPMd in monkeys. In a similar fashion to the invasive electrical stimulation studies that targeted perilesional M1 discussed in a previous section *e.g.*(Plautz et al., 2003), they applied 100 Hz subthreshold stimulation continuously during therapy sessions for several weeks after a focal lesion to the M1 hand area. However, in contrast to perilesional M1 stimulation, PMd stimulation did not lead to improvements in therapeutic gains relative to

controls, nor did it lead to increased digit representation in PMd (Plautz et al., 2016). It also had the unexpected effect of inducing decreased digit representation in PMv. Normally, in this model of focal M1 lesions, rehabilitation and functional recovery are accompanied by increased PMv digit representation (Frost et al., 2003; Dancause, 2013). Note that these results should be taken with a grain of salt, as this was a proof of principle study, and used few animals to perform their analyses. Nonetheless, considering the preferential role PMv seems to play in recovery from focal M1 lesions, perhaps future stimulation approaches would benefit from targeting PMv, rather than PMd, to enhance recovery in this model.

To conclude, while we have provided some initial quantifications of the rapid reorganization that takes place in the PMd, some additional data, possibly from one more monkey with well-placed arrays and with better electrophysiological signals, would be ideal to extend and truly validate our initial observations. That being said, our initial results point to a more attenuated reorganization of PMd relative to PMv after unilateral M1 injury, which appears consistent with observations from other studies using this model.

6.2.2 The supplementary motor cortex

The supplementary motor cortex (SMA) is another premotor area that, while not the focus of this thesis, is involved in voluntary motor control and can play a role in recovery. Like other premotor areas, it can be subdivided into two parts, a rostral ('Pre-SMA') and caudal portion ('SMA-proper') (Luppino et al., 1993; Geyer et al., 2000; Picard and Strick, 2001). It is the caudal SMA-proper that is most implicated in more direct motor control, and that will be the focus of discussion here. The SMA is notably involved in the sequential control of movements, and can directly control distal movements of the hand (Maier et al., 2002; Boudrias et al., 2010), consistent with its somatotopy that contains a hand representation area (Gould et al., 1986; Mitz and Wise, 1987; Luppino et al., 1991). It appears to play a particularly important role in the initiation and coordination of bimanual movements (Kermadi et al., 1998), as inactivation of SMA induces delays in the initiation and timing of bimanual movements without causing any observable motor deficits in hand use during movement (Kermadi et al., 1997). As all premotor areas, it is reciprocally connected with M1, and is an origin of corticospinal projections (Dum and Strick, 1991; Luppino et al., 1993, 1994). It also has numerous transcallosal interconnections with its homologue (McGuire et al., 1991) and some with the hand representation area of the M1

of the other hemisphere (Rouiller et al., 1994). Like PMv and PMd, SMA can also modulate the outputs of the M1 hand area of both hemispheres (Cote et al., 2020).

The SMA has been suggested to contribute to functional recovery following cortical injury. For example, in the monkey, following a lesion that affects M1 and part of premotor cortex, the ipsilesional SMA will show increased corticospinal projections that are correlated with functional recovery (McNeal et al., 2010). Furthermore, a second lesion to SMA after recovery reinstates motor deficits (McNeal et al., 2010). Monkey SMA can also show increased motor representation area that is proportional to lesion size (Eisner-Janowicz et al., 2008). However, in this case the sizes of the lesions needed to induce SMA expansion were quite large, and included not just M1, but the PMv and PMd hand representation areas. Furthermore, changes in map size and their relationship to functional recovery were not as clear-cut as what has been described for PMv (Frost et al., 2003; Dancause, 2013). In particular, there was an initial contraction of SMA maps in the first 3 weeks after injury, which was then followed by an expansion over the next 10 weeks. In parallel, behavioral recovery was only observed during the first 3 weeks after the injury, and then was relatively constant and limited for the remaining 10 weeks. Thus, the association between increased SMA map size and recovery is not clear. Furthermore, the expansion of SMA maps mostly concerned more proximal wrist and forearm movement representations rather than digit representations. This is consistent with the suggestion that the influence of SMA on motor neuron pools in the spinal cord is greater for proximal rather than distal muscles (Boudrias et al., 2006). Finally, the hand representation area of SMA is much smaller than in PMv (Dancause, 2013). As such, for much smaller lesions that only affect the M1 hand area as in our model, the role of SMA in recovery of hand dexterity specifically may be more limited than for PMv, and its influence on functional recovery may become more prominent primarily for larger lesions such as those that extend to PMv and PMd. Therefore, one might hypothesize that an exploration of neural reorganization of bilateral SMA after unilateral M1 inactivation will reveal that it is less affected than bilateral PMv.

Nonetheless, there are some indications that even in the case of a focal lesion to the M1 hand area, important changes take place in both the ipsilesional SMA (iSMA) and the contralesional SMA (cSMA). First of all, microscopic examination of pyramidal neuron density in the SMA of both hemispheres show important structural changes several weeks/months

following the loss of inputs from M1 (Contestabile et al., 2018). This study used SMI-32 staining, which is selective for pyramidal neurons in layers II, III, and V. While the unilateral, focal lesion to the M1 hand area did not lead to an overall significant loss in the number of labelled neurons in SMA across lesioned monkeys relative to controls, it did lead to an interhemispheric asymmetrical pyramidal neuron density between the hemispheres that was not present in controls. Interestingly, this bias was not always directed towards the same hemisphere depending on the size of the lesion. In layer V, smaller M1 lesions were correlated with a bias towards ipsilesional hemisphere (i.e. more pyramidal neurons in iSMA than cSMA), whereas larger lesions were correlated with bias towards contralesional hemisphere (i.e. more pyramidal neurons in cSMA than iSMA). Thus, the impact of the M1 lesion on bilateral SMA neuron density was correlated with the size of the lesion. Furthermore, these asymmetries in neuron density were correlated with the duration of functional recovery (i.e. how long it took the animals to reach a behavioral improvement plateau): the longer the functional recovery, the greater the bias towards the contralesional hemisphere. In layer III, the changes were less systematic than in layer V but were in same direction. However, they were not correlated to lesion size. One possible explanation for this difference between layers III and V is that while both layers are a source of corticocortical projections, those in layer V also have corticospinal projections. Since SMA has been shown to undergo axonal sprouting in the spinal cord after unilateral M1 lesion (McNeal et al., 2010; Morecraft et al., 2015), as more M1 corticospinal axon terminals degenerate with larger M1 lesions, this probably leaves more space for corticospinal axons from SMA layer V to sprout and extend to the spinal cord.

Finally, changes of SMA single-neuron activity after a focal lesion of the M1 hand area suggest a role of this area in functional recovery of the hand (Aizawa et al., 1991). When learning a task that involves the hand, SMA neurons often show activity during movement planning (Tanji et al., 1988). However, after a monkey was overtrained on a finger flexion with the right or left hand, this premovement activity disappeared from most SMA neurons, suggesting that its presence is possibly related to task learning but disappears following motor automation (Aizawa et al., 1991). Interestingly, following recovery from a lesion to the M1 hand area, neural recordings in bilateral SMA revealed that many neurons again displayed premovement activity (Aizawa et al., 1991). This reinstatement of premovement activity was observed during use of either hand and in both SMA. However, some differences between

hemispheres were nonetheless present. In the iSMA, the greatest number of neurons showed a selective return of premovement activity exclusively for the paretic hand, whereas in the cSMA, most of the neurons showing premovement activity were hand non-specific, being active prior to movement onset during use of either hand. As such, it is possible that "relearning" of the task after the lesion involved a reorganization of SMA activity to different extents in both hemispheres, such that it became once again involved in motor planning.

To conclude, it is clear that reorganization in premotor areas other than PMv play a role in recovery from focal M1 lesions, and therefore likely undergo rapid changes in neural activity after cortical injury. The SMA remains an interesting candidate whose rapid reorganization has yet to be explored. This could be done using a similar experimental paradigm as we have used here in this thesis, by reversibly inactivating the M1 hand area with muscimol during continuous recordings. Because the SMA is located on the midline surface of the hemisphere and "wraps" around it in the macaque, its location renders the use of arrays more challenging. However, the availability of arrays whose electrode lengths can be individually specified (such as floating microprobe arrays, used in our studies; MicroProbes for Life Science, Gaithersburg, USA) or new multi-electrode linear shanks with numerous recording sites along its length (e.g. linear microprobe arrays; MicroProbes for Life Science, Gaithersburg, USA), can be used to address these challenges and allow recording from multiple neurons simultaneously in this area. Based on the above discussion, while we expect to see changes in neural activity in bilateral SMA, it is likely that such changes will nonetheless be less pronounced that what we observed in PMv, which appears to play a more direct role in unimanual grasping than SMA.

6.3 Exploring relationships between neural reorganization and lesion size, location, and time from injury

6.3.1 Effect of lesion size on rapid reorganization

An interesting question to explore concerns how the rapid reorganization of neural activity that we observed would change with increasing sizes of M1 inactivation. As discussed at several points throughout the different sections of this thesis, the extent of reorganization of premotor areas after cortical injury in the monkey, in both the ipsilesional and contralesional hemisphere,

is notably dependent on the size of the lesion. Furthermore, as the extent of the lesion becomes greater, reorganization of the contralesional hemisphere becomes more pronounced. As such, it would be interesting to see if a similar pattern emerges in the rapid reorganization of single-neuron activity that occurs in the motor-related areas studied in the current thesis.

In our current experiments, we focused on neural reorganization that occurred following M1 inactivations that were large enough to induce deficits, but where animals were still able to perform the task with the paretic hand for at least a few trials. This mostly included experiments where 1 × 0.75 µL of muscimol were injected into M1, as well as one experiment where 2 × 0.75 µL was injected, and one experiment where 3 × 0.75 µL was injected. We actually performed several more experiments with larger inactivation sizes, where 2, 3, 4, and even 5 × 0.75 µL of muscimol were injected to inactivate larger and larger extents of M1, which were not discussed in the present thesis. However, for these injections, the monkeys were unable to perform the task with the paretic hand at all at the post 0.5 h time point. Instead, to characterize deficits we had them attempt reaches to food morsels held manually by the experimenters using large forceps and presented in front of the monkeys. As such, we chose to shelve those data for the time being as we were interested in specifically comparing neural activity in a rigorous and behaviorally comparable manner during use of the paretic hand relative to the non-paretic hand and with performance on the same automated pellet retrieval task prior to inactivation, which would not have been possible with the larger inactivations and the alternate reaching task.

This collected but unprocessed data would allow us to explore the question of the effect of lesion size on rapid neural reorganization of motor areas in both hemispheres. One approach would be to focus exclusively on the non-paretic hand, since monkeys were able to perform the task without noticeable deficits regardless of the unilateral inactivation size. In the experiments presented in this thesis, we observed important changes during non-paretic hand use in all areas studied. Importantly, we also observed that the neural changes in bilateral PMv during use of the non-paretic hand became more pronounced at the Post 3 h time point, where paretic hand deficits were the most substantial, relative to the Post 0.5 h time point (Moreau-Debord et al., 2021). As deficits regressed, so did the changes in neural activity during use of the non-paretic hand. As such, we hypothesize that a similar effect would likely be observed with larger inactivation sizes. Namely, more pronounced changes would be observed with larger relative to smaller

inactivation sizes. At the population level, this might manifest by more neurons losing their modulation during grasp. In within-neuron analyses, we would expect to see a greater attenuation of discharge rates at the time of pre peak discharge, where neurons where maximally active during grasp prior to the inactivation, particularly in iPMv and cM1.

While analysis of changes in neural activity during use of the non-paretic hand is more readily accessible, some possibilities do exist to explore neural changes during use of the paretic hand when performance on the pellet retrieval task is impossible. In particular, an analysis could be performed looking at associations between neural activity and activation of different specific muscles thanks to our EMG recordings. Changes in the associations between neural activity and single muscles or muscle synergies could then be explored and quantified based on different inactivation sizes. We would hypothesize that larger lesions would lead to a greater attenuation of neural activity associated particularly to distal muscles relative to proximal muscles, and a greater detuning of neural activity relative to the timing of distal muscle use in all areas studied.

6.3.2 Effect of somatosensory versus motor lesions on rapid reorganization

Another interesting question to explore would be how rapid neural reorganization occurs in the distributed motor network following somatosensory, or combined sensorimotor, inactivation. Indeed, stroke can often affect somatosensory cortex, and not just motor-related areas (Abela et al., 2012; Borich et al., 2015; Kessner et al., 2019). Damage to primary somatosensory cortex (S1) often results in a reduction or loss of voluntary motor control and of somatic stimulus perception. Behavioral studies conducted in adult macaque monkeys have shown that lesions to S1 distal forelimb representations lead to deficits in the discrimination of tactile stimuli as well as severe functional impairment in hand use (Cole and Glees, 1954; Semmes and Mishkin, 1965; Semmes and Porter, 1972; LaMotte and Mountcastle, 1979). Fortunately, recovery of sensation and of manipulative function develops progressively after restricted S1 lesions (Cole and Glees, 1954; Glassman, 1971). This sensory recovery is accompanied by cortical reorganization in perilesional and intact areas of S1, in a parallel to what occurs in motor cortex during recovery from motor deficits (Jenkins and Merzenich, 1987; Doetsch et al., 1990; Xerri et al., 1998).

Concerning motor recovery, it has been suggested that lesions to somatosensory cortices interfere with the capacity to recover motor function after stroke (Abela et al., 2012). More specifically, the extent to which the lesion affected somatosensory areas and somatosensory

performance is correlated to the outcome of functional recovery. However, the rate of recovery depends on lesion load to M1. Therefore, there appears to be an interplay between injury to somatosensory and motor cortex, with lesions to somatosensory areas influencing recovery outcome, and lesions to the motor cortex affecting recovery dynamics (Abela et al., 2012).

Finally, somatosensory, motor, or sensorimotor lesions or inactivations can induce rapid reorganization of sensory processing in the ipsilesional but also the contralesional hemisphere in anesthetized animals (Clarey et al., 1996; Ding et al., 2011; Mohajerani et al., 2011). For example, while sensory-evoked neuronal responses to passive, external stimulation often become attenuated in the ipsilesional hemisphere, they can become enhanced in the contralesional hemisphere (Clarey et al., 1996; Mohajerani et al., 2011).

It is unknown how rapid neural reorganization takes place in the bihemispheric distributed motor network of awake behaving animals following a focal S1 inactivation, or an M1+S1 inactivation. Furthermore, it would be interesting to compare such changes with those reported in the current thesis for purely focal M1 inactivation. Fortunately, initial datasets to perform these analyses exist. In our experiments, the cortical chamber that was implanted in our monkeys allowed us access to S1. In several experiments, we specifically inactivated S1 with 1, 2, or 3 × 0.75 μL of muscimol during continuous neural recordings. In addition, we performed several inactivations that targeted both S1 and M1 with several muscimol injections. Following S1 inactivations, monkeys were able to perform the task, but displayed clearly somatosensory deficits. More specifically, they showed some difficulty in properly orienting their digits around the pellets once contact had been made, and they applied inappropriate, often excessive, amounts of force with their digits to grasp the pellets. However, analysis of the changes in neural activity that accompanied these deficits have not yet been performed. Similarly to M1 inactivation, we would expect to see important changes in neural activity across the motor network. As S1 lesions can induce long-term and lasting perturbations in the fidelity of sensory-evoked responses across wide swaths of cortex (Sweetnam and Brown, 2013), we hypothesize that a widespread detuning of neural discharge rates will also occur across motor and premotor cortex similarly to what was seen for M1 inactivation, particularly upon contact with the task apparatus containing the pellet to be retrieved. However, in the monkey S1 connections to premotor cortex appear to be relatively sparce both intrahemispherically (Jones et al., 1978; Pons and Kaas, 1986) and

interhemispherically (Killackey et al., 1983; Gould et al., 1986), with premotor cortex instead receiving numerous peripheral somatosensory inputs of its own (Wiesendanger et al., 1985; Hummelsheim et al., 1988) and being more strongly interconnected with S2 (Gerbella et al., 2011; Gharbawie et al., 2011b). Thus, taken together with the preferential role of PMv in using visual, rather than somatosensory, information for grasping, we would expect neural changes to be more attenuated in bilateral PMv than what was observed during M1 inactivation.

6.3.3 Evolution of neural reorganization after a focal M1 lesion

In the current experiments, we focused on immediate changes in neural activity. However, one question that remains is how these changes across the distributed motor network would evolve with time as animals recover from an actual cortical injury. Such an experiment could be performed using a similar setup as used in the experiments presented in this thesis. However, instead of using muscimol to reversibly inactivate the M1 hand area, a permanent lesion would instead be performed, for example by using targeted endothelium-1 injections which have been used before in the lab. Arrays placed in motor and premotor cortex in both hemispheres could then be used to track the neural reorganization that takes place in the distributed motor network as monkeys recover fine dexterity of the hand on reach and grasp tasks.

With regards to reorganization of neural discharge timing, one study in particular provides interesting clues as to how neural synchrony across the motor network may progress after injury and during recovery (Khanna et al., 2021). As part of their experiments, they reported on the evolving changes in neural activation patterns that occurred at the population level in perilesional cortex (PLC) of monkeys following motor or sensorimotor lesions. In all cases, the M1 hand area was destroyed. The animals performed reach and grasp tasks. They characterized changes in task-related neural activity as recovery progressed. Interestingly, they observed that while behavior in single trials early in recovery was unsurprisingly slower than prior to the lesion, there was nonetheless a subset of trials that were executed quickly and successfully. By averaging the patterns of PLC population activity over these fast, rewarded trials on each day of recovery, they obtained a template per session that provided an estimate of the PLC population pattern encoding successful task performance despite deficits. They then compared single trial patterns of activity to this template of successful patterns per session. They found that, as recovery progressed, the patterns of population activity during single trials became

more and more similar to those of the trial-averaged "successful" templates such that single trial template matching significantly increased as recovery progressed. As such, the similarity of single trial activity to the template tracked improvements and was correlated with recovery. These results demonstrate that recovery is accompanied by increases in temporally precise co-firing of task-related neural activity in PLC that were likely shaped by early successes. Put another way, patterns of neural activity when animals did succeed at the task despite deficits early in recovery likely informed the motor network as to the pattern of activity it 'should' have to properly perform the task and served as a driving force to push the system towards that neural pattern endpoint.

The changes observed during recovery from motor deficits in the Khanna et al. (2021) study are reminiscent of what takes place in motor cortex during adaptation to external perturbations or motor learning of new tasks, where populations of neurons can produce new patterns of activity to maintain existing or enable new behavioral capabilities (Li et al., 2001; Jarosiewicz et al., 2008; Oby et al., 2019; Zhou et al., 2019). More precisely, the motor system first attempts to learn new tasks by reassociating preexisting patterns of neural activity with different intended movements (Golub et al., 2018), and if this is not possible, then it will form new neural patterns over several days (Oby et al., 2019).

It is well known that premotor cortex is also involved in motor learning and adaptation (Dayan and Cohen, 2011). Error-correction signals involved in on-line motor control adaptation exist in premotor cortex (Wolpert and Miall, 1996; Inoue et al., 2016), and during learning, there is an upregulation of activity in the premotor cortex of both hemispheres (Honda et al., 1998; Grafton et al., 2002; Floyer-Lea and Matthews, 2005). In addition, inactivation of PMv impairs visuomotor adaptation in monkeys (Kurata and Hoshi, 1999). We therefore hypothesize that a similar emergence of temporally precise co-firing of task-related neural activity as observed in the PLC of the Khanna et al. (2021) experiments would occur in other premotor areas, such as bilateral PMv, and that this "retuning" would also be correlated with recovery as monkeys "relearn" the task.

Finally, while the different motor and premotor areas may all show equivalent retuning in parallel during recovery, one interesting possibility is that the rate of this retuning may not be equal in all areas studied. In line with this, it has been shown that, during human motor learning,

changes in somatosensory cortical excitability precede those in motor cortex (Ohashi et al., 2019). Considering the hierarchical organization of the motor network and the preferential role of premotor cortex in higher-order processing of motor control, it is possible that retuning of neural activity in premotor cortex may precede M1 retuning to some degree, such that it helps drive functional reorganization of perilesional M1. Future studies will hopefully shed light on some of these questions.

7. General conclusions

In the current work we demonstrated that a localized, unilateral and reversible cortical injury to the M1 hand area induces extensive and complex neuronal reorganization in both hemispheres at the very onset of motor impairments. These neuronal changes appeared within minutes after brain injury and were heterogenous both within and across areas of the cortical motor network. They occurred in the two hemispheres during movements of both the paretic and non-paretic arms, and they varied during different phases of movement. The most pronounced changes took place in the PMv of both hemispheres, with a general decrease of activity in the iPMv, and notable time-specific increases of activity in the cPMv. In contrast, the neuronal activity of the cM1 appeared to be particularly resilient following inactivation of its homologue. These findings constitute a first step in a much needed and timely effort to unravel the complex neuronal correlates of the reorganization that takes place across the distributed motor network after brain injury. Furthermore, our results have important implications for neuromodulatory therapeutic protocols that target motor cortex for stroke rehabilitation and strongly suggest premotor cortex as a viable target for such interventions. Future studies will be required to extend these results to other premotor areas of interest and quantify how the neural reorganization that we observed is dependent on lesion size and location, and how it progresses with time from injury. Fortunately, initial datasets exist for preliminary explorations of some of these questions.

Bibliography

Abasi A, Danielsen NP, Leung J, Muhammad AKMG, Patel S, Gulati T (2021) Epidural cerebellar stimulation drives widespread neural synchrony in the intact and stroke perilesional cortex. J NeuroEngineering Rehabil 18.

Abela E, Missimer J, Wiest R, Federspiel A, Hess C, Sturzenegger M, Weder B (2012) Lesions to primary sensory and posterior parietal cortices impair recovery from hand paresis after stroke. PLoS One 7:e31275.

Ackerley SJ, Stinear CM, Barber PA, Byblow WD (2010) Combining theta burst stimulation with training after subcortical stroke. Stroke 41:1568-1572.

Adeyemo BO, Simis M, Macea DD, Fregni F (2012) Systematic review of parameters of stimulation, clinical trial design characteristics, and motor outcomes in non-invasive brain stimulation in stroke. Front Psychiatry 3:88.

Adkins-Muir DL, Jones TA (2003) Cortical electrical stimulation combined with rehabilitative training: enhanced functional recovery and dendritic plasticity following focal cortical ischemia in rats. Neurol Res 25:780-788.

Aggarwal V, Mollazadeh M, Davidson AG, Schieber MH, Thakor NV (2013) State-based decoding of hand and finger kinematics using neuronal ensemble and LFP activity during dexterous reach-to-grasp movements. J Neurophysiol 109:3067-3081.

Aizawa H, Mushiake H, Inase M, Tanji J (1990) An output zone of the monkey primary motor cortex specialized for bilateral hand movement. Exp Brain Res 82:219-221.

Aizawa H, Inase M, Mushiake H, Shima K, Tanji J (1991) Reorganization of activity in the supplementary motor area associated with motor learning and functional recovery. Exp Brain Res 84:668-671.

Alagona G, Delvaux V, Gerard P, De Pasqua V, Pennisi G, Delwaide PJ, Nicoletti F, Maertens de Noordhout A (2001) Ipsilateral motor responses to focal transcranial magnetic stimulation in healthy subjects and acute-stroke patients. Stroke 32:1304-1309.

Alexander GE, Crutcher MD (1990a) Preparation for movement: neural representations of intended direction in three motor areas of the monkey. J Neurophysiol 64:133-150.

Alexander GE, Crutcher MD (1990b) Neural representations of the target (goal) of visually guided arm movements in three motor areas of the monkey. J Neurophysiol 64:164-178.

Alia C, Spalletti C, Lai S, Panarese A, Lamola G, Bertolucci F, Vallone F, Di Garbo A, Chisari C, Micera S, Caleo M (2017) Neuroplastic Changes Following Brain Ischemia and their Contribution to Stroke Recovery: Novel Approaches in Neurorehabilitation. Front Cell Neurosci 11:76.

Allred RP, Cappellini CH, Jones TA (2010) The "good" limb makes the "bad" limb worse: experience-dependent interhemispheric disruption of functional outcome after cortical infarcts in rats. Behav Neurosci 124:124-132.

Alstott J, Breakspear M, Hagmann P, Cammoun L, Sporns O (2009) Modeling the impact of lesions in the human brain. PLoS Comput Biol 5:e1000408.

Ameli M, Grefkes C, Kemper F, Riegg FP, Rehme AK, Karbe H, Fink GR, Nowak DA (2009) Differential effects of high-frequency repetitive transcranial magnetic stimulation over ipsilesional primary motor cortex in cortical and subcortical middle cerebral artery stroke. Ann Neurol 66:298-309.

Ames KC, Churchland MM (2019) Motor cortex signals for each arm are mixed across hemispheres and neurons yet partitioned within the population response. Elife 8.

Antal A, Paulus W (2013) Transcranial alternating current stimulation (tACS). Front Hum Neurosci 7:317.

Arikan R, Blake NM, Erinjeri JP, Woolsey TA, Giraud L, Highstein SM (2002) A method to measure the effective spread of focally injected muscimol into the central nervous system with electrophysiology and light microscopy. J Neurosci Methods 118:51-57.
Asanuma H (1975) Recent developments in the study of the columnar arrangement of neurons within the motor cortex. Physiol Rev 55:143-156.
Asanuma H, Pavlides C (1997) Neurobiological basis of motor learning in mammals. Neuroreport 8:i-vi.
Au-Yeung SS, Wang J, Chen Y, Chua E (2014) Transcranial direct current stimulation to primary motor area improves hand dexterity and selective attention in chronic stroke. Am J Phys Med Rehabil 93:1057-1064.
Bajaj S, Butler AJ, Drake D, Dhamala M (2015) Functional organization and restoration of the brain motor-execution network after stroke and rehabilitation. Front Hum Neurosci 9:173.
Bansal AK, Vargas-Irwin CE, Truccolo W, Donoghue JP (2011) Relationships among low-frequency local field potentials, spiking activity, and three-dimensional reach and grasp kinematics in primary motor and ventral premotor cortices. J Neurophysiol 105:1603-1619.
Bansal AK, Truccolo W, Vargas-Irwin CE, Donoghue JP (2012) Decoding 3D reach and grasp from hybrid signals in motor and premotor cortices: spikes, multiunit activity, and local field potentials. J Neurophysiol 107:1337-1355.
Baron MS, Wichmann T, Ma D, DeLong MR (2002) Effects of transient focal inactivation of the basal ganglia in parkinsonian primates. J Neurosci 22:592-599.
Barry MD, Boddington LJ, Igelstrom KM, Gray JP, Shemmell J, Tseng KY, Oorschot DE, Reynolds JN (2014) Utility of intracerebral theta burst electrical stimulation to attenuate interhemispheric inhibition and to promote motor recovery after cortical injury in an animal model. Exp Neurol 261:258-266.
Bates KA, Rodger J (2015) Repetitive transcranial magnetic stimulation for stroke rehabilitation-potential therapy or misplaced hope? Restor Neurol Neurosci 33:557-569.
Bauswein E, Fromm C, Werner W, Ziemann U (1991) Phasic and tonic responses of premotor and primary motor cortex neurons to torque changes. Exp Brain Res 86:303-310.
Beaule V, Tremblay S, Theoret H (2012) Interhemispheric control of unilateral movement. Neural Plast 2012:627816.
Bennett KM, Lemon RN (1996) Corticomotoneuronal contribution to the fractionation of muscle activity during precision grip in the monkey. J Neurophysiol 75:1826-1842.
Bestmann S, Baudewig J, Siebner HR, Rothwell JC, Frahm J (2004) Functional MRI of the immediate impact of transcranial magnetic stimulation on cortical and subcortical motor circuits. Eur J Neurosci 19:1950-1962.
Biber MP, Kneisley LW, LaVail JH (1978) Cortical neurons projecting to the cervical and lumbar enlargements of the spinal cord in young and adult rhesus monkeys. Exp Neurol 59:492-508.
Biernaskie J, Corbett D (2001) Enriched rehabilitative training promotes improved forelimb motor function and enhanced dendritic growth after focal ischemic injury. J Neurosci 21:5272-5280.
Biernaskie J, Chernenko G, Corbett D (2004) Efficacy of rehabilitative experience declines with time after focal ischemic brain injury. J Neurosci 24:1245-1254.
Biernaskie J, Szymanska A, Windle V, Corbett D (2005) Bi-hemispheric contribution to functional motor recovery of the affected forelimb following focal ischemic brain injury in rats. Eur J Neurosci 21:989-999.
Binkofski F, Buccino G, Posse S, Seitz RJ, Rizzolatti G, Freund H (1999a) A fronto-parietal circuit for object manipulation in man: evidence from an fMRI-study. Eur J Neurosci 11:3276-3286.
Binkofski F, Buccino G, Stephan KM, Rizzolatti G, Seitz RJ, Freund HJ (1999b) A parieto-premotor network for object manipulation: evidence from neuroimaging. Exp Brain Res 128:210-213.

Block F, Dihne M, Loos M (2005) Inflammation in areas of remote changes following focal brain lesion. Prog Neurobiol 75:342-365.
Boddington LJ, Reynolds JNJ (2017) Targeting interhemispheric inhibition with neuromodulation to enhance stroke rehabilitation. Brain Stimul 10:214-222.
Boddington LJ, Gray JP, Schulz JM, Reynolds JNJ (2020) Low-intensity contralesional electrical theta burst stimulation modulates ipsilesional excitability and enhances stroke recovery. Exp Neurol 323:113071.
Boggio PS, Alonso-Alonso M, Mansur CG, Rigonatti SP, Schlaug G, Pascual-Leone A, Fregni F (2006) Hand function improvement with low-frequency repetitive transcranial magnetic stimulation of the unaffected hemisphere in a severe case of stroke. Am J Phys Med Rehabil 85:927-930.
Bonini L, Ugolotti Serventi F, Bruni S, Maranesi M, Bimbi M, Simone L, Rozzi S, Ferrari PF, Fogassi L (2012) Selectivity for grip type and action goal in macaque inferior parietal and ventral premotor grasping neurons. J Neurophysiol 108:1607-1619.
Borich MR, Brodie SM, Gray WA, Ionta S, Boyd LA (2015) Understanding the role of the primary somatosensory cortex: Opportunities for rehabilitation. Neuropsychologia 79:246-255.
Borra E, Gerbella M, Rozzi S, Luppino G (2017) The macaque lateral grasping network: A neural substrate for generating purposeful hand actions. Neurosci Biobehav Rev 75:65-90.
Borra E, Belmalih A, Gerbella M, Rozzi S, Luppino G (2010) Projections of the hand field of the macaque ventral premotor area F5 to the brainstem and spinal cord. J Comp Neurol 518:2570-2591.
Borra E, Belmalih A, Calzavara R, Gerbella M, Murata A, Rozzi S, Luppino G (2008) Cortical connections of the macaque anterior intraparietal (AIP) area. Cereb Cortex 18:1094-1111.
Bortoff GA, Strick PL (1993) Corticospinal terminations in two new-world primates: further evidence that corticomotoneuronal connections provide part of the neural substrate for manual dexterity. J Neurosci 13:5105-5118.
Boudreau MJ, Brochier T, Pare M, Smith AM (2001) Activity in ventral and dorsal premotor cortex in response to predictable force-pulse perturbations in a precision grip task. J Neurophysiol 86:1067-1078.
Boudrias MH, Belhaj-Saif A, Park MC, Cheney PD (2006) Contrasting properties of motor output from the supplementary motor area and primary motor cortex in rhesus macaques. Cereb Cortex 16:632-638.
Boudrias MH, Lee SP, Svojanovsky S, Cheney PD (2010) Forelimb muscle representations and output properties of motor areas in the mesial wall of rhesus macaques. Cereb Cortex 20:704-719.
Boussaoud D, Tanne-Gariepy J, Wannier T, Rouiller EM (2005) Callosal connections of dorsal versus ventral premotor areas in the macaque monkey: a multiple retrograde tracing study. BMC Neurosci 6:67.
Bowery NG, Smart TG (2006) GABA and glycine as neurotransmitters: a brief history. Br J Pharmacol 147 Suppl 1:S109-119.
Braun C, Staudt M, Schmitt C, Preissl H, Birbaumer N, Gerloff C (2007) Crossed cortico-spinal motor control after capsular stroke. Eur J Neurosci 25:2935-2945.
Brinkman J, Kuypers HG (1973) Cerebral control of contralateral and ipsilateral arm, hand and finger movements in the split-brain rhesus monkey. Brain 96:653-674.
Broadmann K (1909) Vergleichende Lokalisationslehre der grosshirnrinde [Comparative localization in the cerebral hemispheres]. Leipzig, Germany: J.A. Barth.
Brochier T, Boudreau MJ, Pare M, Smith AM (1999) The effects of muscimol inactivation of small regions of motor and somatosensory cortex on independent finger movements and force control in the precision grip. Exp Brain Res 128:31-40.
Brosamle C, Schwab ME (1997) Cells of origin, course, and termination patterns of the ventral, uncrossed component of the mature rat corticospinal tract. J Comp Neurol 386:293-303.

Brown JA, Lutsep H, Cramer SC, Weinand M (2003) Motor cortex stimulation for enhancement of recovery after stroke: case report. Neurol Res 25:815-818.
Brown JA, Lutsep HL, Weinand M, Cramer SC (2006) Motor cortex stimulation for the enhancement of recovery from stroke: a prospective, multicenter safety study. Neurosurgery 58:464-473.
Brozzoli C, Makin TR, Cardinali L, Holmes NP, Farne A (2012) Peripersonal Space: A Multisensory Interface for Body-Object Interactions. In: The Neural Bases of Multisensory Processes (Murray MM, Wallace MT, eds). Boca Raton (FL).
Bruni S, Gerbella M, Bonini L, Borra E, Coude G, Ferrari PF, Fogassi L, Maranesi M, Roda F, Simone L, Serventi FU, Rozzi S (2018) Cortical and subcortical connections of parietal and premotor nodes of the monkey hand mirror neuron network. Brain Struct Funct 223:1713-1729.
Buch ER, Mars RB, Boorman ED, Rushworth MF (2010) A network centered on ventral premotor cortex exerts both facilitatory and inhibitory control over primary motor cortex during action reprogramming. J Neurosci 30:1395-1401.
Buetefisch CM (2015) Role of the Contralesional Hemisphere in Post-Stroke Recovery of Upper Extremity Motor Function. Front Neurol 6:214.
Buetefisch CM, Hines B, Shuster L, Pergami P, Mathes A (2011) Motor demand-dependent improvement in accuracy following low-frequency transcranial magnetic stimulation of left motor cortex. J Neurophysiol 106:1614-1621.
Bundy DT, Leuthardt EC (2019) The Cortical Physiology of Ipsilateral Limb Movements. Trends Neurosci 42:825-839.
Bundy DT, Szrama N, Pahwa M, Leuthardt EC (2018) Unilateral, 3D Arm Movement Kinematics Are Encoded in Ipsilateral Human Cortex. J Neurosci 38:10042-10056.
Buss A, Brook GA, Kakulas B, Martin D, Franzen R, Schoenen J, Noth J, Schmitt AB (2004) Gradual loss of myelin and formation of an astrocytic scar during Wallerian degeneration in the human spinal cord. Brain 127:34-44.
Buss A, Pech K, Merkler D, Kakulas BA, Martin D, Schoenen J, Noth J, Schwab ME, Brook GA (2005) Sequential loss of myelin proteins during Wallerian degeneration in the human spinal cord. Brain 128:356-364.
Butefisch CM, Netz J, Wessling M, Seitz RJ, Homberg V (2003) Remote changes in cortical excitability after stroke. Brain 126:470-481.
Butefisch CM, Wessling M, Netz J, Seitz RJ, Homberg V (2008) Relationship between interhemispheric inhibition and motor cortex excitability in subacute stroke patients. Neurorehabil Neural Repair 22:4-21.
Butefisch CM, Kleiser R, Korber B, Muller K, Wittsack HJ, Homberg V, Seitz RJ (2005) Recruitment of contralesional motor cortex in stroke patients with recovery of hand function. Neurology 64:1067-1069.
Buys EJ, Lemon RN, Mantel GW, Muir RB (1986) Selective facilitation of different hand muscles by single corticospinal neurones in the conscious monkey. J Physiol 381:529-549.
Cabel DW, Cisek P, Scott SH (2001) Neural activity in primary motor cortex related to mechanical loads applied to the shoulder and elbow during a postural task. J Neurophysiol 86:2102-2108.
Caminiti R, Johnson PB, Galli C, Ferraina S, Burnod Y (1991) Making arm movements within different parts of space: the premotor and motor cortical representation of a coordinate system for reaching to visual targets. J Neurosci 11:1182-1197.
Campbell AW (1905) Histological studies on the localization of cerebral function. Cambridge, UK: Cambridge University Press.
Cao Y, D'Olhaberriague L, Vikingstad EM, Levine SR, Welch KM (1998) Pilot study of functional MRI to assess cerebral activation of motor function after poststroke hemiparesis. Stroke 29:112-122.

Caramia MD, Palmieri MG, Giacomini P, Iani C, Dally L, Silvestrini M (2000) Ipsilateral activation of the unaffected motor cortex in patients with hemiparetic stroke. Clin Neurophysiol 111:1990-1996.
Carey LM, Abbott DF, Egan GF, Bernhardt J, Donnan GA (2005) Motor impairment and recovery in the upper limb after stroke: behavioral and neuroanatomical correlates. Stroke 36:625-629.
Carey LM, Abbott DF, Egan GF, O'Keefe GJ, Jackson GD, Bernhardt J, Donnan GA (2006) Evolution of brain activation with good and poor motor recovery after stroke. Neurorehabil Neural Repair 20:24-41.
Carrera E, Tononi G (2014) Diaschisis: past, present, future. Brain 137:2408-2422.
Carter AR, Astafiev SV, Lang CE, Connor LT, Rengachary J, Strube MJ, Pope DL, Shulman GL, Corbetta M (2010) Resting interhemispheric functional magnetic resonance imaging connectivity predicts performance after stroke. Ann Neurol 67:365-375.
Castiello U (2005) The neuroscience of grasping. Nat Rev Neurosci 6:726-736.
Castiello U, Begliomini C (2008) The cortical control of visually guided grasping. Neuroscientist 14:157-170.
Cerri G, Shimazu H, Maier MA, Lemon RN (2003) Facilitation from ventral premotor cortex of primary motor cortex outputs to macaque hand muscles. J Neurophysiol 90:832-842.
Chail A, Saini RK, Bhat PS, Srivastava K, Chauhan V (2018) Transcranial magnetic stimulation: A review of its evolution and current applications. Ind Psychiatry J 27:172-180.
Chen R, Classen J, Gerloff C, Celnik P, Wassermann EM, Hallett M, Cohen LG (1997) Depression of motor cortex excitability by low-frequency transcranial magnetic stimulation. Neurology 48:1398-1403.
Cheney PD, Fetz EE (1985) Comparable patterns of muscle facilitation evoked by individual corticomotoneuronal (CM) cells and by single intracortical microstimuli in primates: evidence for functional groups of CM cells. J Neurophysiol 53:786-804.
Chollet F, DiPiero V, Wise RJ, Brooks DJ, Dolan RJ, Frackowiak RS (1991) The functional anatomy of motor recovery after stroke in humans: a study with positron emission tomography. Ann Neurol 29:63-71.
Chouinard PA, Leonard G, Paus T (2005) Role of the primary motor and dorsal premotor cortices in the anticipation of forces during object lifting. J Neurosci 25:2277-2284.
Cisek P, Crammond DJ, Kalaska JF (2003) Neural activity in primary motor and dorsal premotor cortex in reaching tasks with the contralateral versus ipsilateral arm. J Neurophysiol 89:922-942.
Civardi C, Cantello R, Asselman P, Rothwell JC (2001) Transcranial magnetic stimulation can be used to test connections to primary motor areas from frontal and medial cortex in humans. Neuroimage 14:1444-1453.
Clarey JC, Tweedale R, Calford MB (1996) Interhemispheric modulation of somatosensory receptive fields: evidence for plasticity in primary somatosensory cortex. Cereb Cortex 6:196-206.
Colby CL (1998) Action-oriented spatial reference frames in cortex. Neuron 20:15-24.
Cole J, Glees P (1954) Effects of small lesions in sensory cortex in trained monkeys. J Neurophysiol 17:1-13.
Collins CE, Xu X, Khaytin I, Kaskan PM, Casagrande VA, Kaas JH (2005) Optical imaging of visually evoked responses in the middle temporal area after deactivation of primary visual cortex in adult primates. Proc Natl Acad Sci U S A 102:5594-5599.
Contestabile A, Colangiulo R, Lucchini M, Gindrat AD, Hamadjida A, Kaeser M, Savidan J, Wyss AF, Rouiller EM, Schmidlin E (2018) Asymmetric and Distant Effects of a Unilateral Lesion of the Primary Motor Cortex on the Bilateral Supplementary Motor Areas in Adult Macaque Monkeys. J Neurosci 38:10644-10656.
Cote SL, Hamadjida A, Quessy S, Dancause N (2017) Contrasting Modulatory Effects from the Dorsal and Ventral Premotor Cortex on Primary Motor Cortex Outputs. J Neurosci 37:5960-5973.

Cote SL, Elgbeili G, Quessy S, Dancause N (2020) Modulatory effects of the supplementary motor area on primary motor cortex outputs. J Neurophysiol 123:407-419.
Coude G, Ferrari PF, Roda F, Maranesi M, Borelli E, Veroni V, Monti F, Rozzi S, Fogassi L (2011) Neurons controlling voluntary vocalization in the macaque ventral premotor cortex. PLoS One 6:e26822.
Cramer SC, Nelles G, Benson RR, Kaplan JD, Parker RA, Kwong KK, Kennedy DN, Finklestein SP, Rosen BR (1997) A functional MRI study of subjects recovered from hemiparetic stroke. Stroke 28:2518-2527.
Crammond DJ, Kalaska JF (1996) Differential relation of discharge in primary motor cortex and premotor cortex to movements versus actively maintained postures during a reaching task. Exp Brain Res 108:45-61.
Crammond DJ, Kalaska JF (2000) Prior information in motor and premotor cortex: activity during the delay period and effect on pre-movement activity. J Neurophysiol 84:986-1005.
Crofts A, Kelly ME, Gibson CL (2020) Imaging Functional Recovery Following Ischemic Stroke: Clinical and Preclinical fMRI Studies. J Neuroimaging 30:5-14.
Crutcher MD, Alexander GE (1990) Movement-related neuronal activity selectively coding either direction or muscle pattern in three motor areas of the monkey. J Neurophysiol 64:151-163.
Cuadrado ML, Egido JA, Gonzalez-Gutierrez JL, Varela-De-Seijas E (1999) Bihemispheric contribution to motor recovery after stroke: A longitudinal study with transcranial doppler ultrasonography. Cerebrovasc Dis 9:337-344.
Cunningham DA, Varnerin N, Machado A, Bonnett C, Janini D, Roelle S, Potter-Baker K, Sankarasubramanian V, Wang X, Yue G, Plow EB (2015) Stimulation targeting higher motor areas in stroke rehabilitation: A proof-of-concept, randomized, double-blinded placebo-controlled study of effectiveness and underlying mechanisms. Restor Neurol Neurosci 33:911-926.
Dafotakis M, Grefkes C, Eickhoff SB, Karbe H, Fink GR, Nowak DA (2008) Effects of rTMS on grip force control following subcortical stroke. Exp Neurol 211:407-412.
Dancause N (2006) Vicarious function of remote cortex following stroke: recent evidence from human and animal studies. Neuroscientist 12:489-499.
Dancause N (2013) Plasticity in the motor network following primary motor cortex lesion. Adv Exp Med Biol 782:61-86.
Dancause N, Touvykine B, Mansoori BK (2015) Inhibition of the contralesional hemisphere after stroke: reviewing a few of the building blocks with a focus on animal models. Prog Brain Res 218:361-387.
Dancause N, Barbay S, Frost SB, Mahnken JD, Nudo RJ (2007) Interhemispheric connections of the ventral premotor cortex in a new world primate. J Comp Neurol 505:701-715.
Dancause N, Duric V, Barbay S, Frost SB, Stylianou A, Nudo RJ (2008) An additional motor-related field in the lateral frontal cortex of squirrel monkeys. Cereb Cortex 18:2719-2728.
Dancause N, Barbay S, Frost SB, Plautz EJ, Stowe AM, Friel KM, Nudo RJ (2006a) Ipsilateral connections of the ventral premotor cortex in a new world primate. J Comp Neurol 495:374-390.
Dancause N, Barbay S, Frost SB, Zoubina EV, Plautz EJ, Mahnken JD, Nudo RJ (2006b) Effects of small ischemic lesions in the primary motor cortex on neurophysiological organization in ventral premotor cortex. J Neurophysiol 96:3506-3511.
Dancause N, Barbay S, Frost SB, Plautz EJ, Chen D, Zoubina EV, Stowe AM, Nudo RJ (2005) Extensive cortical rewiring after brain injury. J Neurosci 25:10167-10179.
Dancause N, Barbay S, Frost SB, Plautz EJ, Popescu M, Dixon PM, Stowe AM, Friel KM, Nudo RJ (2006c) Topographically divergent and convergent connectivity between premotor and primary motor cortex. Cereb Cortex 16:1057-1068.
Davare M, Lemon R, Olivier E (2008) Selective modulation of interactions between ventral premotor cortex and primary motor cortex during precision grasping in humans. J Physiol 586:2735-2742.

Davare M, Kraskov A, Rothwell JC, Lemon RN (2011) Interactions between areas of the cortical grasping network. Curr Opin Neurobiol 21:565-570.
Davare M, Montague K, Olivier E, Rothwell JC, Lemon RN (2009) Ventral premotor to primary motor cortical interactions during object-driven grasp in humans. Cortex 45:1050-1057.
Day BL, Rothwell JC, Thompson PD, Maertens de Noordhout A, Nakashima K, Shannon K, Marsden CD (1989) Delay in the execution of voluntary movement by electrical or magnetic brain stimulation in intact man. Evidence for the storage of motor programs in the brain. Brain 112 (Pt 3):649-663.
Dayan E, Cohen LG (2011) Neuroplasticity subserving motor skill learning. Neuron 72:443-454.
Dea M, Hamadjida A, Elgbeili G, Quessy S, Dancause N (2016) Different Patterns of Cortical Inputs to Subregions of the Primary Motor Cortex Hand Representation in Cebus apella. Cereb Cortex 26:1747-1761.
Del Vecchio M, Caruana F, Sartori I, Pelliccia V, Lo Russo G, Rizzolatti G, Avanzini P (2019) Ipsilateral somatosensory responses in humans: the tonic activity of SII and posterior insular cortex. Brain Struct Funct 224:9-18.
Del Vecchio M, Caruana F, Sartori I, Pelliccia V, Zauli FM, Lo Russo G, Rizzolatti G, Avanzini P (2020) Action execution and action observation elicit mirror responses with the same temporal profile in human SII. Commun Biol 3:80.
Di Lazzaro V, Oliviero A, Profice P, Insola A, Mazzone P, Tonali P, Rothwell JC (1999) Direct demonstration of interhemispheric inhibition of the human motor cortex produced by transcranial magnetic stimulation. Exp Brain Res 124:520-524.
Di Lazzaro V, Rothwell JC, Talelli P, Capone F, Ranieri F, Wallace AC, Musumeci G, Dileone M (2013) Inhibitory theta burst stimulation of affected hemisphere in chronic stroke: a proof of principle, sham-controlled study. Neurosci Lett 553:148-152.
di Pellegrino G, Fadiga L, Fogassi L, Gallese V, Rizzolatti G (1992) Understanding motor events: a neurophysiological study. Exp Brain Res 91:176-180.
Di Pino G, Pellegrino G, Assenza G, Capone F, Ferreri F, Formica D, Ranieri F, Tombini M, Ziemann U, Rothwell JC, Di Lazzaro V (2014) Modulation of brain plasticity in stroke: a novel model for neurorehabilitation. Nat Rev Neurol 10:597-608.
Dias EC, Kiesau M, Segraves MA (1995) Acute activation and inactivation of macaque frontal eye field with GABA-related drugs. J Neurophysiol 74:2744-2748.
Diedrichsen J, Wiestler T, Krakauer JW (2013) Two distinct ipsilateral cortical representations for individuated finger movements. Cereb Cortex 23:1362-1377.
Dijkhuizen RM, Ren J, Mandeville JB, Wu O, Ozdag FM, Moskowitz MA, Rosen BR, Finklestein SP (2001) Functional magnetic resonance imaging of reorganization in rat brain after stroke. Proc Natl Acad Sci U S A 98:12766-12771.
Dijkhuizen RM, Singhal AB, Mandeville JB, Wu O, Halpern EF, Finklestein SP, Rosen BR, Lo EH (2003) Correlation between brain reorganization, ischemic damage, and neurologic status after transient focal cerebral ischemia in rats: a functional magnetic resonance imaging study. J Neurosci 23:510-517.
Ding MC, Wang Q, Lo EH, Stanley GB (2011) Cortical excitation and inhibition following focal traumatic brain injury. J Neurosci 31:14085-14094.
Doetsch GS, Johnston KW, Hannan CJ, Jr. (1990) Physiological changes in the somatosensory forepaw cerebral cortex of adult raccoons following lesions of a single cortical digit representation. Exp Neurol 108:162-175.
Donchin O, Gribova A, Steinberg O, Bergman H, Vaadia E (1998) Primary motor cortex is involved in bimanual coordination. Nature 395:274-278.

Donchin O, Gribova A, Steinberg O, Mitz AR, Bergman H, Vaadia E (2002) Single-unit activity related to bimanual arm movements in the primary and supplementary motor cortices. J Neurophysiol 88:3498-3517.
Donoghue JP, Leibovic S, Sanes JN (1992) Organization of the forelimb area in squirrel monkey motor cortex: representation of digit, wrist, and elbow muscles. Exp Brain Res 89:1-19.
Downey JE, Quick KM, Schwed N, Weiss JM, Wittenberg GF, Boninger ML, Collinger JL (2020) The Motor Cortex Has Independent Representations for Ipsilateral and Contralateral Arm Movements But Correlated Representations for Grasping. Cereb Cortex 30:5400-5409.
Dromerick AW, Geed S, Barth J, Brady K, Giannetti ML, Mitchell A, Edwardson MA, Tan MT, Zhou Y, Newport EL, Edwards DF (2021) Critical Period After Stroke Study (CPASS): A phase II clinical trial testing an optimal time for motor recovery after stroke in humans. Proc Natl Acad Sci U S A 118.
Dromerick AW, Edwardson MA, Edwards DF, Giannetti ML, Barth J, Brady KP, Chan E, Tan MT, Tamboli I, Chia R, Orquiza M, Padilla RM, Cheema AK, Mapstone ME, Fiandaca MS, Federoff HJ, Newport EL (2015) Critical periods after stroke study: translating animal stroke recovery experiments into a clinical trial. Front Hum Neurosci 9:231.
Dum RP, Strick PL (1991) The origin of corticospinal projections from the premotor areas in the frontal lobe. J Neurosci 11:667-689.
Dum RP, Strick PL (1996) Spinal cord terminations of the medial wall motor areas in macaque monkeys. J Neurosci 16:6513-6525.
Dum RP, Strick PL (2002) Motor areas in the frontal lobe of the primate. Physiol Behav 77:677-682.
Dum RP, Strick PL (2005) Frontal lobe inputs to the digit representations of the motor areas on the lateral surface of the hemisphere. J Neurosci 25:1375-1386.
Duque J, Hummel F, Celnik P, Murase N, Mazzocchio R, Cohen LG (2005) Transcallosal inhibition in chronic subcortical stroke. Neuroimage 28:940-946.
Edeline JM, Hars B, Hennevin E, Cotillon N (2002) Muscimol diffusion after intracerebral microinjections: a reevaluation based on electrophysiological and autoradiographic quantifications. Neurobiol Learn Mem 78:100-124.
Ehrsson HH, Fagergren E, Forssberg H (2001) Differential fronto-parietal activation depending on force used in a precision grip task: an fMRI study. J Neurophysiol 85:2613-2623.
Ehrsson HH, Fagergren A, Jonsson T, Westling G, Johansson RS, Forssberg H (2000) Cortical activity in precision- versus power-grip tasks: an fMRI study. J Neurophysiol 83:528-536.
Eickhoff SB, Grefkes C (2011) Approaches for the integrated analysis of structure, function and connectivity of the human brain. Clin EEG Neurosci 42:107-121.
Eisner-Janowicz I, Barbay S, Hoover E, Stowe AM, Frost SB, Plautz EJ, Nudo RJ (2008) Early and late changes in the distal forelimb representation of the supplementary motor area after injury to frontal motor areas in the squirrel monkey. J Neurophysiol 100:1498-1512.
Elsner B, Kugler J, Pohl M, Mehrholz J (2013) Transcranial direct current stimulation (tDCS) for improving function and activities of daily living in patients after stroke. Cochrane Database Syst Rev:CD009645.
Escudero JV, Sancho J, Bautista D, Escudero M, Lopez-Trigo J (1998) Prognostic value of motor evoked potential obtained by transcranial magnetic brain stimulation in motor function recovery in patients with acute ischemic stroke. Stroke 29:1854-1859.
Evarts EV (1966) Pyramidal tract activity associated with a conditioned hand movement in the monkey. J Neurophysiol 29:1011-1027.
Evarts EV (1968) Relation of pyramidal tract activity to force exerted during voluntary movement. J Neurophysiol 31:14-27.
Evarts EV, Tanji J (1976) Reflex and intended responses in motor cortex pyramidal tract neurons of monkey. J Neurophysiol 39:1069-1080.

Evinger C, Kaneko CR, Fuchs AF (1982) Activity of omnipause neurons in alert cats during saccadic eye movements and visual stimuli. J Neurophysiol 47:827-844.
Fagg AH, Arbib MA (1998) Modeling parietal-premotor interactions in primate control of grasping. Neural Netw 11:1277-1303.
Fang PC, Stepniewska I, Kaas JH (2005) Ipsilateral cortical connections of motor, premotor, frontal eye, and posterior parietal fields in a prosimian primate, Otolemur garnetti. J Comp Neurol 490:305-333.
Ferbert A, Priori A, Rothwell JC, Day BL, Colebatch JG, Marsden CD (1992) Interhemispheric inhibition of the human motor cortex. J Physiol 453:525-546.
Ferrier D (1874) On the Localisation of the Functions of the Brain. Br Med J 2:766-767.
Filimon F (2010) Human cortical control of hand movements: parietofrontal networks for reaching, grasping, and pointing. Neuroscientist 16:388-407.
Floyer-Lea A, Matthews PM (2005) Distinguishable brain activation networks for short- and long-term motor skill learning. J Neurophysiol 94:512-518.
Fluet MC, Baumann MA, Scherberger H (2010) Context-specific grasp movement representation in macaque ventral premotor cortex. J Neurosci 30:15175-15184.
Fogassi L, Gallese V, Fadiga L, Luppino G, Matelli M, Rizzolatti G (1996) Coding of peripersonal space in inferior premotor cortex (area F4). J Neurophysiol 76:141-157.
Fogassi L, Gallese V, Buccino G, Craighero L, Fadiga L, Rizzolatti G (2001) Cortical mechanism for the visual guidance of hand grasping movements in the monkey: A reversible inactivation study. Brain 124:571-586.
Fogassi L, Gallese V, di Pellegrino G, Fadiga L, Gentilucci M, Luppino G, Matelli M, Pedotti A, Rizzolatti G (1992) Space coding by premotor cortex. Exp Brain Res 89:686-690.
Forno LS (1983) Reaction of the substantia nigra to massive basal ganglia infarction. Acta Neuropathol 62:96-102.
Fregni F, Boggio PS, Valle AC, Rocha RR, Duarte J, Ferreira MJ, Wagner T, Fecteau S, Rigonatti SP, Riberto M, Freedman SD, Pascual-Leone A (2006) A sham-controlled trial of a 5-day course of repetitive transcranial magnetic stimulation of the unaffected hemisphere in stroke patients. Stroke 37:2115-2122.
Fridman EA, Hanakawa T, Chung M, Hummel F, Leiguarda RC, Cohen LG (2004) Reorganization of the human ipsilesional premotor cortex after stroke. Brain 127:747-758.
Friel KM, Nudo RJ (1998) Recovery of motor function after focal cortical injury in primates: compensatory movement patterns used during rehabilitative training. Somatosens Mot Res 15:173-189.
Friel KM, Barbay S, Frost SB, Plautz EJ, Stowe AM, Dancause N, Zoubina EV, Nudo RJ (2007) Effects of a rostral motor cortex lesion on primary motor cortex hand representation topography in primates. Neurorehabil Neural Repair 21:51-61.
Friel KM, Barbay S, Frost SB, Plautz EJ, Hutchinson DM, Stowe AM, Dancause N, Zoubina EV, Quaney BM, Nudo RJ (2005) Dissociation of sensorimotor deficits after rostral versus caudal lesions in the primary motor cortex hand representation. J Neurophysiol 94:1312-1324.
Fritsch G, Hitzig E (2009) Electric excitability of the cerebrum (Uber die elektrische Erregbarkeit des Grosshirns). Epilepsy Behav 15:123-130.
Frost SB, Barbay S, Friel KM, Plautz EJ, Nudo RJ (2003) Reorganization of remote cortical regions after ischemic brain injury: a potential substrate for stroke recovery. J Neurophysiol 89:3205-3214.
Fu QG, Suarez JI, Ebner TJ (1993) Neuronal specification of direction and distance during reaching movements in the superior precentral premotor area and primary motor cortex of monkeys. J Neurophysiol 70:2097-2116.

Fu QG, Flament D, Coltz JD, Ebner TJ (1995) Temporal encoding of movement kinematics in the discharge of primate primary motor and premotor neurons. J Neurophysiol 73:836-854.
Fulton JF (1935) A Note on the Definition of the "Motor" and "Premotor" Areas. Brain:311-316.
Gallese V, Fadiga L, Fogassi L, Rizzolatti G (1996) Action recognition in the premotor cortex. Brain 119 (Pt 2):593-609.
Gallese V, Murata A, Kaseda M, Niki N, Sakata H (1994) Deficit of hand preshaping after muscimol injection in monkey parietal cortex. Neuroreport 5:1525-1529.
Gangitano M, Valero-Cabre A, Tormos JM, Mottaghy FM, Romero JR, Pascual-Leone A (2002) Modulation of input-output curves by low and high frequency repetitive transcranial magnetic stimulation of the motor cortex. Clin Neurophysiol 113:1249-1257.
Ganguly K, Secundo L, Ranade G, Orsborn A, Chang EF, Dimitrov DF, Wallis JD, Barbaro NM, Knight RT, Carmena JM (2009) Cortical representation of ipsilateral arm movements in monkey and man. J Neurosci 29:12948-12956.
Gardner EP, Ro JY, Babu KS, Ghosh S (2007) Neurophysiology of prehension. II. Response diversity in primary somatosensory (S-I) and motor (M-I) cortices. J Neurophysiol 97:1656-1670.
Gardner WJ (1933) Removal of the right cerebral hemisphere for infiltrating glioma: report of a case. Journal of the American Medical Association 101:823-826.
Gentilucci M, Rizzolatti G (1990) Cortical motor control of arm and hand movements. In: Vision and Action: The Control of Grasping (Goodale MA, ed), pp 147-162. Norwood, N.J.: Ablex.
Gentilucci M, Scandolara C, Pigarev IN, Rizzolatti G (1983) Visual responses in the postarcuate cortex (area 6) of the monkey that are independent of eye position. Exp Brain Res 50:464-468.
Gentilucci M, Fogassi L, Luppino G, Matelli M, Camarda R, Rizzolatti G (1988) Functional organization of inferior area 6 in the macaque monkey. I. Somatotopy and the control of proximal movements. Exp Brain Res 71:475-490.
Gentilucci M, Castiello U, Corradini ML, Scarpa M, Umilta C, Rizzolatti G (1991) Influence of different types of grasping on the transport component of prehension movements. Neuropsychologia 29:361-378.
Georgopoulos AP (1995) Current issues in directional motor control. Trends Neurosci 18:506-510.
Georgopoulos AP, Taira M, Lukashin A (1993) Cognitive neurophysiology of the motor cortex. Science 260:47-52.
Georgopoulos AP, Ashe J, Smyrnis N, Taira M (1992) The motor cortex and the coding of force. Science 256:1692-1695.
Georgopoulos AP, Lurito JT, Petrides M, Schwartz AB, Massey JT (1989) Mental rotation of the neuronal population vector. Science 243:234-236.
Gerbella M, Belmalih A, Borra E, Rozzi S, Luppino G (2011) Cortical connections of the anterior (F5a) subdivision of the macaque ventral premotor area F5. Brain Struct Funct 216:43-65.
Gerloff C, Braun C, Staudt M, Hegner YL, Dichgans J, Krageloh-Mann I (2006a) Coherent corticomuscular oscillations originate from primary motor cortex: evidence from patients with early brain lesions. Hum Brain Mapp 27:789-798.
Gerloff C, Bushara K, Sailer A, Wassermann EM, Chen R, Matsuoka T, Waldvogel D, Wittenberg GF, Ishii K, Cohen LG, Hallett M (2006b) Multimodal imaging of brain reorganization in motor areas of the contralesional hemisphere of well recovered patients after capsular stroke. Brain 129:791-808.
Geyer S, Matelli M, Luppino G, Zilles K (2000) Functional neuroanatomy of the primate isocortical motor system. Anat Embryol (Berl) 202:443-474.
Gharbawie OA, Stepniewska I, Kaas JH (2011a) Cortical connections of functional zones in posterior parietal cortex and frontal cortex motor regions in new world monkeys. Cereb Cortex 21:1981-2002.

Gharbawie OA, Stepniewska I, Qi H, Kaas JH (2011b) Multiple parietal-frontal pathways mediate grasping in macaque monkeys. J Neurosci 31:11660-11677.
Glassman RB (1971) Recovery following sensorimotor cortical damage: evoked potentials, brain stimulation and motor control. Exp Neurol 33:16-29.
Glees P, Cole J, Whitty CW, Cairns H (1950) The effects of lesions in the cingular gyrus and adjacent areas in monkeys. J Neurol Neurosurg Psychiatry 13:178-190.
Godschalk M, Mitz AR, van Duin B, van der Burg H (1995) Somatotopy of monkey premotor cortex examined with microstimulation. Neurosci Res 23:269-279.
Golestani AM, Tymchuk S, Demchuk A, Goodyear BG, Group V-S (2013) Longitudinal evaluation of resting-state FMRI after acute stroke with hemiparesis. Neurorehabil Neural Repair 27:153-163.
Golub MD, Sadtler PT, Oby ER, Quick KM, Ryu SI, Tyler-Kabara EC, Batista AP, Chase SM, Yu BM (2018) Learning by neural reassociation. Nat Neurosci 21:607-616.
Gould HJ, 3rd, Cusick CG, Pons TP, Kaas JH (1983) The relation of callosal connections to microstimulation maps of precentral motor cortex in own monkeys. Soc Neurosci Abstr 9:303.
Gould HJ, 3rd, Cusick CG, Pons TP, Kaas JH (1986) The relationship of corpus callosum connections to electrical stimulation maps of motor, supplementary motor, and the frontal eye fields in owl monkeys. J Comp Neurol 247:297-325.
Grafton ST, Hazeltine E, Ivry RB (2002) Motor sequence learning with the nondominant left hand. A PET functional imaging study. Exp Brain Res 146:369-378.
Graziano MS, Gross CG (1994) The representation of extrapersonal space: a possible role for bimodal visual-tactile neurons. In: The Cognitive Neurosciences (Gazzaniga MS, ed), pp 1021-1034. Cambridge, MA: MIT Press.
Graziano MS, Yap GS, Gross CG (1994) Coding of visual space by premotor neurons. Science 266:1054-1057.
Grefkes C, Fink GR (2014) Connectivity-based approaches in stroke and recovery of function. Lancet Neurol 13:206-216.
Grefkes C, Nowak DA, Wang LE, Dafotakis M, Eickhoff SB, Fink GR (2010) Modulating cortical connectivity in stroke patients by rTMS assessed with fMRI and dynamic causal modeling. Neuroimage 50:233-242.
Grefkes C, Nowak DA, Eickhoff SB, Dafotakis M, Kust J, Karbe H, Fink GR (2008) Cortical connectivity after subcortical stroke assessed with functional magnetic resonance imaging. Ann Neurol 63:236-246.
Gregoriou GG, Borra E, Matelli M, Luppino G (2006) Architectonic organization of the inferior parietal convexity of the macaque monkey. J Comp Neurol 496:422-451.
Groppa S, Schlaak BH, Munchau A, Werner-Petroll N, Dunnweber J, Baumer T, van Nuenen BF, Siebner HR (2012) The human dorsal premotor cortex facilitates the excitability of ipsilateral primary motor cortex via a short latency cortico-cortical route. Hum Brain Mapp 33:419-430.
Guggenmos DJ, Azin M, Barbay S, Mahnken JD, Dunham C, Mohseni P, Nudo RJ (2013) Restoration of function after brain damage using a neural prosthesis. Proc Natl Acad Sci U S A 110:21177-21182.
Hamadjida A, Dea M, Deffeyes J, Quessy S, Dancause N (2016) Parallel Cortical Networks Formed by Modular Organization of Primary Motor Cortex Outputs. Curr Biol 26:1737-1743.
Hanajima R, Ugawa Y, Machii K, Mochizuki H, Terao Y, Enomoto H, Furubayashi T, Shiio Y, Uesugi H, Kanazawa I (2001) Interhemispheric facilitation of the hand motor area in humans. J Physiol 531:849-859.
Hannanu FF, Zeffiro TA, Lamalle L, Heck O, Renard F, Thuriot A, Krainik A, Hommel M, Detante O, Jaillard A, Group I-HS (2017) Parietal operculum and motor cortex activities predict motor recovery in moderate to severe stroke. Neuroimage Clin 14:518-529.

Hao Z, Wang D, Zeng Y, Liu M (2013) Repetitive transcranial magnetic stimulation for improving function after stroke. Cochrane Database Syst Rev:CD008862.
Hasse JM, Briggs F (2017) Corticogeniculate feedback sharpens the temporal precision and spatial resolution of visual signals in the ferret. Proc Natl Acad Sci U S A 114:E6222-E6230.
Hatsopoulos N, Joshi J, O'Leary JG (2004) Decoding continuous and discrete motor behaviors using motor and premotor cortical ensembles. J Neurophysiol 92:1165-1174.
He SQ, Dum RP, Strick PL (1993) Topographic organization of corticospinal projections from the frontal lobe: motor areas on the lateral surface of the hemisphere. J Neurosci 13:952-980.
He SQ, Dum RP, Strick PL (1995) Topographic organization of corticospinal projections from the frontal lobe: motor areas on the medial surface of the hemisphere. J Neurosci 15:3284-3306.
Heming EA, Cross KP, Takei T, Cook DJ, Scott SH (2019) Independent representations of ipsilateral and contralateral limbs in primary motor cortex. Elife 8.
Hendrix CM, Mason CR, Ebner TJ (2009) Signaling of grasp dimension and grasp force in dorsal premotor cortex and primary motor cortex neurons during reach to grasp in the monkey. J Neurophysiol 102:132-145.
Hepp-Reymond M, Kirkpatrick-Tanner M, Gabernet L, Qi HX, Weber B (1999) Context-dependent force coding in motor and premotor cortical areas. Exp Brain Res 128:123-133.
Hepp-Reymond MC, Husler EJ, Maier MA, Ql HX (1994) Force-related neuronal activity in two regions of the primate ventral premotor cortex. Can J Physiol Pharmacol 72:571-579.
Herrmann CS, Rach S, Neuling T, Struber D (2013) Transcranial alternating current stimulation: a review of the underlying mechanisms and modulation of cognitive processes. Front Hum Neurosci 7:279.
Herter TM, Korbel T, Scott SH (2009) Comparison of neural responses in primary motor cortex to transient and continuous loads during posture. J Neurophysiol 101:150-163.
Hess G, Aizenman CD, Donoghue JP (1996) Conditions for the induction of long-term potentiation in layer II/III horizontal connections of the rat motor cortex. J Neurophysiol 75:1765-1778.
Hess R, Murata K (1974) Effects of glutamate and GABA on specific response properties of neurones in the visual cortex. Exp Brain Res 21:285-297.
Hilles B (1966) Common mode of action of three agents that decrease the transient change in sodium permeablility in nerves. Nature 210:1220-1222.
Hilles B (1977) THe pH-dependent rate of action of local anesthetics on the node of Ranvier. Journal of General Physiology 69:475-496.
Hinton T, Johnston AR (2018) GABA, the major inhibitory neurotransmitter in the brain. In: Reference Module in Biomedical Sciences.
Hocherman S, Wise SP (1991) Effects of hand movement path on motor cortical activity in awake, behaving rhesus monkeys. Exp Brain Res 83:285-302.
Hoffman DS, Strick PL (1995) Effects of a primary motor cortex lesion on step-tracking movements of the wrist. J Neurophysiol 73:891-895.
Honda M, Deiber MP, Ibanez V, Pascual-Leone A, Zhuang P, Hallett M (1998) Dynamic cortical involvement in implicit and explicit motor sequence learning. A PET study. Brain 121 (Pt 11):2159-2173.
Hoogewoud F, Hamadjida A, Wyss AF, Mir A, Schwab ME, Belhaj-Saif A, Rouiller EM (2013) Comparison of functional recovery of manual dexterity after unilateral spinal cord lesion or motor cortex lesion in adult macaque monkeys. Front Neurol 4:101.
Hordacre B, Austin D, Brown KE, Graetz L, Parees I, De Trane S, Vallence AM, Koblar S, Kleinig T, McDonnell MN, Greenwood R, Ridding MC, Rothwell JC (2021) Evidence for a Window of Enhanced Plasticity in the Human Motor Cortex Following Ischemic Stroke. Neurorehabil Neural Repair 35:307-320.

Horn U, Roschka S, Eyme K, Walz AD, Platz T, Lotze M (2016) Increased ventral premotor cortex recruitment after arm training in an fMRI study with subacute stroke patients. Behav Brain Res 308:152-159.
Hoshi E, Tanji J (2002) Contrasting neuronal activity in the dorsal and ventral premotor areas during preparation to reach. J Neurophysiol 87:1123-1128.
Hoshi E, Tanji J (2006) Differential involvement of neurons in the dorsal and ventral premotor cortex during processing of visual signals for action planning. J Neurophysiol 95:3596-3616.
Houser CR, Hendry SH, Jones EG, Vaughn JE (1983) Morphological diversity of immunocytochemically identified GABA neurons in the monkey sensory-motor cortex. J Neurocytol 12:617-638.
Hsu WY, Cheng CH, Liao KK, Lee IH, Lin YY (2012) Effects of repetitive transcranial magnetic stimulation on motor functions in patients with stroke: a meta-analysis. Stroke 43:1849-1857.
Huang M, Harvey RL, Stoykov ME, Ruland S, Weinand M, Lowry D, Levy R (2008) Cortical stimulation for upper limb recovery following ischemic stroke: a small phase II pilot study of a fully implanted stimulator. Top Stroke Rehabil 15:160-172.
Huang YZ, Rothwell JC (2004) The effect of short-duration bursts of high-frequency, low-intensity transcranial magnetic stimulation on the human motor cortex. Clin Neurophysiol 115:1069-1075.
Huang YZ, Edwards MJ, Rounis E, Bhatia KP, Rothwell JC (2005) Theta burst stimulation of the human motor cortex. Neuron 45:201-206.
Hummel F, Cohen LG (2005) Improvement of motor function with noninvasive cortical stimulation in a patient with chronic stroke. Neurorehabil Neural Repair 19:14-19.
Hummel FC, Cohen LG (2006) Non-invasive brain stimulation: a new strategy to improve neurorehabilitation after stroke? Lancet Neurol 5:708-712.
Hummel FC, Celnik P, Pascual-Leone A, Fregni F, Byblow WD, Buetefisch CM, Rothwell J, Cohen LG, Gerloff C (2008) Controversy: Noninvasive and invasive cortical stimulation show efficacy in treating stroke patients. Brain Stimul 1:370-382.
Hummelsheim H, Bianchetti M, Wiesendanger M, Wiesendanger R (1988) Sensory inputs to the agranular motor fields: a comparison between precentral, supplementary-motor and premotor areas in the monkey. Exp Brain Res 69:289-298.
Huntley GW, Jones EG (1991) Relationship of intrinsic connections to forelimb movement representations in monkey motor cortex: a correlative anatomic and physiological study. J Neurophysiol 66:390-413.
Inman CS, James GA, Hamann S, Rajendra JK, Pagnoni G, Butler AJ (2012) Altered resting-state effective connectivity of fronto-parietal motor control systems on the primary motor network following stroke. Neuroimage 59:227-237.
Inoue M, Uchimura M, Kitazawa S (2016) Error Signals in Motor Cortices Drive Adaptation in Reaching. Neuron 90:1114-1126.
Isa T, Ohki Y, Seki K, Alstermark B (2006) Properties of propriospinal neurons in the C3-C4 segments mediating disynaptic pyramidal excitation to forelimb motoneurons in the macaque monkey. J Neurophysiol 95:3674-3685.
Isa T, Ohki Y, Alstermark B, Pettersson LG, Sasaki S (2007) Direct and indirect cortico-motoneuronal pathways and control of hand/arm movements. Physiology (Bethesda) 22:145-152.
Jakobson LS, Goodale MA (1991) Factors affecting higher-order movement planning: a kinematic analysis of human prehension. Exp Brain Res 86:199-208.
Jarosiewicz B, Chase SM, Fraser GW, Velliste M, Kass RE, Schwartz AB (2008) Functional network reorganization during learning in a brain-computer interface paradigm. Proc Natl Acad Sci U S A 105:19486-19491.

Jeannerod M (1981) Intersegmental coordination during reaching at natural visual objects. In: Attention and Performance IX (Long J, Badeley A, eds), pp 153-169. Hillsdale: Lawrence Erlbaum Associates.
Jeannerod M (1984) The timing of natural prehension movements. J Mot Behav 16:235-254.
Jeannerod M, Arbib MA, Rizzolatti G, Sakata H (1995) Grasping objects: the cortical mechanisms of visuomotor transformation. Trends Neurosci 18:314-320.
Jenkins WM, Merzenich MM (1987) Reorganization of neocortical representations after brain injury: a neurophysiological model of the bases of recovery from stroke. Prog Brain Res 71:249-266.
Jenny AB (1979) Commissural projections of the cortical hand motor area in monkeys. J Comp Neurol 188:137-145.
Johansen-Berg H, Rushworth MF, Bogdanovic MD, Kischka U, Wimalaratna S, Matthews PM (2002) The role of ipsilateral premotor cortex in hand movement after stroke. Proc Natl Acad Sci U S A 99:14518-14523.
Johnson PB, Ferraina S, Bianchi L, Caminiti R (1996) Cortical networks for visual reaching: physiological and anatomical organization of frontal and parietal lobe arm regions. Cereb Cortex 6:102-119.
Johnston GA (2014) Muscimol as an ionotropic GABA receptor agonist. Neurochem Res 39:1942-1947.
Jones EG, Wise SP (1977) Size, laminar and columnar distribution of efferent cells in the sensory-motor cortex of monkeys. J Comp Neurol 175:391-438.
Jones EG, Coulter JD, Hendry SH (1978) Intracortical connectivity of architectonic fields in the somatic sensory, motor and parietal cortex of monkeys. J Comp Neurol 181:291-347.
Jones EG, Coulter JD, Wise SP (1979) Commissural columns in the sensory-motor cortex of monkeys. J Comp Neurol 188:113-135.
Jones RD, Donaldson IM, Parkin PJ (1989) Impairment and recovery of ipsilateral sensory-motor function following unilateral cerebral infarction. Brain 112 (Pt 1):113-132.
Jones TA (2017) Motor compensation and its effects on neural reorganization after stroke. Nat Rev Neurosci 18:267-280.
Jones TA, Jefferson SC (2011) Reflections of experience-expectant development in repair of the adult damaged brain. Dev Psychobiol 53:466-475.
Kaas JH (1995) The organization of callosal connections in primates. In: Epilepsy and the Corpus Callosum 2, pp 15-27: Springer.
Kaas JH, Gharbawie OA, Stepniewska I (2013) Cortical networks for ethologically relevant behaviors in primates. Am J Primatol 75:407-414.
Kakei S, Hoffman DS, Strick PL (1999) Muscle and movement representations in the primary motor cortex. Science 285:2136-2139.
Kakuda W, Abo M, Kobayashi K, Momosaki R, Yokoi A, Fukuda A, Ito H, Tominaga A, Umemori T, Kameda Y (2011) Anti-spastic effect of low-frequency rTMS applied with occupational therapy in post-stroke patients with upper limb hemiparesis. Brain Inj 25:496-502.
Kalaska JF, Hyde ML (1985) Area 4 and area 5: differences between the load direction-dependent discharge variability of cells during active postural fixation. Exp Brain Res 59:197-202.
Kalaska JF, Caminiti R, Georgopoulos AP (1983) Cortical mechanisms related to the direction of two-dimensional arm movements: relations in parietal area 5 and comparison with motor cortex. Exp Brain Res 51:247-260.
Kalaska JF, Cohen DA, Hyde ML, Prud'homme M (1989) A comparison of movement direction-related versus load direction-related activity in primate motor cortex, using a two-dimensional reaching task. J Neurosci 9:2080-2102.
Kalaska JF, Scott SH, Cisek P, Sergio LE (1997) Cortical control of reaching movements. Curr Opin Neurobiol 7:849-859.

Kang X, Schieber MH, Thakor NV (2012) Decoding of finger, hand and arm kinematics using switching linear dynamical systems with pre-motor cortical ensembles. Annu Int Conf IEEE Eng Med Biol Soc 2012:1732-1735.
Karl JM, Whishaw IQ (2013) Different evolutionary origins for the reach and the grasp: an explanation for dual visuomotor channels in primate parietofrontal cortex. Front Neurol 4:208.
Kaufman MT, Churchland MM, Santhanam G, Yu BM, Afshar A, Ryu SI, Shenoy KV (2010) Roles of monkey premotor neuron classes in movement preparation and execution. J Neurophysiol 104:799-810.
Kermadi I, Liu Y, Tempini A, Rouiller EM (1997) Effects of reversible inactivation of the supplementary motor area (SMA) on unimanual grasp and bimanual pull and grasp performance in monkeys. Somatosens Mot Res 14:268-280.
Kermadi I, Liu Y, Tempini A, Calciati E, Rouiller EM (1998) Neuronal activity in the primate supplementary motor area and the primary motor cortex in relation to spatio-temporal bimanual coordination. Somatosens Mot Res 15:287-308.
Kessner SS, Schlemm E, Cheng B, Bingel U, Fiehler J, Gerloff C, Thomalla G (2019) Somatosensory Deficits After Ischemic Stroke. Stroke 50:1116-1123.
Khanna P, Totten D, Novik L, Roberts J, Morecraft RJ, Ganguly K (2021) Low-frequency stimulation enhances ensemble co-firing and dexterity after stroke. Cell 184:912-930 e920.
Khedr EM, Ahmed MA, Fathy N, Rothwell JC (2005) Therapeutic trial of repetitive transcranial magnetic stimulation after acute ischemic stroke. Neurology 65:466-468.
Khedr EM, Etraby AE, Hemeda M, Nasef AM, Razek AA (2010) Long-term effect of repetitive transcranial magnetic stimulation on motor function recovery after acute ischemic stroke. Acta Neurol Scand 121:30-37.
Killackey HP, Gould HJ, 3rd, Cusick CG, Pons TP, Kaas JH (1983) The relation of corpus callosum connections to architectonic fields and body surface maps in sensorimotor cortex of new and old world monkeys. J Comp Neurol 219:384-419.
Kim K, Yoo SJ, Kim SY, Lee T, Lim SH, Jang JE, Je M, Moon C, Choi JW (2021) Subthreshold electrical stimulation as a low power electrical treatment for stroke rehabilitation. Sci Rep 11:14048.
Kim SY, Jones TA (2010) Lesion size-dependent synaptic and astrocytic responses in cortex contralateral to infarcts in middle-aged rats. Synapse 64:659-671.
Kim YH, Park JW, Ko MH, Jang SH, Lee PK (2004) Facilitative effect of high frequency subthreshold repetitive transcranial magnetic stimulation on complex sequential motor learning in humans. Neurosci Lett 367:181-185.
Kim YH, You SH, Ko MH, Park JW, Lee KH, Jang SH, Yoo WK, Hallett M (2006) Repetitive transcranial magnetic stimulation-induced corticomotor excitability and associated motor skill acquisition in chronic stroke. Stroke 37:1471-1476.
Kinsbourne M (1977) Hemi-neglect and hemisphere rivalry. Adv Neurol 18:41-49.
Kinsbourne M (1980) Dichotic imbalance due to isolated hemisphere occlusion or directional rivalry? Brain Lang 11:221-224.
Kirton A, Chen R, Friefeld S, Gunraj C, Pontigon AM, Deveber G (2008) Contralesional repetitive transcranial magnetic stimulation for chronic hemiparesis in subcortical paediatric stroke: a randomised trial. Lancet Neurol 7:507-513.
Kleim JA, Bruneau R, VandenBerg P, MacDonald E, Mulrooney R, Pocock D (2003) Motor cortex stimulation enhances motor recovery and reduces peri-infarct dysfunction following ischemic insult. Neurol Res 25:789-793.
Kobayashi M, Hutchinson S, Theoret H, Schlaug G, Pascual-Leone A (2004) Repetitive TMS of the motor cortex improves ipsilateral sequential simple finger movements. Neurology 62:91-98.

Koch G, Franca M, Mochizuki H, Marconi B, Caltagirone C, Rothwell JC (2007) Interactions between pairs of transcranial magnetic stimuli over the human left dorsal premotor cortex differ from those seen in primary motor cortex. J Physiol 578:551-562.
Koch G, Franca M, Del Olmo MF, Cheeran B, Milton R, Alvarez Sauco M, Rothwell JC (2006) Time course of functional connectivity between dorsal premotor and contralateral motor cortex during movement selection. J Neurosci 26:7452-7459.
Kokinovic B, Medini P (2018) Loss of GABAB -mediated interhemispheric synaptic inhibition in stroke periphery. J Physiol 596:1949-1964.
Kraskov A, Dancause N, Quallo MM, Shepherd S, Lemon RN (2009) Corticospinal neurons in macaque ventral premotor cortex with mirror properties: a potential mechanism for action suppression? Neuron 64:922-930.
Kraskov A, Prabhu G, Quallo MM, Lemon RN, Brochier T (2011) Ventral premotor-motor cortex interactions in the macaque monkey during grasp: response of single neurons to intracortical microstimulation. J Neurosci 31:8812-8821.
Kraskov A, Philipp R, Waldert S, Vigneswaran G, Quallo MM, Lemon RN (2014) Corticospinal mirror neurons. Philos Trans R Soc Lond B Biol Sci 369:20130174.
Kubota K (1996) Motor cortical muscimol injection disrupts forelimb movement in freely moving monkeys. Neuroreport 7:2379-2384.
Kuhtz-Buschbeck JP, Gilster R, Wolff S, Ulmer S, Siebner H, Jansen O (2008) Brain activity is similar during precision and power gripping with light force: an fMRI study. Neuroimage 40:1469-1481.
Kurata K (2007) Laterality of movement-related activity reflects transformation of coordinates in ventral premotor cortex and primary motor cortex of monkeys. J Neurophysiol 98:2008-2021.
Kurata K (2010) Conditional selection of contra- and ipsilateral forelimb movements by the dorsal premotor cortex in monkeys. J Neurophysiol 103:262-277.
Kurata K, Tanji J (1986) Premotor cortex neurons in macaques: activity before distal and proximal forelimb movements. J Neurosci 6:403-411.
Kurata K, Wise SP (1988) Premotor cortex of rhesus monkeys: set-related activity during two conditional motor tasks. Exp Brain Res 69:327-343.
Kurata K, Hoffman DS (1994) Differential effects of muscimol microinjection into dorsal and ventral aspects of the premotor cortex of monkeys. J Neurophysiol 71:1151-1164.
Kurata K, Hoshi E (1999) Reacquisition deficits in prism adaptation after muscimol microinjection into the ventral premotor cortex of monkeys. J Neurophysiol 81:1927-1938.
Lacquaniti F, Guigon E, Bianchi L, Ferraina S, Caminiti R (1995) Representing spatial information for limb movement: role of area 5 in the monkey. Cereb Cortex 5:391-409.
Lacroix S, Havton LA, McKay H, Yang H, Brant A, Roberts J, Tuszynski MH (2004) Bilateral corticospinal projections arise from each motor cortex in the macaque monkey: a quantitative study. J Comp Neurol 473:147-161.
Lai SM, Studenski S, Duncan PW, Perera S (2002) Persisting consequences of stroke measured by the Stroke Impact Scale. Stroke 33:1840-1844.
LaMotte RH, Mountcastle VB (1979) Disorders in somesthesis following lesions of parietal lobe. J Neurophysiol 42:400-419.
Lang CE, Schieber MH (2004) Reduced muscle selectivity during individuated finger movements in humans after damage to the motor cortex or corticospinal tract. J Neurophysiol 91:1722-1733.
Lashley KS (1929) Brain mechanisms and intelligence: a quantitative study of injuries to the brain. Chicago: Chicago Press.
Lashley KS (1930) Basic neural mechanisms in behavior. Psychol Rev 37:1-24.

Latifi S, Mitchell S, Habibey R, Hosseini F, Donzis E, Estrada-Sanchez AM, Nejad HR, Levine M, Golshani P, Carmichael ST (2020) Neuronal Network Topology Indicates Distinct Recovery Processes after Stroke. Cereb Cortex 30:6363-6375.
Lawrence DG, Porter R, Redman SJ (1985) Corticomotoneuronal synapses in the monkey: light microscopic localization upon motoneurons of intrinsic muscles of the hand. J Comp Neurol 232:499-510.
Lefebvre S, Thonnard JL, Laloux P, Peeters A, Jamart J, Vandermeeren Y (2014) Single session of dual-tDCS transiently improves precision grip and dexterity of the paretic hand after stroke. Neurorehabil Neural Repair 28:100-110.
Lemon RN (1993) The G. L. Brown Prize Lecture. Cortical control of the primate hand. Exp Physiol 78:263-301.
Lemon RN (2008) Descending pathways in motor control. Annu Rev Neurosci 31:195-218.
Lemon RN, Johansson RS, Westling G (1995) Corticospinal control during reach, grasp, and precision lift in man. J Neurosci 15:6145-6156.
Levy R, Ruland S, Weinand M, Lowry D, Dafer R, Bakay R (2008) Cortical stimulation for the rehabilitation of patients with hemiparetic stroke: a multicenter feasibility study of safety and efficacy. J Neurosurg 108:707-714.
Levy RM, Harvey RL, Kissela BM, Winstein CJ, Lutsep HL, Parrish TB, Cramer SC, Venkatesan L (2016) Epidural Electrical Stimulation for Stroke Rehabilitation: Results of the Prospective, Multicenter, Randomized, Single-Blinded Everest Trial. Neurorehabil Neural Repair 30:107-119.
Leyton ASF, Sherrington CS (1917) Observations on the Excitable Cortex of the Chimpanzee, Orang-Utan, and Gorilla. Quarterly Journal of Experimental Physiology:135-222.
Li CS, Padoa-Schioppa C, Bizzi E (2001) Neuronal correlates of motor performance and motor learning in the primary motor cortex of monkeys adapting to an external force field. Neuron 30:593-607.
Li N, Daie K, Svoboda K, Druckmann S (2016) Robust neuronal dynamics in premotor cortex during motor planning. Nature 532:459-464.
Li N, Chen TW, Guo ZV, Gerfen CR, Svoboda K (2015) A motor cortex circuit for motor planning and movement. Nature 519:51-56.
Lidow MS, Goldman-Rakic PS, Gallager DW, Geschwind DH, Rakic P (1989) Distribution of major neurotransmitter receptors in the motor and somatosensory cortex of the rhesus monkey. Neuroscience 32:609-627.
Liepert J, Zittel S, Weiller C (2007) Improvement of dexterity by single session low-frequency repetitive transcranial magnetic stimulation over the contralesional motor cortex in acute stroke: a double-blind placebo-controlled crossover trial. Restor Neurol Neurosci 25:461-465.
Liepert J, Dettmers C, Terborg C, Weiller C (2001) Inhibition of ipsilateral motor cortex during phasic generation of low force. Clin Neurophysiol 112:114-121.
Liew SL, Santarnecchi E, Buch ER, Cohen LG (2014) Non-invasive brain stimulation in neurorehabilitation: local and distant effects for motor recovery. Front Hum Neurosci 8:378.
Liu Y, Rouiller EM (1999) Mechanisms of recovery of dexterity following unilateral lesion of the sensorimotor cortex in adult monkeys. Exp Brain Res 128:149-159.
Liuzzi G, Horniss V, Zimerman M, Gerloff C, Hummel FC (2011) Coordination of uncoupled bimanual movements by strictly timed interhemispheric connectivity. J Neurosci 31:9111-9117.
Lotze M, Markert J, Sauseng P, Hoppe J, Plewnia C, Gerloff C (2006) The role of multiple contralesional motor areas for complex hand movements after internal capsular lesion. J Neurosci 26:6096-6102.
Loubinoux I, Carel C, Pariente J, Dechaumont S, Albucher JF, Marque P, Manelfe C, Chollet F (2003) Correlation between cerebral reorganization and motor recovery after subcortical infarcts. Neuroimage 20:2166-2180.

Ludemann-Podubecka J, Bosl K, Nowak DA (2016) Inhibition of the contralesional dorsal premotor cortex improves motor function of the affected hand following stroke. Eur J Neurol 23:823-830.
Luppino G, Matelli M, Camarda R, Rizzolatti G (1993) Corticocortical connections of area F3 (SMA-proper) and area F6 (pre-SMA) in the macaque monkey. J Comp Neurol 338:114-140.
Luppino G, Matelli M, Camarda R, Rizzolatti G (1994) Corticospinal projections from mesial frontal and cingulate areas in the monkey. Neuroreport 5:2545-2548.
Luppino G, Murata A, Govoni P, Matelli M (1999) Largely segregated parietofrontal connections linking rostral intraparietal cortex (areas AIP and VIP) and the ventral premotor cortex (areas F5 and F4). Exp Brain Res 128:181-187.
Luppino G, Matelli M, Camarda RM, Gallese V, Rizzolatti G (1991) Multiple representations of body movements in mesial area 6 and the adjacent cingulate cortex: an intracortical microstimulation study in the macaque monkey. J Comp Neurol 311:463-482.
Lurito JT, Georgakopoulos T, Georgopoulos AP (1991) Cognitive spatial-motor processes. 7. The making of movements at an angle from a stimulus direction: studies of motor cortical activity at the single cell and population levels. Exp Brain Res 87:562-580.
Maeda F, Keenan JP, Tormos JM, Topka H, Pascual-Leone A (2000a) Modulation of corticospinal excitability by repetitive transcranial magnetic stimulation. Clin Neurophysiol 111:800-805.
Maeda F, Keenan JP, Tormos JM, Topka H, Pascual-Leone A (2000b) Interindividual variability of the modulatory effects of repetitive transcranial magnetic stimulation on cortical excitability. Exp Brain Res 133:425-430.
Maier MA, Bennett KM, Hepp-Reymond MC, Lemon RN (1993) Contribution of the monkey corticomotoneuronal system to the control of force in precision grip. J Neurophysiol 69:772-785.
Maier MA, Armand J, Kirkwood PA, Yang HW, Davis JN, Lemon RN (2002) Differences in the corticospinal projection from primary motor cortex and supplementary motor area to macaque upper limb motoneurons: an anatomical and electrophysiological study. Cereb Cortex 12:281-296.
Mansoori BK, Jean-Charles L, Touvykine B, Liu A, Quessy S, Dancause N (2014) Acute inactivation of the contralesional hemisphere for longer durations improves recovery after cortical injury. Exp Neurol 254:18-28.
Mansur CG, Fregni F, Boggio PS, Riberto M, Gallucci-Neto J, Santos CM, Wagner T, Rigonatti SP, Marcolin MA, Pascual-Leone A (2005) A sham stimulation-controlled trial of rTMS of the unaffected hemisphere in stroke patients. Neurology 64:1802-1804.
Maranesi M, Roda F, Bonini L, Rozzi S, Ferrari PF, Fogassi L, Coude G (2012) Anatomo-functional organization of the ventral primary motor and premotor cortex in the macaque monkey. Eur J Neurosci 36:3376-3387.
Marconi B, Genovesio A, Giannetti S, Molinari M, Caminiti R (2003) Callosal connections of dorso-lateral premotor cortex. Eur J Neurosci 18:775-788.
Marconi B, Genovesio A, Battaglia-Mayer A, Ferraina S, Squatrito S, Molinari M, Lacquaniti F, Caminiti R (2001) Eye-hand coordination during reaching. I. Anatomical relationships between parietal and frontal cortex. Cereb Cortex 11:513-527.
Marshall RS, Zarahn E, Alon L, Minzer B, Lazar RM, Krakauer JW (2009) Early imaging correlates of subsequent motor recovery after stroke. Ann Neurol 65:596-602.
Martin JH (1991) Autoradiographic estimation of the extent of reversible inactivation produced by microinjection of lidocaine and muscimol in the rat. Neurosci Lett 127:160-164.
Martin JH, Ghez C (1993) Differential impairments in reaching and grasping produced by local inactivation within the forelimb representation of the motor cortex in the cat. Exp Brain Res 94:429-443.
Martin JH, Ghez C (1999) Pharmacological inactivation in the analysis of the central control of movement. J Neurosci Methods 86:145-159.

Matelli M, Luppino G, Rizzolatti G (1985) Patterns of cytochrome oxidase activity in the frontal agranular cortex of the macaque monkey. Behav Brain Res 18:125-136.
Matelli M, Camarda R, Glickstein M, Rizzolatti G (1986) Afferent and efferent projections of the inferior area 6 in the macaque monkey. J Comp Neurol 251:281-298.
Matsumoto RR (1989) GABA receptors: are cellular differences reflected in function? Brain Res Brain Res Rev 14:203-225.
Matsumura M, Sawaguchi T, Oishi T, Ueki K, Kubota K (1991) Behavioral deficits induced by local injection of bicuculline and muscimol into the primate motor and premotor cortex. J Neurophysiol 65:1542-1553.
Matsuzaka Y, Aizawa H, Tanji J (1992) A motor area rostral to the supplementary motor area (presupplementary motor area) in the monkey: neuronal activity during a learned motor task. J Neurophysiol 68:653-662.
Mayston MJ, Harrison LM, Stephens JA (1999) A neurophysiological study of mirror movements in adults and children. Ann Neurol 45:583-594.
McDonnell MN, Stinear CM (2017) TMS measures of motor cortex function after stroke: A meta-analysis. Brain Stimul 10:721-734.
McGuire PK, Bates JF, Goldman-Rakic PS (1991) Interhemispheric integration: I. Symmetry and convergence of the corticocortical connections of the left and the right principal sulcus (PS) and the left and the right supplementary motor area (SMA) in the rhesus monkey. Cereb Cortex 1:390-407.
McKiernan BJ, Marcario JK, Karrer JH, Cheney PD (1998) Corticomotoneuronal postspike effects in shoulder, elbow, wrist, digit, and intrinsic hand muscles during a reach and prehension task. J Neurophysiol 80:1961-1980.
McNeal DW, Darling WG, Ge J, Stilwell-Morecraft KS, Solon KM, Hynes SM, Pizzimenti MA, Rotella DL, Vanadurongvan T, Morecraft RJ (2010) Selective long-term reorganization of the corticospinal projection from the supplementary motor cortex following recovery from lateral motor cortex injury. J Comp Neurol 518:586-621.
Meehan SK, Dao E, Linsdell MA, Boyd LA (2011) Continuous theta burst stimulation over the contralesional sensory and motor cortex enhances motor learning post-stroke. Neurosci Lett 500:26-30.
Menz VK, Schaffelhofer S, Scherberger H (2015) Representation of continuous hand and arm movements in macaque areas M1, F5, and AIP: a comparative decoding study. J Neural Eng 12:056016.
Messier J, Kalaska JF (2000) Covariation of primate dorsal premotor cell activity with direction and amplitude during a memorized-delay reaching task. J Neurophysiol 84:152-165.
Meyer BU, Roricht S, Grafin von Einsiedel H, Kruggel F, Weindl A (1995) Inhibitory and excitatory interhemispheric transfers between motor cortical areas in normal humans and patients with abnormalities of the corpus callosum. Brain 118 (Pt 2):429-440.
Meyer KL, Dempsey RJ, Roy MW, Donaldson DL (1985) Somatosensory evoked potentials as a measure of experimental cerebral ischemia. J Neurosurg 62:269-275.
Michaels JA, Scherberger H (2018) Population coding of grasp and laterality-related information in the macaque fronto-parietal network. Sci Rep 8:1710.
Michelot D, Melendez-Howell LM (2003) Amantia muscaria: Chemistry, biology, toxicology, and ethnomycology. Mycol Res 107:131-146.
Mink JW, Thach WT (1991) Basal ganglia motor control. III. Pallidal ablation: normal reaction time, muscle cocontraction, and slow movement. J Neurophysiol 65:330-351.
Mitz AR, Wise SP (1987) The somatotopic organization of the supplementary motor area: intracortical microstimulation mapping. J Neurosci 7:1010-1021.

Mitz AR, Godschalk M, Wise SP (1991) Learning-dependent neuronal activity in the premotor cortex: activity during the acquisition of conditional motor associations. J Neurosci 11:1855-1872.
Miyai I, Suzuki T, Kang J, Kubota K, Volpe BT (1999) Middle cerebral artery stroke that includes the premotor cortex reduces mobility outcome. Stroke 30:1380-1383.
Miyai I, Yagura H, Hatakenaka M, Oda I, Konishi I, Kubota K (2003) Longitudinal optical imaging study for locomotor recovery after stroke. Stroke 34:2866-2870.
Mohajerani MH, Aminoltejari K, Murphy TH (2011) Targeted mini-strokes produce changes in interhemispheric sensory signal processing that are indicative of disinhibition within minutes. Proc Natl Acad Sci U S A 108:E183-191.
Moore TL, Pessina MA, Finklestein SP, Kramer BC, Killiany RJ, Rosene DL (2013) Recovery of fine motor performance after ischemic damage to motor cortex is facilitated by cell therapy in the rhesus monkey. Somatosens Mot Res 30:185-196.
Moreau-Debord I, Serrano E, Quessy S, Dancause N (2021) Rapid and Bihemispheric Reorganization of Neuronal Activity in Premotor Cortex after Brain Injury. J Neurosci 41:9112-9128.
Morecraft RJ, Ge J, Stilwell-Morecraft KS, McNeal DW, Pizzimenti MA, Darling WG (2013) Terminal distribution of the corticospinal projection from the hand/arm region of the primary motor cortex to the cervical enlargement in rhesus monkey. J Comp Neurol 521:4205-4235.
Morecraft RJ, Ge J, Stilwell-Morecraft KS, McNeal DW, Hynes SM, Pizzimenti MA, Rotella DL, Darling WG (2015) Vulnerability of the medial frontal corticospinal projection accompanies combined lateral frontal and parietal cortex injury in rhesus monkey. J Comp Neurol 523:669-697.
Mountcastle VB, Atluri PP, Romo R (1992) Selective output-discriminative signals in the motor cortex of waking monkeys. Cereb Cortex 2:277-294.
Muakkassa KF, Strick PL (1979) Frontal lobe inputs to primate motor cortex: evidence for four somatotopically organized 'premotor' areas. Brain Res 177:176-182.
Muellbacher W, Facchini S, Boroojerdi B, Hallett M (2000) Changes in motor cortex excitability during ipsilateral hand muscle activation in humans. Clin Neurophysiol 111:344-349.
Muir KW, Tyrrell P, Sattar N, Warburton E (2007) Inflammation and ischaemic stroke. Curr Opin Neurol 20:334-342.
Munk H (1881) Uber die Funktionen der Grosshirnrinde. In: Hirshwald A (ed) Gesammelte Mitteilungen aus den Jahren (Hirshwald A, ed), pp 1877-1880. Berlin.
Murase N, Duque J, Mazzocchio R, Cohen LG (2004) Influence of interhemispheric interactions on motor function in chronic stroke. Ann Neurol 55:400-409.
Murata A, Fadiga L, Fogassi L, Gallese V, Raos V, Rizzolatti G (1997) Object representation in the ventral premotor cortex (area F5) of the monkey. J Neurophysiol 78:2226-2230.
Murata Y, Higo N, Hayashi T, Nishimura Y, Sugiyama Y, Oishi T, Tsukada H, Isa T, Onoe H (2015) Temporal plasticity involved in recovery from manual dexterity deficit after motor cortex lesion in macaque monkeys. J Neurosci 35:84-95.
Murray EA, Coulter JD (1981) Organization of corticospinal neurons in the monkey. J Comp Neurol 195:339-365.
Murray EA, Mishkin M (1984) Relative contributions of SII and area 5 to tactile discrimination in monkeys. Behav Brain Res 11:67-83.
Nair DG, Hutchinson S, Fregni F, Alexander M, Pascual-Leone A, Schlaug G (2007) Imaging correlates of motor recovery from cerebral infarction and their physiological significance in well-recovered patients. Neuroimage 34:253-263.
Nakayama Y, Yokoyama O, Hoshi E (2015) Distinct neuronal organizations of the caudal cingulate motor area and supplementary motor area in monkeys for ipsilateral and contralateral hand movements. J Neurophysiol 113:2845-2858.

Nawrot M, Aertsen A, Rotter S (1999) Single-trial estimation of neuronal firing rates: from single-neuron spike trains to population activity. J Neurosci Methods 94:81-92.
Nelissen K, Vanduffel W (2011) Grasping-related functional magnetic resonance imaging brain responses in the macaque monkey. J Neurosci 31:8220-8229.
Nishimura Y, Onoe H, Morichika Y, Perfiliev S, Tsukada H, Isa T (2007) Time-dependent central compensatory mechanisms of finger dexterity after spinal cord injury. Science 318:1150-1155.
Nitsche MA, Schauenburg A, Lang N, Liebetanz D, Exner C, Paulus W, Tergau F (2003) Facilitation of implicit motor learning by weak transcranial direct current stimulation of the primary motor cortex in the human. J Cogn Neurosci 15:619-626.
Nomura EM, Gratton C, Visser RM, Kayser A, Perez F, D'Esposito M (2010) Double dissociation of two cognitive control networks in patients with focal brain lesions. Proc Natl Acad Sci U S A 107:12017-12022.
Nowak DA, Grefkes C, Ameli M, Fink GR (2009) Interhemispheric competition after stroke: brain stimulation to enhance recovery of function of the affected hand. Neurorehabil Neural Repair 23:641-656.
Nowak DA, Grefkes C, Dafotakis M, Eickhoff S, Kust J, Karbe H, Fink GR (2008) Effects of low-frequency repetitive transcranial magnetic stimulation of the contralesional primary motor cortex on movement kinematics and neural activity in subcortical stroke. Arch Neurol 65:741-747.
Nudo RJ (2006) Mechanisms for recovery of motor function following cortical damage. Curr Opin Neurobiol 16:638-644.
Nudo RJ, Milliken GW (1996) Reorganization of movement representations in primary motor cortex following focal ischemic infarcts in adult squirrel monkeys. J Neurophysiol 75:2144-2149.
Nudo RJ, Wise BM, SiFuentes F, Milliken GW (1996) Neural substrates for the effects of rehabilitative training on motor recovery after ischemic infarct. Science 272:1791-1794.
Nudo RJ, Larson D, Plautz EJ, Friel KM, Barbay S, Frost SB (2003) A squirrel monkey model of poststroke motor recovery. ILAR J 44:161-174.
O'Shea J, Sebastian C, Boorman ED, Johansen-Berg H, Rushworth MF (2007) Functional specificity of human premotor-motor cortical interactions during action selection. Eur J Neurosci 26:2085-2095.
Oby ER, Golub MD, Hennig JA, Degenhart AD, Tyler-Kabara EC, Yu BM, Chase SM, Batista AP (2019) New neural activity patterns emerge with long-term learning. Proc Natl Acad Sci U S A 116:15210-15215.
Ogawa T, Yoshida Y, Okudera T, Noguchi K, Kado H, Uemura K (1997) Secondary thalamic degeneration after cerebral infarction in the middle cerebral artery distribution: evaluation with MR imaging. Radiology 204:255-262.
Ogden R, Franz SI (1917) On cerebral motor control: the recovery of function from experimentally produced hemiplegia. Psychbiol 1.
Ohashi H, Gribble PL, Ostry DJ (2019) Somatosensory cortical excitability changes precede those in motor cortex during human motor learning. J Neurophysiol 122:1397-1405.
Omrani M, Pruszynski JA, Murnaghan CD, Scott SH (2014) Perturbation-evoked responses in primary motor cortex are modulated by behavioral context. J Neurophysiol 112:2985-3000.
Orczykowski ME, Arndt KR, Palitz LE, Kramer BC, Pessina MA, Oblak AL, Finklestein SP, Mortazavi F, Rosene DL, Moore TL (2018) Cell based therapy enhances activation of ventral premotor cortex to improve recovery following primary motor cortex injury. Exp Neurol 305:13-25.
Orru G, Conversano C, Hitchcott PK, Gemignani A (2020) Motor stroke recovery after tDCS: a systematic review. Reviews in the Neurosciences 31:201-218.
Otani S, Blond O, Desce JM, Crepel F (1998) Dopamine facilitates long-term depression of glutamatergic transmission in rat prefrontal cortex. Neuroscience 85:669-676.

Pandarinath C, Ames KC, Russo AA, Farshchian A, Miller LE, Dyer EL, Kao JC (2018) Latent Factors and Dynamics in Motor Cortex and Their Application to Brain-Machine Interfaces. J Neurosci 38:9390-9401.
Pandya DN, Vignolo LA (1971) Intra- and interhemispheric projections of the precentral, premotor and arcuate areas in the rhesus monkey. Brain Res 26:217-233.
Papadourakis V, Raos V (2017) Evidence for the representation of movement kinematics in the discharge of F5 mirror neurons during the observation of transitive and intransitive actions. J Neurophysiol 118:3215-3229.
Papadourakis V, Raos V (2019) Neurons in the Macaque Dorsal Premotor Cortex Respond to Execution and Observation of Actions. Cereb Cortex 29:4223-4237.
Pare M, Guitton D (1998) Brain stem omnipause neurons and the control of combined eye-head gaze saccades in the alert cat. J Neurophysiol 79:3060-3076.
Park CH, Chang WH, Ohn SH, Kim ST, Bang OY, Pascual-Leone A, Kim YH (2011) Longitudinal changes of resting-state functional connectivity during motor recovery after stroke. Stroke 42:1357-1362.
Park MC, Belhaj-Saif A, Gordon M, Cheney PD (2001) Consistent features in the forelimb representation of primary motor cortex in rhesus macaques. J Neurosci 21:2784-2792.
Partsalis AM, Zhang Y, Highstein SM (1995) Dorsal Y group in the squirrel monkey. II. Contribution of the cerebellar flocculus to neuronal responses in normal and adapted animals. J Neurophysiol 73:632-650.
Pascual-Leone A, Valls-Sole J, Wassermann EM, Hallett M (1994) Responses to rapid-rate transcranial magnetic stimulation of the human motor cortex. Brain 117 (Pt 4):847-858.
Paulignan Y, Jeannerod M, MacKenzie C, Marteniuk R (1991) Selective perturbation of visual input during prehension movements. 2. The effects of changing object size. Exp Brain Res 87:407-420.
Pavlides C, Miyashita E, Asanuma H (1993) Projection from the sensory to the motor cortex is important in learning motor skills in the monkey. J Neurophysiol 70:733-741.
Paz JT, Christian CA, Parada I, Prince DA, Huguenard JR (2010) Focal cortical infarcts alter intrinsic excitability and synaptic excitation in the reticular thalamic nucleus. J Neurosci 30:5465-5479.
Peinemann A, Reimer B, Loer C, Quartarone A, Munchau A, Conrad B, Siebner HR (2004) Long-lasting increase in corticospinal excitability after 1800 pulses of subthreshold 5 Hz repetitive TMS to the primary motor cortex. Clin Neurophysiol 115:1519-1526.
Penfield W, Boldrey E (1937) Somatic Motor and Sensory Representation in the Cerebral Cortex of Man as Studied by Electrical Stimulation. Brain:389-443.
Penfield W, Welch K (1951) The supplementary motor area of the cerebral cortex; a clinical and experimental study. AMA Arch Neurol Psychiatry 66:289-317.
Petri S, Krampfl K, Hashemi F, Grothe C, Hori A, Dengler R, Bufler J (2003) Distribution of GABAA receptor mRNA in the motor cortex of ALS patients. J Neuropathol Exp Neurol 62:1041-1051.
Picard N, Smith AM (1992) Primary motor cortical activity related to the weight and texture of grasped objects in the monkey. J Neurophysiol 68:1867-1881.
Picard N, Strick PL (2001) Imaging the premotor areas. Curr Opin Neurobiol 11:663-672.
Pineiro R, Pendlebury ST, Smith S, Flitney D, Blamire AM, Styles P, Matthews PM (2000) Relating MRI changes to motor deficit after ischemic stroke by segmentation of functional motor pathways. Stroke 31:672-679.
Plautz EJ, Barbay S, Frost SB, Friel KM, Dancause N, Zoubina EV, Stowe AM, Quaney BM, Nudo RJ (2003) Post-infarct cortical plasticity and behavioral recovery using concurrent cortical stimulation and rehabilitative training: a feasibility study in primates. Neurol Res 25:801-810.
Plautz EJ, Barbay S, Frost SB, Zoubina EV, Stowe AM, Dancause N, Eisner-Janowicz I, Bury SD, Taylor MD, Nudo RJ (2016) Effects of Subdural Monopolar Cortical Stimulation Paired With Rehabilitative

Training on Behavioral and Neurophysiological Recovery After Cortical Ischemic Stroke in Adult Squirrel Monkeys. Neurorehabil Neural Repair 30:159-172.
Plewnia C, Lotze M, Gerloff C (2003) Disinhibition of the contralateral motor cortex by low-frequency rTMS. Neuroreport 14:609-612.
Plow EB, Carey JR, Nudo RJ, Pascual-Leone A (2009) Invasive cortical stimulation to promote recovery of function after stroke: a critical appraisal. Stroke 40:1926-1931.
Plow EB, Cunningham DA, Varnerin N, Machado A (2015) Rethinking stimulation of the brain in stroke rehabilitation: why higher motor areas might be better alternatives for patients with greater impairments. Neuroscientist 21:225-240.
Plow EB, Cunningham DA, Beall E, Jones S, Wyant A, Bonnett C, Yue GH, Lowe M, Wang XF, Sakaie K, Machado A (2013) Effectiveness and neural mechanisms associated with tDCS delivered to premotor cortex in stroke rehabilitation: study protocol for a randomized controlled trial. Trials 14:331.
Pomeroy VM, Cloud G, Tallis RC, Donaldson C, Nayak V, Miller S (2007) Transcranial magnetic stimulation and muscle contraction to enhance stroke recovery: a randomized proof-of-principle and feasibility investigation. Neurorehabil Neural Repair 21:509-517.
Pons TP, Kaas JH (1986) Corticocortical connections of area 2 of somatosensory cortex in macaque monkeys: a correlative anatomical and electrophysiological study. J Comp Neurol 248:313-335.
Prabhu G, Shimazu H, Cerri G, Brochier T, Spinks RL, Maier MA, Lemon RN (2009) Modulation of primary motor cortex outputs from ventral premotor cortex during visually guided grasp in the macaque monkey. J Physiol 587:1057-1069.
Preuss TM, Stepniewska I, Kaas JH (1996) Movement representation in the dorsal and ventral premotor areas of owl monkeys: a microstimulation study. J Comp Neurol 371:649-676.
Pruszynski JA, Omrani M, Scott SH (2014) Goal-dependent modulation of fast feedback responses in primary motor cortex. J Neurosci 34:4608-4617.
Pruszynski JA, Kurtzer I, Nashed JY, Omrani M, Brouwer B, Scott SH (2011) Primary motor cortex underlies multi-joint integration for fast feedback control. Nature 478:387-390.
Quessy S, Cote SL, Hamadjida A, Deffeyes J, Dancause N (2016) Modulatory Effects of the Ipsi and Contralateral Ventral Premotor Cortex (PMv) on the Primary Motor Cortex (M1) Outputs to Intrinsic Hand and Forearm Muscles in Cebus apella. Cereb Cortex 26:3905-3920.
Ramanathan DS, Guo L, Gulati T, Davidson G, Hishinuma AK, Won SJ, Knight RT, Chang EF, Swanson RA, Ganguly K (2018) Low-frequency cortical activity is a neuromodulatory target that tracks recovery after stroke. Nat Med 24:1257-1267.
Raos V, Franchi G, Gallese V, Fogassi L (2003) Somatotopic organization of the lateral part of area F2 (dorsal premotor cortex) of the macaque monkey. J Neurophysiol 89:1503-1518.
Raos V, Umilta MA, Gallese V, Fogassi L (2004) Functional properties of grasping-related neurons in the dorsal premotor area F2 of the macaque monkey. J Neurophysiol 92:1990-2002.
Raos V, Umilta MA, Murata A, Fogassi L, Gallese V (2006) Functional properties of grasping-related neurons in the ventral premotor area F5 of the macaque monkey. J Neurophysiol 95:709-729.
Rathelot JA, Strick PL (2006) Muscle representation in the macaque motor cortex: an anatomical perspective. Proc Natl Acad Sci U S A 103:8257-8262.
Rathelot JA, Strick PL (2009) Subdivisions of primary motor cortex based on cortico-motoneuronal cells. Proc Natl Acad Sci U S A 106:918-923.
Rehme AK, Fink GR, von Cramon DY, Grefkes C (2011a) The role of the contralesional motor cortex for motor recovery in the early days after stroke assessed with longitudinal FMRI. Cereb Cortex 21:756-768.
Rehme AK, Eickhoff SB, Wang LE, Fink GR, Grefkes C (2011b) Dynamic causal modeling of cortical activity from the acute to the chronic stage after stroke. Neuroimage 55:1147-1158.

Rehme AK, Eickhoff SB, Rottschy C, Fink GR, Grefkes C (2012) Activation likelihood estimation meta-analysis of motor-related neural activity after stroke. Neuroimage 59:2771-2782.
Rehme AK, Volz LJ, Feis DL, Eickhoff SB, Fink GR, Grefkes C (2015) Individual prediction of chronic motor outcome in the acute post-stroke stage: Behavioral parameters versus functional imaging. Hum Brain Mapp 36:4553-4565.
Reis J, Schambra HM, Cohen LG, Buch ER, Fritsch B, Zarahn E, Celnik PA, Krakauer JW (2009) Noninvasive cortical stimulation enhances motor skill acquisition over multiple days through an effect on consolidation. Proc Natl Acad Sci U S A 106:1590-1595.
Reis J, Robertson EM, Krakauer JW, Rothwell J, Marshall L, Gerloff C, Wassermann EM, Pascual-Leone A, Hummel F, Celnik PA, Classen J, Floel A, Ziemann U, Paulus W, Siebner HR, Born J, Cohen LG (2008) Consensus: Can transcranial direct current stimulation and transcranial magnetic stimulation enhance motor learning and memory formation? Brain Stimul 1:363-369.
Restani L, Cerri C, Pietrasanta M, Gianfranceschi L, Maffei L, Caleo M (2009) Functional masking of deprived eye responses by callosal input during ocular dominance plasticity. Neuron 64:707-718.
Riehle A, Requin J (1989) Monkey primary motor and premotor cortex: single-cell activity related to prior information about direction and extent of an intended movement. J Neurophysiol 61:534-549.
Riehle A, Requin J (1995) Neuronal correlates of the specification of movement direction and force in four cortical areas of the monkey. Behav Brain Res 70:1-13.
Riehle A, MacKay WA, Requin J (1994) Are extent and force independent movement parameters? Preparation- and movement-related neuronal activity in the monkey cortex. Exp Brain Res 99:56-74.
Ritchie JM (1979) A pharmacological approach to the structure of sodium channels in myelinated axons. Annu Rev Neurosci 2:341-362.
Rizzolatti G (1987) Functional organization of inferior area 6. Ciba Found Symp 132:171-186.
Rizzolatti G, Fadiga L (1998) Grasping objects and grasping action meanings: the dual role of monkey rostroventral premotor cortex (area F5). Novartis Found Symp 218:81-95; discussion 95-103.
Rizzolatti G, Luppino G (2001) The cortical motor system. Neuron 31:889-901.
Rizzolatti G, Craighero L (2004) The mirror-neuron system. Annu Rev Neurosci 27:169-192.
Rizzolatti G, Luppino G (2015) Premotor Cortex. In: International Encyclopedia of the Social and Behavioral Sciences, 2nd edition, pp 846-851: Elsevier Ltd.
Rizzolatti G, Luppino G, Matelli M (1998) The organization of the cortical motor system: new concepts. Electroencephalogr Clin Neurophysiol 106:283-296.
Rizzolatti G, Scandolara C, Matelli M, Gentilucci M (1981a) Afferent properties of periarcuate neurons in macaque monkeys. I. Somatosensory responses. Behav Brain Res 2:125-146.
Rizzolatti G, Scandolara C, Matelli M, Gentilucci M (1981b) Afferent properties of periarcuate neurons in macaque monkeys. II. Visual responses. Behav Brain Res 2:147-163.
Rizzolatti G, Fadiga L, Gallese V, Fogassi L (1996) Premotor cortex and the recognition of motor actions. Brain Res Cogn Brain Res 3:131-141.
Rizzolatti G, Fadiga L, Fogassi L, Gallese V (1997) The space around us. Science 277:190-191.
Rizzolatti G, Cattaneo L, Fabbri-Destro M, Rozzi S (2014) Cortical mechanisms underlying the organization of goal-directed actions and mirror neuron-based action understanding. Physiol Rev 94:655-706.
Rizzolatti G, Camarda R, Fogassi L, Gentilucci M, Luppino G, Matelli M (1988) Functional organization of inferior area 6 in the macaque monkey. II. Area F5 and the control of distal movements. Exp Brain Res 71:491-507.
Rocha S, Silva E, Foerster A, Wiesiolek C, Chagas AP, Machado G, Baltar A, Monte-Silva K (2016) The impact of transcranial direct current stimulation (tDCS) combined with modified constraint-

induced movement therapy (mCIMT) on upper limb function in chronic stroke: a double-blind randomized controlled trial. Disabil Rehabil 38:653-660.
Roland PE, Skinhoj E, Lassen NA, Larsen B (1980) Different cortical areas in man in organization of voluntary movements in extrapersonal space. J Neurophysiol 43:137-150.
Romo R, Hernandez A, Zainos A, Lemus L, Brody CD (2002) Neuronal correlates of decision-making in secondary somatosensory cortex. Nat Neurosci 5:1217-1225.
Rosenzweig ES, Brock JH, Culbertson MD, Lu P, Moseanko R, Edgerton VR, Havton LA, Tuszynski MH (2009) Extensive spinal decussation and bilateral termination of cervical corticospinal projections in rhesus monkeys. J Comp Neurol 513:151-163.
Rossiter HE, Eaves C, Davis E, Boudrias MH, Park CH, Farmer S, Barnes G, Litvak V, Ward NS (2012) Changes in the location of cortico-muscular coherence following stroke. Neuroimage Clin 2:50-55.
Rouiller EM, Moret V, Liang F (1993) Comparison of the connectional properties of the two forelimb areas of the rat sensorimotor cortex: support for the presence of a premotor or supplementary motor cortical area. Somatosens Mot Res 10:269-289.
Rouiller EM, Babalian A, Kazennikov O, Moret V, Yu XH, Wiesendanger M (1994) Transcallosal connections of the distal forelimb representations of the primary and supplementary motor cortical areas in macaque monkeys. Exp Brain Res 102:227-243.
Rouiller EM, Yu XH, Moret V, Tempini A, Wiesendanger M, Liang F (1998) Dexterity in adult monkeys following early lesion of the motor cortical hand area: the role of cortex adjacent to the lesion. Eur J Neurosci 10:729-740.
Rozzi S, Ferrari PF, Bonini L, Rizzolatti G, Fogassi L (2008) Functional organization of inferior parietal lobule convexity in the macaque monkey: electrophysiological characterization of motor, sensory and mirror responses and their correlation with cytoarchitectonic areas. Eur J Neurosci 28:1569-1588.
Rozzi S, Calzavara R, Belmalih A, Borra E, Gregoriou GG, Matelli M, Luppino G (2006) Cortical connections of the inferior parietal cortical convexity of the macaque monkey. Cereb Cortex 16:1389-1417.
Sakata H, Taira M, Murata A, Mine S (1995) Neural mechanisms of visual guidance of hand action in the parietal cortex of the monkey. Cereb Cortex 5:429-438.
Sakatani K, Iizuka H, Young W (1990) Somatosensory evoked potentials in rat cerebral cortex before and after middle cerebral artery occlusion. Stroke 21:124-132.
Sandrini M, Cohen LG (2013) Noninvasive brain stimulation in neurorehabilitation. Handb Clin Neurol 116C:499-524.
Sawan SAE, Reda AM, Kamel AH, Ali MAM (2020) Transcranial direct current stimulation (tDCS) its effect on improving dysphagia in stroke patients. J Neurol Psychiatry Neurosurg 56.
Schabrun SM, Ridding MC, Miles TS (2008) Role of the primary motor and sensory cortex in precision grasping: a transcranial magnetic stimulation study. Eur J Neurosci 27:750-756.
Schaechter JD, Perdue KL (2008) Enhanced cortical activation in the contralesional hemisphere of chronic stroke patients in response to motor skill challenge. Cereb Cortex 18:638-647.
Schaffelhofer S, Scherberger H (2016) Object vision to hand action in macaque parietal, premotor, and motor cortices. Elife 5.
Schieber MH, Hibbard LS (1993) How somatotopic is the motor cortex hand area? Science 261:489-492.
Schieber MH, Poliakov AV (1998) Partial inactivation of the primary motor cortex hand area: effects on individuated finger movements. J Neurosci 18:9038-9054.
Schmidlin E, Brochier T, Maier MA, Kirkwood PA, Lemon RN (2008) Pronounced reduction of digit motor responses evoked from macaque ventral premotor cortex after reversible inactivation of the primary motor cortex hand area. J Neurosci 28:5772-5783.

Schmitt AB, Brook GA, Buss A, Nacimiento W, Noth J, Kreutzberg GW (1998) Dynamics of microglial activation in the spinal cord after cerebral infarction are revealed by expression of MHC class II antigen. Neuropathol Appl Neurobiol 24:167-176.
Schmitt AB, Buss A, Breuer S, Brook GA, Pech K, Martin D, Schoenen J, Noth J, Love S, Schroder JM, Kreutzberg GW, Nacimiento W (2000) Major histocompatibility complex class II expression by activated microglia caudal to lesions of descending tracts in the human spinal cord is not associated with a T cell response. Acta Neuropathol 100:528-536.
Scott SH, Kalaska JF (1995) Changes in motor cortex activity during reaching movements with similar hand paths but different arm postures. J Neurophysiol 73:2563-2567.
Scott SH, Kalaska JF (1997) Reaching movements with similar hand paths but different arm orientations. I. Activity of individual cells in motor cortex. J Neurophysiol 77:826-852.
Seeburg PH, Wisden W, Verdoorn TA, Pritchett DB, Werner P, Herb A, Luddens H, Sprengel R, Sakmann B (1990) The GABAA receptor family: molecular and functional diversity. Cold Spring Harb Symp Quant Biol 55:29-40.
Seitz RJ, Kleiser R, Butefisch CM (2005) Reorganization of cerebral circuits in human brain lesion. Acta Neurochir Suppl 93:65-70.
Seitz RJ, Hoflich P, Binkofski F, Tellmann L, Herzog H, Freund HJ (1998) Role of the premotor cortex in recovery from middle cerebral artery infarction. Arch Neurol 55:1081-1088.
Semmes J, Mishkin M (1965) Somatosensory Loss in Monkeys after Ipsilateral Cortical Ablation. J Neurophysiol 28:473-486.
Semmes J, Porter L (1972) A comparison of precentral and postcentral cortical lesions on somatosensory discrimination in the monkey. Cortex 8:249-264.
Seniow J, Bilik M, Lesniak M, Waldowski K, Iwanski S, Czlonkowska A (2012) Transcranial magnetic stimulation combined with physiotherapy in rehabilitation of poststroke hemiparesis: a randomized, double-blind, placebo-controlled study. Neurorehabil Neural Repair 26:1072-1079.
Shadmehr RA, Wise SP (2005) The Computational Neurobiology of Reaching and Pointing: A Foundation for Motor Learning. Cambridge, MA: MIT Press.
Shen L, Alexander GE (1997a) Neural correlates of a spatial sensory-to-motor transformation in primary motor cortex. J Neurophysiol 77:1171-1194.
Shen L, Alexander GE (1997b) Preferential representation of instructed target location versus limb trajectory in dorsal premotor area. J Neurophysiol 77:1195-1212.
Shenoy KV, Sahani M, Churchland MM (2013) Cortical control of arm movements: a dynamical systems perspective. Annu Rev Neurosci 36:337-359.
Shimazu H, Maier MA, Cerri G, Kirkwood PA, Lemon RN (2004) Macaque ventral premotor cortex exerts powerful facilitation of motor cortex outputs to upper limb motoneurons. J Neurosci 24:1200-1211.
Shimizu T, Hosaki A, Hino T, Sato M, Komori T, Hirai S, Rossini PM (2002) Motor cortical disinhibition in the unaffected hemisphere after unilateral cortical stroke. Brain 125:1896-1907.
Shinoda Y, Yokota J, Futami T (1981) Divergent projection of individual corticospinal axons to motoneurons of multiple muscles in the monkey. Neurosci Lett 23:7-12.
Siegel JS, Ramsey LE, Snyder AZ, Metcalf NV, Chacko RV, Weinberger K, Baldassarre A, Hacker CD, Shulman GL, Corbetta M (2016) Disruptions of network connectivity predict impairment in multiple behavioral domains after stroke. Proc Natl Acad Sci U S A 113:E4367-4376.
Sigler A, Mohajerani MH, Murphy TH (2009) Imaging rapid redistribution of sensory-evoked depolarization through existing cortical pathways after targeted stroke in mice. Proc Natl Acad Sci U S A 106:11759-11764.
Silasi G, Murphy TH (2014) Stroke and the connectome: how connectivity guides therapeutic intervention. Neuron 83:1354-1368.

Sitaram R, Veit R, Stevens B, Caria A, Gerloff C, Birbaumer N, Hummel F (2012) Acquired control of ventral premotor cortex activity by feedback training: an exploratory real-time FMRI and TMS study. Neurorehabil Neural Repair 26:256-265.
Small SL, Hlustik P, Noll DC, Genovese C, Solodkin A (2002) Cerebellar hemispheric activation ipsilateral to the paretic hand correlates with functional recovery after stroke. Brain 125:1544-1557.
Smith MC, Stinear CM (2016) Transcranial magnetic stimulation (TMS) in stroke: Ready for clinical practice? J Clin Neurosci 31:10-14.
Smith WS, Fetz EE (2009) Synaptic linkages between corticomotoneuronal cells affecting forelimb muscles in behaving primates. J Neurophysiol 102:1040-1048.
Solomons CD, Shanmugasundaram V (2019) A review of transcranial electrical stimulation methods in stroke rehabilitation. Neurol India 67:417-423.
Song M, Shin Y, Yun K (2014) Beta-frequency EEG activity increased during transcranial direct current stimulation. Neuroreport 25:1433-1436.
Soteropoulos DS, Edgley SA, Baker SN (2011) Lack of evidence for direct corticospinal contributions to control of the ipsilateral forelimb in monkey. J Neurosci 31:11208-11219.
Spinks RL, Kraskov A, Brochier T, Umilta MA, Lemon RN (2008) Selectivity for grasp in local field potential and single neuron activity recorded simultaneously from M1 and F5 in the awake macaque monkey. J Neurosci 28:10961-10971.
Stark E, Asher I, Abeles M (2007) Encoding of reach and grasp by single neurons in premotor cortex is independent of recording site. J Neurophysiol 97:3351-3364.
Stedman A, Davey NJ, Ellaway PH (1998) Facilitation of human first dorsal interosseous muscle responses to transcranial magnetic stimulation during voluntary contraction of the contralateral homonymous muscle. Muscle Nerve 21:1033-1039.
Stepniewska I, Preuss TM, Kaas JH (1993) Architectonics, somatotopic organization, and ipsilateral cortical connections of the primary motor area (M1) of owl monkeys. J Comp Neurol 330:238-271.
Stepniewska I, Preuss TM, Kaas JH (2006) Ipsilateral cortical connections of dorsal and ventral premotor areas in New World owl monkeys. J Comp Neurol 495:691-708.
Stepniewska I, Gharbawie OA, Burish MJ, Kaas JH (2014) Effects of muscimol inactivations of functional domains in motor, premotor, and posterior parietal cortex on complex movements evoked by electrical stimulation. J Neurophysiol 111:1100-1119.
Stinear CM, Walker KS, Byblow WD (2001) Symmetric facilitation between motor cortices during contraction of ipsilateral hand muscles. Exp Brain Res 139:101-105.
Stinear CM, Petoe MA, Byblow WD (2015) Primary Motor Cortex Excitability During Recovery After Stroke: Implications for Neuromodulation. Brain Stimul 8:1183-1190.
Sweetnam DA, Brown CE (2013) Stroke induces long-lasting deficits in the temporal fidelity of sensory processing in the somatosensory cortex. J Cereb Blood Flow Metab 33:91-96.
Takahashi K, Best MD, Huh N, Brown KA, Tobaa AA, Hatsopoulos NG (2017) Encoding of Both Reaching and Grasping Kinematics in Dorsal and Ventral Premotor Cortices. J Neurosci 37:1733-1746.
Takasawa M, Oku N, Osaki Y, Kinoshita H, Imaizumi M, Yoshikawa T, Kimura Y, Kajimoto K, Sasagaki M, Kitagawa K, Hori M, Hatazawa J (2003) Cerebral and cerebellar activation in power and precision grip movements: an H2 15O positron emission tomography study. J Cereb Blood Flow Metab 23:1378-1382.
Takatsuru Y, Fukumoto D, Yoshitomo M, Nemoto T, Tsukada H, Nabekura J (2009) Neuronal circuit remodeling in the contralateral cortical hemisphere during functional recovery from cerebral infarction. J Neurosci 29:10081-10086.

Takei T, Crevecoeur F, Herter TM, Cross KP, Scott SH (2018) Correlations Between Primary Motor Cortex Activity with Recent Past and Future Limb Motion During Unperturbed Reaching. J Neurosci 38:7787-7799.
Takeuchi N, Tada T, Toshima M, Ikoma K (2010) Correlation of motor function with transcallosal and intracortical inhibition after stroke. J Rehabil Med 42:962-966.
Takeuchi N, Chuma T, Matsuo Y, Watanabe I, Ikoma K (2005) Repetitive transcranial magnetic stimulation of contralesional primary motor cortex improves hand function after stroke. Stroke 36:2681-2686.
Takeuchi N, Toshima M, Chuma T, Matsuo Y, Ikoma K (2008) Repetitive transcranial magnetic stimulation of the unaffected hemisphere in a patient who was forced to use the affected hand. Am J Phys Med Rehabil 87:74-77.
Talelli P, Greenwood RJ, Rothwell JC (2007) Exploring Theta Burst Stimulation as an intervention to improve motor recovery in chronic stroke. Clin Neurophysiol 118:333-342.
Talelli P, Wallace A, Dileone M, Hoad D, Cheeran B, Oliver R, VandenBos M, Hammerbeck U, Barratt K, Gillini C, Musumeci G, Boudrias MH, Cloud GC, Ball J, Marsden JF, Ward NS, Di Lazzaro V, Greenwood RG, Rothwell JC (2012) Theta burst stimulation in the rehabilitation of the upper limb: a semirandomized, placebo-controlled trial in chronic stroke patients. Neurorehabil Neural Repair 26:976-987.
Tang Q, Li G, Liu T, Wang A, Feng S, Liao X, Jin Y, Guo Z, He B, McClure MA, Xing G, Mu Q (2015) Modulation of interhemispheric activation balance in motor-related areas of stroke patients with motor recovery: Systematic review and meta-analysis of fMRI studies. Neurosci Biobehav Rev 57:392-400.
Tanji J, Okano K, Sato KC (1987) Relation of neurons in the nonprimary motor cortex to bilateral hand movement. Nature 327:618-620.
Tanji J, Okano K, Sato KC (1988) Neuronal activity in cortical motor areas related to ipsilateral, contralateral, and bilateral digit movements of the monkey. J Neurophysiol 60:325-343.
Tanne-Gariepy J, Rouiller EM, Boussaoud D (2002) Parietal inputs to dorsal versus ventral premotor areas in the macaque monkey: evidence for largely segregated visuomotor pathways. Exp Brain Res 145:91-103.
Taub E, Uswatte G, Morris DM (2003) Improved motor recovery after stroke and massive cortical reorganization following Constraint-Induced Movement therapy. Phys Med Rehabil Clin N Am 14:S77-91, ix.
Tazoe T, Perez MA (2013) Speed-dependent contribution of callosal pathways to ipsilateral movements. J Neurosci 33:16178-16188.
Teskey GC, Flynn C, Goertzen CD, Monfils MH, Young NA (2003) Cortical stimulation improves skilled forelimb use following a focal ischemic infarct in the rat. Neurol Res 25:794-800.
Thach WT (1978) Correlation of neural discharge with pattern and force of muscular activity, joint position, and direction of intended next movement in motor cortex and cerebellum. J Neurophysiol 41:654-676.
Theys T, Pani P, van Loon J, Goffin J, Janssen P (2012) Selectivity for three-dimensional shape and grasping-related activity in the macaque ventral premotor cortex. J Neurosci 32:12038-12050.
Theys T, Pani P, van Loon J, Goffin J, Janssen P (2013) Three-dimensional shape coding in grasping circuits: a comparison between the anterior intraparietal area and ventral premotor area F5a. J Cogn Neurosci 25:352-364.
Tinazzi M, Zanette G (1998) Modulation of ipsilateral motor cortex in man during unimanual finger movements of different complexities. Neurosci Lett 244:121-124.

Tokuno H, Nambu A (2000) Organization of nonprimary motor cortical inputs on pyramidal and nonpyramidal tract neurons of primary motor cortex: An electrophysiological study in the macaque monkey. Cereb Cortex 10:58-68.
Tortella G, Casati R, Aparicio LV, Mantovani A, Senco N, D'Urso G, Brunelin J, Guarienti F, Selingardi PM, Muszkat D, Junior Bde S, Valiengo L, Moffa AH, Simis M, Borrione L, Brunoni AR (2015) Transcranial direct current stimulation in psychiatric disorders. World J Psychiatry 5:88-102.
Touvykine B, Elgbeili G, Quessy S, Dancause N (2020) Interhemispheric modulations of motor outputs by the rostral and caudal forelimb areas in rats. J Neurophysiol 123:1355-1368.
Touvykine B, Mansoori BK, Jean-Charles L, Deffeyes J, Quessy S, Dancause N (2016) The Effect of Lesion Size on the Organization of the Ipsilesional and Contralesional Motor Cortex. Neurorehabil Neural Repair 30:280-292.
Travis AM (1955) Neurological deficiencies after ablation of the precentral motor area in Macaca mulatta. Brain 78:155-173.
Umilta MA, Brochier T, Spinks RL, Lemon RN (2007) Simultaneous recording of macaque premotor and primary motor cortex neuronal populations reveals different functional contributions to visuomotor grasp. J Neurophysiol 98:488-501.
Umilta MA, Escola L, Intskirveli I, Grammont F, Rochat M, Caruana F, Jezzini A, Gallese V, Rizzolatti G (2008) When pliers become fingers in the monkey motor system. Proc Natl Acad Sci U S A 105:2209-2213.
Urban J, Kossut M, Hess G (2002) Long-term depression and long-term potentiation in horizontal connections of the barrel cortex. Eur J Neurosci 16:1772-1776.
Valero-Cabre A, Amengual JL, Stengel C, Pascual-Leone A, Coubard OA (2017) Transcranial magnetic stimulation in basic and clinical neuroscience: A comprehensive review of fundamental principles and novel insights. Neurosci Biobehav Rev 83:381-404.
Vallone F, Lai S, Spalletti C, Panarese A, Alia C, Micera S, Caleo M, Di Garbo A (2016) Post-Stroke Longitudinal Alterations of Inter-Hemispheric Correlation and Hemispheric Dominance in Mouse Pre-Motor Cortex. PLoS One 11:e0146858.
van Lieshout ECC, van der Worp HB, Visser-Meily JMA, Dijkhuizen RM (2019) Timing of Repetitive Transcranial Magnetic Stimulation Onset for Upper Limb Function After Stroke: A Systematic Review and Meta-Analysis. Front Neurol 10:1269.
van Meer MP, Otte WM, van der Marel K, Nijboer CH, Kavelaars A, van der Sprenkel JW, Viergever MA, Dijkhuizen RM (2012) Extent of bilateral neuronal network reorganization and functional recovery in relation to stroke severity. J Neurosci 32:4495-4507.
van Meer MP, van der Marel K, Wang K, Otte WM, El Bouazati S, Roeling TA, Viergever MA, Berkelbach van der Sprenkel JW, Dijkhuizen RM (2010) Recovery of sensorimotor function after experimental stroke correlates with restoration of resting-state interhemispheric functional connectivity. J Neurosci 30:3964-3972.
Vargas-Irwin CE, Franquemont L, Black MJ, Donoghue JP (2015) Linking Objects to Actions: Encoding of Target Object and Grasping Strategy in Primate Ventral Premotor Cortex. J Neurosci 35:10888-10897.
Vesia M, Culham JC, Jegatheeswaran G, Isayama R, Le A, Davare M, Chen R (2018) Functional interaction between human dorsal premotor cortex and the ipsilateral primary motor cortex for grasp plans: a dual-site TMS study. Neuroreport 29:1355-1359.
Vigneswaran G, Philipp R, Lemon RN, Kraskov A (2013) M1 corticospinal mirror neurons and their role in movement suppression during action observation. Curr Biol 23:236-243.
Vogt C, Vogt O (1919) Ergebnisse unserer Hirnforschung [Results of our brain research]. Jounrnal Fur Psychologie und Neurologie 25:277-462.

Volz LJ, Rehme AK, Michely J, Nettekoven C, Eickhoff SB, Fink GR, Grefkes C (2016) Shaping Early Reorganization of Neural Networks Promotes Motor Function after Stroke. Cereb Cortex 26:2882-2894.
Volz LJ, Sarfeld AS, Diekhoff S, Rehme AK, Pool EM, Eickhoff SB, Fink GR, Grefkes C (2015) Motor cortex excitability and connectivity in chronic stroke: a multimodal model of functional reorganization. Brain Struct Funct 220:1093-1107.
von Monakow C (1914) Die Lokalisation im Grosshirn und der Abbau der Funktion durch kortikale Herde. Wiesbaden.
Waitzman DM, Silakov VL, DePalma-Bowles S, Ayers AS (2000) Effects of reversible inactivation of the primate mesencephalic reticular formation. I. Hypermetric goal-directed saccades. J Neurophysiol 83:2260-2284.
Wang CC, Wang CP, Tsai PY, Hsieh CY, Chan RC, Yeh SC (2014) Inhibitory repetitive transcranial magnetic stimulation of the contralesional premotor and primary motor cortices facilitate poststroke motor recovery. Restor Neurol Neurosci 32:825-835.
Wang L, Yu C, Chen H, Qin W, He Y, Fan F, Zhang Y, Wang M, Li K, Zang Y, Woodward TS, Zhu C (2010) Dynamic functional reorganization of the motor execution network after stroke. Brain 133:1224-1238.
Wannier TM, Maier MA, Hepp-Reymond MC (1991) Contrasting properties of monkey somatosensory and motor cortex neurons activated during the control of force in precision grip. J Neurophysiol 65:572-589.
Ward NS (2005) Mechanisms underlying recovery of motor function after stroke. Postgrad Med J 81:510-514.
Ward NS (2007) Future perspectives in functional neuroimaging in stroke recovery. Eura Medicophys 43:285-294.
Ward NS (2015) Does neuroimaging help to deliver better recovery of movement after stroke? Curr Opin Neurol 28:323-329.
Ward NS, Cohen LG (2004) Mechanisms underlying recovery of motor function after stroke. Arch Neurol 61:1844-1848.
Ward NS, Brown MM, Thompson AJ, Frackowiak RS (2003a) Neural correlates of outcome after stroke: a cross-sectional fMRI study. Brain 126:1430-1448.
Ward NS, Brown MM, Thompson AJ, Frackowiak RS (2003b) Neural correlates of motor recovery after stroke: a longitudinal fMRI study. Brain 126:2476-2496.
Weber R, Ramos-Cabrer P, Justicia C, Wiedermann D, Strecker C, Sprenger C, Hoehn M (2008) Early prediction of functional recovery after experimental stroke: functional magnetic resonance imaging, electrophysiology, and behavioral testing in rats. J Neurosci 28:1022-1029.
Weiller C, Chollet F, Friston KJ, Wise RJ, Frackowiak RS (1992) Functional reorganization of the brain in recovery from striatocapsular infarction in man. Ann Neurol 31:463-472.
Weinrich M, Wise SP (1982) The premotor cortex of the monkey. J Neurosci 2:1329-1345.
Weinrich M, Wise SP, Mauritz KH (1984) A neurophysiological study of the premotor cortex in the rhesus monkey. Brain 107 (Pt 2):385-414.
Werner W, Bauswein E, Fromm C (1991) Static firing rates of premotor and primary motor cortical neurons associated with torque and joint position. Exp Brain Res 86:293-302.
Wessel MJ, Zimerman M, Hummel FC (2015) Non-invasive brain stimulation: an interventional tool for enhancing behavioral training after stroke. Front Hum Neurosci 9:265.
Westlake KP, Hinkley LB, Bucci M, Guggisberg AG, Byl N, Findlay AM, Henry RG, Nagarajan SS (2012) Resting state alpha-band functional connectivity and recovery after stroke. Exp Neurol 237:160-169.

Whishaw IQ, Karl JM (2014) The contribution of the reach and the grasp to shaping brain and behaviour. Can J Exp Psychol 68:223-235.
Wiesendanger M, Hummelsheim H, Bianchetti M (1985) Sensory input to the motor fields of the agranular frontal cortex: a comparison of the precentral, supplementary motor and premotor cortex. Behav Brain Res 18:89-94.
Wilke M, Kagan I, Andersen RA (2012) Functional imaging reveals rapid reorganization of cortical activity after parietal inactivation in monkeys. Proc Natl Acad Sci U S A 109:8274-8279.
Wisden W, Laurie DJ, Monyer H, Seeburg PH (1992) The distribution of 13 GABAA receptor subunit mRNAs in the rat brain. I. Telencephalon, diencephalon, mesencephalon. J Neurosci 12:1040-1062.
Wise SP, Murray EA (2000) Arbitrary associations between antecedents and actions. Trends Neurosci 23:271-276.
Wise SP, di Pellegrino G, Boussaoud D (1996) The premotor cortex and nonstandard sensorimotor mapping. Can J Physiol Pharmacol 74:469-482.
Wise SP, Boussaoud D, Johnson PB, Caminiti R (1997) Premotor and parietal cortex: corticocortical connectivity and combinatorial computations. Annu Rev Neurosci 20:25-42.
Wise SP, Moody SL, Blomstrom KJ, Mitz AR (1998) Changes in motor cortical activity during visuomotor adaptation. Exp Brain Res 121:285-299.
Wolpaw JR (1980) Amplitude of responses to perturbation in primate sensorimotor cortex as a function of task. J Neurophysiol 44:1139-1147.
Wolpert DM, Miall RC (1996) Forward Models for Physiological Motor Control. Neural Netw 9:1265-1279.
Woolsey CN, Settlage PH, Meyer DR, Sencer W, Pinto Hamuy T, Travis AM (1952) Patterns of localization in precentral and "supplementary" motor areas and their relation to the concept of a premotor area. Res Publ Assoc Res Nerv Ment Dis 30:238-264.
Xerri C, Merzenich MM, Peterson BE, Jenkins W (1998) Plasticity of primary somatosensory cortex paralleling sensorimotor skill recovery from stroke in adult monkeys. J Neurophysiol 79:2119-2148.
Xu J, Branscheidt M, Schambra H, Steiner L, Widmer M, Diedrichsen J, Goldsmith J, Lindquist M, Kitago T, Luft AR, Krakauer JW, Celnik PA, Group SS (2019) Rethinking interhemispheric imbalance as a target for stroke neurorehabilitation. Ann Neurol 85:502-513.
Yamamoto T, Hayashi T, Murata Y, Ose T, Higo N (2019) Premotor Cortical-Cerebellar Reorganization in a Macaque Model of Primary Motor Cortical Lesion and Recovery. J Neurosci 39:8484-8496.
Zant JD, Strick PL (1978) The cells of origin of interhemispheric connections in the primate motor cortex. Soc Neurosci Abstr 4:308.
Zeiler SR, Hubbard R, Gibson EM, Zheng T, Ng K, O'Brien R, Krakauer JW (2016) Paradoxical Motor Recovery From a First Stroke After Induction of a Second Stroke: Reopening a Postischemic Sensitive Period. Neurorehabil Neural Repair 30:794-800.
Zhang Y, Partsalis AM, Highstein SM (1995) Properties of superior vestibular nucleus flocculus target neurons in the squirrel monkey. II. Signal components revealed by reversible flocculus inactivation. J Neurophysiol 73:2279-2292.
Zhou X, Tien RN, Ravikumar S, Chase SM (2019) Distinct types of neural reorganization during long-term learning. J Neurophysiol 121:1329-1341.
Zhu LL, Lindenberg R, Alexander MP, Schlaug G (2010) Lesion load of the corticospinal tract predicts motor impairment in chronic stroke. Stroke 41:910-915.